Supporting Information

Synthesis, Oligomerization and Catalytic Studies of a Redox-Active Ni4-Cubane: A detailed Mechanistic Investigation

Saroj Kumar Kushvaha, [a†] Maria Francis, [b†] Jayasree Kumar, [a] Ekta Nag, [b] Prathap Ravichandran, [a] Sudipta Roy*[b] and Kartik Chandra Mondal*[a]

[a]Department of Chemistry, Indian Institute of Technology Madras, Chennai 600036, India.
[b]Department of Chemistry, Indian Institute of Science Education and Research (IISER) Tirupati 517507, India.
† Both authors contributed equally.

Table of Contents

1. General remarks

All catalytic reactions were performed under Argon atmosphere. The progress of all the catalytic reactions were monitored by thin layer chromatography (TLC, Merck silica gel 60 F 254) upon visualization of the TLC plate under UV light (250 nm). Different charring reagents, such as phosphomolybdic acid/ethanol, ninhydrin/acetic acid solution and iodine were used to visualize various starting materials and products spots on TLC plates. Indole, pyrrole and furan were purchased from commercial sources and used directly. Substituted pyrroles, indoles, furoate esters and diazoesters were synthesized following the reported literatures.[S1-S2] Silica gel (240-400 mesh) for column chromatography was purchased from the commercial source. HPLC grade dichloromethane (DCM) and toluene were purchased from the commercial sources and poured in a solvent purification system (SPS, MB-SPS-5). All the catalytic reactions were carried out in dry solvents collected from the SPS. Polar solvents required for the syntheses of the nickel complexes, e.g., methanol, dimethyl formamide (DMF), dimethyl sulfoxide (DMSO) and acetone were purchased from commercial source and used as it is. The bulk solvents for column chromatography, such as ethyl acetate (EtOAc) and *n*-hexane were received from the commercial source and steam distilled prior to the usage. ^{1}H and ^{13}C NMR spectra of all synthesized compounds were recorded on Bruker AV 400 (400 MHz) and Bruker AV III (500 MHz) spectrometer using $CDCl_3$, DMSO-D6 as solvents. The chemical shift values for all the organic molecules were reported in δ (ppm) relative to $CDCl_3$ at 7.26 ppm (^{1}H NMR) and 77.0 ppm (^{13}C NMR). The following abbreviations were used to describe the peak multiplicity in ^{1}H NMR spectra: s (singlet), d (doublet), dd (doublet of doublet), td (triplet of doublet), t (triplet), q (quartet), m (multiplet). High resolution mass spectra were recorded on a “TOF analyzer” spectrometer in an electrospray mode. Infrared spectra were recorded on a Bruker ALPHA FT-IR spectrometer. Cyclic voltammetry studies were performed on a Metrohm Multi-Autolab PGSTAT204. GC analysis was carried out using a DB-5 column (30 m, 0.25 mm, 0.25µ). Elemental analysis was performed in Thermo scientific flash 2000 elemental analyzer. UV-Visible spectra were recorded in Jasco V-650 Spectrophotometer.

2. Syntheses of complexes 1-3

2.1. Synthesis of ligands: Diprotic Schiff base ligands $(OH)_2L$-Me was synthesized by condensing *o*-vanillin with 4-methyl-2-aminophenol in MeOH and isolated as dark orange crystalline precipitate in good yield (80%).[S3-S5] Complexes **1-3** were synthesized under aerobic condition. Complex $[Ni_4((O^-)_2L\text{-}Me)_4(s)_4]$ (**3**) was synthesized under aerobic conditions in excellent yield (94%). It is stable in ambient atmosphere for several months.

2.2. Synthesis of $[Ni_4((O^-)_2L\text{-}Me)_4(s)_4]$ (3) [s = solvent = MeOH/H_2O]: A 1:1 molar mixture of $NiCl_2{\cdot}6H_2O$ (10 mmol; 2.38 g) and (H_2L-Me) (10 mmol; 2.57 g) was dissolved in 150 mL of MeOH and stirred for 15 min to obtain a clear solution. Et_3N (20 mmol; 2.0 g) (two equivalents) was added dropwise over 5 min to obtain a clear orange-brown solution. Dark orange-brown precipitate was isolated in 94% (2.94 g) yield. Block like single crystals were obtained when this same reaction was performed with double volume of MeOH (300 mL). The poor diffraction of single crystal diffraction of X-ray was encountered. Several attempts failed to produce desired diffraction.

Elemental analysis (Calcd.) of $[Ni_4((O^-)_2L\text{-}Me)_4(s)_4]$ (**3**): C 54.82 (54.74), H 5.31 (5.29), N 3.73 (3.87), Cl <0.02 (0.0) which closely matches with $[Ni_4((O^-)_2L\text{-}Me)_4(MeOH)_4]{\cdot}2MeOH$. **IR (KBr, cm^{-1}):** 2965, 2917, 2851, 1601, 1535, 1486, 1460, 1433, 1381, 1323, 1297, 1258, 1231, 1202, 1170, 1143, 1121, 1100, 1020, 971, 858, 822, 729, 668, 594.

Ni(II) ions (with s = 1; g = 2) of complex **3** are ferromagnetically coupled having spin ground state S = 4 at very low temperature.

ESI-MS (m/z): 1253 as $[M+H]^+$, 1275 as $[M+Na]^+$, 627 as $[M+2H]^{2+}$; M = $[Ni_4((O^-)_2L\text{-}Me)_4]$, **$(O^-)_2$L-Me** = $C_{15}H_{13}NO_3$. **3** was dried in open air when it was stored over a filter paper for 3-4 h at room temperature.

ESI mass spectrometric studies showed the formation of both **2** and **3**. The former complex was only isolated when following slight controlled experiment.

2.3. Synthesis of $[Ni_4((O^-)_2L\text{-}Me)_3((O_{al}^-)(OH)L)Cl]$ (2): To Synthesize **2**, 0.1 mmol (23.7 mg) of $NiCl_2{\cdot}6H_2O$ and 0.1 mmol (25.7 mg) of ligand (H_2L-Me) was stirred in 20 ml of mixture of solvents (3:1 by volume; MeOH and CH_3CN) for 10 min to obtain golden-yellow color solution. On adding, 0.15 mmol (15 mg) of triethylamine base into this solution, color changes to brownish. The reaction mixture was further stirred for 10 min and was left for slow evaporation. After six days of slow evaporation brownish color crystals were formed. A suitable orange-yellowish block-shape crystal was mounted for single crystal X-ray diffraction. During the course of data collection, we observed that there are few distinct yellow crystals of **1**·2MeOH, we collected SC-XRD data for that crystal and it turned out that the crystal has different crystal structure but same nuclearity. This suggests that **2** is formed via intermediacy of **1**·2MeOH. As SC-XRD data reveals, the complex **1**·2MeOH has two bridged chlorine atoms and **2** has one chlorine atom in the crystal structure. The elementary (C, H, N and Cl) analysis suggests presence of one chlorine atom suggesting dominance of **2** in the bulk. The few dark green-black blocks of **1**·2MeOH suitable for X-ray single crystal diffraction were obtained when the mother liquor of the reaction solution was close to the dryness.

Elemental analysis (Cald.) of $[Ni_4((O^-)_2L\text{-}Me)_3((O_{al}^-)(OH)L)Cl]$ (**2**): C 55.45 (55.76), H 4.25 (4.13), N 4.48 (4.34), Cl 2.41 (2.74). **Selected IR bands** (KBr; cm^{-1}): $\tilde{\nu}$ = 2919(s), 2338(s), 1606(m), 1502(s), 1299(s), 726(m).

3. Detail characterization of complexes 1-3

3.1. UV-vis spectra of complex 3

The UV-Vis spectrum of the complex **3** is recorded in various solvents viz. chloroform, acetonitrile, dichloromethane, dimethyl sulfoxide (DMSO), dimethylformamide, tetrahydrofuran and toluene in 10 micro molar concentration at room temperature.

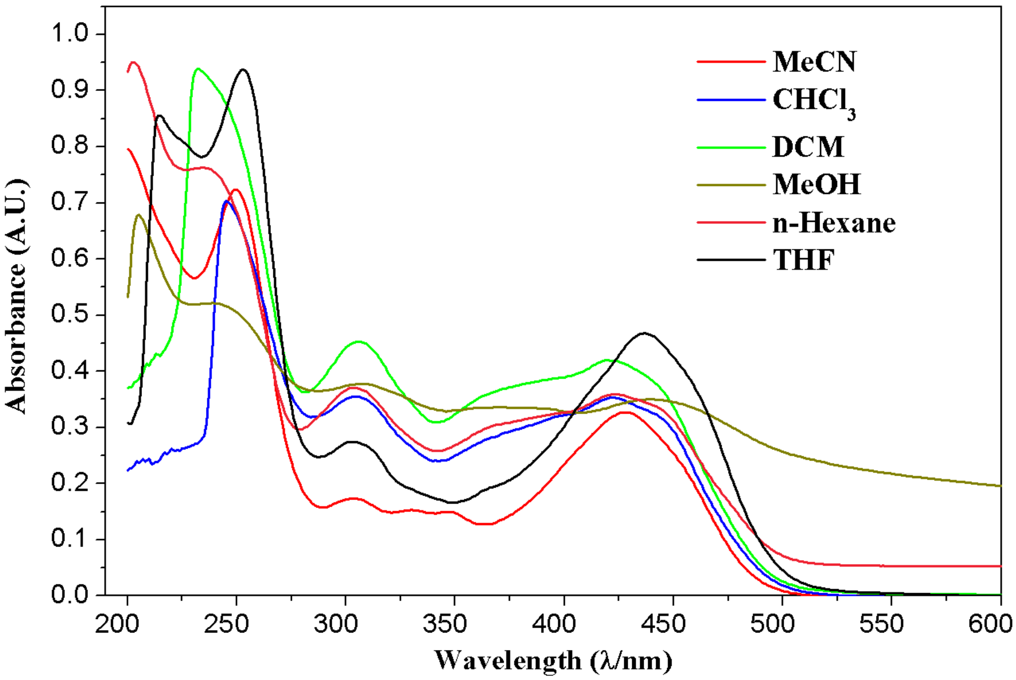

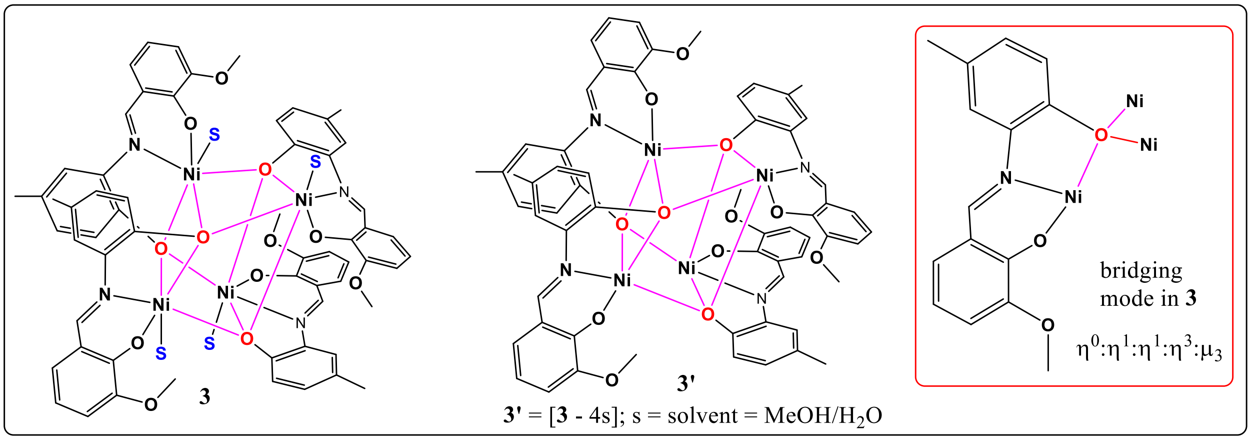

3' = [**3** - 4s]; s = solvent = MeOH/H$_2$O

Figure S1. UV-vis spectra of **3** in different solvents. The UV-vis absorption bands for **3** in different solvents: THF (296.6, 239.0 nm), toluene (303.2, 349.4 nm), CHCl3 (242.52, 297.1, 347.6 nm), DMSO (259.2, 302.3, 415.8 nm), MeCN (293.4, 408.8 nm), DMF (295.6, 409.2 nm) and DCM (284, 297.1, 346.8 nm).

3.2. Magnetic susceptibility measurement of complex 3

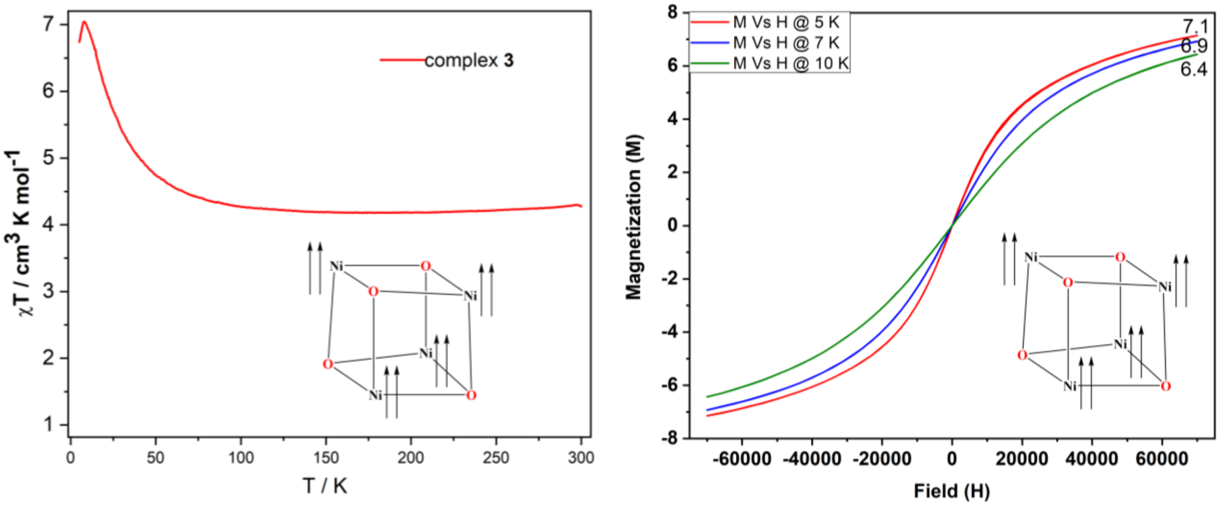

Figure S2. χT vs T (H = 0.1 T) (left) and M vs H (right) plots of complex **3**.

The temperature dependent direct-current (dc) magnetic susceptibility of 3 was measured under an applied dc magnetic field of 1000 Oe in the temperature range of 5-300 K (Figure S2). The μ_3-O bridges present between Ni(II) ions facilitate magnetic exchange interactions. The Ni-O-Ni bond angles decide the type of interaction between metal ions. The room temperature χ_MT value is 4.29 cm^3 mol^{-1} K which is higher than the theoretically calculated spin only value for four Ni(II) ions (4.04 cm^3 mol^{-1} K with g = 2.0). The higher χ_MT value is due to slight value of g (> 2.0). The χ_MT value remains almost constant on cooling down sample from 300 to 100 K, that happens probably due to presence of weak magnetic interactions among Ni(II) ions in this temperature range (The spin centers are randomized in this temperature range). However, χ_MT value increases (the separations among the magnetic energy levels are populated/depopulated below 100 K following temperature dependent Boltzmann distribution) sharply thereafter and reaches maximum value of 8.10 cm^3 mol^{-1} K at 6 K. The steady increase in χ_MT value 100 K is due to moderate ferromagnetic interactions in this temperature range. On further cooling, $\chi_M T$ value slightly decreases due to zero field splitting (ZFS). M vs H plot suggest that spin ground state of 3 is S = 4. Magnetization (M = dE/dH; χ = dM/dH) did not reach saturation at 5 K. The expected saturation of magnetization of 8 (if g = 2). The experimental magnetization of 7.10 μ_B under applied magnetic field of 7 T at 5 K.

3.3. NMR spectroscopic data of complex 3

^{1}H NMR spectrum of complex 3

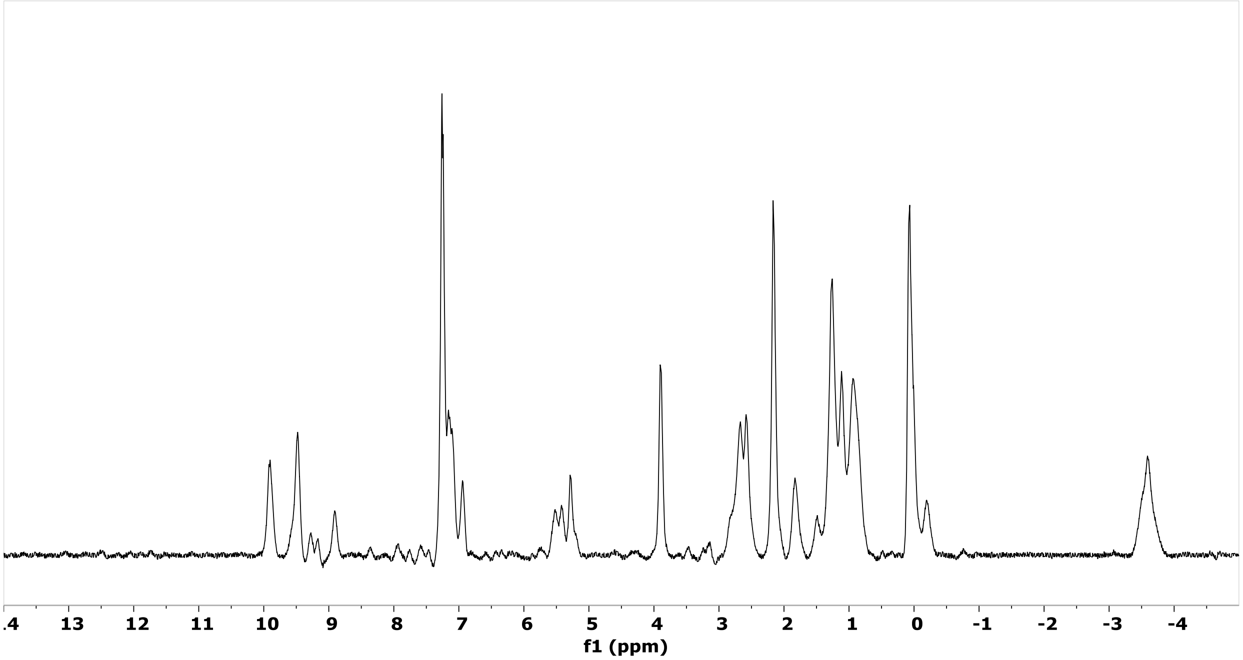

Figure S3. ^{1}H NMR spectrum of complex **3** (with higher concentration) in $CDCl_3$. It is a paramagnetic complex with S = 4 spin ground state.

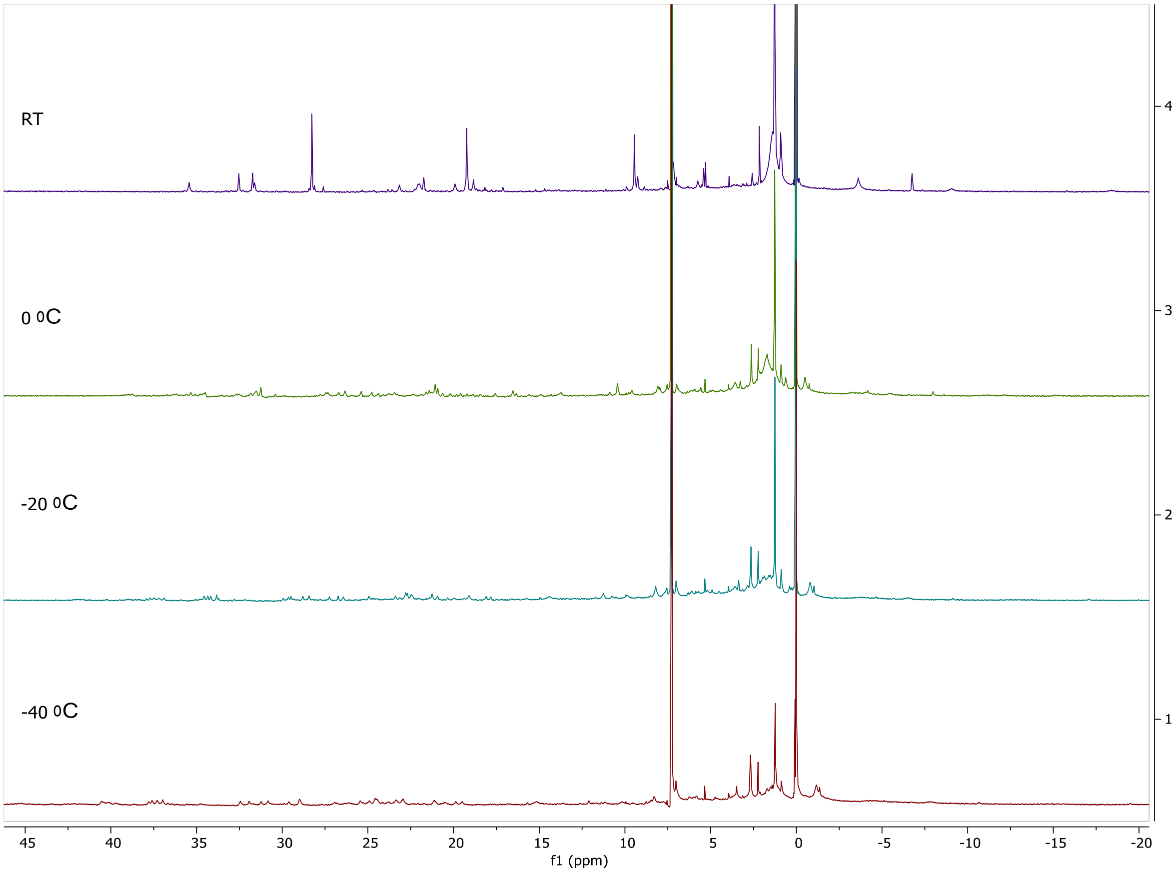

Figure S4. Temperature dependent ^{1}H NMR spectrum of complex **3** in $CDCl_3$.

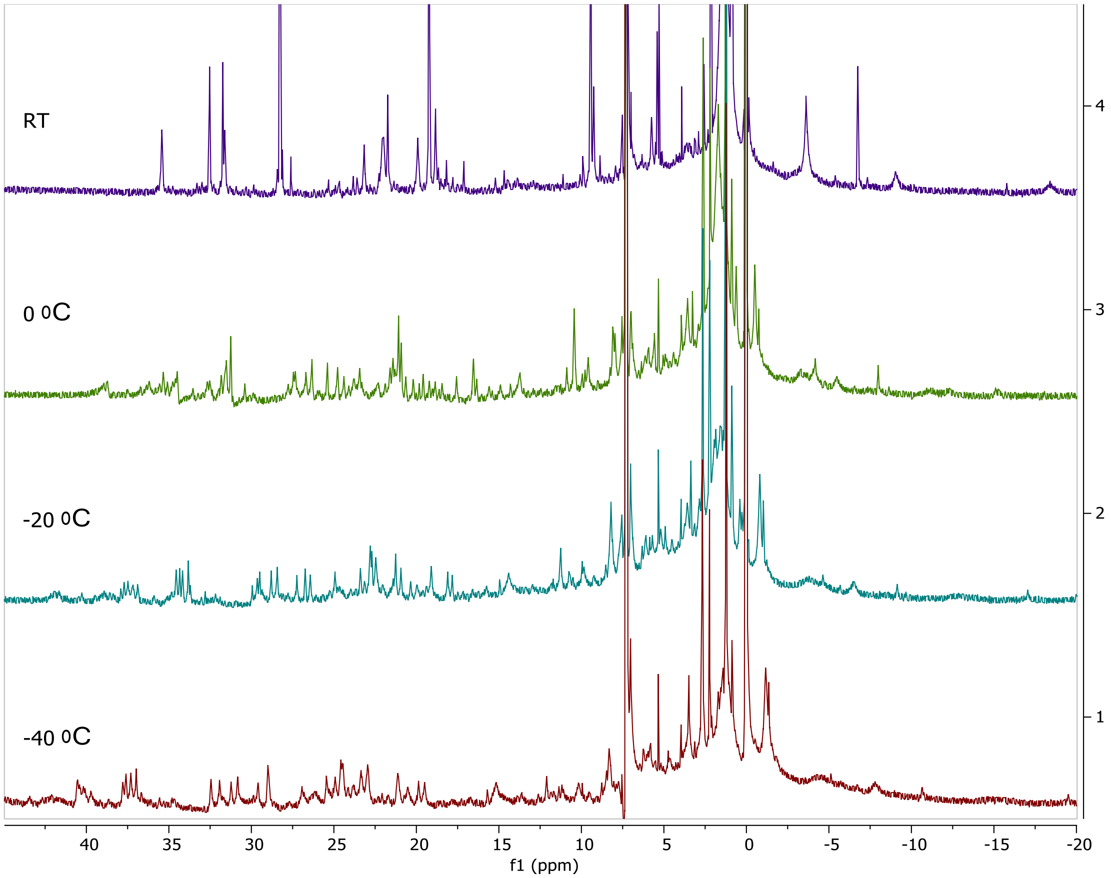

Figure S5. Temperature dependent ^{1}H NMR spectrum of complex **3** in $CDCl_3$ (expanded).

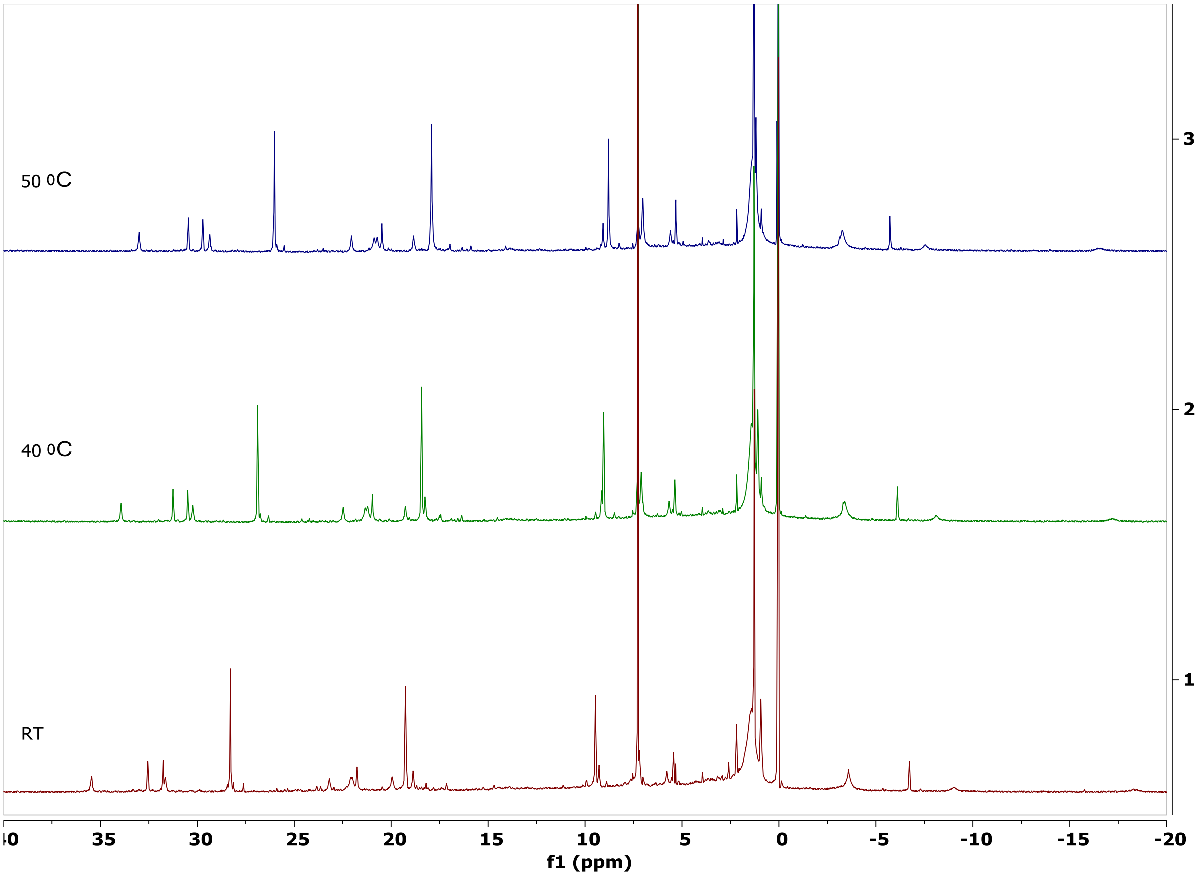

Figure S6. Temperature dependent ^{1}H NMR spectrum of complex **3** in $CDCl_3$. Increase in temperature leads to the well resolves signals in the spectra.

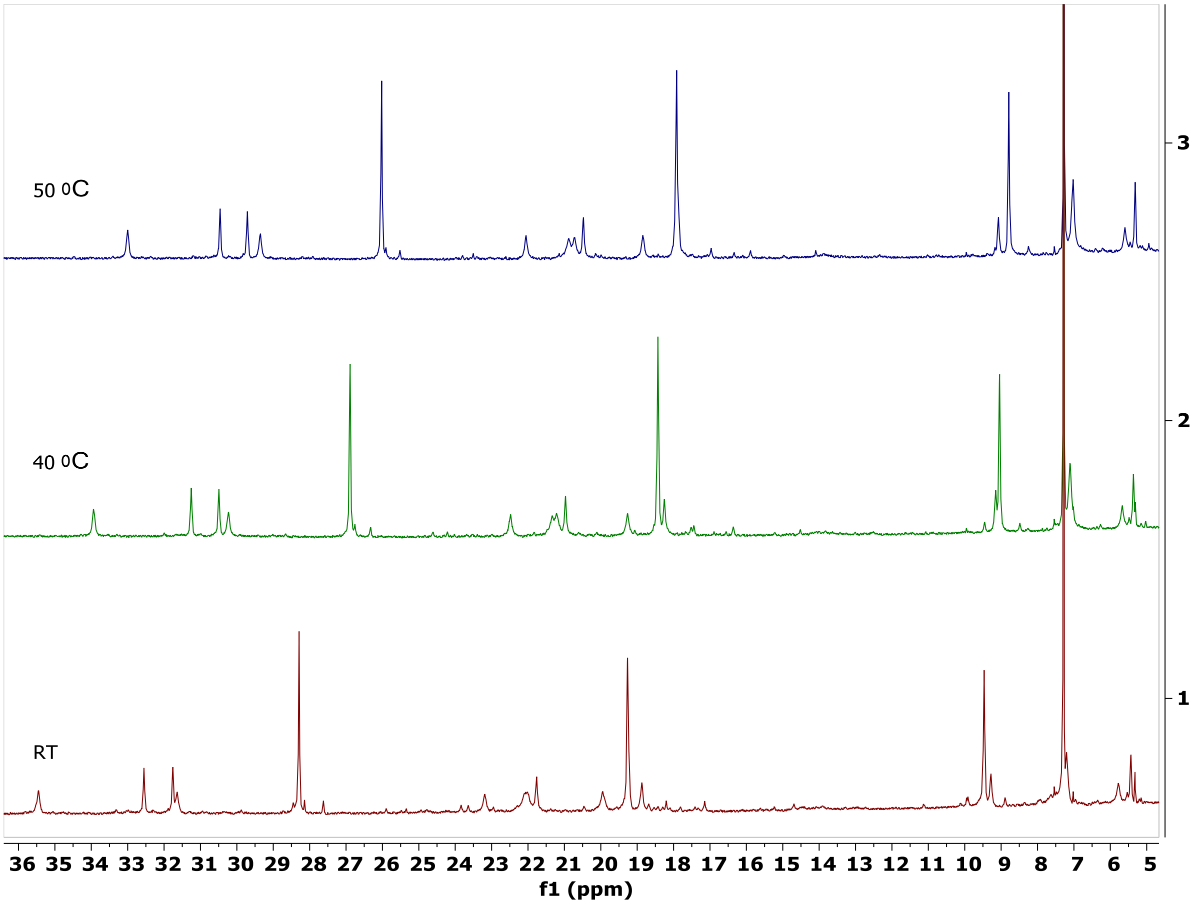

Figure S7. Temperature dependent ^{1}H NMR spectrum of complex **3** in $CDCl_3$ (expanded).

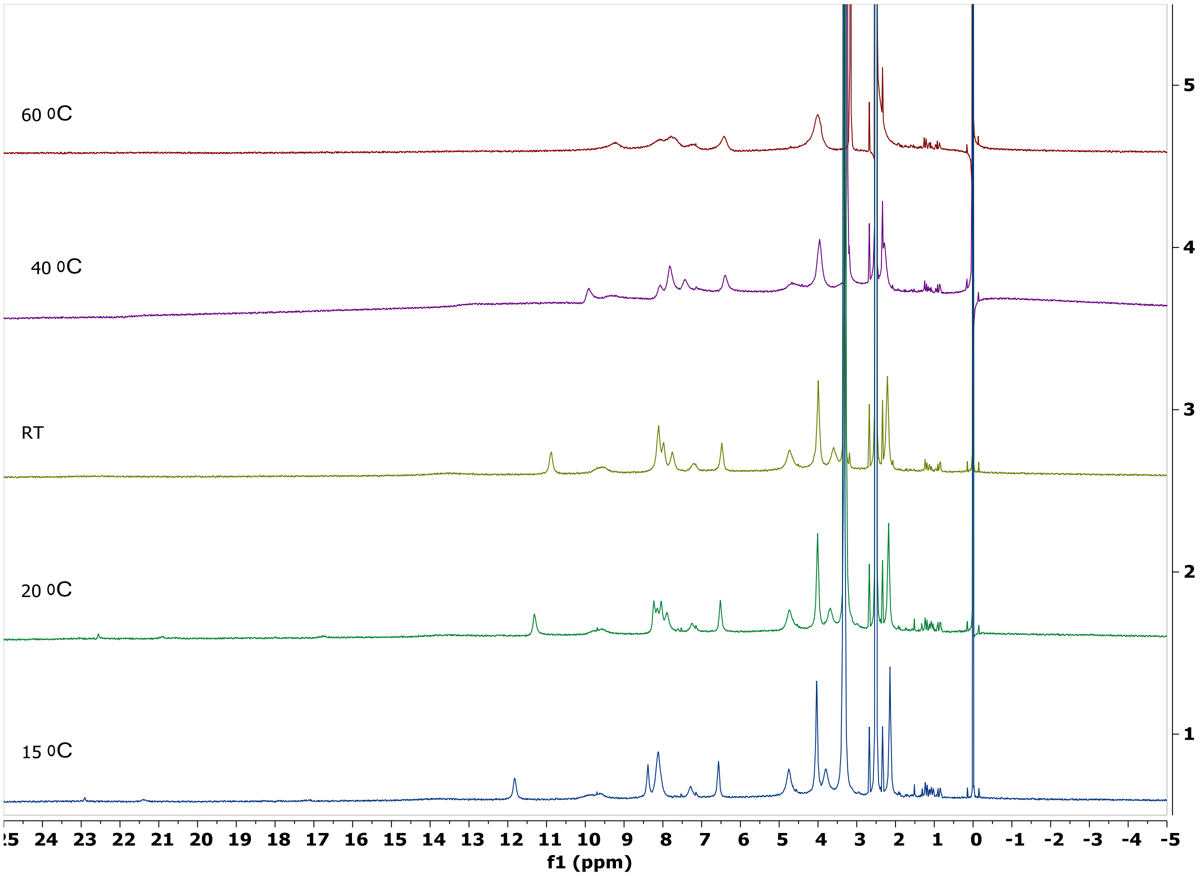

Figure S8. Temperature dependent ^{1}H NMR spectrum of complex **3** in DMSO-D6. Lowering the temperature of the sample led to the well-resolved spectral lines.

3.4. Thermogravimetric analysis of complex 2

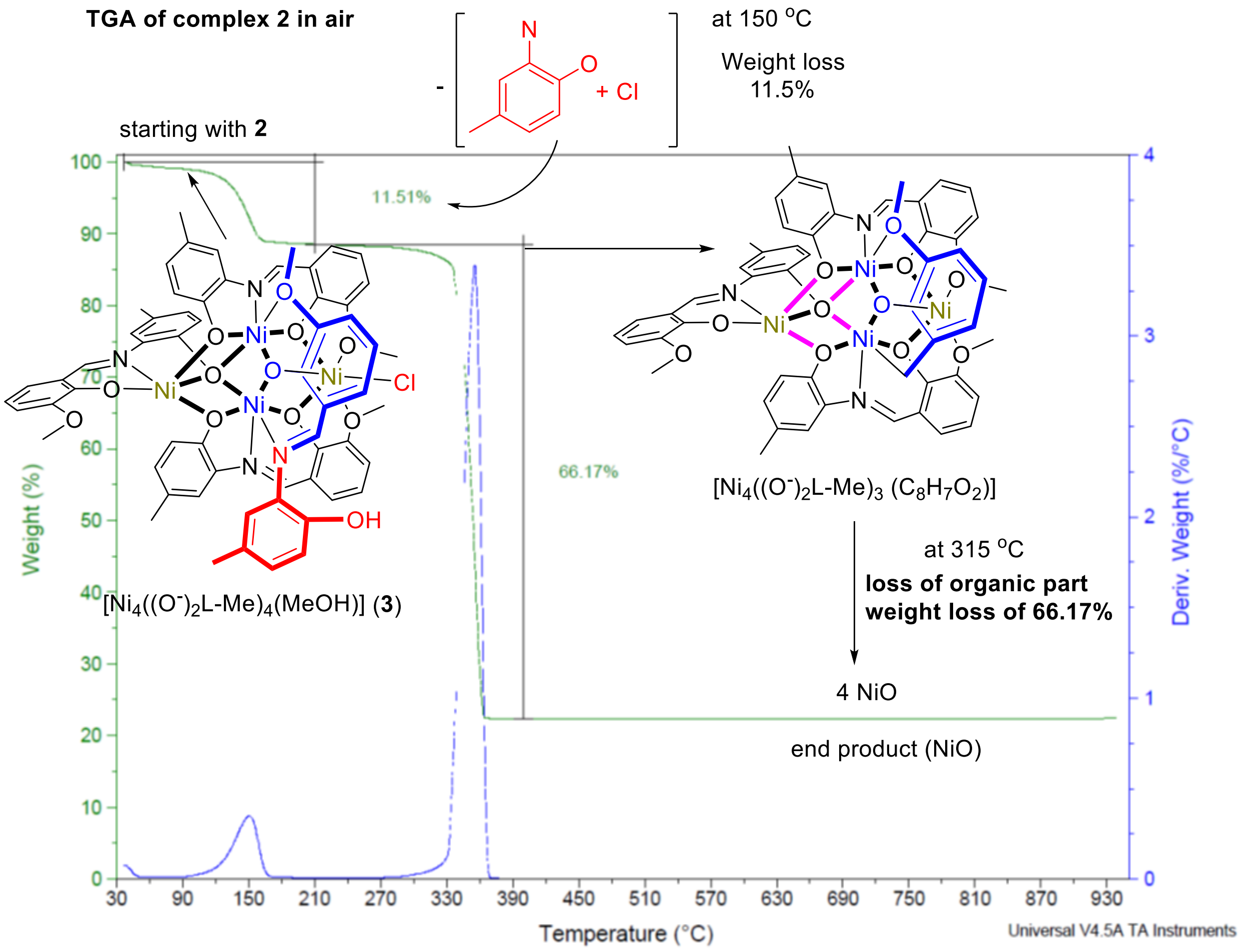

Figure S9. TGA of complex **2** in air. The first weight loss of 11.5% at 150 °C is due to loss of 4-methyl-aminophenol unit and coordinated chloride ion (shown in red color). The second weight loss of 66.2% at 315 °C is due to loss of all remaining organic ligand parts leading to the formation of final product as NiO.

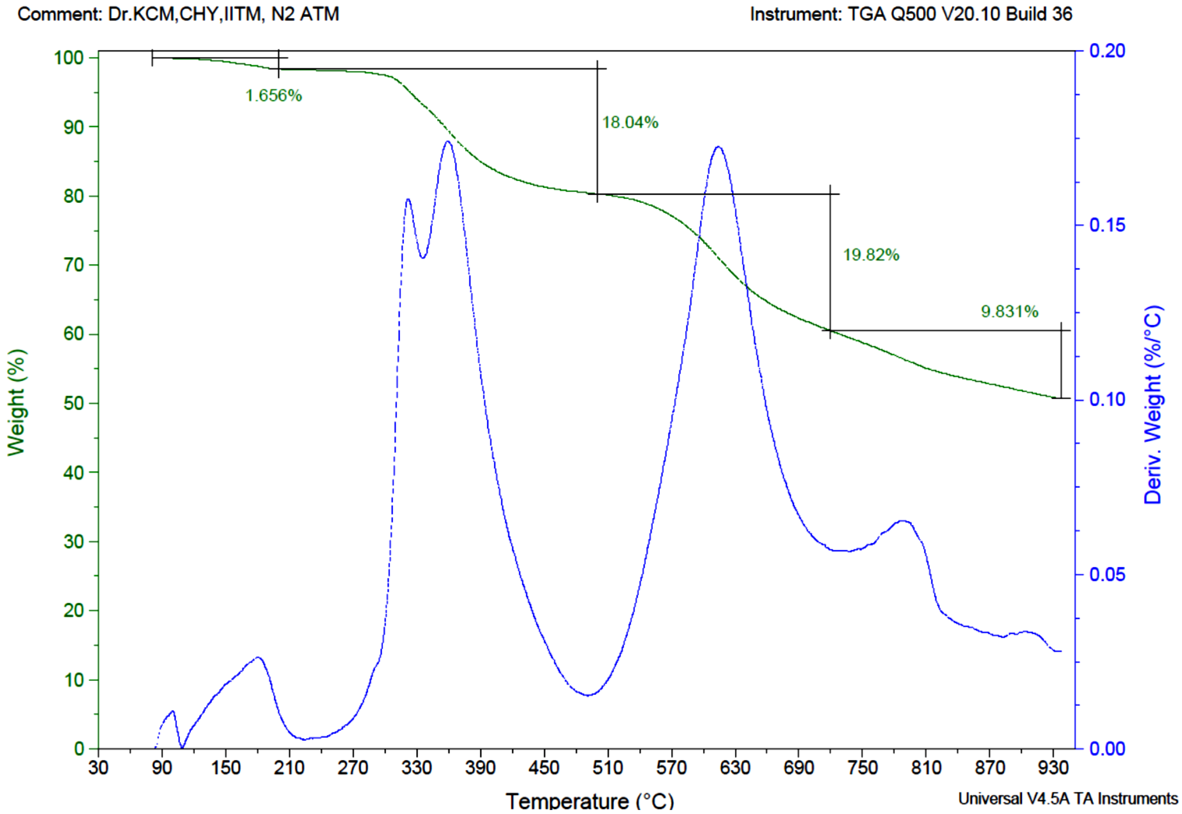

Figure S10. TGA of complex **2** under argon atmosphere. First weight loss of 1.66% possibly is due to the loss of a water molecule. Then second weight losses of nearly 18-19% is due to loss of L-Me ligand donating the O-atom to Ni-core. The decomposition at 930 °C is not complete.

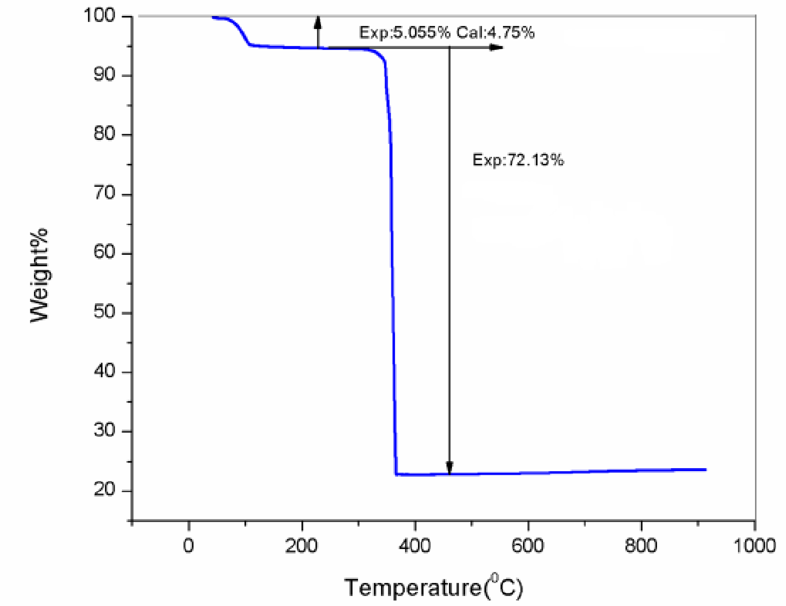

Figure S11. TGA of complex (**3**) in air. The first weight loss of 5.0 % at 50 °C is due to loss of two coordinated methanol ligands (shown in red color). The second weight loss of 72.13% above 360 °C is due to loss of all remaining organic ligand parts leading to the formation of final product as NiO.

3.5. IR Spectra of complexes 2-3

The IR spectrum of the complexes were recorded by preparing KBr pellet which covers the range of 400-4000 cm^{-1}. A small amount of sample was grinded with KBr until it becomes uniformly distributed and dried under sodium lamp for some time. The disc like pellet was prepared by using a pressed pellet sampling technique.

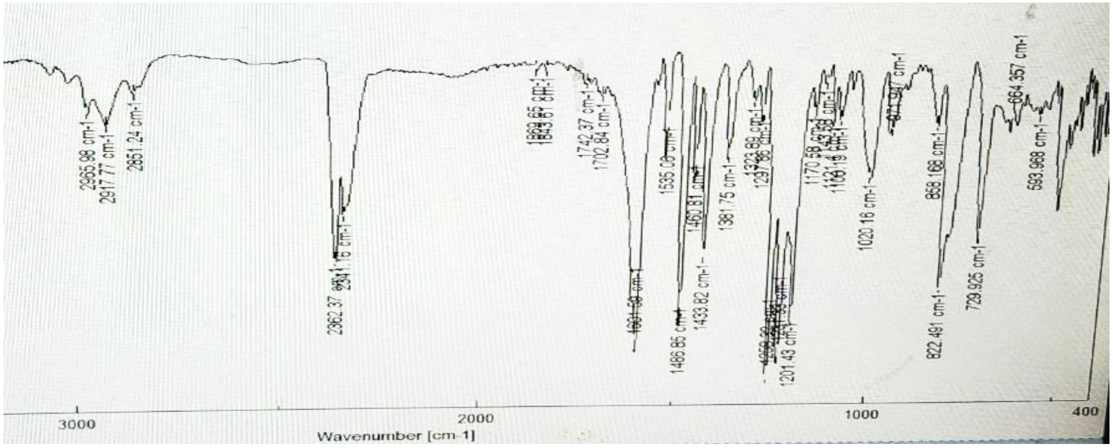

Figure S12. IR spectrum of **3**. The bands at 2367 and 2341 cm^{-1} are due to background.

2965, 2917, 2851, 1601, 1535, 1486, 1460, 1433, 1381, 1323, 1297, 1258, 1231, 1202, 1170, 1143, 1121, 1100, 1020, 971, 858, 822, 729, 668, 594 cm^{-1}.

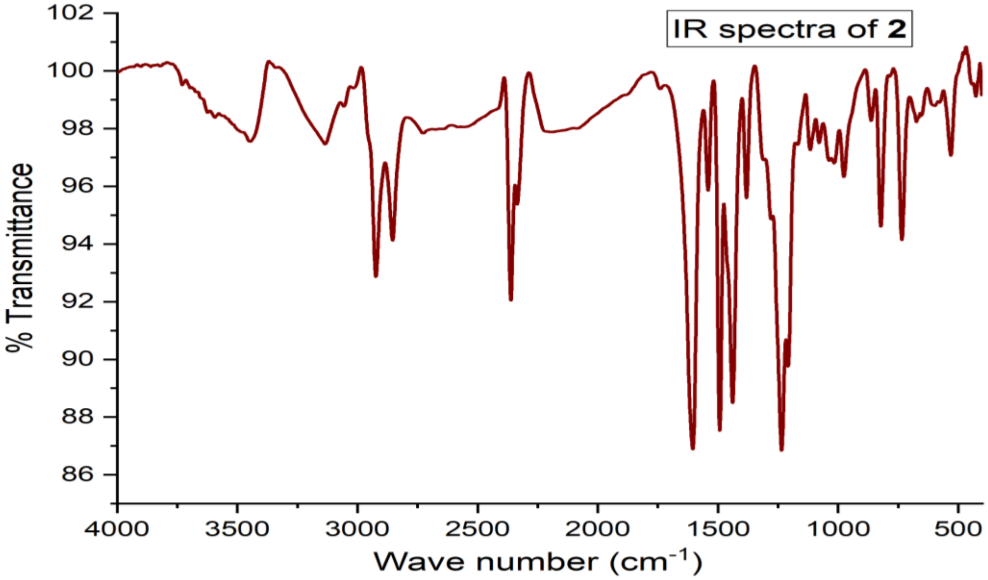

Figure S13. IR spectrum of complex **2**.

4. Computational details

All the geometry optimizations were performed in M06-2X/def2-SVPP. The single point energy calculations were performed on the optimized coordinates M06-2X/def2-SVPP. The NBO calculations and wavefunction generation were performed using the same level of theory and basis set.

4.1. Computational studies of various O-donor ligands

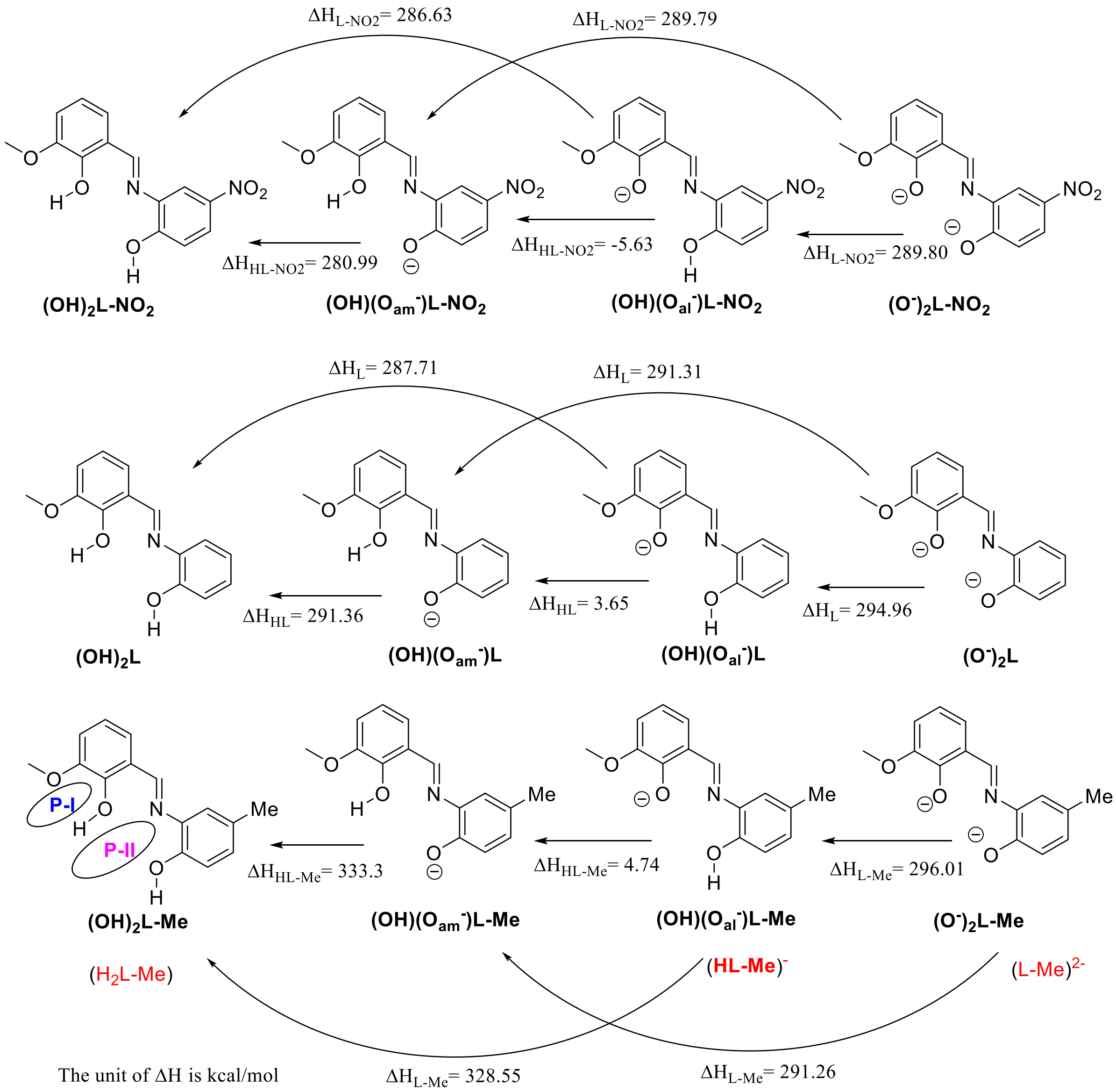

Figure S14. Calculated proton affinity values of mono- and d-anionic ligands $(HO)_2LR$ with different substitutions (R = NO_2, H, Me) at M06-2X/def2SVPP level of theory. For simplicity: $(OH)_2L$-Me = H_2L-Me, $(O^-)_2L$-Me = L-Me^{2-}, $(O^-)(OH)L$-Me = HL-Me$^-$.

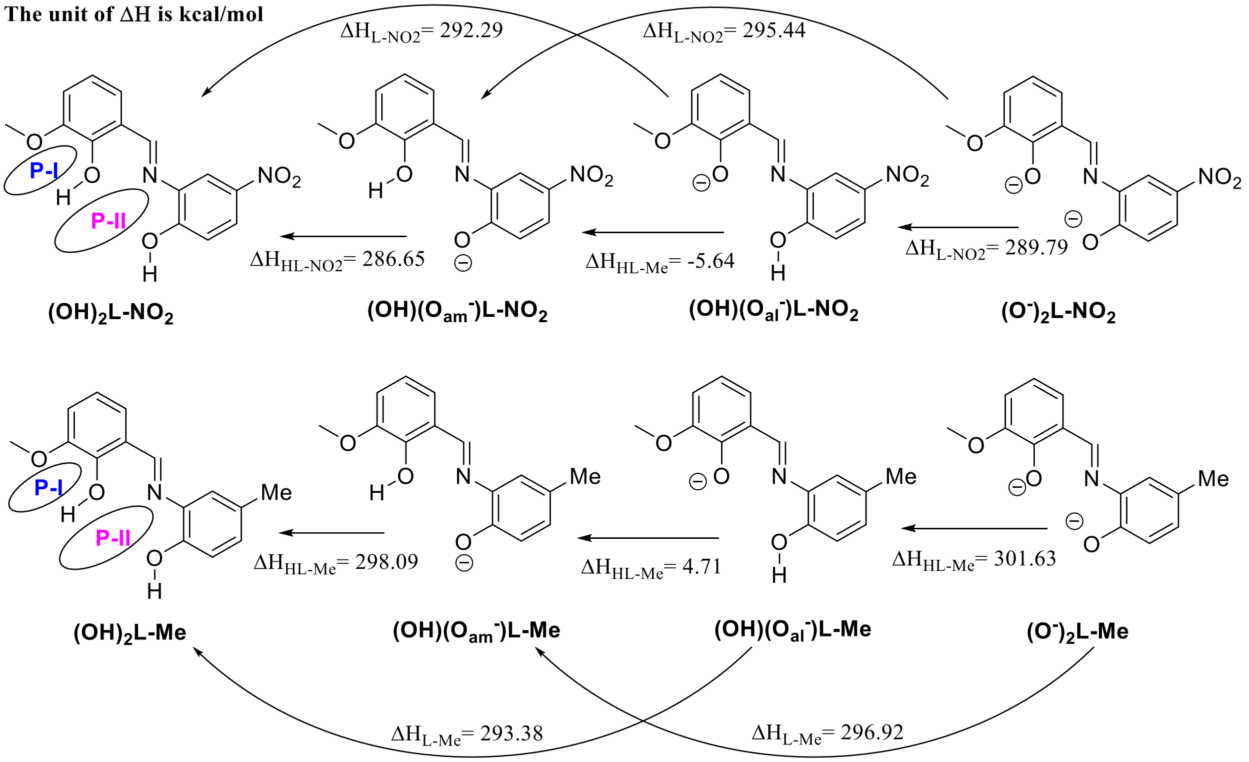

Figure S15. Calculated proton affinity values of mono- and di-anionic ligands $(HO)_2LR$ with different substitutions (R = NO_2, Me) at M06-2X/def2SVP.

The Tables S1-S3 show the natural charges, energy of HOMO and LUMO and electron density distribution on HOMO and LUMO. NBO calculations have been performed using M06-2X/def2SVPP level of theory. The natural charges on selected atoms are given in Table S1. When $O_{aldehyde}$ (O_{al}) is deprotonated, the negative charge on the O-atom increases, from -0.721 to -0.839. There is also significant change in the $C_{aldehyde}$ (C_{al}) also. There is an increase observed from 0.350 to 0.414. The HOMO of anion is significantly raised when compared to the neutral ligand. This implies that the ability for coordination to Ni(II) ions increased when the ligand undergoes deprotonation. The HOMO of the neutral ligand is majorly located on the imine bond and also on the phenyl rings. There are also minor contributions located on the oxygen atoms of the alcohol group. After deprotonation, electron density is majorly located on the deprotonated oxygen atom and on the phenyl-ring bonded to it.

When the deprotonation was O$_{am}$, similar observations were observed. The natural charge on the deprotonated O increased considerably negatively. The charge on carbon bonded to the O also increased slightly. The charge on the imine C and N is also deviated because on the resonance of the ring. The coordination ability is increased compared to the neutral ligand. The HOMO majorly constitutes the lone pair on the deprotonated O$_{phenol}$ and the electron density on the phenyl ring. The LUMO of the both the mono-deprotonated structures are similar.

When both the alcohols are deprotonated, the overall electron density has increased. The charges on both the O-atoms increased considerably, so do the charges of carbon atoms bonded to them. When it is compared to the neutral and mono-anions ligands, the HOMO of the di-anion ligand is more destabilized. This indicates that the di-anion has the most binding ability. The HOMO contributes to the electron density over deprotonated O-atoms, phenyl rings and also the imine bond. The LUMO of all the ligands were observed similar.

Table S1. Natural charges on selected atoms of the ligands.

	(OH)$_2$L-Me	**(O$_{al}^{-}$)(OH)L-Me^{-}**	**(O$_{am}^{-}$)(OH)L-Me^{-}**	**(O^{-})$_2$L-Me^{2-}**
O(al)	-0.721	-0.839	-0.726	-0.855
C(al)	0.350	0.414	0.335	0.401
C(im)	0.156	0.155	0.105	0.126
N(im)	-0.518	-0.575	-0.506	-0.555
C(am)	0.339	0.330	0.395	0.381
O(am)	-0.720	-0.724	-0.870	-0.888

Table S2. Energies of HOMOs and LUMOs of the ligands **(OH)$_2$L-Me**, **(O$_{al}^-$)(OH)L-Me$^-$**, **(O$_{am}^-$)(OH)L-Me$^-$**, **(O$^-$)$_2$L-Me^{2-}**.

	(OH)$_2$L-Me	**(O$_{al}^-$)(OH)L-Me$^-$**	**(O$_{am}^-$)(OH)L-Me$^-$**	**(O$^-$)$_2$L-Me^{2-}**
HOMO	-7.04 eV	-5.77 eV	-5.52 eV	-5.20 eV
LUMO	-0.79 eV	-0.23 eV	-0.46 eV	0.14 eV

Table S3. HOMOs and LUMOs of the ligands **(OH)$_2$L-Me**, **(O$_{al}^-$)(OH)L-Me$^-$**, **(O$_{am}^-$)(OH)L-Me$^-$**, **(O$^-$)$_2$L-Me^{2-}**.

Ligand	**HOMO**	**LUMO**
(OH)$_2$L-Me	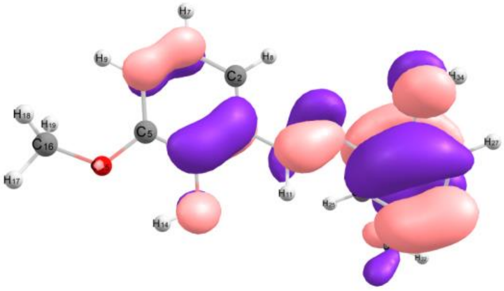	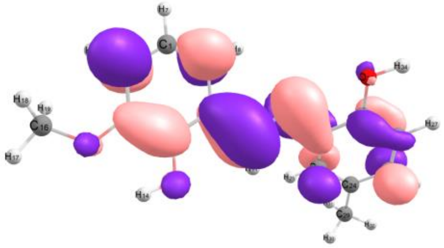
(O$_{al}^-$)(OH)L-Me$^-$	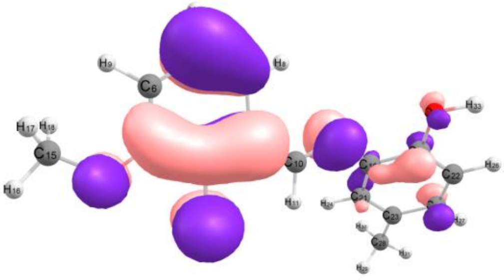	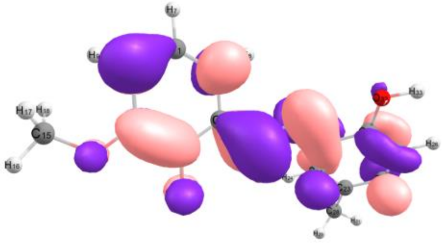
(O$_{am}^-$) (OH)L-Me$^-$	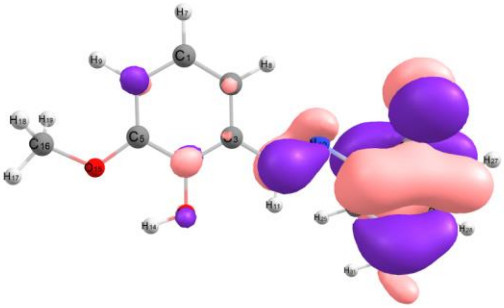	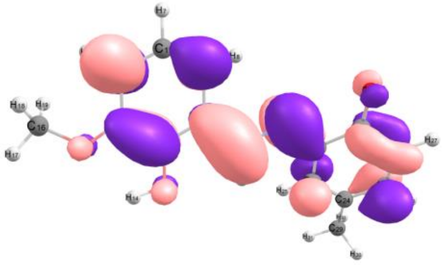

$(O^-)_2L\text{-}Me^{2-}$

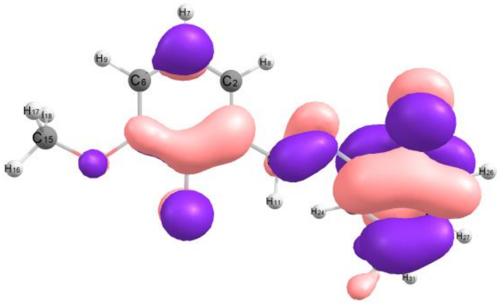

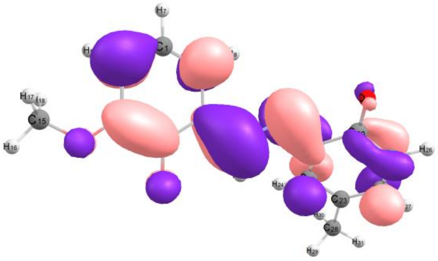

AIM analysis of the ligands:

QTAIM is a great tool now to analyze the topology and structural features of a molecule. A critical point can be defined as a point in space where the first derivative of electron density (ED) vanishes. Considering the second derivative one can differentiate between local minima and a local maximum. Bond path is defined as a single line of maximum electron density between two nuclei. A bond can indicate all kind of chemical interaction which can be either weak or strong. Bond critical point (BCP) is the point on the bond path with lowest value of electron density. Intersection of bond path and zero flux density surface is at the BCP.

Topological analysis has been carried out to analyze the electron density **(ρ_r)** of all the neutral and anionic ligands using Bader's quantum theory of atoms in molecules.[S6] The atoms bonded together are joined by a line called bond path.[S7] The bond critical point BCP (3,-1) along the bond path represents the point where electron density reaches minimum. The nature of bond is provided by the magnitude of electron density $\boldsymbol{\rho_r}$ and Laplacian of electron density $\boldsymbol{\nabla^2\rho_r}$ at BCP.[S8]

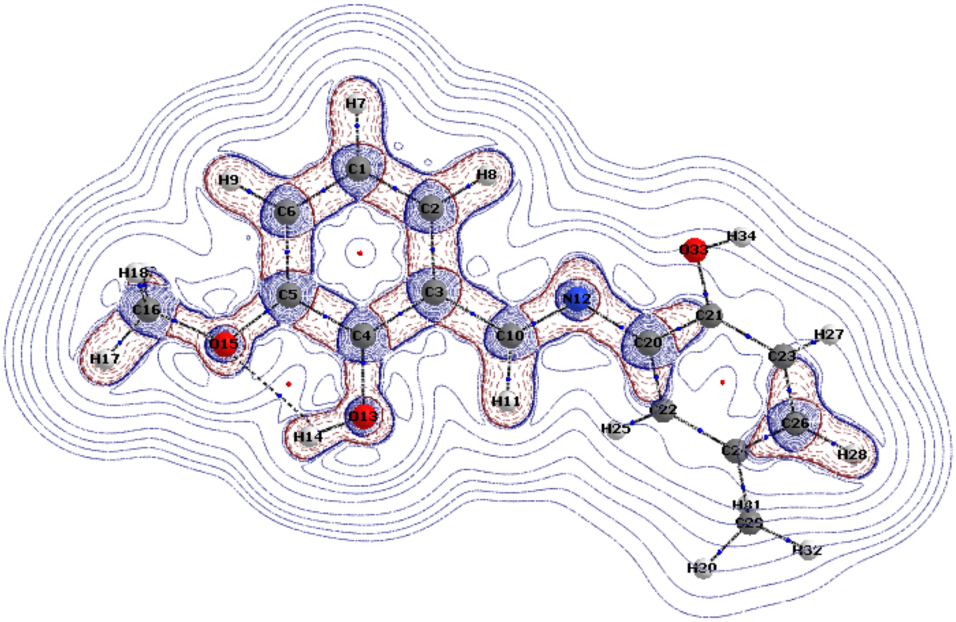

Figure S16. Contour plot of Laplacian distribution [$\nabla^2\boldsymbol{\rho}$ (r)] in the C3-C4-O13 plane of **neutral (OH)$_2$L-Me** ligand. Solid blue lines indicate the areas of charge concentration ($\nabla^2\boldsymbol{\rho}$ (r) < 0) while dotted purple lines denotes charge depletion ($\nabla^2\boldsymbol{\rho}$ (r) > 0). Solid black lines connecting atomic nuclei are the bond paths.

Table S4. Electron density (ρ), Laplacian and bond ellipticity (ε) of neutral (OH)$_2$L-Me ligand.

Bond	$\boldsymbol{\rho}$	$\boldsymbol{\nabla^2\rho}$	**ε**
C4-O13	0.290	-0.211	0.011
C10 - N12	+0.375	-0.633	+0.175
C21 - O33	+0.284	-0.215	+0.021

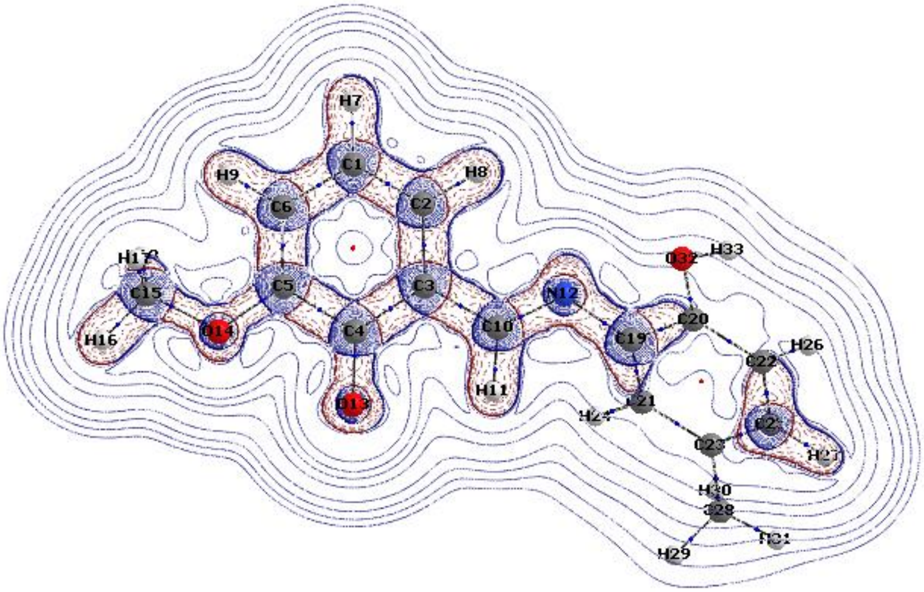

Figure S17. Contour plot of Laplacian distribution [$\nabla^2\boldsymbol{\rho}$ (r)] in the C3-C4-O13 plane of monoanionic **(O_{al}^{-})(OH)L-Me** ligand. Solid blue lines indicate the areas of charge concentration ($\nabla^2\boldsymbol{\rho}$ (r) < 0) while dotted purple lines denotes charge depletion ($\nabla^2\boldsymbol{\rho}$ (r) > 0). Solid lines connecting atomic nuclei (black) are the bond paths.

Table S5. Electron density (ρ), Laplacian and bond ellipticity (ε) of (O_{al}^{-})(OH)L-Me⁻ ligand.

Bond	ρ	$\nabla^2\rho$	ε
C4 - O13	+0.361	-0.070	+0.004
C10 - N12	+0.367	-0.701	+0.134
C20 - O32	+0.283	-0.213	+0.017

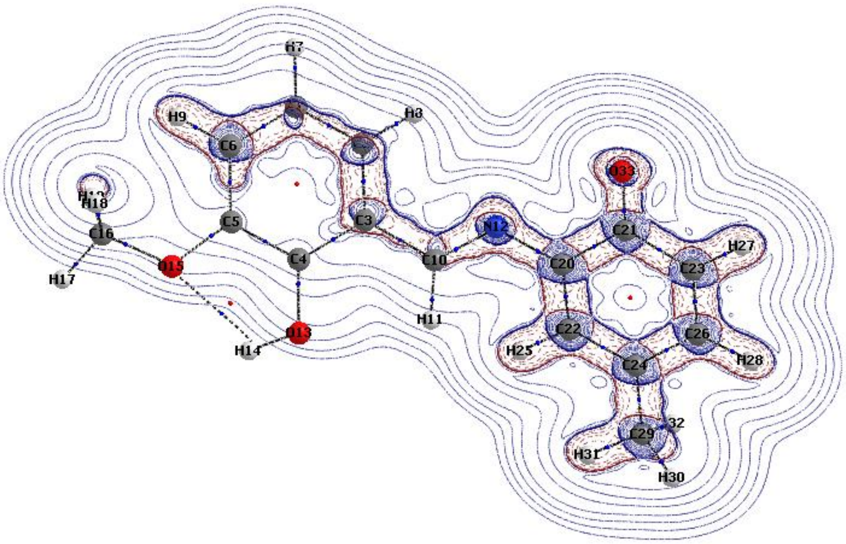

Figure S18. Contour plot of Laplacian distribution [$\nabla^2\boldsymbol{\rho}$ (r)] in the O33-C21-C20 plane of monoanionic **(O_{am}^{-})(OH)L-Me** ligand. Solid blue lines indicate the areas of charge concentration ($\nabla^2\boldsymbol{\rho}$ (r) < 0) while dotted purple lines denotes charge depletion ($\nabla^2\boldsymbol{\rho}$ (r) > 0). Solid lines connecting atomic nuclei (black) are the bond paths.

Table S6. Electron density (ρ), Laplacian and bond ellipticity (ε) of (O_{am}^{-})(OH)L-Me ligand.

Bond	ρ	$\nabla^2\rho$	ε
C4 - O13	+0.287	-0.214	+0.005
C10 - N12	+0.374	-0.622	+0.215
C21 - O33	+0.355	-0.132	+0.008

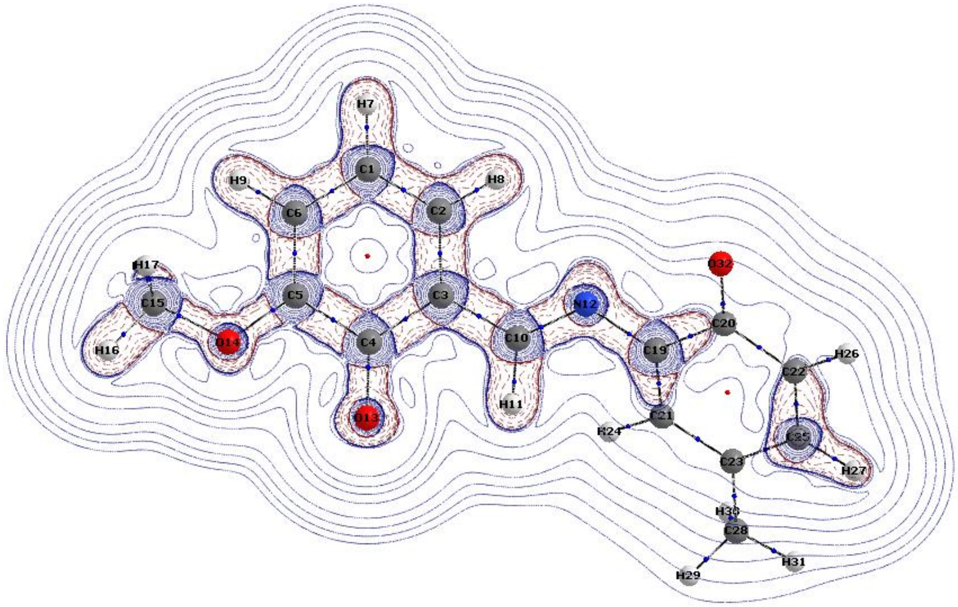

Figure S19. Contour plot of Laplacian distribution [$\nabla^2\boldsymbol{\rho}$ (r)] in the C3-C4-O13 plane of dianionic **$(O^{-})_2$L-Me** ligand. Solid blue lines indicate the areas of charge concentration ($\nabla^2\boldsymbol{\rho}$ (r) < 0) while dotted purple lines denotes charge depletion ($\nabla^2\boldsymbol{\rho}$ (r) > 0). Solid lines connecting atomic nuclei (black) are the bond paths.

Table S7. Electron density (ρ), Laplacian and bond ellipticity (ε) of $(O^{-})_2$L-Me ligand.

Bond	$\boldsymbol{\rho}$	$\boldsymbol{\nabla^2\rho}$	**ε**
C4 - O13	+0.357383	-0.105771	+0.004063
C10 - N12	+0.369904	-0.673917	+0.167942
C20 - O32	+0.351973	-0.164598	+0.006386

Tables S8-S10 show the natural charges, the energy of HOMO and LUMO and electron density distribution on HOMO and LUMO. NBO calculations were performed using M06-2X/def2SVPP level of theory and basis set. The natural charges on selected atoms are given in Table S8. When O_{al} is deprotonated, the negative charge on the O-atom increases, from -0.719 to -0.829. There is also a significant change in the $C_{aldehyde}$. There is an increase observed from 0.355 to 0.421. The charge on C_{im} decreased from 0.169 to 0.158. The negative charge on N_{imine} is also increased considerably from -0.522 to -0.582. There are no considerable changes observed on the aminophenol part of the Schiff's base ligand.

The HOMO of the anion is significantly raised from -7.34 eV to -5.84 eV when compared to the neutral ligand. This implies that the binding ability of the ligand increased when the ligand undergoes deprotonation. The HOMO of the neutral ligand is majorly located on the imine bond and also on the phenyl rings. There are also minor contributions located on the oxygen atoms of the alcohol group. After deprotonation, the electron density is majorly located on the deprotonated oxygen atom and the phenyl ring associated with it.

When the deprotonation site is changed from $O_{aldehyde}$ (O_{al}) to $O_{aminophenol}$ (O_{am}) similar changes are observed. When the natural charges on the aldehyde part remained almost the same, significant changes are noted in the amine part of the Schiff base. The charge on the C_{am} is increased from 0.394 to 0.456. The negative charge on O_{am} is also increased negatively from 0.695 to -0.774. The energy of the HOMO is lesser than $HL\text{-}NO_2^-$ (O_{al}^-) implies that the nucleophilic character is decreased for $HL\text{-}NO_2$ (O_{am}^-). However, the energy of the LUMO is lesser for this ligand. The HOMO is majorly concentrated on the phenyl ring associated with the deprotonated oxygen atom. The imine bond also contributes slightly to the HOMO. There is a slight extension of electron density to the other aldehyde phenyl ring in LUMO. This was not observed in the neutral, other mono-anion, and the di-anion ligand.

When both the alcoholic hydrogens are deprotonated, the natural charge all over the molecule has changed. The electron densities all over the molecule have increased. The charges on both the O-atoms have increases negatively. An increase in the charge on the C-atoms attached to it also noted. The energy of HOMO is the highest for the dianion ligand. In other words, we can say that the nucleophilic character is more for this ligand. The energy of LUMO is lowest for the di-anion. The HOMO constitutes the lone pair on the oxygen atoms, imine bond, and the electron delocalization over the phenyl rings.

Table S8: Natural charges on selected atoms for different forms of ligand **$(OH)_2L\text{-}NO_2$**: **$(OH)_2L\text{-}NO_2$, $(OH)_2L\text{-}NO_2$, $(O_{am}^-)(OH)L\text{-}NO_2^-$, $(O^-)_2L\text{-}NO_2^{2-}$**.

	$(OH)_2L\text{-}NO_2$	**$(O_{al}^-)(OH)L\text{-}NO_2^-$**	**$(O_{am}^-)(OH)L\text{-}NO_2^-$**	**$(O^-)_2L\text{-}NO_2^{2-}$**
O(al)	-0.719	-0.829	-0.722	-0.845
C(al)	0.355	0.421	0.345	0.409
C(im)	0.169	0.165	0.138	0.144
N(im)	-0.522	-0.582	-0.511	-0.565
C(am)	0.394	0.386	0.456	0.453
O(am)	-0.695	-0.699	-0.773	-0.779

Table S9: HOMO and LUMO energies of **$(OH)_2L\text{-}NO_2$, $(OH)_2L\text{-}NO_2$, $(O_{am}^{-})(OH)L\text{-}NO_2^{-}$, $(O^{-})_2L\text{-}NO_2^{2-}$**.

	$(OH)_2L\text{-}NO_2$	**$(O_{al}^{-})(OH)L\text{-}NO_2^{-}$**	**$(O_{am}^{-})(OH)L\text{-}NO_2^{-}$**	**$(O^{-})_2L\text{-}NO_2^{2-}$**
HOMO	-7.34 eV	-5.84 eV	-6.26 eV	-5.58 eV
LUMO	-1.36 eV	-1.24 eV	-0.88 eV	-0.72 eV

Table S10: HOMOs and LUMOs of the ligands **$(OH)_2L\text{-}NO_2$, $(OH)_2L\text{-}NO_2$, $(O_{am}^{-})(OH)L\text{-}NO_2^{-}$, $(O^{-})_2L\text{-}NO_2^{2-}$**.

Ligand	HOMO	LUMO
$(OH)_2L\text{-}NO_2$	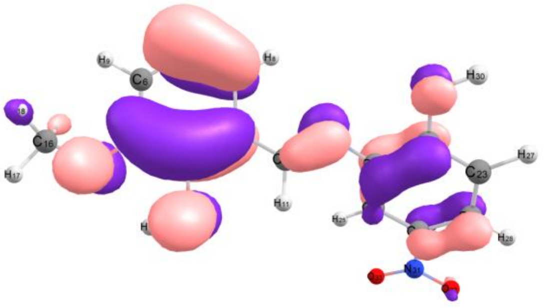	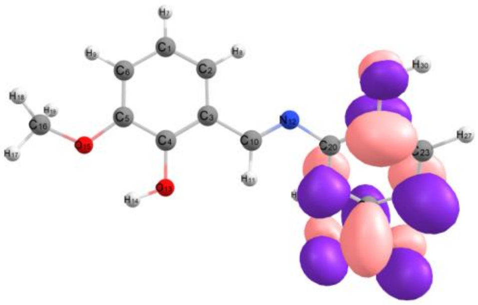
$(O_{al}^{-})(OH)L\text{-}NO^{2-}$	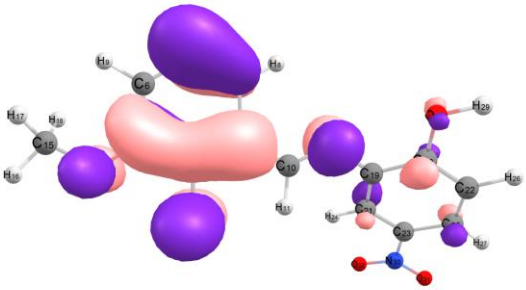	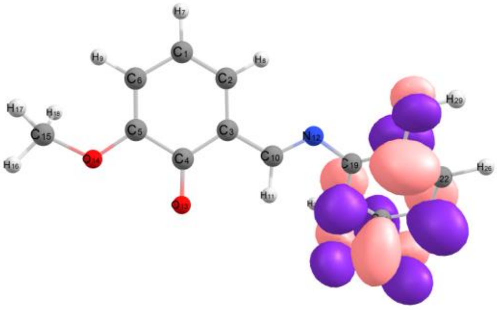
$(O_{am}^{-})(OH)L\text{-}NO^{2-}$	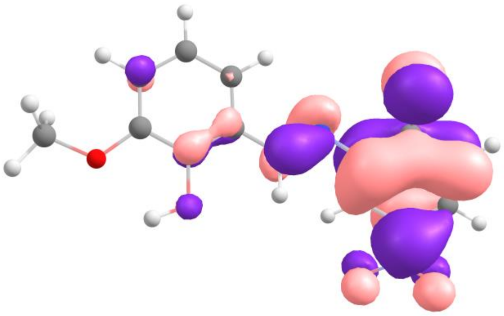	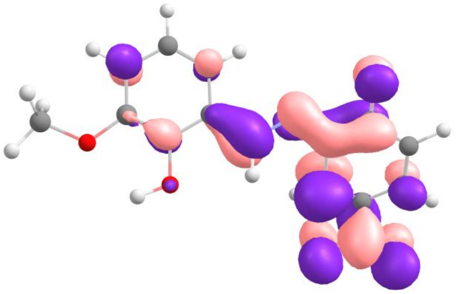

$(O^{-})_2L$-NO_2^{2-}	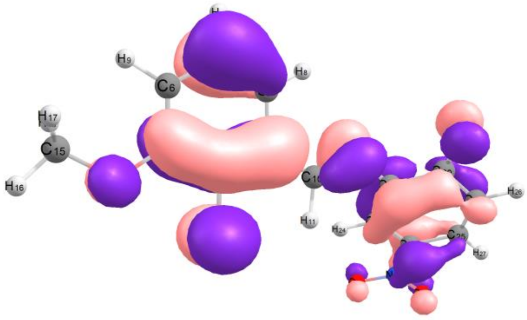	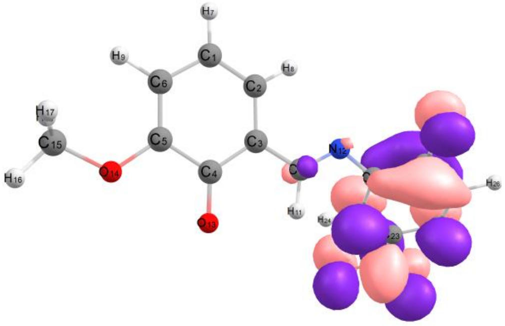

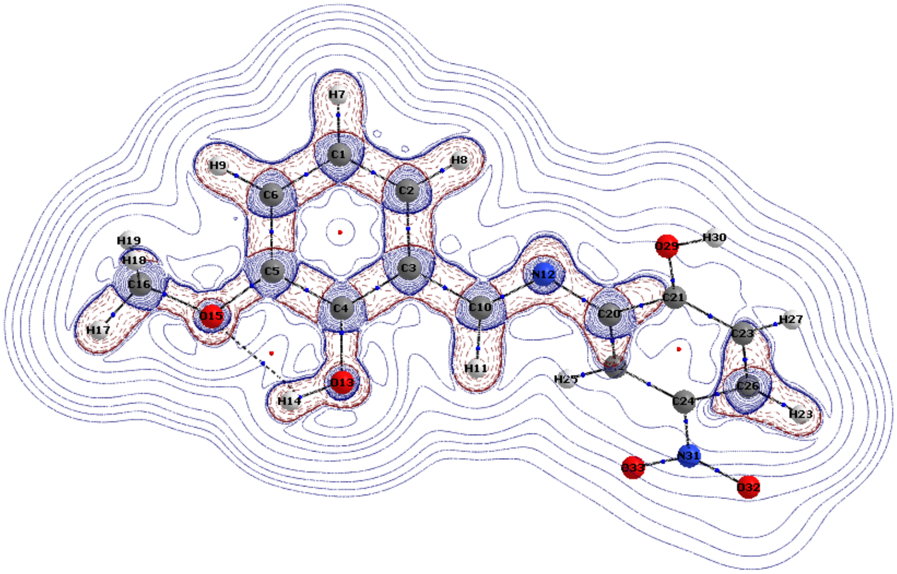

Figure S20. Contour plot of Laplacian distribution [$\nabla^2\boldsymbol{\rho}$ (r)] in the C3-C4-O13 plane of neutral **H_2L-NO_2** ligand. Solid blue lines indicate the areas of charge concentration ($\nabla^2\boldsymbol{\rho}$ (r) < 0) while dotted purple lines denotes charge depletion ($\nabla^2\boldsymbol{\rho}$ (r) > 0). Solid lines connecting atomic nuclei (black) are the bond paths.

Table S11. Electron density (*ρ*), Laplacian and bond ellipticity (ε) of neutral $(OH)_2L$-NO_2 ligand.

Bond	ρ	$\nabla^2\rho$	ε
C4 - O13	+0.291	-0.208	+0.012
C10 - N12	+0.374	-0.635	+0.162
C21 - O29	+0.298	-0.183	+0.036

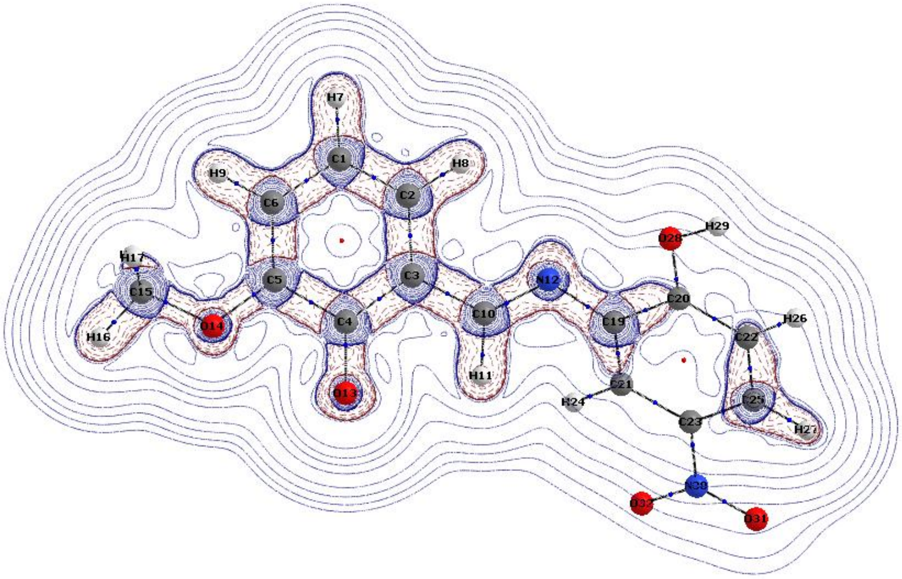

Figure S21. Contour plot of Laplacian distribution [$\nabla^2\boldsymbol{\rho}$ (r)] in the C3-C4-O13 plane of monoanioninc **HL-NO$_2$(O$_{al}^{-}$)** ligand. Solid blue lines indicate the areas of charge concentration ($\nabla^2\boldsymbol{\rho}$ (r) < 0) while dotted purple lines denotes charge depletion ($\nabla^2\boldsymbol{\rho}$ (r) > 0). Solid lines connecting atomic nuclei (black) are the bond paths.

Table S12. Electron density (ρ), Laplacian and bond ellipticity (ε) of neutral (O$_{al}^{-}$)(OH)L-NO$_2$ ligand.

Bond	$\boldsymbol{\rho}$	$\boldsymbol{\nabla^2\rho}$	**ε**
C4 - O13	+0.362	-0.049	+0.005
C10 - N12	+0.365	-0.717	+0.119
C20 - O28	+0.295	-0.180	+0.035

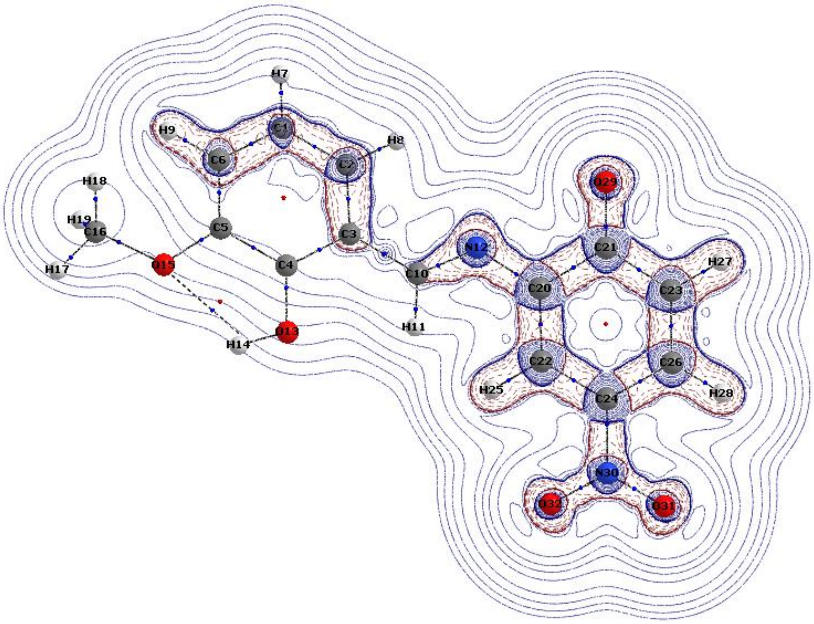

Figure S22. Contour plot of Laplacian distribution [$\nabla^2\boldsymbol{\rho}$ (r)] in the C20-C21-O29 plane of monoanionic **HL-NO$_2$(O$_{am}^-$)** ligand. Solid blue lines indicate the areas of charge concentration ($\nabla^2\boldsymbol{\rho}$ (r) $<$ 0) while dotted purple lines denotes charge depletion ($\nabla^2\boldsymbol{\rho}$ (r) $>$ 0). Solid lines connecting atomic nuclei (black) are the bond paths.

Table S13. Electron density (ρ), Laplacian and bond ellipticity (ε) of neutral (O$_{am}^-$)(OH)L-NO$_2$ ligand.

Bond	ρ	$\nabla^2\boldsymbol{\rho}$	ε
C4 - O13	+0.289	-0.211	+0.009
C10 - N12	+0.375	-0.624	+0.190
C21 - O29	+0.372	+0.077	+0.012

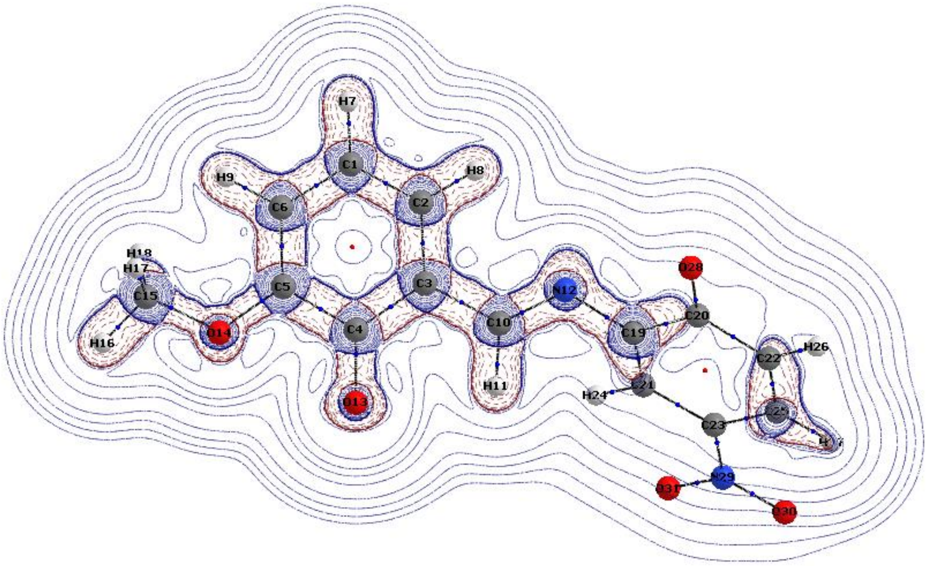

Figure S23. Contour plot of Laplacian distribution [$\nabla^2\boldsymbol{\rho}$ (r)] in the C3-C4-O13 plane of dianionic **$(O^-)_2$L-NO_2** ligand. Solid blue lines indicate the areas of charge concentration ($\nabla^2\boldsymbol{\rho}$ (r) < 0) while dotted purple lines denotes charge depletion ($\nabla^2\boldsymbol{\rho}$ (r) > 0). Solid lines connecting atomic nuclei (black) are the bond paths.

Table S14. Electron density (ρ), Laplacian and bond ellipticity (ε) of $(O^-)_2$L-NO_2 ligand.

Bond	$\boldsymbol{\rho}$	$\boldsymbol{\nabla^2\rho}$	**ε**
C4 - O13	+0.359	-0.083	+0.005
C10 - N12	+0.368	-0.684	+0.148
C21 - O29	+0.371	+0.072	+0.010

The computed Molecular Electrostatic Potential (MEP) maps of neutral $(OH)_2$L-Me and the corresponding mono- and di-anionic ligands showing different electronic environment across the O_2 (P-I) and O_2N (P-II) pockets.

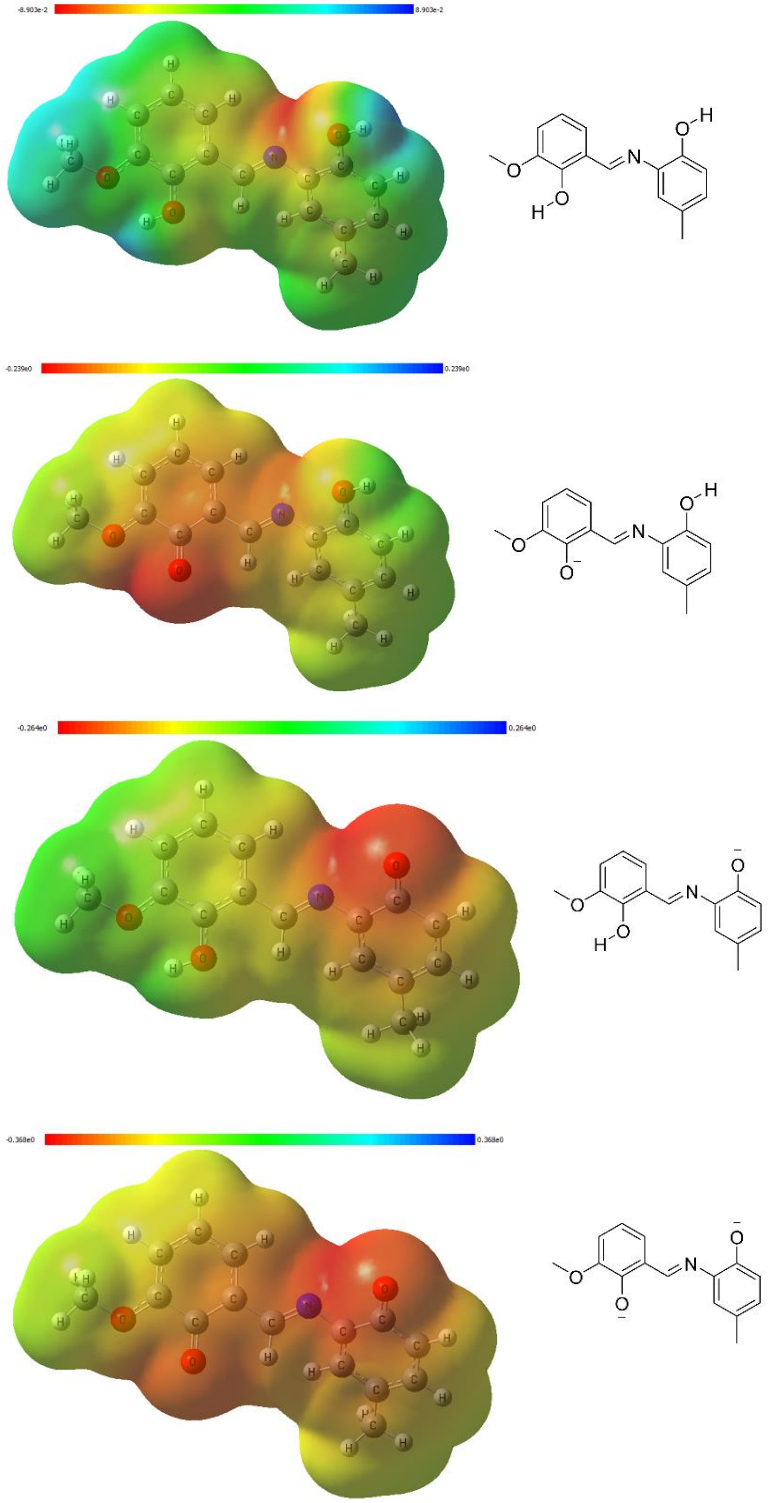

Figure S24. MEP plots (computed at iso-density surface value of 0.0004 a.u) of neutral, mono- and di-deprotonated $(OH)_2$L-Me ligand.

The computed Molecular Electrostatic Potential (MEP) maps of neutral $(OH)_2L\text{-}NO_2$ and the corresponding mono- and di-anionic ligands showing different electronic environment across the O_2 (P-I) and O_2N (P-II) pockets.

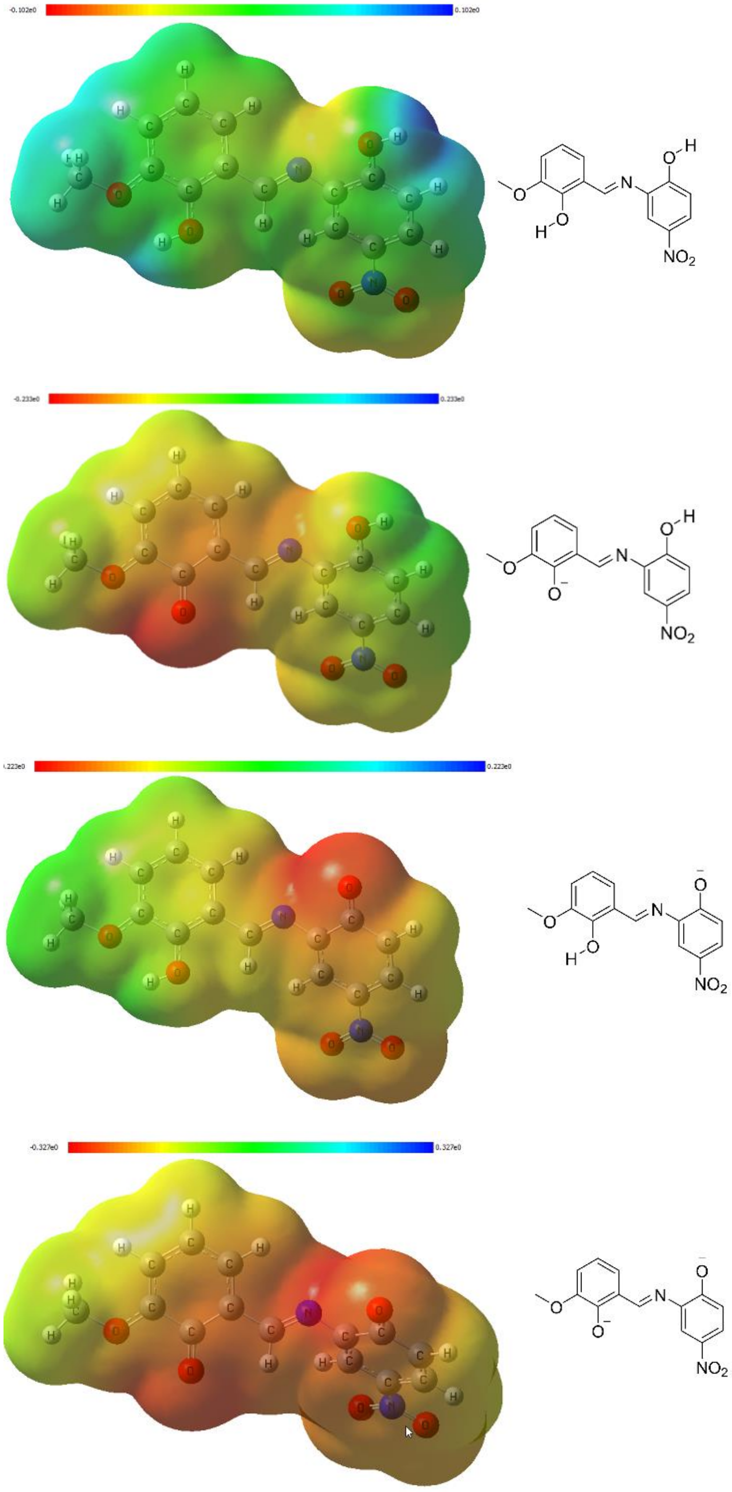

Figure S25. MEP plots (computed at iso-density surface value of 0.0004 a.u) of neutral, mono- and di-deprotonated of $(OH)_2L\text{-}NO_2$ ligand.

The computed Molecular Electrostatic Potential (MEP) maps of neutral (OH)$_2$L-H and corresponding mono- and di-anionic ligands showing different electronic environment across the O$_2$ (P-I) and O$_2$N (P-II) pockets.

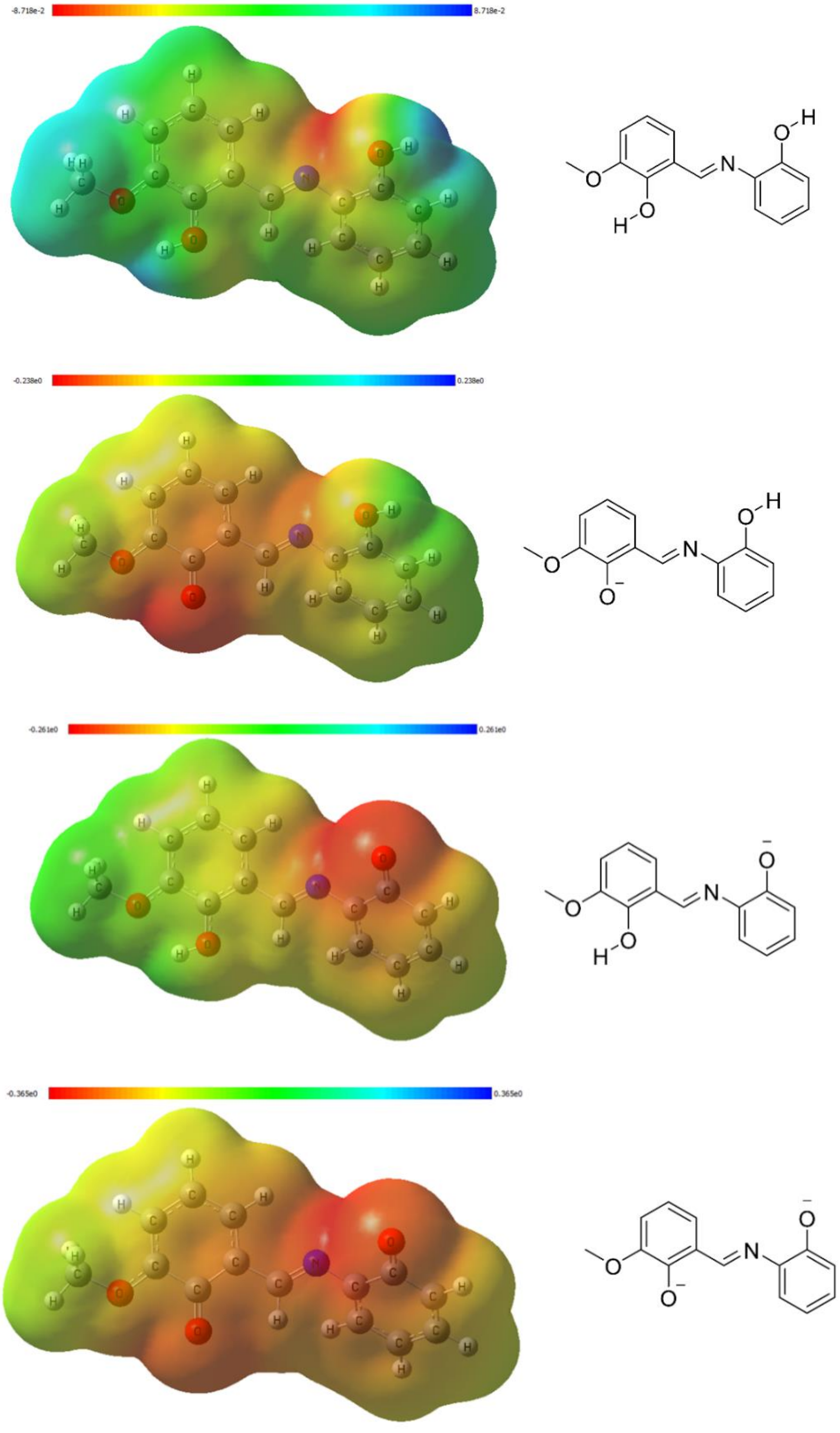

Figure S26. MEP plots (computed at iso-density surface value of 0.0004 a.u) of neutral, mono- and di-deprotonated of (OH)$_2$L-H ligand.

5. X-ray single crystal diffraction of complexes 1-2.

Single-crystal data were collected on a Bruker Axs Kappa Apex2 CCD diffractometer,[S9] with graphite-monochromated Mo-K_α (λ = 0.71073 Å) radiation at 200 K. The data was integrated using SAINT PLUS[S10] and absorption correction was done using multi-scan absorption correction method (SADABS).[S11] The structure was solved by direct method (SHELXS-97) and refined using SHELXL-2018/3 program and WinGX v1.70.01[S12-14] programs packages. All non-hydrogen atoms were refined anisotropically.

The single crystals of **1-2** have been grown from MeOH solvent. The single crystal suitable for diffraction was only grown from DMF solution by dissolving complex **3** in it. The single crystals of **3** which have been grown from MeOH solvent do not sufficiently diffracted by X-ray. The single crystal of **3** cracked when diffracted by X-ray (during collection of full data). The structure has been shown for connectivity only.

The immersion oil was purchased from Sigma Aldrich. The crystals were picked up with spatula and placed into degassed immersion oil on a glass plate and mounted under argon flow. The X-ray single crystal data were collected in SAIF, IIT Madras using APEX2 X-ray diffractometer having molybdenum X-ray source. The average data collection time was 7 h for a single crystal under flow of argon gas at room temperature or at 200 K.

Table S15. Crystallographic data for **1** and **2.**

Compound	**$[Ni_4((O_{al}^-)_2L\text{-}Me)_2((O_{al}^-)(OH)L\text{-}Me)_2Cl_2(MeOH(MeCN)]\cdot 2MeOH$ (1)**	**$[Ni_4((O^-)_2L\text{-}Me)_3((O_{al}^-)(OH)L\text{-}Me)Cl]$ (2)**	**$[Ni_4((O^-)_2L\text{-}Me)_4(H_2O)_2]$ (3·2DMF)**
Empirical formula	$C_{64}H_{58}Cl_2N_5Ni_4O_{14}$	$C_{60}H_{53}ClN_4Ni_4O_{12}$	
CCDC no.	2006271	2006270	
Molecular weight	1426.89	1292.35	
Mo K_α radiation	λ = 0.71076 Å		
Crystal size [mm^3]	0.09 × 0.08 × 0.06	0.12 × 0.10 × 0.08	
Crystal system	Triclinic,	Monoclinic	
Space group	P-1	$P2_1/c$	
a [Å]	14.070(7)	16.831(2)	15.59 (2)
b [Å]	14.216(8)	23.697(5),	17.26 (2)

c [Å]	19.039(11)	14.715(3)	18.02 (3)
α [°]	76.64(3)	90	75.11 (4)
β [°]	68.85(2)	92.577(8)	88.71 (4)
γ [°]	63.449(18)	90	67.08 (4)
V [Å^3]	3166(3)	5863.1 (2)	4300 (10)
Z	2	4	
Temperature [K]	200(2)	200(2)	
ρ [Mgm^{-3}]	1.497	1.464	
μ [mm^{-1}]	1.32	1.38	
F (000)	1470	2664	
θ-area [°]	3.2–26.4	1.63 to 25.206	
Total number of reflections	118920	35932	
Unique reflections	12969	10269	
R_{int}	0.101	0.155	
Number of restraints	0	0	
Parameters	802	738	
$R1$ [$I>2\sigma(I)$]	0.0559	0.0630	
$wR2$ [$I>2\sigma(I)$]	0.1540	0.1295	
$R1$ [all data]	0.0941	0.1593	
$wR2$ [all data]	0.1842	0.1622	
GooF	1.06	0.932	
Extinction coefficient	n/a	n/a	
Largest diff. peak / hole			
max. / min. [e · Å^{-3}]	1.65 / −0.46	0.67 / −0.69	

Table S16. Selected bond lengths (Å) angles (°) around Ni-centers of complexes **1** and **2**.

Complex 1	**Complex 1**	**Complex 2**	**Complex 2**
N1—Ni4	2.007 (4)	Ni1—O12	1.955 (5)
N2—Ni2	2.003 (4)	Ni1—O6	1.987 (4)
N3—Ni1	2.011 (4)	Ni1—O4	1.989 (5)
N4—Ni3	2.081 (4)	Ni1—N4	2.035 (6)
N5—Ni3	1.996 (4)	Ni1—O5	2.252 (5)
O2—Ni1	1.997 (4)	Ni2—O1	1.986 (4)

O3—Ni1	2.032 (4)	Ni2—N2	1.990 (6)
O4—Ni4	2.026 (3)	Ni2—O8	2.034 (5)
O5—Ni4	1.977 (3)	Ni2—O4	2.042 (4)
O6—Ni4	2.172 (4)	Ni2—N1	2.088 (6)
O7—Ni3	1.962 (3)	Ni2—O5	2.176 (5)
O7—Ni4	2.014 (3)	Ni3—N3	1.991 (6)
O8—Ni3	2.041 (3)	Ni3—O1	2.007 (5)
O9—Ni2	2.013 (3)	Ni3—O7	2.051 (5)
O10—Ni2	1.965 (3)	Ni3—O5	2.073 (4)
O10—Ni1	2.007 (3)	Ni3—O6	2.084 (5)
O11—Ni1	2.250 (4)	Ni3—O2	2.200 (5)
O14—Ni2	2.101 (4)	Ni4—O7	1.982 (5)
Ni1—Cl1	2.5267 (16)	Ni4—O8	2.025 (4)
Ni2—Cl1	2.4088 (16)	Ni4—Cl1	2.188 (2)
Ni2—Cl2	2.609 (2)	Ni4—O9	2.220 (5)
Ni3—Cl2	2.4035 (18)	Ni4—O10	2.388 (5)
Ni3—Cl1	2.7037 (18)		
Ni4—Cl2	2.5416 (18)		
Ni3—O7—Ni4	108.66 (15)	Ni2—O1—Ni3	106.5 (2)
Ni2—O10—Ni1	109.33 (15)	Ni1—O4—Ni2	102.0 (2)
Ni2—Cl1—Ni1	82.05 (6)	Ni3—O5—Ni2	97.7 (2)
Ni2—Cl1—Ni3	85.32 (6)	Ni3—O5—Ni1	93.44 (18)
Ni1—Cl1—Ni3	133.19 (6)	Ni2—O5—Ni1	90.08 (17)
Ni3—Cl2—Ni4	81.50 (5)	Ni1—O6—Ni3	101.4 (2)
Ni3—Cl2—Ni2	87.55 (6)	Ni4—O7—Ni3	112.6 (2)
Ni4—Cl2—Ni2	135.02 (6)	Ni4—O8—Ni2	111.0 (2)

Table S17. Selected bond angles (°) around Ni-centers of complex **1**.

O2—Ni1—O10	91.10 (14)
O2—Ni1—N3	91.37 (15)
O10—Ni1—N3	177.53 (16)
O2—Ni1—O3	171.45 (13)
O10—Ni1—O3	96.18 (14)
N3—Ni1—O3	81.37 (15)
O2—Ni1—O11	91.02 (14)
O10—Ni1—O11	74.66 (13)
N3—Ni1—O11	105.33 (14)
O3—Ni1—O11	86.60 (14)
O2—Ni1—Cl1	92.57 (11)
O10—Ni1—Cl1	80.72 (10)
N3—Ni1—Cl1	99.13 (12)
O3—Ni1—Cl1	93.02 (11)
O11—Ni1—Cl1	155.18 (9)
O10—Ni2—N2	93.05 (15)
O10—Ni2—O9	174.78 (14)
N2—Ni2—O9	83.49 (15)
O10—Ni2—O14	86.90 (14)
N2—Ni2—O14	95.89 (16)
O9—Ni2—O14	89.56 (14)
O10—Ni2—Cl1	84.62 (10)
N2—Ni2—Cl1	171.93 (13)
O9—Ni2—Cl1	99.33 (10)
O14—Ni2—Cl1	91.71 (11)
O10—Ni2—Cl2	96.11 (11)

N2—Ni2—Cl2	85.06 (13)
O9—Ni2—Cl2	87.50 (11)
O14—Ni2—Cl2	176.80 (10)
Cl1—Ni2—Cl2	87.50 (6)
O7—Ni3—N5	91.65 (15)
O7—Ni3—O8	173.41 (13)
N5—Ni3—O8	81.78 (15)
O7—Ni3—N4	90.43 (16)
N5—Ni3—N4	93.35 (16)
O8—Ni3—N4	89.44 (16)
O7—Ni3—Cl2	85.60 (10)
N5—Ni3—Cl2	173.31 (12)
O8—Ni3—Cl2	100.98 (10)
N4—Ni3—Cl2	92.77 (12)
O7—Ni3—Cl1	97.28 (11)
N5—Ni3—Cl1	88.82 (12)
O8—Ni3—Cl1	83.18 (11)
N4—Ni3—Cl1	171.93 (12)
Cl2—Ni3—Cl1	85.48 (5)
O5—Ni4—N1	92.30 (16)
O5—Ni4—O7	90.80 (14)
N1—Ni4—O7	174.25 (16)
O5—Ni4—O4	173.20 (14)
N1—Ni4—O4	81.30 (15)
O7—Ni4—O4	95.39 (14)
O5—Ni4—O6	88.65 (16)
N1—Ni4—O6	98.39 (17)

O7—Ni4—O6	76.83 (14)	
O4—Ni4—O6		90.01 (16)
O5—Ni4—Cl2		90.66 (12)
N1—Ni4—Cl2		103.86 (14)
O7—Ni4—Cl2		80.93 (10)
O4—Ni4—Cl2		93.09 (12)
O6—Ni4—Cl2		157.74 (11)

Table S18. Selected bond angles (°) around Ni-centers of complex **2**.

O12—Ni1—O6	105.1 (2)
O12—Ni1—O4	100.2 (2)
O6—Ni1—O4	114.6 (2)
O12—Ni1—N4	93.5 (2)
O6—Ni1—N4	124.1 (2)
O4—Ni1—N4	113.0 (2)
O12—Ni1—O5	171.6 (2)
O6—Ni1—O5	80.22 (17)
O4—Ni1—O5	83.12 (18)
N4—Ni1—O5	78.1 (2)
O1—Ni2—N2	174.4 (2)
O1—Ni2—O8	87.70 (19)

N2—Ni2—O8	90.5 (2)
O1—Ni2—O4	98.71 (19)
N2—Ni2—O4	82.5 (2)
O8—Ni2—O4	170.7 (2)
O1—Ni2—N1	88.3 (2)
N2—Ni2—N1	97.1 (2)
O8—Ni2—N1	96.3 (2)
O4—Ni2—N1	90.7 (2)
O1—Ni2—O5	76.93 (18)
N2—Ni2—O5	97.8 (2)
O8—Ni2—O5	91.05 (18)
O4—Ni2—O5	83.86 (18)
N1—Ni2—O5	163.3 (2)
N3—Ni3—O1	173.0 (2)
N3—Ni3—O7	93.0 (2)
O1—Ni3—O7	85.3 (2)
N3—Ni3—O5	108.1 (2)
O1—Ni3—O5	78.89 (19)
O7—Ni3—O5	96.92 (18)

N3—Ni3—O6	81.9 (2)
O1—Ni3—O6	100.1 (2)
O7—Ni3—O6	174.3 (2)
O5—Ni3—O6	82.40 (18)
N3—Ni3—O2	97.3 (2)
O1—Ni3—O2	75.99 (19)
O7—Ni3—O2	91.2 (2)
O5—Ni3—O2	152.86 (19)
O6—Ni3—O2	92.0 (2)
O7—Ni4—O8	106.90 (19)
O7—Ni4—Cl1	131.03 (15)
O8—Ni4—Cl1	110.59 (15)
O7—Ni4—O9	113.0 (2)
O8—Ni4—O9	74.95 (18)
Cl1—Ni4—O9	106.34 (16)
O7—Ni4—O10	72.65 (18)
O8—Ni4—O10	148.1 (2)
Cl1—Ni4—O10	90.36 (15)
O9—Ni4—O10	76.15 (18)

Theoretical calculations on various fragments of the nickel complex:

All the geometry optimizations were performed in M06-2X/def2-SVPP. The single point energy calculations were performed on the optimized coordinates M06-2X/def2-SVPP. The NBO calculations and wavefunction generation were performed using the same level of theory and basis set.

The tridentate Ni complex (**Y**) was optimized in singlet and triplet state. The energy for these states were found -2367.0135624 and -2367.040262 hartrees respectively. It is evident from the values that the triplet state is less in energy than the singlet state. The energy difference between these states are 16.75 kcal/mol. The optimized structure in triplet state is given in the Figure S22 and selected bond lengths are represented in the Table S19.

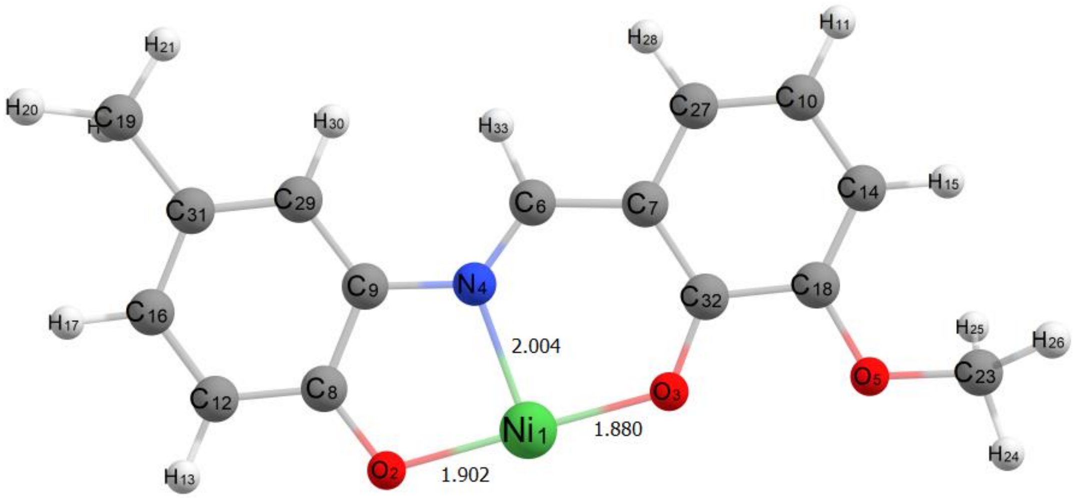

Figure S27. Optimized structure of **Y**.

Table S19. Selected Bond lengths (Å), bond angles and torsion angle (°) of **Y**.

O2-Ni1	1.902
O3-Ni1	1.880
N4-Ni1	2.004
O2-Ni1-N4	85.798
O3-Ni1-N4	94.836
O2-Ni1-N4-O3	179.363

Since the stable ground state is triplet the highest occupied orbital is singly occupied, ie., SUMO. The SOMO is composed of the lone pair on oxygen (p type), delocalization on the pheny; ring and π-type orbital of the imine bond. A significant contribution of oxygen lone pair (p type) and filled d orbital of Ni can be seen in SOMO-1. The HOMO-2 features the π-type orbital of the imine bond, lone pair on oxygen and the filled d orbitals. The HOMO-3 is composed of the lone pair of oxygen, filled d orbital of Ni and electron delocalization over the ligand. Along with the above features HOMO-4 has the contribution of N lone pair. An extensive delocalization over the O-Ni-O core can be seen in HOMO-5. The major contribution of the LUMO id from the ligand's lone pairs and the imine bond and also a minor contribution from Ni's unfilled d orbitals. LUMO-1 features the unfilled d orbital of Ni. LUMO+2, LUMO+3, and LUMO+4 reveals the major contribution from the ligand. Along with the contribution from ligand, LUMO+5 has the contribution from N-Ni bond (2p orbital of N and 2d orbital of Ni).

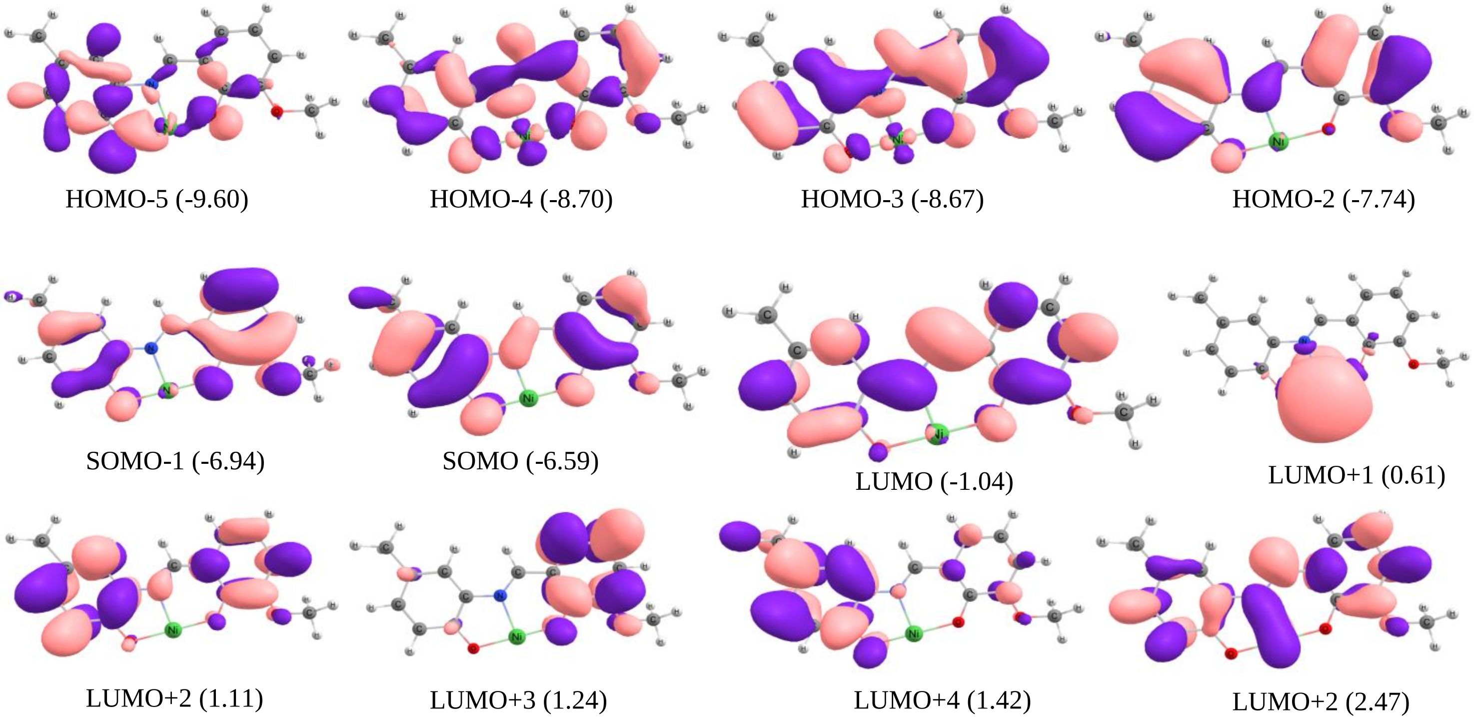

HOMO-5 (-9.60)

HOMO-4 (-8.70)

HOMO-3 (-8.67)

HOMO-2 (-7.74)

SOMO-1 (-6.94)

SOMO (-6.59)

LUMO (-1.04)

LUMO+1 (0.61)

LUMO+2 (1.11)

LUMO+3 (1.24)

LUMO+4 (1.42)

LUMO+2 (2.47)

Figure S28. HOMO-5 to LUMO+5 of (L-Me)Ni (**Y**) calculated at M06-2/def2SVPP level of theory. The value in the brackets denote the energy of the orbital in eV.

Table S20. Natural Charges on selected atoms of **Y**.

Atom	Natural charge
Ni	1.416
O_{am}	-0.882
O_{al}	-0.851
N_{im}	-0.627

AIM analysis on various fragments of nickel complexes:

The strength of a bond is represented by the electron density at the BCP (ρ). Generally, when ρ is greater than 0.20 au it is considered as an electron sharing or a covalent bond. If it is less than 0.10 it is likely to be a closed shell interaction. Table 21 represents ρ of selected bonds. We know that the donor atoms of one the ligand is donated its lone pair to the vacant d orbitals of Ni, thus forming a coordinate bond. The value of ρ in the table also indicating the same. The sum of three curvatures of density (λ_1, λ_2, and λ_3) at the critical point is the Laplacian at the BCP. For a covalent bond two negative curvatures are dominant. So, the Laplacian will be negative. For closed shell interaction the Laplacian of the electron density at the BCP is positive. The coordinate nature of the Ni-N/O is thus verified. Ellipticity measures the π character of the bond. There is significant variation of ellipticity in the Ni-O bonds and the Ni-N bond. This indicates that the extend of π-contribution is different in these bonds. An additional parameter is η. It is the ratio of modulus of λ_1 to λ_3. For a closed shell interaction, it will be less than unity and it will increase with the covalent character of the bond. The values observed for the **Y** is less than unity again underlines the fact that there is no covalent character in the Ni-O/N bond.

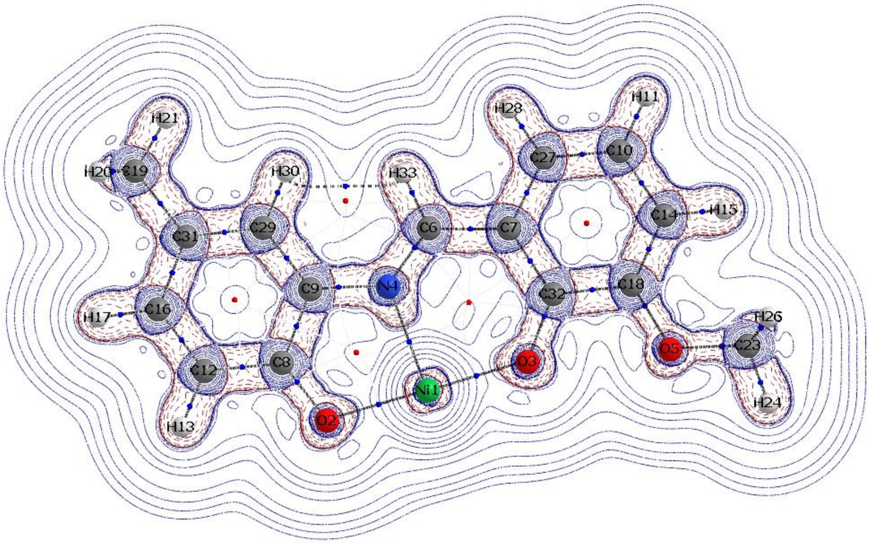

Figure S29. Contour plot of Laplacian distribution [$\nabla^2\boldsymbol{\rho}$ (r)] in the O2-Ni1-N4 plane of fragment **Y**. Solid blue lines indicate the areas of charge concentration ($\nabla^2\boldsymbol{\rho}$ (r) < 0) while dotted purple lines denotes charge depletion ($\nabla^2\boldsymbol{\rho}$ (r) > 0). Solid lines connecting atomic nuclei (black) are the bond paths.

Table S21. ED and Laplacian at the BCPs of **Y**.

Bond	**ρ (a.u.)**	**$\nabla^2\rho$**	**ε**	**η**
Ni1 - N4	+0.082	+0.492	+0.013	0.140
Ni1 - O2	+0.094	+0.659	+0.352	0.173
Ni1 - O3	+0.096	+0.711	+0.382	0.171

The five coordinated Ni complex (**X**) is optimized in the triplet state and its energy was found to be -2943.3527236 Hartrees. A chloride ion and a methanol molecule is present in the coordination sphere of the Ni centre. The O_{am} is protonated whereas, the O_{al} stays deprotonated. The Ni centre is in a distorted square pyramidal geometry with the methanol molecule in its axial position. The selected bond distances and angles of **X** are given in the Table S22.

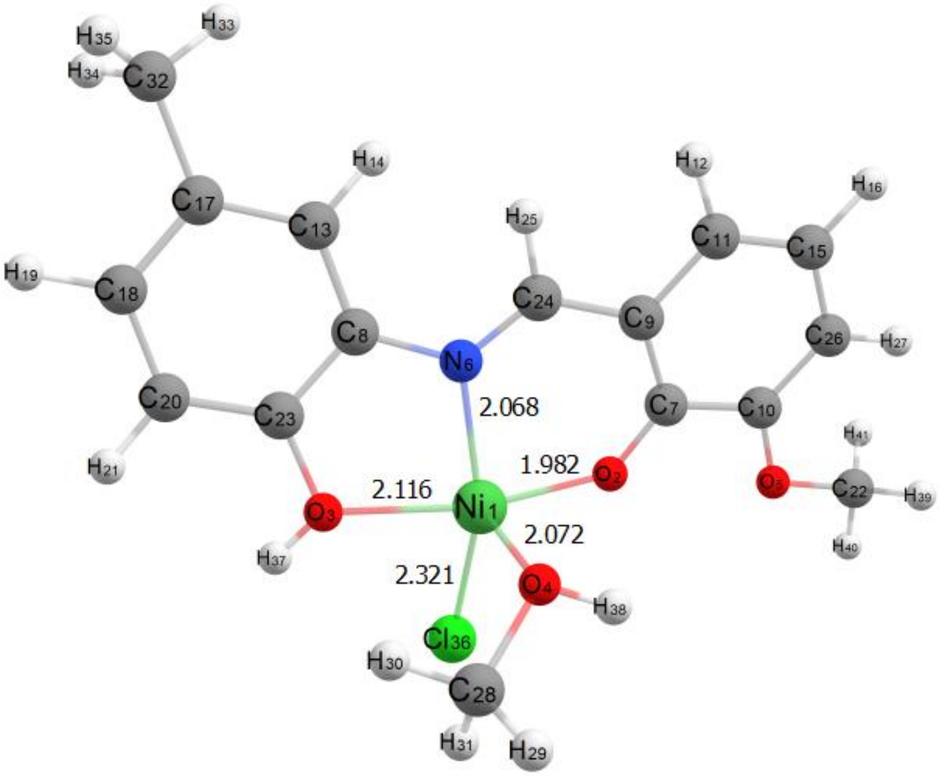

Figure S30. The optimized structure of **X**.

Table S22: Selected Bond lengths (Å) and angles (º) of **X**.

O2-Ni1	1.982
O3-Ni1	2.116
N6-Ni1	2.068
O4-Ni1	2.072
Cl36-Ni1	2.321
O2-Ni1-Cl36	101.200
O3-Ni1-N4	77.570
O2-Ni1-N4	90.822
O3-Ni1-Cl36	89.372
O2-Ni1-O4	90.943

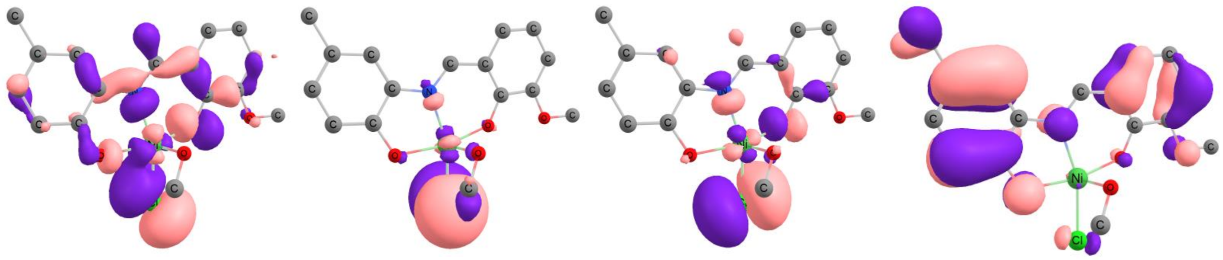

HOMO-5 (-8.49) HOMO-4 (-8.36) HOMO-3 (-8.34) HOMO-2 (-8.04)

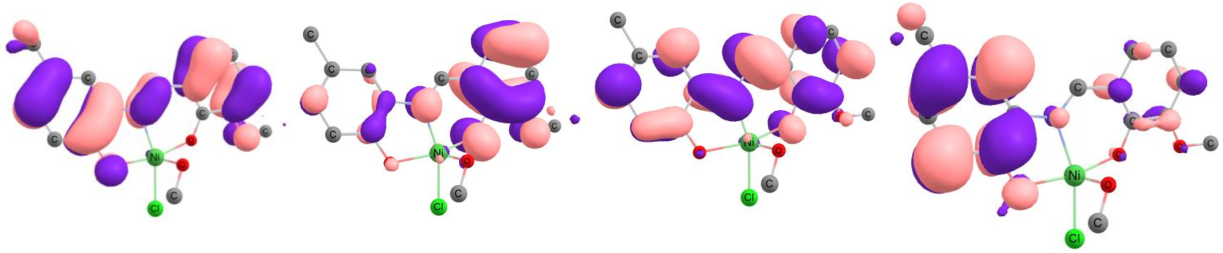

SOMO-1 (-7.36) SOMO (-6.58) LUMO (-1.06) LUMO+1 (0.77)

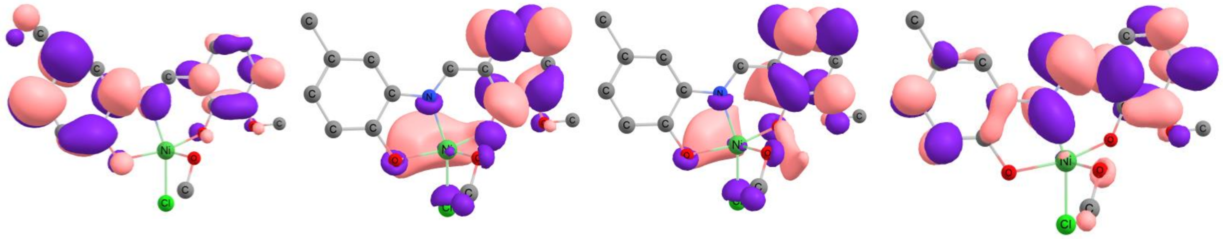

LUMO+2 (1.06) LUMO+3 (1.35) LUMO+4 (1.39) LUMO+5 (2.49)

Figure S31. HOMO-5 to LUMO+5 of **X** calculated at M06-2/def2SVPP level of theory. The value in the brackets denote the energy of the orbital in eV.

The highest occupied state is singly occupied, i.e., SOMO. The major contribution of the orbital is from the ligand and its lone pair on N and O. A minor contribution from filled d orbital of Ni can be seen. The SOMO-1 is mainly located on the phenyl rings of the ligand and the imine bond (π-type). HOMO-2 features the lone pairs on N, Os and chlorine atom. The HOMO-3 and HOMO-4 orbital is mainly featuring the lone pair on Cl atom and slight contribution from the filled d orbital of Ni and the lone pair of the donating atoms. The LUMO is predominantly from the ligand, the imine bond (π-type), the lone pair on O and the phenyl rings and very slightly from the vacant d orbital of the Ni. In LUMO+1and LUMO+2 and LUMO+5, there is no contribution from Ni, the ligand constitutes the major part. The LUMO+3 and LUMO+4 are composed of the extensive delocalization of O-Ni-O core.

Table S23: Natural Charges on selected atoms of **X**.

Atom	Natural charge
Ni	1.150
O_{am}	-0.734
O_{al}	-0.796
N_{im}	-0.620
Cl	-0.693
O_{MeOH}	-0.776

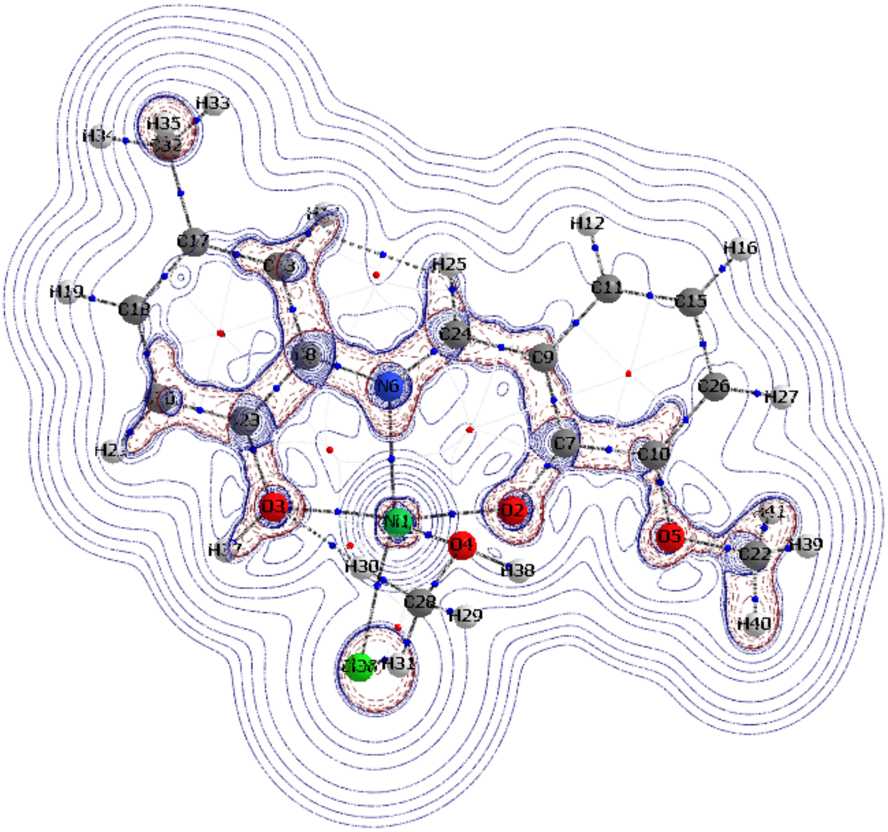

Figure S32. Contour plot of Laplacian distribution [$\nabla^2\boldsymbol{\rho}$ (r)] in the O3-Ni1-N6 plane of fragment **Y**. Solid blue lines indicate the areas of charge concentration ($\nabla^2\boldsymbol{\rho}$ (r) < 0) while dotted purple lines denotes charge depletion ($\nabla^2\boldsymbol{\rho}$ (r) > 0). Solid lines connecting atomic nuclei (black) are the bond paths.

Table S24. ED and Laplacian at the BCPs of fragment **X**.

Bond	**ρ (au)**	**$\nabla^2\rho$**	**Ellipticity**	**η**
Ni1 – N6	0.069	0.413	0.116	0.134
Ni1 - O2	0.071	0.530	0.079	0.093
Ni1 - O3	0.049	0.334	0.237	0.122
Ni1 - Cl36	0.057	0.232	0.232	0.151
Ni1 - O4	0.056	0.396	0.111	0.108

The ED at the BCP (ρ) for all the bonds coordinated to Ni have the value less than 0.10 au. This indicates that any of these bonds are an electron sharing (covalent) bond. All these bonds are to be likely to be a closed shell interaction. For a closed shell interaction, the sign of the sum of three curvatures of density at the critical point, i.e., the Laplacian at the BCP is a positive value. The same is observed for the atoms bonded to Ni. Ellipticity measures the π character of the bond. The extend of the π character is different for every atom. Another parameter defining a bond is η. The value will increase as the covalent nature of the bond increases. For a covalent bond the value will be greater than unity. Its noted that η for all the selected bond is very less than unity. It again emphasis the fact that all these bonds have no covalent character and it likely to a coordinate bond.

The half of the complex **1** is constructed by combination of **Y** and **X**. The half of the complex **1** is optimized in its singlet and quintet state. The energy corresponding to these states are -5310.3980733 and -5310.490042 Hartrees, respectively. These values indicate that the quintet state is more stable than the singlet. The energy difference between these states is 57.71 kcal/mol. The Ni1 centre is in distorted octahedral geometry whereas, the Ni2 centre is in distorted square pyramidal geometry. Both the Ni centres are bound together by the chloride and alkoxide bridging. The Ni centres are 3.178 Å away from each other. There is also a hydrogen bond present between the H of methanol and the O_{al} (1.582 Å).

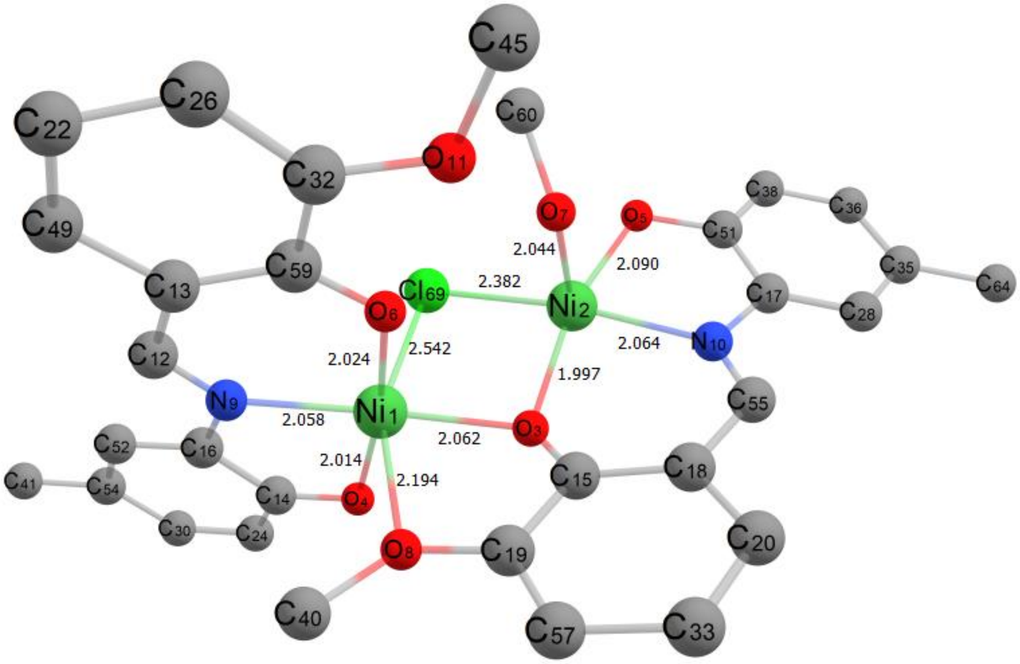

Figure S33. The optimized structure of half of the complex **1**.

Table S25. Selected Bond lengths (Å) of half of the complex **1**.

O6-Ni1	2.024
O3-Ni1	2.062
N9-Ni1	2.058
O8-Ni1	2.194
O4-Ni1	2.014
Cl69-Ni1	2.542
O3-Ni2	1.997
O5-Ni2	2.090
N10-Ni2	2.064
O7-Ni2	2.044
Cl69-Ni2	2.382

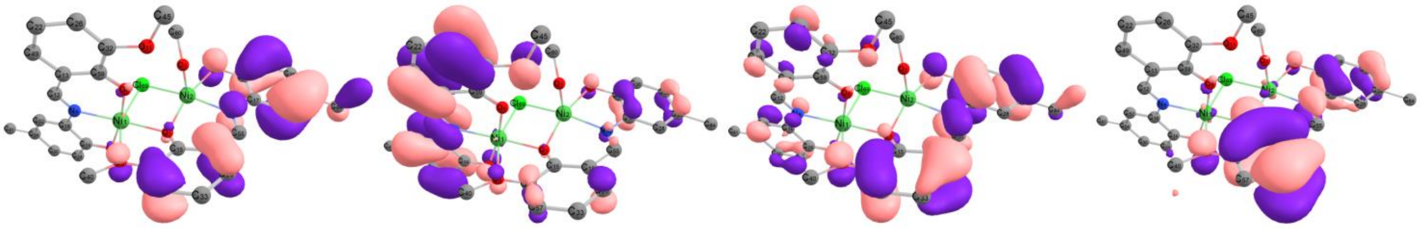

HOMO-5 (-8.18) HOMO-4 (-7.59) SOMO-3 (-7.56) SOMO-2 (-7.11)

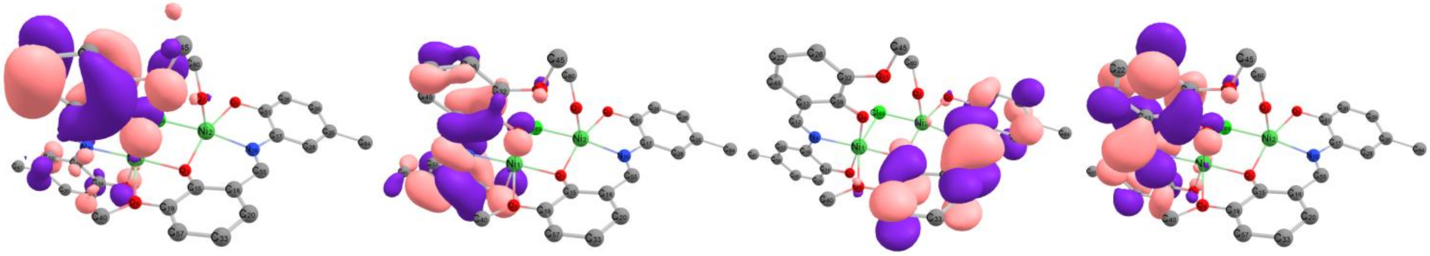

SOMO-1 (-6.78) SOMO (-6.19) LUMO (-1.29) LUMO+1 (-0.84)

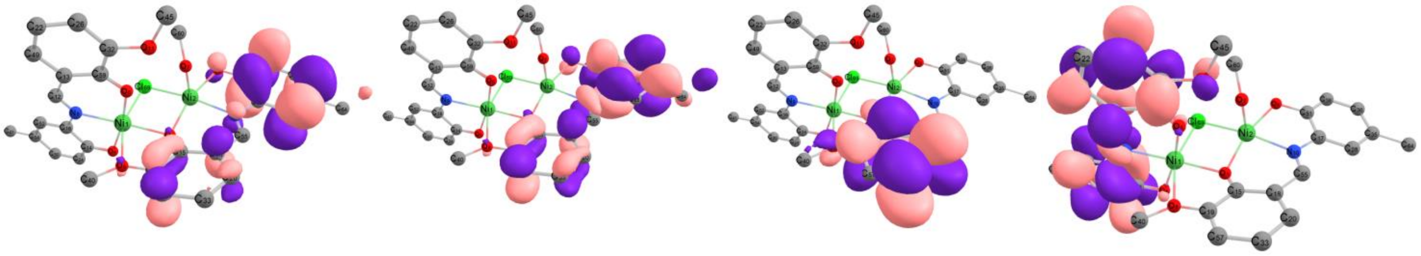

LUMO+2 (0.68) LUMO+3 (0.92) LUMO+4 (1.03) LUMO+5 (1.25)

Figure S34. HOMO-5 to LUMO+5 of half of the complex **1** calculated at M06-2/def2SVPP level of theory. The value in the brackets denote the energy of the orbital in eV

Since the more stable state is quintet the four highest occupied orbitals are singly occupied. The SOMO and SOMO-1 are mainly constituted on the tridentate ligand coordinated to Ni1 centre and very slight contribution Ni1 d orbital can be seen. In SOMO-2 and HOMO-5, the major contribution is from the Ni2 bonded ligand and a minor contribution from both the filled d orbitals of Ni. The SOMO-3 features the electron delocalization of ligand bonded to the Ni2 centre, whereas, HOMO-4 features the electron delocalization on the Ni1 bonded ligand. The only contribution of LUMO, LUMO+2, LUMO+3 and LUMO+4 are from Ni2 centre and the associated ligand. There is no contribution from Ni1. LUMO+1 and LUMO+5 are located on the Ni1 centre and the bonded ligand.

Table S26. Natural Charges on selected atoms of half of the complex **1**.

Atom	Natural charge
Ni1	1.135
O3	-0.817
O4	-0.843
O6	-0.816
O8	-0.580
N9	-0.587
Cl69	-0.585
Ni2	1.202
O7	-0.735
O5	-0.735
N10	-0.602

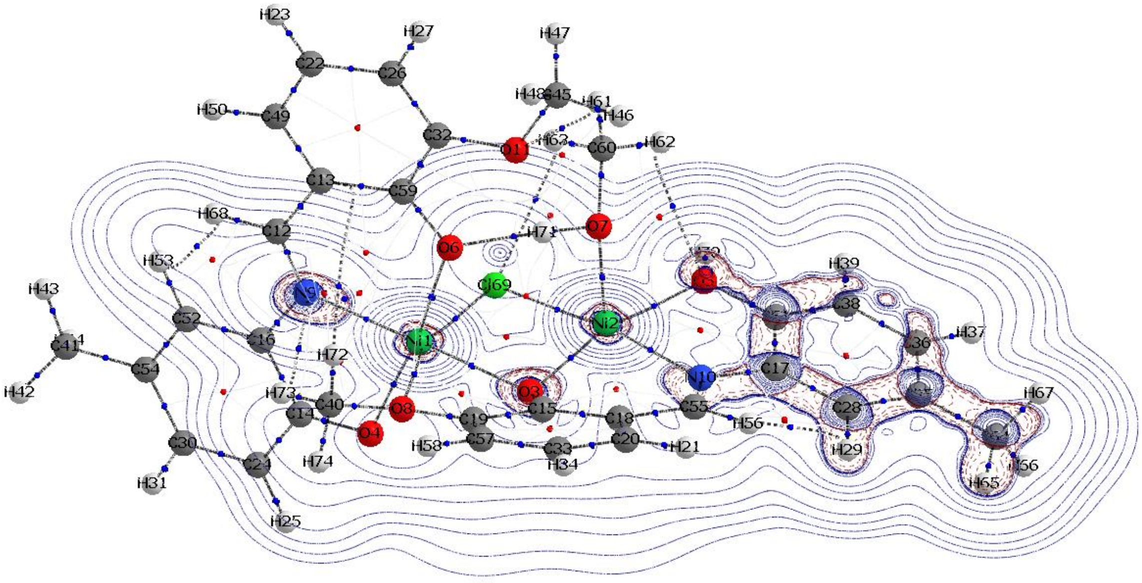

Figure S35. Contour plot of Laplacian distribution [$\nabla^2\boldsymbol{\rho}$ (r)] in the Ni1-Cl69-Ni2 plane of complex **1**. Solid blue lines indicate the areas of charge concentration ($\nabla^2\boldsymbol{\rho}$ (r) < 0) while dotted purple lines denotes charge depletion ($\nabla^2\boldsymbol{\rho}$ (r) > 0). Solid lines connecting atomic nuclei (black) are the bond paths.

Table S27. Extracted parameters for of half of the complex **1** from QTAIM calculations.

Bond	$\boldsymbol{\rho}$ **(au)**	$\nabla^2\boldsymbol{\rho}$	**Ellipticity**	**η**
Ni1 - Cl69	0.035	0.123	0.218	0.152
Ni1 - N9	0.07	0.435	0.139	0.124
Ni1 - O3	0.059	0.405	0.105	0.115
Ni1 - O4	0.069	0.472	0.134	0.123
Ni1 - O6	0.064	0.462	0.09	0.385
Ni1 - O8	0.042	0.248	0.276	0.135
Ni2 - Cl69	0.049	0.2	0.094	0.135
Ni2 - N10	0.069	0.418	0.066	0.13
Ni2 - O3	0.069	0.503	0.027	0.114
Ni2 - O5	0.053	0.363	0.209	0.125
Ni2 - O7	0.062	0.431	0.076	0.11

The ED at the BCP (ρ) for all the bonds coordinated to Ni have the value less than 0.10 au. This indicates that any of these bonds are an electron sharing (covalent) bond. If ρ is more than 0.2 au it is generally considered as covalent bond. All these bonds are to be likely to be a closed shell interaction. The Laplacian at the BCP is positive for noncovalent interactions. Here also we observe a positive value for the Laplacian at the BCP. Ellipticity explains the π character of a bond. As this value increases π character of the bond increases. Various extend of π character is seen in the bonds of the complex. It is noted that η for all the selected bond is very less than unity. It again emphasis the fact that all these bonds have no covalent character and it likely to a coordinate bond.

6. Details of catalytic activities of complex 3 [$Ni_4((O_{al}^-)_2L\text{-}Me)_4(H_2O)_4$]·2DMF

6.1. General procedures for the syntheses of various aromatic heterocycles (6) and diazoesters (7)

6.1.1. Syntheses of aromatic heterocycles (6):

General procedure 1: *N*-Boc protection of aromatic heterocyclic compounds:[15]

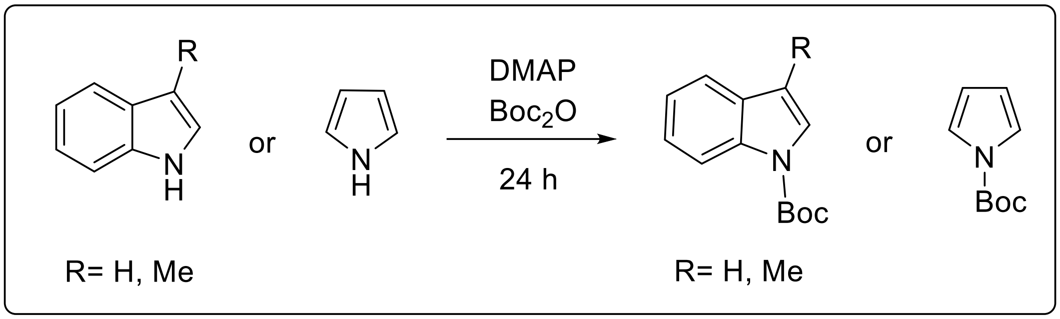

A mixture of indole/pyrrole derivative (1 equiv), di-^{t}butyl dicarbonate (1.2 equiv) and DMAP (0.15 equiv) were taken in a 250 mL flask. To this 60 mL of dry acetonitrile was added under argon atmosphere. Thereafter, the reaction mixture was allowed for stirring at room temperature for 24 h. After completion of the reaction, as monitored by TLC, the reaction mixture was quenched with $NaHCO_3$ solution and extracted with ethyl acetate. The organic layer was passed through anhydrous Na_2SO_4 and evaporated under rotary evaporator under reduced pressure. The reaction mixture was further purified by column chromatography on silica gel with hexane/ EtOAc (10:1) as an eluent to afford the corresponding *N*-Boc protected indoles/pyrroles.

General procedure 2: Syntheses of *N*-Pivaloyl Indoles and Pyrroles:[16]

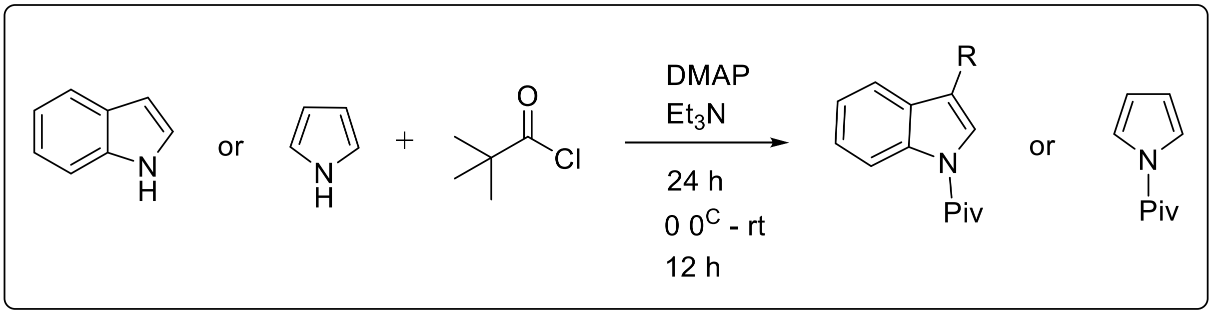

Indole/pyrrole (1 equiv) and DMAP (0.1 equiv) were weighed into a round bottom flask. The flask was purged with argon and dry DCM was added to yield a clear, colorless solution. Triethyl amine (1.48 equiv) was added and the flask was submerged into an ice-water bath and cooled to 0°C. Pivaloyl chloride (1.17 equiv) was added to the flask slowly (over a period of 1 min) via syringe and the reaction was then allowed to stir at 0°C for ~10 min The reaction mixture was allowed to warm to room temperature and stirred overnight. The progress of the reaction was monitored by TLC. DCM was removed by rotary evaporation and the residue was partitioned between diethyl ether and a saturated solution of ammonium chloride. The layers were separated and the ether layer was washed with brine. The combined aqueous layers were extracted with diethyl ether and the combined organic fractions were passed through Na_2SO_4 and evaporated to dryness. The crude product was purified by subjecting to column chromatography on silica gel with 1% diethyl ether in hexanes as the eluant to afford the pure product.

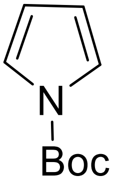

6a

***Tert*-butyl 1H-pyrrole-1-carboxylate (6a):** ^{1}**NMR** (400 MHz, $CDCl_3$, ppm) *δ:* 7.16 (s, 2H), 6.13 (s, 2H), 1.52 (s, 9H); ^{13}**C NMR** (101 MHz, $CDCl_3$, ppm) *δ:* 148.95, 119.97, 111.84, 83.53, 27.99.

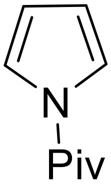

6b

2,2-dimethyl-1-(1H-pyrrol-1-yl)propan-1-one (6b): ^{1}**H NMR** (400 MHz, $CDCl_3$, ppm) *δ:* 7.35 (s, 2H), 6.16 (s, 2H), 1.36 (s, 9H); ^{13}**C NMR** (101 MHz, $CDCl_3$, ppm) *δ*: 175.83, 120.57, 111.91, 40.60, 28.52.

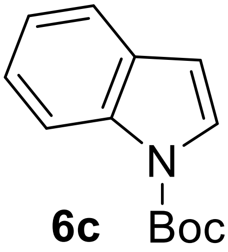

6c

***Tert*-butyl 1H-indole-1-carboxylate (6c):** ^{1}**H NMR** (400 MHz, $CDCl_3$, ppm) *δ*: 8.05 (d, *J* = 8 Hz, 1H), 7.48 (s, 1H), 7.46 (d, *J* = 8 Hz, 1H), 7.20 (t, *J* = 8 Hz, 1H), 7.1 (t, *J* = 8 Hz, 1H), 6.44 (d, *J* = 4 Hz, 1H), 1.55 (s, 9H); ^{13}**C NMR** (101 MHz, $CDCl_3$, ppm) *δ*: 149.85, 130.64, 125.92, 124.24, 122.69, 120.99, 115.22, 107.34, 83.63, 28.24.

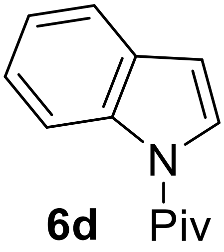

6d

1-(1H-indol-1-yl)-2,2-dimethylpropan-1-one (6d): ^{1}**H NMR** (400 MHz, $CDCl_3$, ppm) *δ*: 8.44 (d, J = 8 Hz, 1H), 7.65 (d, J = 4 Hz, 1H), 7.48 (d, J = 8 Hz, 1H), 7.27 (t, J = 8 Hz, 1H), 7.19 (t, J = 8 Hz, 1H), 6.54 (d, J = 4 Hz, 1H), 1.44 (s, 9H); ^{13}**C NMR** (101 MHz, $CDCl_3$, ppm) *δ*: 177.12, 136.78, 129.41, 125.67, 125.12, 123.56, 120.50, 117.35, 108.25, 41.26, 28.73.

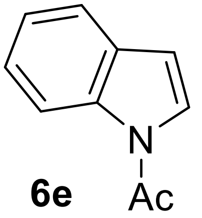
6e

1-(1H-indol-1-yl)ethan-1-one (6e): ^{1}H NMR (400 MHz, $CDCl_3$, ppm) *δ*: 8.49 (d, *J* = 8 Hz, 1H), 7.60 (d, *J* = 8 Hz, 1H), 7.39 (t, *J* = 8 Hz, 2H), 7.31 (t, *J* = 8.0 Hz, 1H), 6.65 (d, *J* = 4 Hz, 1H), 2.62 (s, 3H); **^{13}C NMR** (101 MHz, $CDCl_3$, ppm) *δ*: 168.71, 135.57, 130.48, 125.32, 125.12, 120.89, 116.57, 23.95.

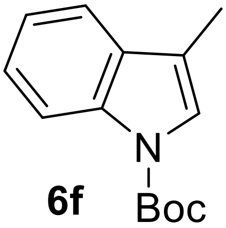
6f

***Tert*-butyl 3-methyl-1H-indole-1-carboxylate (6f): ^{1}H NMR** (400 MHz, $CDCl_3$, ppm) *δ*: 8.11 (s, 1H), 7.48 (d, *J* = 8 Hz, 1H), 7.30 (t, *J* = 8 Hz, 1H), 7.23 (t, *J* = 8 Hz, 1H), 2.25 (s, 3H), 1.65 (s, 9H); **^{13}C NMR** (101 MHz, $CDCl_3$, ppm) *δ*: 149.87, 135.53, 131.50, 124.24, 122.83, 122.33, 116.37, 115.17, 83.17, 28.27, 9.64.

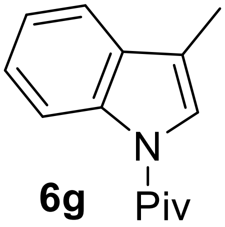
6g

2,2-dimethyl-1-(3-methyl-1H-indol-1-yl)propan-1-one (6g): ^{1}H NMR (400 MHz, $CDCl_3$, ppm) *δ*: 8.43 (d, *J* = 8.0 Hz, 1H), 7.39 (d, *J* = 4 Hz, 2H), 7.26 (t, *J* = 8 Hz, 1H), 7.19 (t, *J* = 8 Hz, 1H), 2.20 (s, 3H), 1.41 (s, 9H); **^{13}C NMR** (101 MHz, $CDCl_3$, ppm) *δ*: 177.12, 136.78, 129.41, 125.67, 125.12, 123.56, 120.50, 117.35, 108.25, 41.26, 28.81.

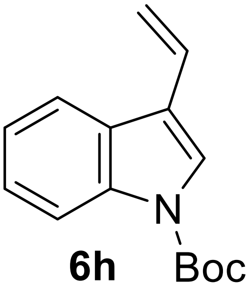
6h

Tert**-butyl 3-vinyl-1H-indole-1-carboxylate (6h): ^{1}H NMR** (400 MHz, $CDCl_3$, ppm) *δ*: 8.07 (s, 1H), 7.69 (d, J = 8 Hz, 1H), 7.52 (s, 1H), 7.25 (t, J = 8 Hz, 1H), 7.17 (t, J = 8 Hz, 1H), 6.70 (dd, J = 16, 12 Hz, 1H), 5.71 (d, J = 20 Hz, 1H), 5.22 (d, J = 12 Hz, 1H), 1.57 (d, J = 4.1 Hz, 9H); **^{13}C NMR** (101 MHz, $CDCl_3$, ppm) *δ*: 149.64, 135.86, 124.65, 128.21, 124.65, 124.02, 122.96, 120.02, 119.29, 115.40, 114.39, 83.83, 28.22.

6.1.2. Syntheses of various diazoesters (7):

6.1.2.1. Procedure for the synthesis of Ethyl 2-diazoacetate (7a):

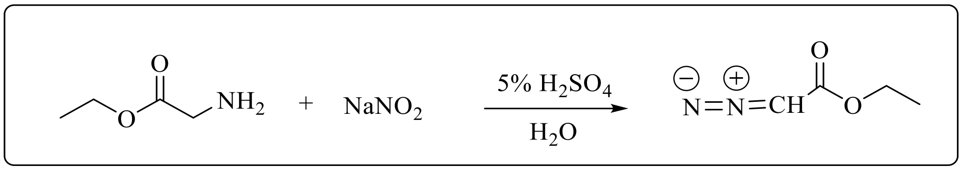

In a 250 mL Schlenk flask, ethyl glycinate hydrochloride (7 gm, 50 mmol, 1 equiv) was dissolved in 12.5 mL of distilled water, to this 30 mL of DCM was added with vigorous stirring. Thereafter, an ice-cold solution of sodium nitrite (3.45 gm of $NaNO_2$ dissolved in 12.5 mL distilled water) was added to the reaction mixture with constant stirring for 30 min. Further, the reaction mixture was cooled to -10 ^{0}C, subsequently 5 % H_2SO_4 (2.60 mL) was added through dropping funnel over a period of 20 min with constant stirring. In this process, the color of the reaction mixture was changed from colorless to light green. After completion of the reaction, the reaction mixture was washed with 5% $NaHCO_3$ solution and then extracted with ethyl acetate. Compound **3a** was isolated as a yellow liquid after evaporation of the ethyl acetate using rotary evaporator under mildly reduced pressure (9.9 g, 87% yield). **^{1}H NMR** (400 MHz, $CDCl_3$, ppm) δ: 4.77 (s, 1H), 4.22 (q, 2H), 1.28 (t, 3H); **^{13}C NMR** (101 MHz, $CDCl_3$, ppm) δ: 166.93, 60.82, 53.46, 14.36.

6.1.2.2. Procedure for the synthesis of *tert*-butyl-2-diazoacetate (7b):

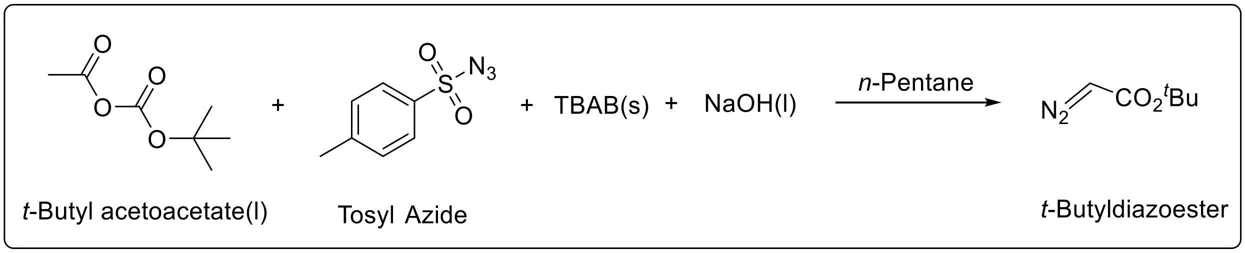

A mixture of *tert*-butyl-diazoacetate (4.11 mL, 25 mmol, 1.0 equiv), TBAB (Tetra-*n*-butylammonium bromide) (161.15 mg, 0.5 mmol, 0.02 equiv) and tosylazide (4.9 gm, 25 mmol, 1.0 equiv) were taken in a 250 mL round bottom flask, to this *n*-pentane 75 mL was added with vigorous stirring at 0 °C. Thereafter, pre-cooled sodium hydroxide solution (3 g in 25 mL of

H_2O) was added to the reaction mixture over a period of 20 min with constant stirring the reaction mixture for 12 h. After completion of the reaction, the reaction mixture was passed through Celite and the resultant organic layer was washed with brine solution and passed through anhydrous Na_2SO_4. Finally, the pure *tert*-butyl 2-diazoacetate was isolated as yellow oil after concentration of the reaction mixture using rotary evaporator under mildly reduced pressure (3 g, 92% yield). **^{1}H NMR** (400 MHz, $CDCl_3$, ppm) δ: 1.48 (s, 9H), 4.61 (s, 1H); **^{13}CNMR** (101 MHz, $CDCl_3$, ppm) δ: 166.19, 81.31, 46.60, 28.25.

General Procedure 3: Synthesis of Aryldiazoacetates:[17]

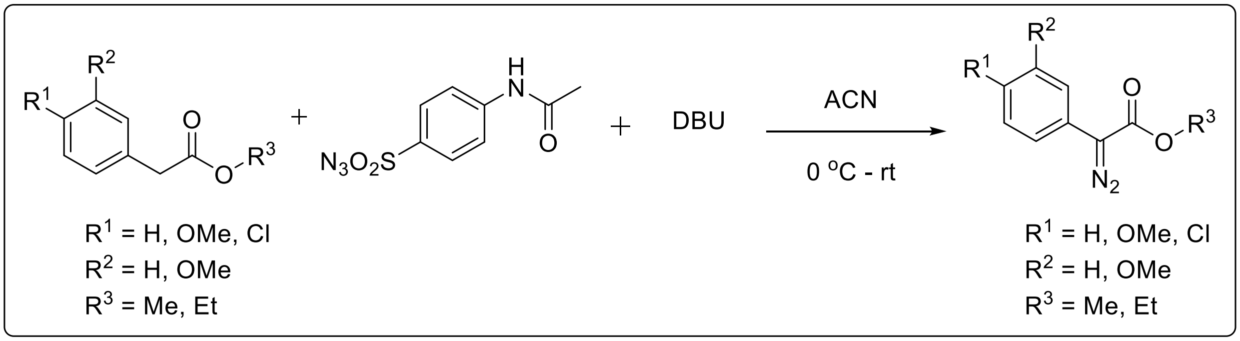

A mixture of ester (1.0 eq) and p-toluenesulfonyl azide (1.2 equiv) was dissolved in MeCN and cooled with an ice bath. DBU (1.2 eq) were added. The reaction mixture was stirred overnight, while slowly warming up to room temperature. The reaction mixture was quenched by adding saturated aq. NH_4Cl. The solution was extracted with diethyl ether and the organic layer was dried over $MgSO_4$ and concentrated under reduced pressure. The product was purified by silica column chromatography *n*-hexane/ethyl acetate.

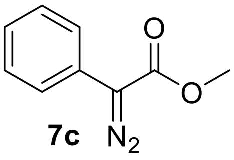

7c

Methyl 2-diazo-2-phenylacetate (7c): ^{1}H NMR ($CDCl_3$, 400 MHz) δ: 7.46 (d, J = 8 Hz, 2H), 7.35 (t, J = 8 Hz, 2H), 7.16 (t, J = 8 Hz, 1H), 3.83 (s, 3H); **^{13}C NMR** (101 MHz, $CDCl_3$, ppm) δ:165.55, 128.95, 125.83, 125.50, 123.95, 51.97.

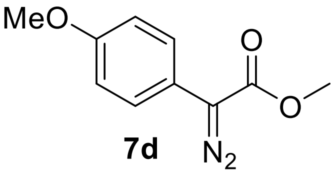

7d

Methyl 2-diazo-2-(4-methoxyphenyl)acetate (7d): ^{1}H NMR ($CDCl_3$, 400 MHz) δ: 7.38 (d, J = 8 Hz, 2H), 6.95 (d, J = 8 Hz,2H), 3.85 (s, 3H), 3.81 (s, 3H); **^{13}C NMR** (101 MHz, $CDCl_3$, ppm) δ: 165.18, 157.08, 124.99, 115.86, 113.61, 54.34, 50.95.

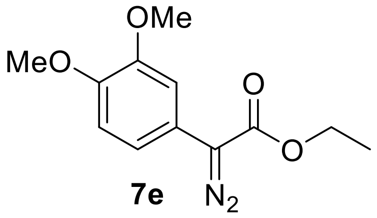
7e

Ethyl 2-diazo-2-(3,4-dimethoxyphenyl)acetate (7e): ^{1}H NMR (400 MHz, CDCl$_3$, ppm) *δ*: 7.19 (s, 1H), 6.81 (d, *J* = 8 Hz, 1H), 6.87 (d, *J* = 8 Hz, 1H), 4.26 (q, *J* = 7.1 Hz, 2H), 3.83 (s, 3H), 3.80 (s, 3H), 1.27 (t, *J* = 8 Hz, 3H); **^{13}C NMR** (101 MHz, CDCl3, ppm) *δ*: 165.75, 149.50, 147.33, 116.43, 116.4, 111.71, 108.40, 55.91, 14.53.

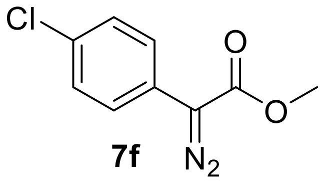
7f

Methyl 2-(4-chlorophenyl)-2-diazoacetate (7f): ^{1}H NMR (400 MHz, CDCl$_3$, ppm) *δ*: 7.35 (d, *J* = 8 Hz, 2H), 7.28 (d, *J* = 8 Hz, 2H), 7.19 (s, 1H), 3.80 (s, 3H); **^{13}C NMR** (101 MHz, CDCl3, ppm) *δ*: 165.32, 131.52, 129.12, 125.08, 124.13, 52.12.

6.2. Optimization of reaction conditions for catalytic cyclopropanation of aromatic heterocycles:

Table S28. Optimization table for complex 3-catalyzed C2-C3 cyclopropanation of aromatic heterocycles[a]

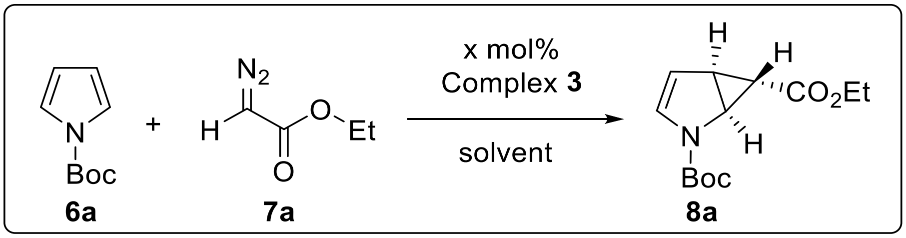

S. No.	6a (mmol)	7a (mmol)	Catalyst (mol%)	Solvent	Temperature in ^{0}C	% Yield of the Product (8a)[b]
1.	5	7.5	Complex **3** 0.25 mol%	DCM	rt	28
2.	5	7.5	Complex **3** 1.25 mol%	DCM	rt	35

3.	5	7.5	Complex **3** 1.87 mol%	DCM	rt	30
4.	5	7.5	Complex **3** 2.5 mol%	DCM	rt	25
5.	5	7	Complex **3** 1.25 mol%	DCM	rt	32
6.	5	7.5	Complex **3** 1.25 mol%	DMF	rt	No reaction[c]
7.	5	7.5	Complex **3** 1.25 mol%	Toluene	100 ^{0}C[d]	25
8.	5	7.5	No catalyst	DCM	rt	No reaction[c]
9.	5	7.5	$Ni_4(L\text{-}H)_4(MeOH)_2$ cubane 1.25 mol%	DCM	rt	16
10.	5	7.5	$Ni_2Dy_2(L\text{-}Me)_4(NO_3)_2(DMF)_2$ 2.5 mol%	Toluene	rt	No reaction[c]
11.	5	7.5	$CuDy(L\text{-}H)_2(Ph_3PO)(NO_3)$ 5 mol%	DCM	rt	No reaction[c]
12	5	7.5	$CuDy(L\text{-}H)_2(Ph_3PO)(NO_3)$ 5 mol%	Toluene	rt	No reaction[c]

[a]Reaction condition: An oven dried Schlenk flask was charged with complex **3** (x mol%) to which a solution of N-Boc pyrrole, **6a** (5 mmol, 1.0 equiv) in dry solvent (3 mL) was added. A solution of ethyl 2-diazoacetate, **7a** (7.5 mmol, 1.5 equiv) in dry solvent (12 mL) was then dropwise added to the Schlenk flask containing **6a** and complex **3** at 0 ^{0}C over a period of 20 min. The temperature of the reaction mixture was then raised to rt or above and kept for stirring over 24 h. [b]Isolated yield of **8a**. [c]Starting material **6a** was recovered back. [d]An oil bath was used for heating the reaction mixture at 100 ^{0}C.

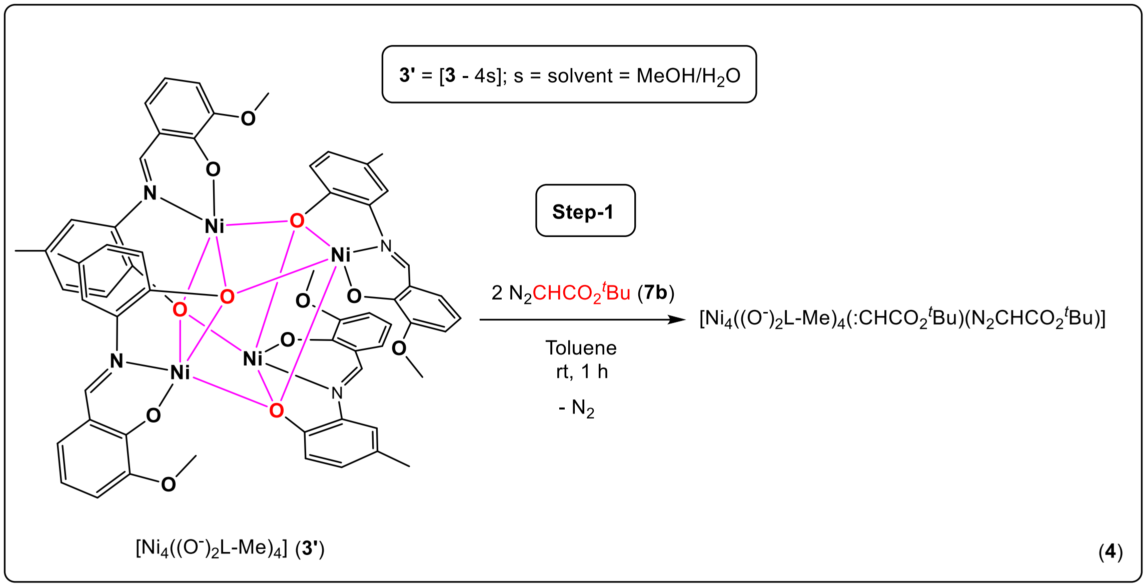

$[Ni_4((O^-)_2L\text{-}Me)_4]$ (**3'**)

(**4**)

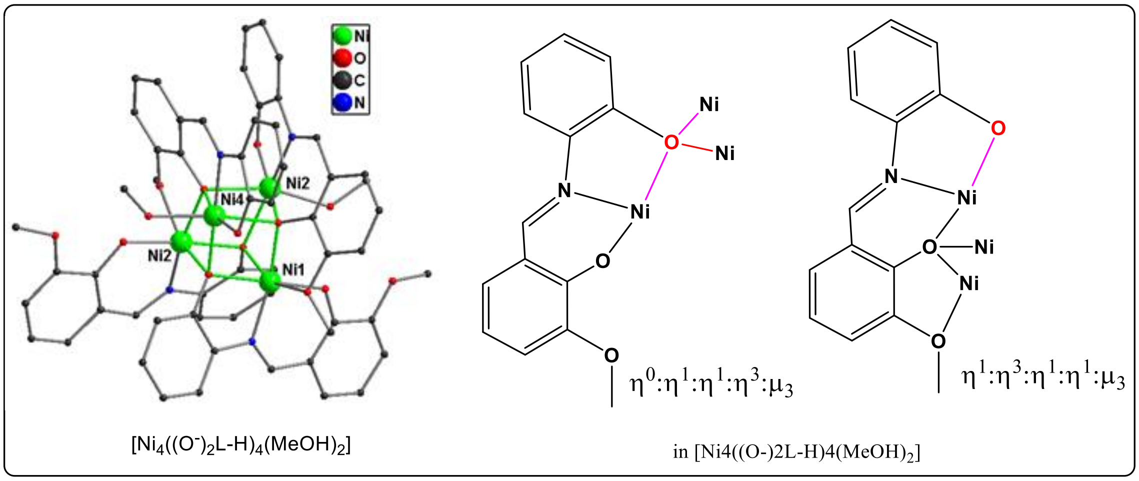

$[Ni_4((O^-)_2L\text{-}H)_4(MeOH)_2]$

in [Ni4((O-)2L-H)4(MeOH)$_2$]

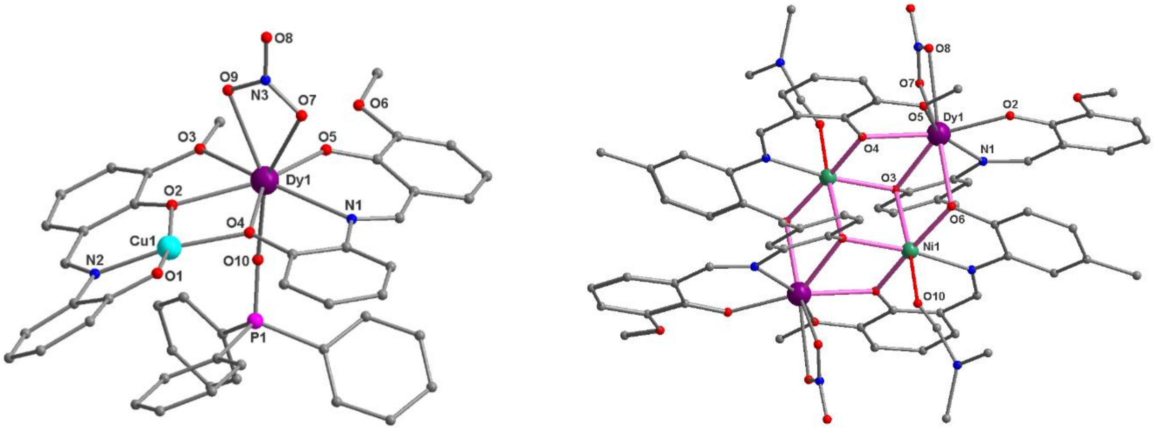

Figure S36. Molecular structures of previously reported complexes (top, left) $[Ni_4(L\text{-}H)_4(MeOH)_2]$ cubane, (top, right) $CuDy(L\text{-}H)_2(Ph_3PO)(NO_3)$, (bottom) $Ni_2Dy_2(L\text{-}Me)_4(NO_3)_2(DMF)_2$ which were given in the optimization table of the organic catalytic reactions.[S1-S3]

6.3.1 General procedure 4 (GP-4) for cyclopropanation of aromatic heterocycles catalyzed by complex 3

1.25 mol% of complex **3** (32 mg) was taken in an oven dried 50 mL schlenk flask. **3** was dissolved in 10 mL dry DCM. A heterocyclic derivative **6** (2 mmol, 1 equiv) was added under argon. Temperature was brought down using an ice bath. To this a solution of diazoester **7** (**7a-7c**) (3 mmol, 1.5 equiv) in 2 mL DCM was added dropwise. After the addition the reaction was allowed to stir for 24 h at room temperature. After the reaction monitored by TLC, the reaction mixture was transferred to a separating funnel and washed with brine. The organic layer was extracted in DCM (3 times). The combined organic layers were dried over Na_2SO_4 and concentrated under reduced pressure. The cyclopropanated product **8** was purified by column chromatography using silica gel (200-400 μm) with *n*-hexane/EtOAc as the eluent to afford the desired cyclopropane carboxylate derivatives **8**.

6.3.2 General procedure 5 (GP-5) for cyclopropanation of aromatic heterocycles catalyzed by complex 3

An oven dried 100 ml Schlenk flask was equipped with a magnetic stir bar and charged with the complex **3** (1.25 mol%) and heterocyclic derivative **6** (2 mmol, 1 equiv). To this 2 mL of dry toluene was added with vigorous stirring under argon atmosphere. Thereafter, the diazoester **7** (**7c-7f**) (3 mmol, 1.5 equiv) was added in 5 mL toluene under argon atmosphere over a period of 30 min. After addition the reaction mixture was allowed for stirring at 100 °C (oil bath temperature) for 24 h. After completion of the reaction (as monitored by TLC), the reaction mixture was washed with the brine solution and extracted with EtOAc. The organic layer was passed through anhydrous Na_2SO_4 and dried using rotary evaporator under reduced pressure. The reaction mixture was further purified by column chromatography on silica gel (200-400 μm) with hexane/EtOAc as the eluent which afforded the desired cyclopropane carboxylate derivatives **8**.

Synthesis of 2-(*Tert*-Butyl)-6-ethyl-2-azabicyclo[3.1.0]hex-3-ene-2,6-dicarboxylate (8a):

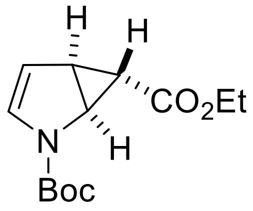

Following General procedure 4 (GP-4), starting from *N*-Boc pyrrole, **6a** (0.334 g, 2 mmol 1.0 equiv), ethyl 2-diazoacetate, **7a** (0.342 g, 3 mmol, 1.5 equiv) and **(L-Me)$_4$Ni$_4$(MeOH)** (0.032 g, 1.25 mol%), **8a** was isolated as colorless gummy solid (0.197 g, 39%). **R*f*** = 0.55 (Hex/EA = 10:1). **^{1}H NMR** (400 MHz, CDCl$_3$, ppm) δ: 6.53-6.37 (m, **1H**, Boc-NC$_{sp2}$*H*), 5.33-5.28 (m, **1H**), 4.37-4.21 (m, **1H**), 4.07-4.04 (m, **2H**, -OCH$_2$C*H$_3$*), 2.73 (s, **1H**), 1.44 (s, **9H**, -C(C*H$_3$*)$_3$), 1.19-1.18 (m, **3H**, -CH$_2$C*H$_3$*), 0.87 (s, **1H**) (signal broadening due to rotamers)[25]; **^{13}C NMR** (101 MHz, CDCl$_3$, ppm) δ: 173.1, 172.8, 151.2, 150.9, 129.7, 129.5, 109.9, 81.6, 60.6, 44.2, 44.0, 32.1, 30.9, 28.2, 28.1, 23.0, 22.8, 14.2 (signal doubling due to rotamers)[25]; **FT-IR υ_{max}** (neat)/cm^{-1}: 2980, 2936, 1707, 1629, 1585, 1459, 1397, 1368, 1336, 1287, 1249, 1158, 1065, 1013, 935, 833, 762, 724; **HRMS** (ESI): *m/z* calculated for $C_{13}H_{20}NO_4$ [M+H]$^+$: 254.1387; found: 254.1390.

Synthesis of Di-*tert*-butyl-2-azabicyclo[3.1.0]hex-3-ene-2,6-dicarboxylate (8b): Following

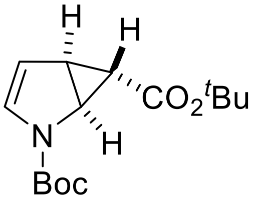

GP-4, starting from *N*-Boc pyrrole, **6a** (836 mg, 5 mmol, 1.0 equiv), *tert*-butyl 2-diazoacetate, **7b** (0.1066 g, 7.5 mmol, 1.5 equiv) and **(L-Me)$_4$Ni$_4$(MeOH)** (0.081 g, 3.12 mol%), **8b** was isolated as a colorless gummy solid (0.548 g, 39%). **R*f*** = 0.45 (Hex/EA = 10:1); **MP:** 70-72 °C; **^{1}H NMR** (400 MHz, CDCl$_3$, ppm) δ: 6.50-6.35 (m, **1H**, Ar*H*), 5.31-5.27 (m, **1H**), 4.32-4.14 (m, **1H**), 2.66 (s, **1H**), 1.44 (s, **9H**, -C(C*H$_3$*)$_3$), 1.37 (s, **9H**, -C(C*H$_3$*)$_3$), 0.90 (s, **1H**) (signal broadening due to rotamers)[25]; **^{13}C NMR** (101 MHz, CDCl$_3$, ppm) δ: 172.4, 172.0, 151.1, 150.9, 130.1, 129.4, 110.0, 81.5, 80.7, 40.0, 43.7, 32.1, 30.6, 28.2, 28.1 (signal doubling due to rotamers)[25]; **FT-IR υ_{max}** (neat)/cm^{-1}: 2977, 2933, 1704, 1585, 1477, 1457, 1392, 1366, 1341, 1291, 1254, 1133, 1020, 939, 896, 851, 829, 761, 720; **HRMS** (ESI): *m/z* calculated for $C_{15}H_{24}NO_4$ [M+H]$^+$: 282.1700; found: 282.1704.

Di-*tert*-butyl fumarate (**8b′**) has been obtained as the minor product (11%, based on the diazoester): **^{1}H NMR** (400 MHz, CDCl$_3$, ppm) δ: 6.65 (s, 2H), 1.48 (s, 18H); **^{13}C NMR** (101 MHz, CDCl$_3$, ppm) δ: 163.40, 133.56, 80.63, 26.96.

2-(*Tert*-butyl) 6-methyl (1S,5S,6R)-6-phenyl-2-azabicyclo[3.1.0]hex-3-ene-2,6-dicarboxylate

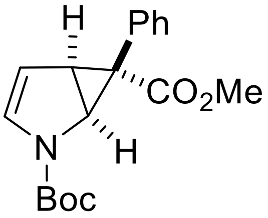

(8c): Following GP-5, starting from *N*-Boc pyrrole, **6a** (0.334 g, 2 mmol, 1.0 equiv), methyl phenyldiazoacetate, **7c** (0.528 g, 3 mmol, 1.5 equiv) and **(L-Me)$_4$Ni$_4$(MeOH)** (0.032 g, 1.25 mol%), **8c** was isolated as a white solid (0.277 g, 44%). **MP**: 125-127 ^{o}C; **R*f*** = 0.35 (Hex/EA = 9:1); ^{1}**H NMR** (400 MHz, CDCl$_3$, ppm) *δ:* 7.25-7.24 (m, **3H**), 7.14-7.09 (m, **2H**), 6.05 (d, *J* = 61.0 Hz, **1H**), 5.16 (d, *J* = 29.6 Hz, **1H**), 4.65 (dd, *J* = 40.1, 6.6 Hz, **2H**), 3.62 (d, *J* = 11.8 Hz, **3H**), 3.32 (d, *J* = 6.4 Hz, **1H**), 1.52 (d, *J* = 57.2 Hz, **9H**); ^{13}**C NMR** (101 MHz, CDCl$_3$, ppm) *δ:* 174.16, 173.86, 151.38, 132.72, 132.45, 131.24, 130.85, 130.55, 127.90, 127.81, 121.42, 127.28, 107.33, 81.6, 52.53, 49.29, 39.61, 38.31, 29.71, 28.17; **HRMS** (ESI): *m/z* calculated for $C_{18}H_{21}NNaO_4$ [M+Na]$^+$: 338.1363; found: 338.1364; **FT-IR** υ_{max} (neat)/cm^{-1}: 2979, 1710, 1474, 1391, 1351, 1242, 1391, 1196, 1149, 748, 731, 700.

2-(*Tert*-butyl) 6-methyl (1S,5S,6R)-6-phenyl-2-azabicyclo[3.1.0]hex-3-ene-2,6-dicarboxylate

(8d): Following GP-5, starting from *N*-pivaloyl pyrrole, **6b** (0.302 g, 2 mmol, 1.0 equiv), methyl phenyldiazoacetate, **7c** (0.528 g, 3 mmol, 1.5 equiv) and **(L-Me)$_4$Ni$_4$(MeOH)** (0.032 g, 1.25 mol%), **8d** was isolated as a white solid (0.281 g, 47%). **MP:** 139-142 ^{o}C; **R*f*** = 0.2 (Hex/EA = 9:1); ^{1}**H NMR** (400 MHz, CDCl$_3$, ppm) *δ:* 7.22-7.21 (m, **3H**), 7.06-7.05 (m, 2**H**), 6.26 (s, **1H**), 5.30 (s, **1H**), 4.90 (d, *J* = 6.6 Hz, **1H**), 3.61 (s, **3H**), 3.26-3.21(m, **1H**), 1.10 (s, **9H**); ^{13}**C NMR** (101 MHz, CDCl$_3$, ppm) *δ:* 175.46, 173.71, 132.75, 130.92, 127.81, 127.32, 109.93, 52.60, 50.32, 39.07, 31.01, 27.59; **HRMS** (ESI): *m/z* calculated for $C_{18}H_{21}NNaO_3$ [M+Na]$^+$: 322.1410; found: 322.1414; $C_{18}H_{22}NNaO_3$ [M+H]$^+$: 300.1590; found: 300.1594; **FT-IR** υ_{max} (neat)/cm^{-1}: 2979, 1704, 1481, 1393, 1236, 1197, 1148, 1086, 1047, 748, 731, 700.

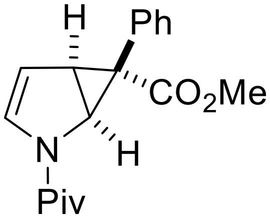

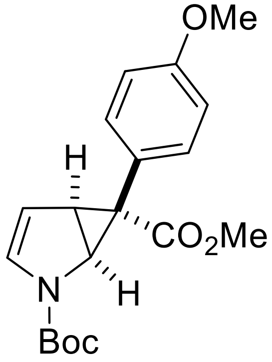

2-(*tert*-butyl) 6-methyl (1S,5S,6R)-6-(4-methoxyphenyl)-2-azabicyclo[3.1.0]hex-3-ene-2,6-dicarboxylate (8e): Following GP-5, starting from *N*-Boc pyrrole, **6a** (0.334 g, 2 mmol, 1.0 equiv), methyl 4-methoxy-phenyldiazoacetate, **7d** (0.619 g, 3 mmol, 1.5 equiv) and **(L-Me)$_4$Ni$_4$(MeOH)** (0.032 g, 1.25 mol%), **8e** was isolated as a colorless gummy solid (0.311 g, 45%). **R_f** = 0.1 (Hex/EA = 4:1); **^{1}H NMR** (400 MHz, $CDCl_3$, ppm) δ: 7.05-7.01 (m, 2H), 6.78 (d, J = 8.7 Hz, 2H), 6.07 (dd, J = 65.0, 3.0 Hz, 1H), 5.14 (d, J = 29.5 Hz, 1H), 4.61 (dd, J = 40, 8. Hz, 1H), 3.77 (s, 3H), 3.61 (d, J = 12 Hz, 3H), 3.28 (d, J = 8 Hz, 1H), 1.51 (d, J = 52 Hz, 9H); **^{13}C NMR** (101 MHz, $CDCl_3$, ppm) δ: 174.18, 158.64, 151.40, 133.75, 130.65, 123.14, 113.33, 107.27, 81.60, 55.09, 52.52, 49.35, 39.74, 38.44, 28.18; **HRMS** (ESI): *m/z* calculated for $C_{19}H_{24}NO_5$ $[M+H]^+$: 346.1657 found = 346.1649; $C_{25}H_{27}NNaO_5$ $[M+Na]^+$: 444.1793; found: 444.1781; **FT-IR** υ_{max} (neat)/cm^{-1}: 2985, 1694, 1508, 1393, 1334, 1236, 1144, 962, 732.

Methyl (1S,5S,6R)-6-(4-methoxyphenyl)-2-pivaloyl-2-azabicyclo[3.1.0]hex-3-ene-6-carboxylate (8f): Following GP-5, starting from *N*-pivaloyl pyrrole, **6b** (0.302 g, 2 mmol, 1.0 equiv), methyl 4-methoxy-phenyldiazoacetate, **7d** (0.619 g, 3 mmol, 1.5 equiv) and **(L-Me)$_4$Ni$_4$(MeOH)** (0.032 g, 1.25 mol%), **8f** was isolated as a colorless gummy solid (0.323 g, 49%). **R_f** = 0.25 (Hex/EA = 9:1); **^{1}H NMR** (400 MHz, $CDCl_3$, ppm) δ: 6.96 (d, *J* = 8.0 Hz, 2H), 6.75 (d, *J* = 8.0 Hz, 2H), 6.29 (s, 1H), 5.28 (s, 1H), 4.86 (d, *J* = 8 Hz, 1H), 3.74 (s, 3H), 3.61 (s, 3H), 3.19 (d, J = 4 Hz 1H), 1.11 (s, 9H); **^{13}C NMR** (101 MHz, $CDCl_3$, ppm) δ: 175.47, 174.03, 158.69, 133.78, 122.87, 113.32, 55.13, 52.58, 50.36, 39.08, 27.64; **HRMS** (ESI): *m/z* calculated for $C_{19}H_{24}NO_4$ $[M+H]^+$: 330.1700; found = 330.1703; **FT-IR** υ_{max} (neat)/cm^{-1}: 2965, 1704, 1643, 1514, 1400, 1335, 1247, 1208, 907, 728, 648.

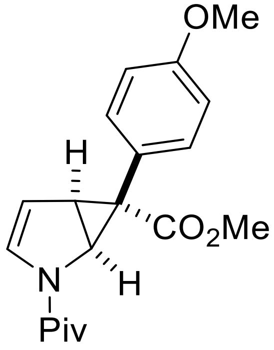

Synthesis of 2-(*Tert*-butyl)-1-ethyl-1a,6b-dihydrocyclopropa[b]indole-1,2(1H)-dicarboxylate (8g): Following the GP-4, starting from *N*-Boc indole, **6c** (0.434 g, 2 mmol, 1.0 equiv), ethyl 2-diazoacetate, **7a** (0.316 g, 3 mmol, 1.5 equiv) and **(L-Me)$_4$Ni$_4$(MeOH)** (0.032 g, 1.25 mol%), **8g** was isolated as a colorless liquid (0.216 g) as a mixture with its *endo*-diastereomer in a ratio of 9:1. Accordingly the corrected yield of the major diastereomer **8g** was calculated as 32%. **R$_f$** = 0.47 (Hex/EA = 10:1); **^{1}H NMR** (400 MHz, CDCl$_3$, ppm) δ: 7.75-7.39 (br, **1H**, Ar*H*), 7.26 (d, *J* = 8 Hz, **1H**, Ar*H*), 7.11 (t, *J* = 8 Hz, **1H**, Ar*H*), 6.92 (t, *J* = 8 Hz, **1H**, Ar*H*), 4.51 (br, **1H**), 4.08 (q, *J* = 4 Hz, **2H**, -OCH_2CH$_3$), 3.12 (d, *J* = 6.56 Hz, **1H**), 1.51 (s, **9H**, -C(CH_3)$_3$), 1.19 (t, *J* = 7.08 Hz, **3H**, -CH_3) 1.11 (s, **1H**); **^{13}C NMR** (101 MHz, CDCl$_3$, ppm) δ: 172.2, 152.5, 127.7, 124.5, 122.5, 115.2, 77.4, 60.9, 45.6, 28.3, 28.2, 24.2, 14.2; **FT-IR υ$_{max}$** (neat)/cm^{-1}: 2978, 2933, 1706, 1632, 1606, 1476, 1370, 1353, 1289, 1254, 1147, 1106, 1068, 1045, 912, 884, 846, 811, 749, 620; **HRMS** (ESI): *m/z* calculated for $C_{17}H_{21}NNaO_4$ [M+Na]$^+$: 326.1363; found: 326.1357.

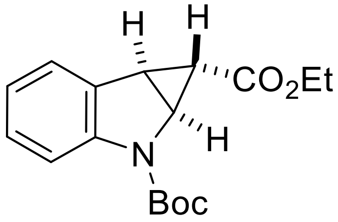

Synthesis of Di-*tert*-butyl-1a,6b-dihydrocyclopropa[b]indole-1,2(1H)-dicarboxylate (8h): Following the GP-4, starting from *N*-Boc indole, **6c** (0.434 g, 2 mmol, 1.0 equiv), *tert*-butyl 2-diazoacetate, **7b** (0.426 g, 3 mmol, 1.5 equiv) and **(L-Me)$_4$Ni$_4$(MeOH)** (0.032 g, 1.25 mol%), **8h** was isolated as a white solid (0.218 g, 33 %). **R$_f$** = 0.53 (Hex/EA = 10:1); **MP:** 83-85 °C; **^{1}H NMR** (400 MHz, CDCl$_3$, ppm) δ: 7.78-7.32 (m, **1H**, Ar*H*), 7.28 (d, *J* = 7.4 Hz, **1H**, Ar*H*), 7.11 (t, *J* = 7.8 Hz, **1H**, Ar*H*), 6.89 (t, *J* = 7.4 Hz, **1H**, Ar*H*), 4.70-4.19 (br, **1H**), 3.06 (dd, *J* = 6.7, 3.0 Hz, **1H**), 1.51 (s, **9H**, -C(CH_3)$_3$), 1.39 (d, **9H**, -C(CH_3)$_3$), 1.04 (s, **1H**) (signal broadening due to rotamers)[25]; **^{13}C NMR** (101 MHz, CDCl$_3$, ppm) δ: 171.4, 152.0, 130.1, 127.6, 124.5, 122.4, 115.4, 81.0, 45.4, 28.3, 28.1, 28.0, 25.2 (signal doubling due to rotamers) [25]; **FT-IR υ$_{max}$** (neat)/cm^{-1}: 2976, 2932, 1705, 1636, 1607, 1477, 1466, 1388, 13564, 1292, 1268, 1255, 1235, 1139, 1105, 1066, 1046, 913, 884, 837, 811, 785, 747, 621; **HRMS** (ESI): *m/z* calculated for $C_{19}H_{26}NO_4$ [M+H]$^+$: 332.1856; found: 332.1817.

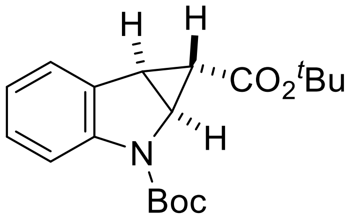

Di-*tert*-butyl fumarate (**8b′**) has been obtained as the minor product (11%, based on the diazoester): **^{1}H NMR** (400 MHz, $CDCl_3$, ppm) δ: 6.65 (s, 2H), 1.48 (s, 18H); **^{13}C NMR** (101 MHz, $CDCl_3$, ppm) δ: 163.40, 133.56, 80.63, 26.96.

2-(*Tert*-butyl)1-methyl-6b-methyl-1-phenyl-1a,6b-dihydrocyclopropa[b]indole-1,2(1H)-dicarboxylate (8i, major product): Following the GP-5, starting from *N*-Boc indole, **6c** (0.434 g, 2 mmol, 1.0 equiv), methyl-2-diazo-2-phenylacetate, **7c** (0.529 g, 3 mmol, 1.5 equiv) and **(L-Me)$_4$Ni$_4$(MeOH)** (0.032 g, 1.25 mol%), **8i** was isolated as a colorless gummy solid (0.394 g, 54%). **R*f*** = 0.25 (Hex/EA = 9:1); **^{1}H NMR** (400 MHz, $CDCl_3$, ppm) δ: 7.43-7.38 (m, **2H**), 7.05-6.90 (m, **7H**), 4.91 (dd, *J* = 43.0, 5.3 Hz, **1H**), 3.73 (s, **1H**), 3.66 (d, *J* = 10.3 Hz, **3H**), 1.65-1.53 (m, **9H**); **^{13}C NMR** (101 MHz, $CDCl_3$, ppm) δ: 173.65, 151.64, 142.42, 141.34, 132.34, 132.01, 30.30 128.39, 127.87, 127.59, 125.57, 125.11, 122.37, 114.62, 81.86, 52.79, 50.57, 35.50, 28.45; **HRMS** (ESI): *m/z* calculated for $C_{22}H_{23}NNaO_4$ $[M+Na]^+$: 388.1519; found: 388.1520; **FT-IR** υ_{max} (neat)/cm^{-1}: 2981, 1712, 1478, 1392, 1354, 1309, 1242, 1195, 1153, 1084, 1049, 729.

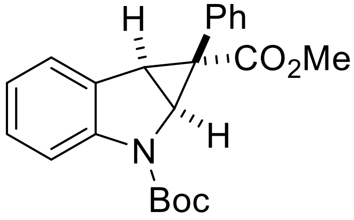

Methyl 2-methyl-7-phenylbicyclo[4.1.0]hept-3-ene-7-carboxylate (8i′, minor product):

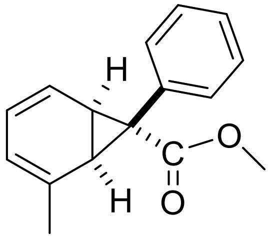

^{1}H NMR (400 MHz, $CDCl_3$, ppm) δ: 7.19-7.16 (m, 3H), 7.05 – 7.03 (m, 2H), 6.03 (dd, *J* = 8, 4 Hz, 1H), 5.72(dd, *J* = 8, 4 Hz, 1H), 5.56 (d, *J* = 5 Hz, 1H), 3.64 (s, 3H), 3.25 (dd, *J* = 8, 4 Hz, 1H), 3.11 (d, *J* = 8 Hz, 1H), 2.10 (s, 3H); **^{13}C NMR** (101 MHz, $CDCl_3$, ppm) δ: 176.17, 132.56, 131.36, 126.10, 125.82, 125.08, 121.08, 120.72, 51.87, 43.87, 41.47, 25.81, 22.97, 20.82.

Methyl (1R,1aS,6bS)-1-phenyl-2-pivaloyl-1,1a,2,6b-tetrahydrocyclopropa[b]indole-1-carboxylate (8j): Following GP-5, starting from *N*-pivaloyl indole, **6d** (0.604 g, 2 mmol, 1.0

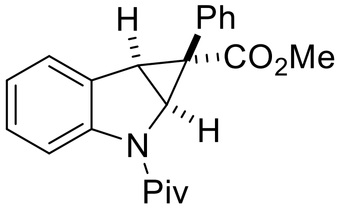

equiv), methyl-2-diazo-2-phenylacetate, **7c** (0.529 g, 3 mmol, 1.5 equiv) and **(L-Me)$_4$Ni$_4$(MeOH)** (0.032 g, 1.25 mol%), **8j** was isolated as a colorless gummy solid (0.356 g, 51%). **R*f*** = 0.3 (Hex/EA = 9:1); **^{1}H NMR** (400 MHz, CDCl$_3$, ppm) *δ:* 7.83 (d, *J* = 7.4 Hz, **1H**), 7.37 (d, *J* = 7.3 Hz, **1H**) 7.04-6.95 (m, **7H**), 5.21 (d, *J* = 7.0 Hz, **1H**), 3.84 (d, *J* = 7.0 Hz, **1H**), 3.69 (s, **3H**), 1.57 (s, **9H**); **^{13}C NMR** (101 MHz, CDCl$_3$, ppm) *δ:* 176.98, 173.41, 144.07, 131.77, 129.95, 128.41, 127.95, 127.66, 127.29, 125.04, 23.56, 117.81, 53.00, 51.85, 40.82, 36.71, 32.31, 28.24; **HRMS** (ESI): *m/z* calculated for $C_{22}H_{24}NO_3$ [M]: 350.1751; found: 350.1751; **FT-IR** υ_{max} (neat)/cm^{-1}: 2979, 1712, 1477, 1391, 1350, 1239, 1194, 1150, 1090, 750, 731, 699.

Methyl 2-methyl-7-phenylbicyclo[4.1.0]hept-3-ene-7-carboxylate (**8i′**) has been obtained as the minor product (15%, based on the diazoester).

Methyl (1R,1aS,6bS)-2-acetyl-1-phenyl-1,1a,2,6b-tetrahydrocyclopropa[b]indole-1-carboxylate (8k): Following GP-5, starting from *N*-acetyl indole, **6e** (0.218 g, 2 mmol, 1.0

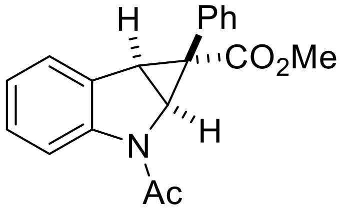

equiv), methyl-2-diazo-2-phenylacetate, **7c** (0.529 g, 3 mmol, 1.5 equiv) and **(L-Me)$_4$Ni$_4$(MeOH)** (0.032 g, 1.25 mol%), **8k** was isolated as a white solid (0.399 g, 65%). **MP:** 173-175 ^{o}C; **R*f*** = 0.3 (Hex/EA = 4:1);**^{1}H NMR** (400 MHz, CDCl$_3$, ppm) *δ*: 7.74 (d, *J* = 7.4 Hz, **1H**), 7.40 (d, *J* = 6.1 Hz, **1H**), 7.06-6.90 (m, **7H**) 4.79 (s, **1H**), 3.79 (d, *J* = 6.9 Hz, **1H**), 3.68 (s, **3H**), 2.54 (s, **3H**); **^{13}C NMR** (101 MHz, CDCl$_3$, ppm) *δ*: 173.13, 68.87, 142.61, 132.16, 131.78, 129.70, 128.78, 128.14, 127.92, 127.92, 127.50, 125.15, 123.68, 116.80, 113.16, 52.97, 51.35, 35.93, 32.86, 24.54; **HRMS** (ESI): *m/z* calculated for $C_{19}H_{18}NO_3$ [M+H]$^+$: 350.1202; found: 308.1278; **FT-IR** υ_{max} (neat)/cm^{-1}: 2986, 1714, 1474, 1393, 1353, 1238, 1191, 1150, 1089, 907, 748, 699.

Methyl 2-methyl-7-phenylbicyclo[4.1.0]hept-3-ene-7-carboxylate (**8i′**) has been obtained as the minor product (12%, based on the diazoester).

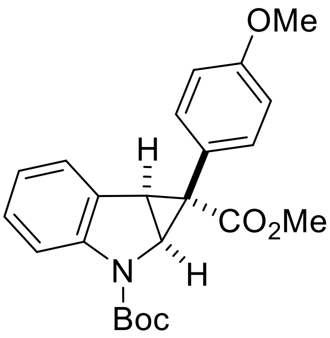

Methyl (1S,5S,6R)-6-(4-methoxyphenyl)-2-pivaloyl-2-azabicyclo[3.1.0]hex-3-ene-6-carboxylate (8l): Following the General procedure-5, starting from *N*-Boc indole, **6c** (0.434 g, 2 mmol, 1.0 equiv), methyl 4-methoxyphenyldiazoacetate, **7d** (0.619 g, 3 mmol, 1.5 equiv) and **(L-Me)$_4$Ni$_4$(MeOH)** (0.032 g, 1.25 mol%), **8l** was isolated as a pale yellow gummy solid (0.625 g, 79%). **R$_f$** = 0.25 (Hex/EA = 4:1); **^{1}H NMR** (400 MHz, CDCl$_3$, ppm) δ: 6.96 (d, *J* = 8.0 Hz, 2H), 6.75 (d, *J* = 8.0 Hz, 2H), 6.29 (s, 1H), 5.28 (s, 1H), 4.86 (d, *J* = 8 Hz, 1H), 3.74 (s, 3H), 3.61 (s, 3H), 3.19 (d, J = 4 Hz 1H), 1.11 (s, 9H); **^{13}C NMR** (101 MHz, CDCl$_3$, ppm) δ: 173.96, 158.48, 152.90, 133.37, 133.00, 128.39, 127.87, 125.04, 122.20, 114.66, 54.95, 50.68, 35.59, 28.47, 14.14; **HRMS** (ESI): *m/z* calculated for $C_{23}H_{25}NO_5$ $[M+Na]^+$: 418.1625; found: 418.1638; **FT-IR** υ_{max} (neat)/cm^{-1}: 2969, 1703, 1514, 1478, 1381, 1323, 1240, 1149, 1110, 1027, 750, 725.

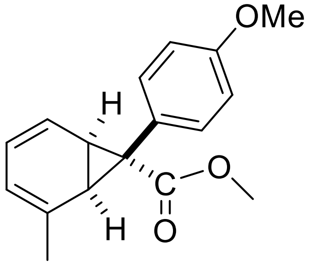

Methyl 7-(4-methoxyphenyl)-2-methylbicyclo[4.1.0]hept-3-ene-7-carboxylate (8l′, minor product): **^{1}H NMR** (400 MHz, CDCl$_3$, ppm) δ: 6.93 (d, J = 8 Hz, 2H), 6.71 (d, J = 8 Hz, 2H), 6.01 (dd, J = 8, 4 Hz, 1H), 5.73 (t, J = 8 Hz 1H), 5.56 (d, J = 2 Hz, 1H), 3.75 (s, 3H), 3.64 (s, 3H), 3.20 (s, 1H), 3.05 (d, J = 8 Hz, 1H), 2.08 (s, 3H). **^{13}C NMR** (101 MHz, CDCl$_3$, ppm) δ: 177.62, 158.24, 133.43, 126.19, 125.05, 122.10, 121.73, 112.67, 55.03, 52.95, 44.44, 41.24, 24.07.

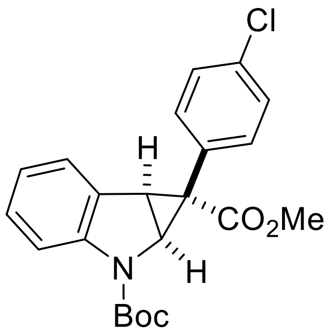

2-(*Tert*-butyl) 1-methyl (1R,1aS,6bS)-1-(4-chlorophenyl)-1a,6b-dihydrocyclopropa[b]indole-1,2(1H)-dicarboxylate (8m): Following the GP-5, starting from *N*-Boc indole, **6c** (0.434 g, 2 mmol, 1.0 equiv), methyl 4-chloro-phenyldiazoacetate, **7f** (0.632 g, 3 mmol, 1.5 equiv) and **(L-Me)$_4$Ni$_4$(MeOH)** (0.032 g, 1.25 mol%), **8m** was isolated as a colorless solid (0.296 g, 37%). **MP**: 155-158 °C; **R$_f$** = 0.5 (Hex/EA = 4:1); **^{1}H NMR** (400 MHz, CDCl$_3$, ppm) δ: 7.37 (d, *J* = 8.0 Hz, 1H), 7.01 6.91 (m, 6H), 4.90 (dd, *J* = 44, 8 Hz, 1H), 3.72 (s, 1H), 3.66 (d, *J* = 20 Hz, 3H), 1.61 (d, *J* = 20 Hz, 9H); **^{13}C NMR** (101 MHz, $CDCl_3$, ppm) δ: 171.88, 140.18, 132.23, 128.21, 124.04, 121.40, 81.01, 49.55, 33.62, 30.41, 27.25, 21.31, 13.05; **HRMS** (ESI): *m/z* calculated for $C_{22}H_{23}NO_4Cl$ $[M+H]^+$: 400.1310; found: 400.1330; **FT-IR** υ_{max} (neat)/cm^{-1}: 2982, 1707, 1479, 1381, 1320, 1245, 1149, 1088, 1015, 720.

2-(*Tert*-butyl) 6-methyl (1S,5S,6R)-6-(4-methoxyphenyl)-2-azabicyclo[3.1.0]hex-3-ene-2,6-dicarboxylate (8n): Following the GP-5, starting from *N*-pivaloyl indole, **6d** (0.402 g, 2 mmol, 1.0 equiv), methyl 4-methoxyphenyldiazoacetate, **7d** (0.619 g, 3 mmol, 1.5 equiv) and **(L-Me)$_4$Ni$_4$(MeOH)** (0.032 g, 1.25 mol%), **8n** was isolated as a colorless crystalline solid (0.622 g, 82%). **MP:** 85- 88 °C; **R$_f$** = 0.3 (Hex/EA = 4:1); **^{1}H NMR** (400 MHz, $CDCl_3$, ppm) δ: 7.84 (d, *J* = 8.0 Hz, 1H), 7.36 (d, *J* = 8 Hz, 1H), 7.04 – 6.93 (m, 2H), 6.88 (d, *J* = 8 Hz, 2H), 6.56 (d, *J* = 8 Hz, 2H), 5.17 (d, *J* = 8.0 Hz, 1H), 3.80 (d, *J* = 8.0 Hz, 1H), 3.69 (s, 3H), 3.65 (s, 3H), 1.55 (s, 9H); **^{13}C NMR** (101 MHz, $CDCl_3$, ppm) δ:177.01, 17.73, 158.45, 144.21, 132.80, 128.45, 127.97, 124.94, 123.51, 121.78, 117.80, 113.23, 54.94, 52.97, 40.79, 36.82, 31.70, 28.33; **HRMS** (ESI): *m/z* calculated for $C_{23}H_{26}NO_4$ $[M+H]^+$: 380.1856; found: 380.1861; **FT-IR** υ_{max} (neat)/cm^{-1}: 2952, 1710, 1660, 1514, 1467, 1356, 1247, 1180, 1031, 755, 728.

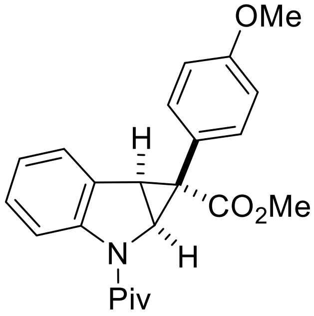

Methyl 7-(4-methoxyphenyl)-2-methylbicyclo[4.1.0]hept-3-ene-7-carboxylate (**8l′**) has been obtained as the minor product (14%, based on the diazoester).

Methyl (1R,1aS,6bS)-2-acetyl-1-(4-methoxyphenyl)-1,1a,2,6b-tetrahydrocyclopropa[b]indole-1-carboxylate (8o): Following the GP-5, starting from *N*-acetyl indole, **6e** (0.318 g, 2 mmol, 1.0 equiv), methyl 4-methoxyphenyldiazoacetate, **7d** (0.619 g, 3 mmol, 1.5 equiv) and **(L-Me)$_4$Ni$_4$(MeOH)** (0.032 g, 1.25 mol%), **8o** was isolated as a white solid (0.580 g, 86%). **MP:** 181-184 °C; **R$_f$** = 0.3 (Hex/EA = 4:1); **^{1}H**

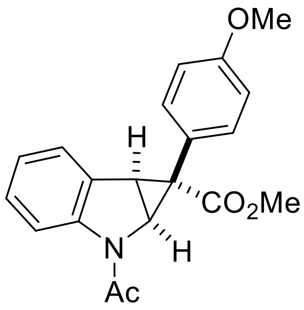

NMR (400 MHz, $CDCl_3$, ppm) δ: 7.77 (d, J = 8.0 Hz, 1H), 7.39 (d, J = 8.0 Hz, 1H), 7.04- 6.95 (m, 3H), 6.80 (d, J = 8.0 Hz, 2H), 6.59 (d, J = 8.0 Hz, 2H), 4.76 (d, J = 8.0 Hz, 1H), 3.76 (d, J = 8.0 Hz, 1H), 3.68 (s, 3H), 3.65 (s, 3H), 2.52 (s, 3H); **^{13}C NMR** (101 MHz, $CDCl_3$, ppm) δ:173.43, 168.91, 158.63, 142.74, 132.74, 128.84, 125.07, 123.65, 121.51, 116.82, 113.51, 54.96, 52.96, 51.46, 36.05, 32.25, 24.56; **HRMS** (ESI): m/z calculated for $C_{20}H_{26}NO_4$ $[M+H]^+$: 338.1387; found: 338.1392; **FT-IR** υ_{max} (neat)/cm^{-1}: 2959, 1710, 1671, 1467, 1384, 1312, 1241, 1191, 955, 758, 705.

Methyl 7-(4-methoxyphenyl)-2-methylbicyclo[4.1.0]hept-3-ene-7-carboxylate (**8l′**) has been obtained as the minor product (10%, based on the diazoester).

2-(*Tert*-butyl) 1-ethyl (1R,1aS,6bS)-1-(3,4-dimethoxyphenyl)-1a,6b-dihydrocyclopropa[b]indole-1,2(1H)-dicarboxylate (8p): Following the GP-5, starting from

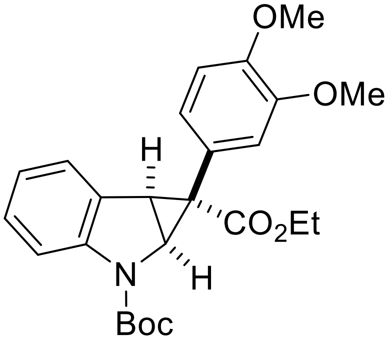

N-Boc indole, **6c** (0.434 g, 2 mmol, 1.0 equiv), methyl 3,4-methoxy-phenyldiazoacetate, **7e** (0.708 g, 3 mmol, 1.5 equiv) and **(L-Me)$_4$Ni$_4$(MeOH)** (0.032 g, 1.25 mol%), **8p** was isolated as a colorless liquid (0.185 g, 21%). **R*f*** = 0.5 (Hex/EA = 4:1); **^{1}H NMR** (400 MHz, $CDCl_3$, ppm) δ: 7.38 (d, J = 4 Hz, 1H), 7.04-6.98 (m, 2H), 6.91 (dt, J = 8, 4 Hz, 1H), 6.59 – 6.34 (m, 3H), 4.88 (dd, J = 44, 8 Hz, 1H), 4.15 (s, 2H), 3.74 (s, 3H), 3.69 (s, 1H), 3.62 (d, J = 16 Hz, 3H), 1.60 (d, J = 24 Hz, 9H), 1.19 (t, J = 8 Hz, 3H); **^{13}C NMR** (101 MHz, $CDCl_3$, ppm) δ: 173.19, 148.04, 129.48, 127.97, 127.75, 125.32, 124.88, 122.16, 115.24, 114.72, 110.27, 82.59, 61.43, 55.53, 34.42, 28.32, 14.25; **HRMS** (ESI): m/z calculated for $C_{25}H_{29}NO_6Na$ $[M+Na]^+$: 462.1887; found: 462.1887; **FT-IR** υ_{max} (neat)/cm^{-1}: 1706, 1520, 1264, 1152, 1029, 732, 698.

Ethyl (1R,1aS,6bS)-1-(3,4-dimethoxyphenyl)-2-pivaloyl-1,1a,2,6b-tetrahydrocyclopropa[b]indole-1-carboxylate (8q): Following the GP-5, starting from *N*-pivaloyl indole, **6d** (0.402 g, 2 mmol, 1.0 equiv), methyl 3,4-methoxy-phenyldiazoacetate, **7e** (0.708 g, 3 mmol, 1.5 equiv) and **(L-Me)$_4$Ni$_4$(MeOH)** (0.032 g, 1.25 mol%), **8q** was isolated as a white gummy solid (0.381 g, 45%). **R$_f$** = 0.25 (Hex/EA = 4:1); **^{1}H NMR** (400 MHz, CDCl$_3$, ppm) δ: 7.84 (d, *J* = 8.0 Hz, **1H**), 7.36 (d, *J* = 6.5 Hz, **1H**), 7.02-6.93 (m, **2H**), 6.59 (s, **2H**), 6.39 (s, **1H**) 5.15 (d, *J* = 7.0 Hz, **1H**), 4.18 (qd, *J* = 6.9, 1.7 Hz, **2H**), 3.80 (d, *J* = 7.0 Hz, **1H**), 1.54 (s, **9H**) 1.19 (t, *J* = 7.1 Hz, **3H**); **^{13}C NMR** (101 MHz, CDCl$_3$, ppm) δ: 176.92, 172.94, 147.92, 144.31, 128.61, 128.61, 128.05, 124.77, 124.35, 123.46, 122.30, 117.93, 115.16, 110.27, 61.68, 55.72, 55.50, 51.87, 40.80, 36.49, 32.26, 51.87, 40.80, 36.49, 32.26, 28.19, 14.29; **HRMS** (ESI): *m/z* calculated for C$_{25}$H$_{30}$NO$_5$ [M+H]$^+$: 424.2118; found: 424.2113; **FT-IR** υmax (neat)/cm^{-1}: 2976, 1702, 1604, 1518, 1462, 1359, 1297, 1245, 1188, 1059, 1026, 974, 938, 883, 853, 804, 757.

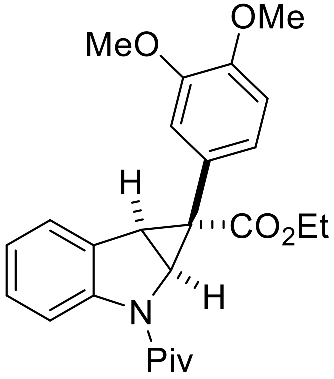

Synthesis of 2-(*Tert*-butyl) 1-ethyl 6b-methyl-1a,6b-dihydrocyclopropa[b]indole-1,2(1H)-dicarboxylate (8r): Following the GP-4, starting from 3-methyl-N-Boc indole, **6f** (0.462 g, 2 mmol, 1.0 equiv), ethyl 2-diazoacetate, **7a** (0.316 g, 3 mmol, 1.5 equiv) and **(L-Me)$_4$Ni$_4$(MeOH)** (0.032 g, 1.25 mol%), **8r** was isolated as a colorless liquid (0.089 g, 28%). **R$_f$** = 0.56 (Hex/EA = 9:1); **^{1}H NMR** (400 MHz, CDCl$_3$) δ ppm: 7.81 (s, **1H**, ArH), 7.32 (d, *J* = 7.4 Hz, **1H**,ArH), 7.21 (t, *J* = 7.8 Hz, **1H**,ArH), 7.02 (t, *J* = 7.5 Hz, **1H**,ArH), 4.53 (s, **1H**, —NC*H*—(CH)$_2$), 4.18 (q, *J* = 7.1 Hz, **2H**, OC(CH_3)$_3$), 1.70 (s, **3H**, —CCH_3), 1.59 (s, **9H**, OC(CH_3)$_3$), 1.28 (t, *J* = 7.1 Hz, **4H**, CH$_2$CH_3, *H*); **^{13}C NMR** (100 MHz, CDCl$_3$) δ ppm: 171.35, 133.63, 127.70, 123.00, 122.97, 122.93, 122.39, 115.49, 93.68, 60.68, 49.90, 28.93, 28.38, 28.05, 14.30, 11.32.

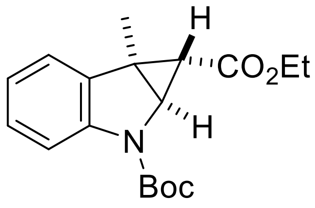

Synthesis of Di-*tert*-butyl-6b-methyl-1a,6b-dihydrocyclopropa[b]indole-1,2(1H)-dicarboxylate (8r′): Following the GP-4, starting from 3-methyl-N-Boc indole, **6f** (0.462 g, 2 mmol, 1.0 equiv), **7b** (0.320 g, 3 mmol, 1.5 equiv) and **(L-Me)$_4$Ni$_4$(MeOH)** (0.032 g, 1.25 mol%), **8r′** was isolated as a yellow liquid (0.079 g, 23%). **R*f*** = 0.43 (Hex/EA = 10:1); **^{1}H NMR** (400 MHz, CDCl$_3$, ppm) *δ*: 8.00-7.33 (m, **1H**, Ar*H*), 7.25 (d, *J* = 7.5 Hz, **1H**, Ar*H*), 7.12 (t, *J* = 7.5 Hz, **1H**, Ar*H*), 6.93 (t, *J* = 7.5 Hz, **1H**, Ar*H*), 4.38 (br, **1H**), 1.62 (s, **3H**), 1.52 (s, **9H**, -C(CH_3)$_3$) 1.12 (s, **9H**, -C(CH_3)$_3$), 1.12 (s, **1H**); **^{13}C NMR** (101 MHz, CDCl$_3$, ppm) *δ*: 174.2, 167.5, 149.4, 127.5, 122.9, 122.3, 115.3, 81.0, 49.6, 28.9, 28.3, 28.0, 11.3; **FT-IR** υ_{max} (neat)/cm^{-1}: 2977, 2932, 1707, 1605, 1477, 1455, 1391, 1365, 1326, 1296, 1270, 1254, 1143, 1114, 1098, 1078, 1057, 1026, 1008, 958, 893, 858, 842, 747, 701, 678; **HRMS** (ESI): *m/z* calculated for $C_{20}H_{28}NO_4$ [M+H]$^+$: 346.2013; found: 346.2009.

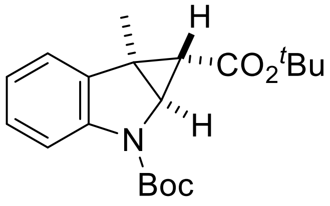

2-(*Tert*-butyl) 1-methyl-6b-methyl-1-phenyl-1a,6b-dihydrocyclopropa[b]indole-1,2(1H)-dicarboxylate (8s): Following the GP-5, starting from 3-methyl-N-Boc indole, **6f** (0.462 g, 2 mmol, 1.0 equiv), methyl-2-diazo-2-phenylacetate, **7c** (0.529 g, 3 mmol, 1.5 equiv) and **(L-Me)$_4$Ni$_4$(MeOH)** (0.032 g, 1.25 mol%), **8s** was isolated as a white solid (0.326 g, 43%). **MP:** 115-120 °C; **R*f*** = 0.5 (Hex/EA = 9:1); **^{1}H NMR** (400 MHz, CDCl$_3$, ppm) *δ*: 7.41-7.31 (m, **2H**), 7.01-6.93 (m, **7H**), 5.00 (d, *J* = 49.7 Hz, **1H**), 3.66 (s, **3H**), 1.84 (s, **3H**), 1.63 (d, *J* = 26.4 Hz, **9H**); **^{13}C NMR** (101 MHz, CDCl$_3$, ppm) *δ*: 172.10, 151.75, 141.67, 132.09, 129.23, 127.82, 127.44, 126.99, 124.15, 123.73, 122.21, 114.34, 81.61, 53.40, 52.51, 39.65, 28.35, 13.26; **HRMS** (ESI): *m/z* calculated for $C_{23}H_{25}NNaO_4$ [M+Na]$^+$: 402.1676; found: 402.1678; **FT-IR** υ_{max} (neat)/cm^{-1}: 2979, 1708, 1477, 1392, 1353, 1240, 1192, 1150, 1087, 749, 730, 701.

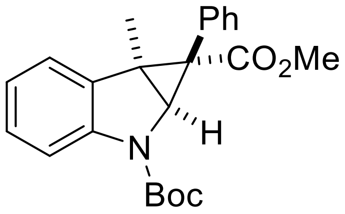

Methyl 2-methyl-7-phenylbicyclo[4.1.0]hept-3-ene-7-carboxylate (**8i′**) has been obtained as the minor product (16%, based on the diazoester).

Methyl (1S,1aS,6bS)-6b-methyl-1-phenyl-2-pivaloyl-1,1a,2,6b-tetrahydrocyclopropa[b]indole-1-carboxylate (8t): Following the GP-5, starting from 3-methyl-N-pivaloyl indole, **6d** (0.430 g, 2 mmol, 1.0 equiv), methyl-2-diazo-2-phenylacetate, **7c** (0.529 g, 3 mmol, 1.5 equiv) and **(L-Me)₄Ni₄(MeOH)** (0.032 g, 1.25 mol%), **8t** was isolated as a colorless gummy solid (0.472 g, 65%). **R*f*** = 0.4 (Hex/EA = 9:1);

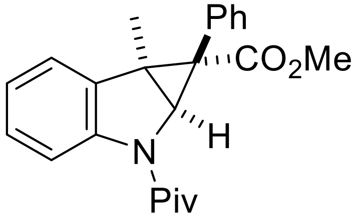

^{1}H NMR (400 MHz, CDCl$_3$, ppm) δ: 7.83-7.81 (m, **1H**), 7.33-7.31 (m, **1H**), 7.00-6.95 (m, **7H**), 5.28 (s, **1H**), 3.69 (s, **3H**), 1.86 (s, **3H**), 1.59 (s, **9H**); **^{13}C NMR** (101 MHz, CDCl$_3$, ppm) δ: 13.26; **^{13}C NMR** (101 MHz, CDCl$_3$, ppm) δ*:* 176.90, 171.93, 143.35, 132.70, 131.58, 131.51, 127.91, 127.46, 127.04, 123.57, 123.40, 117.63, 54.61, 52.78, 40.79, 40.68, 37.27, 28.21, 13.39; **HRMS** (ESI): *m/z* calculated for $C_{23}H_{26}NO_3$ $[M+H]^+$: 364.1907; found: 364.1901; **FT-IR** υ_{max} (neat)/cm^{-1}: 2979, 1713, 1476, 1390, 1352, 1241, 1196, 1150, 747, 729, 702.

Methyl 2-methyl-7-phenylbicyclo[4.1.0]hept-3-ene-7-carboxylate (**8i′**) has been obtained as the minor product (12%, based on the diazoester).

2-(*Tert*-butyl) 1-methyl (1S,1aS,6bS)-1-(4-methoxyphenyl)-6b-methyl-1a,6b-dihydrocyclopropa[b]indole-1,2(1H)-dicarboxylate (8u): Following the GP-5, starting from 3-methyl-N-Boc indole, **6f** (0.462 g, 2 mmol, 1.0 equiv), **7d** (0.619 g, 3 mmol, 1.5 equiv) and **(L-Me)₄Ni₄(MeOH)** (0.032 g, 1.25 mol%), **8u** was isolated as a white solid (0.532 g, 65%). **MP**: 158-160 °C. **R*f*** = 0.4 (Hex/EA = 4:1); **^{1}H NMR** (400 MHz, CDCl$_3$, ppm) δ: 7.31 (d, *J* = 8.0 Hz, 1H), 7.00 – 6.81 (m, 5H), 6.53 (d, *J* = 8.0 Hz, 2H), 4.96 (d, *J* = 48.0 Hz, 1H), 3.65 (d, *J* = 6.4 Hz, 6H), 1.80 (s, 3H), 1.62 (d, *J* = 24 Hz, 9H);**^{13}C NMR** (101 MHz, CDCl$_3$, ppm) δ: 172.41, 158.29, 151.81, 141.78, 133.09, 132.71, 127.84, 122.18, 114.36, 113.00, 81.55, 54.94, 53.38, 52.52, 39.30, 28.48, 13.29; **HRMS** (ESI): *m/z* calculated for $C_{24}H_{27}NNaO_5$ $[M+Na]^+$: 432.1781; found: 432.1792; **FT-IR** υ_{max} (neat)/cm^{-1}: 2973, 1704, 1612, 1513, 1480, 1394, 1351, 1239, 1149, 1092, 1047, 1019, 912, 751, 728.

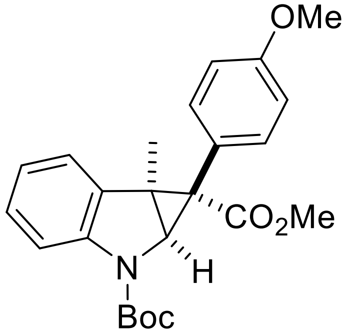

Methyl 7-(4-methoxyphenyl)-2-methylbicyclo[4.1.0]hept-3-ene-7-carboxylate (**8l′**) has been obtained as the minor product (12%, based on the diazoester).

***Tert*-butyl 3-((2S)-2-(methoxycarbonyl)-2-phenylcyclopropyl)-1H-indole-1-carboxylate (8v):** Following the GP-5, starting from 3-methyl-N-Boc indole, **6f** (0.462 g, 2 mmol, 1.0 equiv), methyl-2-diazo-2-phenylacetate, **7c** (0.529 g, 3 mmol, 1.5 equiv) and **(L-Me)$_4$Ni$_4$(MeOH)** (0.032 g, 1.25 mol%), **8v** was isolated as a pale yellow solid (0.532 g, 35%) which was a mixture of two products. **Major product:** **^{1}H NMR** (400 MHz, CDCl$_3$, ppm) δ: 7.61 (d, J = 7.4 Hz, 1H), 7.52 (d, J = 8.0 Hz, 1H), 7.36 – 7.30 (m, 2H), 7.29 – 7.22 (m, 3H), 7.05 – 7.02 (m, 3H), 3.63 (s, 3H), 3.06 (t, J = 8.0 Hz, 1H), 2.15 – 2.07 (m, 1H), 1.72 (dd, J = 8.0, 4.0 Hz, 1H), 1.48 (d, J = 4.0 Hz, 9H); **^{13}C NMR** (101 MHz, CDCl$_3$, ppm) δ: 131.58, 130.30, 128.47, 127.74, 52.74, 36.83, 28.11, 23.94. The ratio between the major and minor products is 3.3:1. The yield of the major product was 33% and that of the minor product was 8% (calculated from the ^{1}H NMR spectrum).

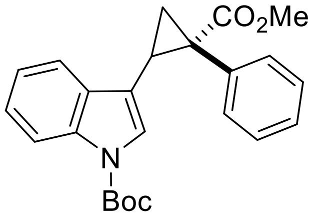

Major product

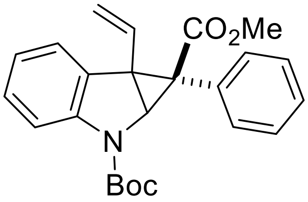

Minor product

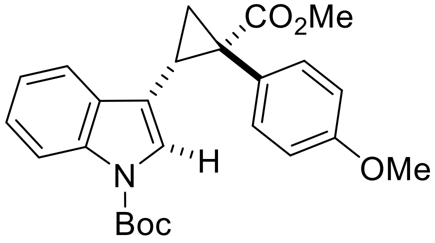

***Tert*-butyl 3-((1S,2S)-2-(methoxycarbonyl)-2-(4-methoxyphenyl)cyclopropyl)-1H-indole-1-carboxylate (8w):** Following the GP-5, starting from *tert*-butyl 3-vinyl-1H-indole-1-carboxylate, **6h** (0.487 g, 2 mmol, 1.0 equiv), methyl 4-methoxy-phenyldiazoacetate, **7d** (0.619 g, 3 mmol, 1.5 equiv) and **(L-Me)$_4$Ni$_4$(MeOH)** (0.032 g, 1.25 mol%), **8w** was isolated as a colorless gummy solid (0.312 g, 37%). **R$_f$** = 0.25 (Hex/EA = 4:1); **^{1}H NMR** (400 MHz, CDCl$_3$, ppm) δ: 8.03 (s, **1H**), 7.68 (d, J = 8.1 Hz, **1H**), 7.31-7.21 (m, **2H**), 7.00 (d, J = 8.6 Hz, 2H), 6.64 (d, J = 8.6 Hz, 2H), 6.51 (s, 1H), 3.69 (s, 6H), 3.09 (t, J = 8.1 Hz, 1H), 2.15 (dd, J = 9.2, 4.4 Hz, 1H), 1.73 (dd, J = 6.9, 4.5 Hz, 1H), 1.55 (s, 9H); **^{13}C NMR** (101 MHz, CDCl$_3$, ppm) δ: 174.73, 158.54, 149.46, 135.21, 132.62, 131.14, 128.40, 127.21, 124.42, 122.58, 118.86, 117.38, 115.17, 114.61, 113.19, 83.39, 55.02, 52.69, 36.11, 28.10, 24.00; **HRMS** (ESI): *m/z* calculated for $C_{25}H_{27}NNaO_5$ $[M+Na]^+$: 444.1792; found: 444.1781; **FT-IR** υ_{max} (neat)/cm^{-1}: 2983, 1720, 1514, 1448, 1366, 1251, 1150, 1076, 904, 734, 650.

***Tert*-butyl 3-((2S)-2-(3,4-dimethoxyphenyl)-2-(ethoxycarbonyl)cyclopropyl)-1H-indole-1-carboxylate (8x):** Following the GP-5, starting from *tert*-butyl 3-vinyl-1H-indole-1-carboxylate, **6h** (0.487 g, 2 mmol, 1.0 equiv), methyl 3,4-methoxy-phenyldiazoacetate, **7e** (0.708 g, 3 mmol, 1.5 equiv) and **(L-Me)₄Ni₄(MeOH)** (0.032 g, 1.25 mol%), **8x** was isolated as a pale yellow solid (0.316 g, 34%). **^{1}H NMR** (400 MHz, $CDCl_3$, ppm) δ: 7.92 (s, 1H), 7.65 (dd, *J* = 6.0, 2.4 Hz, 1H), 7.24-7.17 (m, 3H), 6.66-6.61 (m, 1H), 6.57 (d, *J* = 8.0 Hz, 1H), 6.36 (s, 1H), 4.20-4.02 (m, 2H), 3.70 (s, 3H), 3.15 (s, 2H), 2.98 (t, *J* = 8.0 Hz, 1H), 2.06 (dd, *J* = 8.0, 4.0 Hz, 1H), 1.69 (dd, *J* = 8.0, 4.0 Hz, 1H), 1.51 (d, *J* = 8.0 Hz, 9H), 1.16 (t, *J* = 8.0 Hz, 3H); **^{13}C NMR** (101 MHz, $CDCl_3$, ppm) δ: 174.06, 149.48, 147.64, 135.31, 131.38, 128.00, 124.41, 123.37, 122.59, 118.81, 117.56, 115.40, 114.84, 110.11, 83.64, 55.18, 36.42, 28.13, 23.63, 19.70, 14.28; **HRMS (ESI):** m/z calculated for C26H30NO6 [M+H]+: 452.2068; found: 452.2075; **FT-IR ʋmax (neat)/cm^{-1}:** 2980, 1724, 1514, 1451, 1372, 1255, 1147, 1079, 1030, 766, 746.

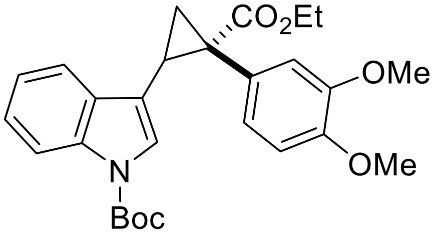

6.3.3 Large scale synthesis of methyl (1R,1aS,6bS)-1-(4-methoxyphenyl)-2-pivaloyl-1,1a,2,6b-tetrahydrocyclopropa[b]indole-1-carboxylate (8n):

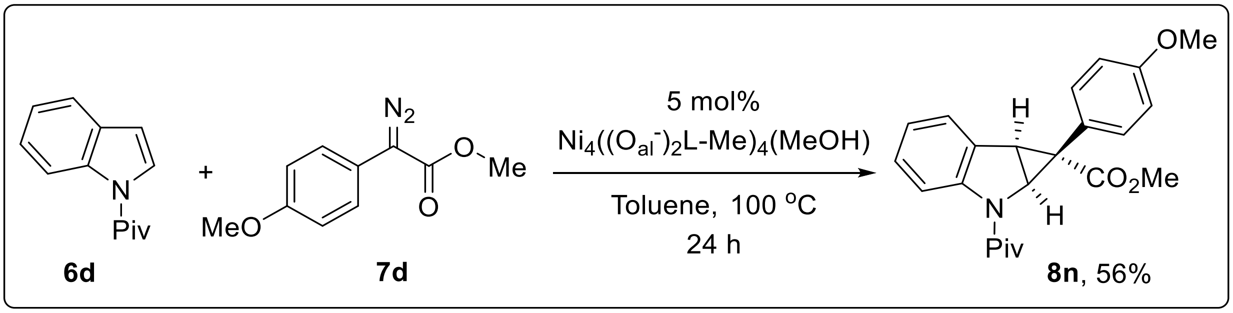

An oven dried 50 ml Schlenk flask was equipped with a magnetic stir bar and charged with the nickel(II) catalyst **$Ni_4((O_{al}^-)_2L\text{-}Me)_4(MeOH)$**, **3** (5 mol%), N-pivaloyl-indole, **6d** (1.005 g, 5 mmol, 1 equiv) and methyl 2-diazo-2-(4-methoxyphenyl)acetate, **7d** (1.545 g, 7.5 mmol, 1.5 equiv), and to this 15 mL of dry toluene was added with vigorous stirring under argon atmosphere. After addition the reaction mixture was allowed for stirring at rt for 15 min and the temperature was increased to 100 °C for 24 h. After completion of the reaction (as monitored by TLC), the reaction mixture was washed with the brine solution and extracted with EtOAc. The organic layer was passed through anhydrous Na_2SO_4 and dried using rotary evaporator under reduced pressure. The reaction mixture was further purified by column chromatography on silica gel (230-400 μm) with hexane/EtOAc as the eluent which afforded the cyclopropanated N-pivaloyl-indole, **8n** in 56% yield (1.056 g) which is comparable with the yield obtained for the 1 mmol scale reaction. The conversion of **6d** to **8n** on the basis of recovered N-methyl-indole **6d** (0.253 g) was found to be 74%.

6.3.4 Competition experiments:

Competition reaction of *N*-Boc indole, 6c with two different diazoesters, 7d and 7f.[a]

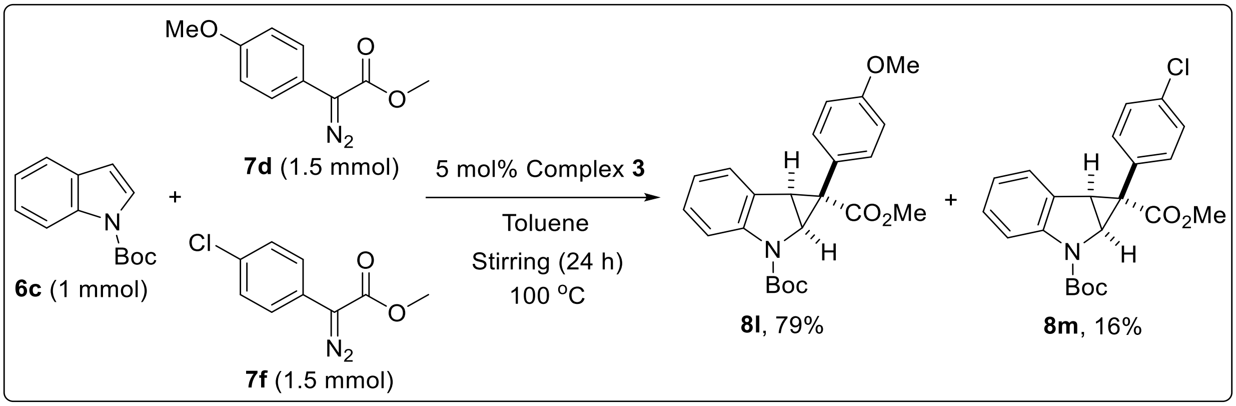

Following the general procedure 5, starting from *N*-boc indole, **6c** (217 mg, 1 mmol, 1.0 equiv), **7d** (309 mg, 1.5 mmol, 1.5 equiv), **7f** (316 mg, 1.5 mmol, 1.5 equiv) and complex **3** (15.7 mg, 5 mol%), the products, **8l** (313 mg, 79%) and **8m** (63.6 mg, 16%) were isolated. [a]An oil bath was used for heating the reaction mixture at 100 °C.

6.3.5. Kinetics Study

Relationship between time of the reaction and conversion of heteroarene (6) to the corresponding cyclopropanated product (8) in the presence of complex 3.

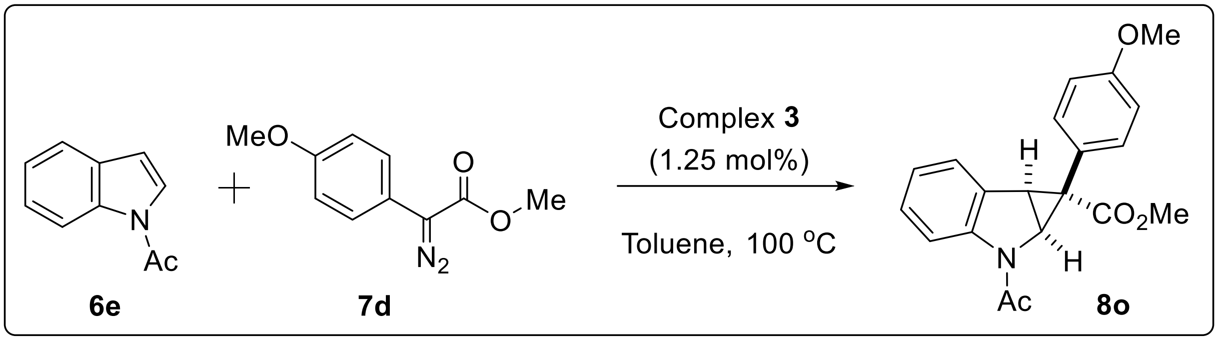

Gas Chromatography:

Five Schlenk tubes were individually charged with 0.15 mmol of the diazoester and 5 mol% of Complex **3** fitted with a magnetic bead. After evacuating and purging with argon for several times, 1 mL of dry toluene (freshly collected from SPS) was added to each Schlenk tube. Later 0.1 mmol of N-acetyl indole, **6e** was added under argon atmosphere to each Schlenk tube. All the Schlenk tubes were then transferred to an oil bath previously heated at 100 °C. After 3 h, one Schlenk tube was removed. Toluene was removed to dryness under vacuum. Then 0.1 mmol of dibromoethane was added as an internal standard, and GC was recorded.

Single Point Internal Standard:

Gas Chromatography is a useful tool that allows us to identify and quantitate individual components in a mixture. There are various methods to perform this experiment. The method we are using here is Single Point Internal standard. There are two parts for this analysis. The first part includes calculation of the response factor by using a known amount of internal standard (IS) and specific compound (SC). We calculated the IRF as 0.643151.

$$Internal\ response\ factor\ (IRF) = \frac{area\ of\ IS\ \times\ amount\ of\ SC}{amount\ of\ IS\ \times\ area\ of\ SC}$$

The second part involves the calculation the amount of unknown compound by adding known amount of IS. The result of this part is summarized in Table S30.

$$Amount\ of\ SC = \frac{amount\ of\ IS\ \times\ area\ of\ SC\ \times\ IRF}{amount\ of\ IS}$$

Table S29:

Sl. No.	Time (h)	Area of IS	Area of SC	Amount of SC (mg)	Yield (%)
1	0.5	57.041	404.063	78.99486	23.41456
2	1	66.000	504.956	85.31914	25.28911
3	1.5	67.301	575.730	95.39689	28.27622
4	2	57.950	548.603	105.5703	31.29167
5	2.5	73.570	716.614	108.6229	32.19649

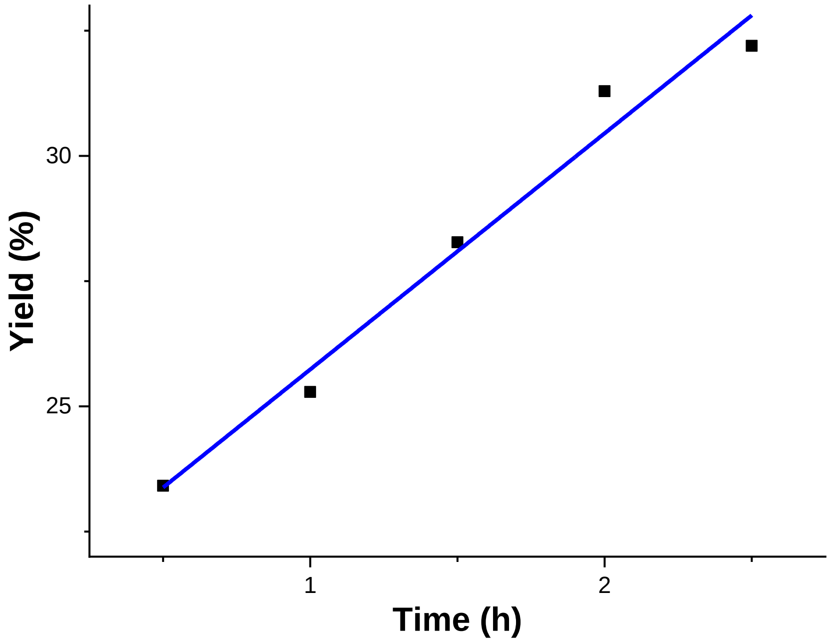

Figure. S37a. Kinetic plot for the nickel catalyzed cyclopropanation of heterocycle (**6e**) with diazoester (**7d**).

The reaction kinetic profile of the Ni catalyzed cyclopropanation was studied for 2.5 h. The time dependent product formation plot indicated that product started forming in 30 min in 23%. After the completion of 2.5 h the yield of **8o** increases to 32%.

NMR:

Five Schlenk tubes were individually charged with 0.15 mmol of the diazoester and 5 mol% of complex **3** fitted with a magnetic bead. After evacuating and purging with argon for several times, 1 mL of dry toluene (freshly collected from SPS) was added to each Schlenk tube. Later 0.1 mmol of N-acetyl indole, **6e** was added under argon atmosphere to each Schlenk tube. All the Schlenk tubes were then transferred to an oil bath previously heated at 100 ^{o}C. After 3 h, one Schlenk tube was removed. Toluene was removed to dryness under vacuum. Then 0.1 mmol of dibromoethane was added as an internal standard, and ^{1}H NMR was recorded. This procedure was followed in every 3 h interval for 15 h. Table S30 summarizes the result of above described experiment.

Table S30:

Time (h)	Yield (%)
3	48
6	53
9	56
12	65
15	70

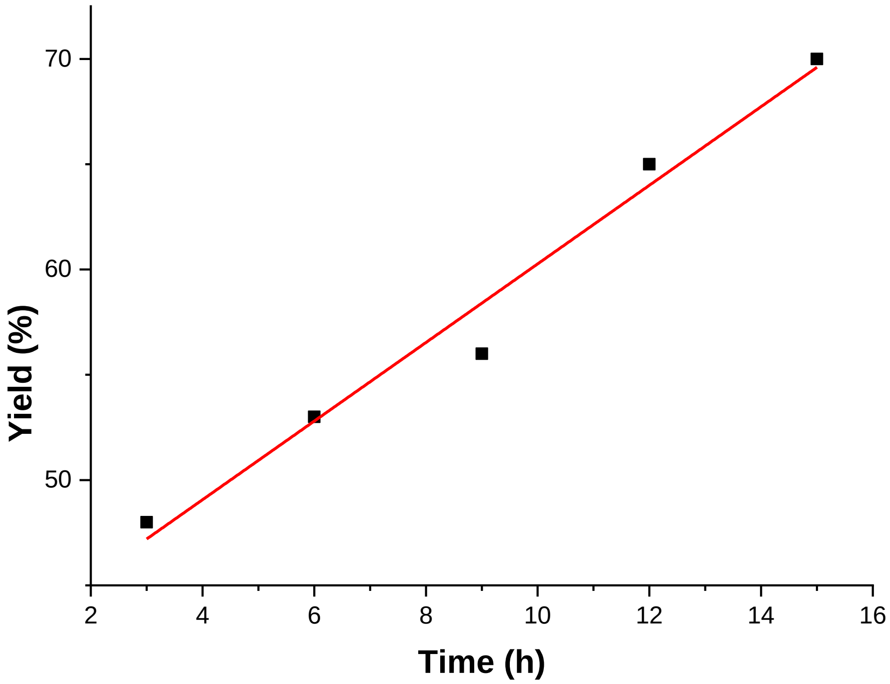

Figure S37b. Kinetic plot for the nickel catalyzed cyclopropanation of heterocycle (**6e**) with diazoester (**7d**). Yield vs. time plot for the conversion of **6e** to **8o**.

The reaction kinetic profile of the Ni-catalyzed cyclopropanation was studied for 15 h is depicted in Figure S37b. After the completion of 15 h the yield of **8o** reaches 70%.

6.4. Determination of relative stereochemistry of the cyclopropanated heteroarene 8u:

6.4.1. General method of crystallization: Suitable single crystals were grown by slow evaporation of the saturated *n*-hexane solution of **8u** after 2 days at rt.

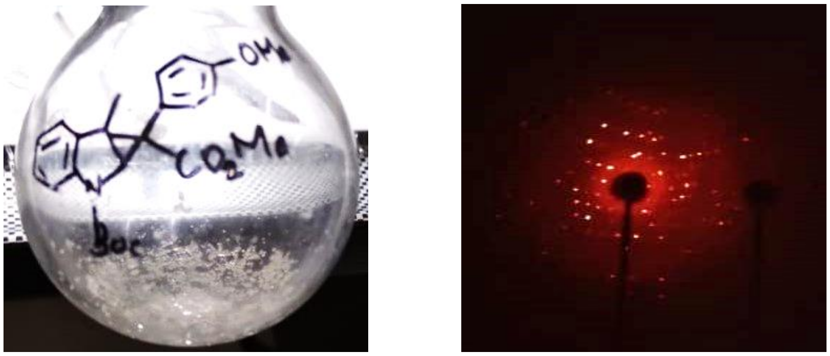

Figure S38. Crystallization of **8u**.

6.4.2. Single crystal X-ray structure of compound 8u.

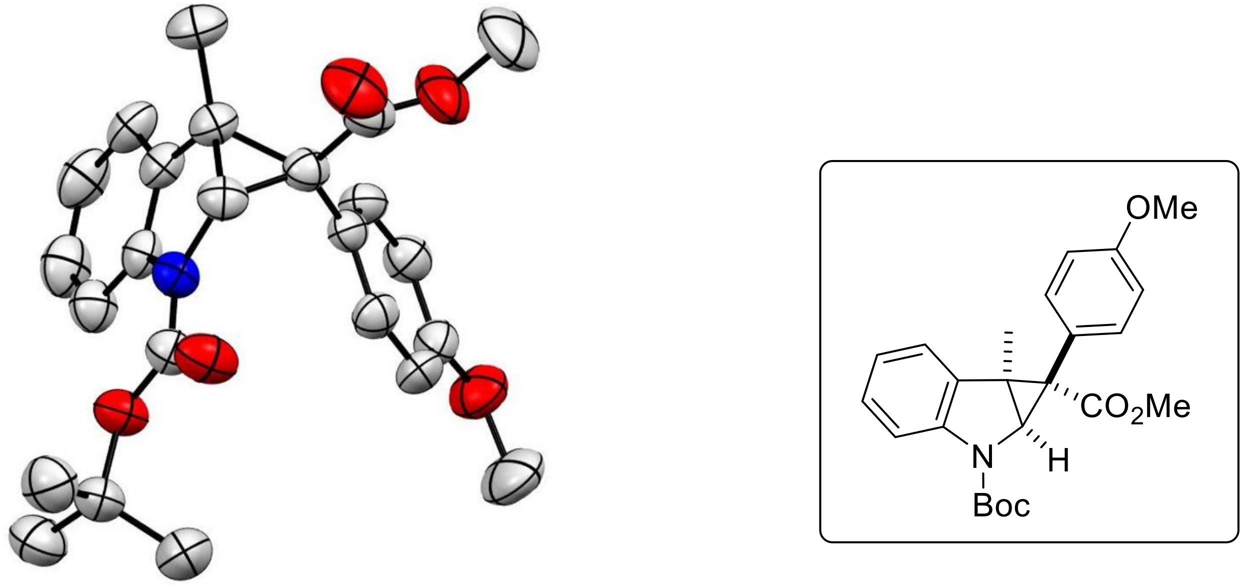

Figure S39. Single crystal X-ray structure of compound **8u**. (ORTEP plot, all the atoms are drawn at 50% probability level).

Table S31. X-ray crystallographic parameters for compound **8u.**

Chemical formula	$C_{24}H_{27}NO_5$
Formula weight	409.46
CCDC Number	2072516
Crystal size (mm)	0.12 × 0.10 × 0.08 mm
Crystal system	Orthorhombic
Space group	$P2_12_12_1$
a (Å)	9.2258 (11)
b (Å)	15.495 (2) Å
c (Å)	15.6334 (16)
α (deg)	90
β (deg)	90
γ (deg)	90
V (Å^3)	2234.9 (5)
Z	4
T (K)	296
λ (Å)	0.71073
D_{calc} (g cm^{-3})	1.217
μ (mm^{-1})	0.09
R_{int}	0.065
R_1 [I > 2σ(I)]^a	0.040
wR_2 (all data)^b	0.104
Total reflections	61760
Independent reflections	4588
Reflections ; $I > 2\sigma(I)$	4000

$\Delta\rho_{max}$	+ 0.12 e Å^{-3}
$\Delta\rho_{min}$	-0.11 e Å^{-3}
GooF	1.03

[a]$R_1 = \Sigma||F_o| - |F_c||/\Sigma|F_o|$; [b]$wR_2 = \{\Sigma[w(F_o^2 - F_c^2)^2]/\Sigma[w(F_o^2)^2]\}^{1/2}$

Table S32. Bond lengths [Å] and angles [°] for compound **8u**

O3—C14	1.374 (3)
C20—C23	1.516 (4)
O3—C24	1.414 (4)
C20—C22	1.521 (4)
O5—C19	1.329 (3)
C23—H23A	0.9600
O5—C20	1.476 (3)
C23—H23B	0.9600
O1—C17	1.204 (3)
C23—H23C	0.9600
O4—C19	1.205 (3)
C22—H22A	0.9600
N1—C19	1.377 (3)
C22—H22B	0.9600
N1—C2	1.419 (3)
C22—H22C	0.9600
N1—C8	1.442 (3)
C18—H18A	0.9600
O2—C17	1.330 (3)
C18—H18B	0.9600
O2—C18	1.451 (3)
C18—H18C	0.9600
C15—C16	1.384 (3)
C16—H16	0.9300

C15—C14	1.386 (3)
C7—C1	1.489 (3)
C15—H15	0.9300
C7—C10	1.512 (3)
C24—H24A	0.9600
C10—H10A	0.9600
C24—H24B	0.9600
C10—H10B	0.9600
C24—H24C	0.9600
C10—H10C	0.9600
C14—C13	1.375 (4)
C1—C6	1.385 (3)
C13—C12	1.395 (3)
C1—C2	1.391 (3)
C13—H13	0.9300
C2—C3	1.385 (3)
C12—C11	1.387 (3)
C3—C4	1.384 (4)
C12—H12	0.9300
C3—H3	0.9300
C11—C16	1.381 (3)
C4—C5	1.370 (4)
C11—C9	1.502 (3)
C4—H4	0.9300
C9—C17	1.493 (3)
C5—C6	1.377 (4)
C9—C8	1.518 (3)
C5—H5	0.9300
C9—C7	1.563 (3)
C6—H6	0.9300
C8—C7	1.504 (3)

C21—H21A	0.9600
C8—H8	0.9800
C21—H21B	0.9600
C20—C21	1.510 (4)
C21—H21C	0.9600
C14—O3—C24	118.0 (3)
C20—C22—H22A	109.5
C19—O5—C20	121.64 (19)
C20—C22—H22B	109.5
C19—N1—C2	130.83 (18)
H22A—C22—H22B	109.5
C19—N1—C8	119.40 (18)
C20—C22—H22C	109.5
C2—N1—C8	109.76 (18)
H22A—C22—H22C	109.5
C17—O2—C18	117.2 (3)
H22B—C22—H22C	109.5
C16—C15—C14	119.7 (2)
O1—C17—O2	123.5 (2)
C16—C15—H15	120.1
O1—C17—C9	125.3 (3)
C14—C15—H15	120.1
O2—C17—C9	111.2 (2)
O3—C24—H24A	109.5
O2—C18—H18A	109.5
O3—C24—H24B	109.5
O2—C18—H18B	109.5
H24A—C24—H24B	109.5
H18A—C18—H18B	109.5
O3—C24—H24C	109.5
O2—C18—H18C	109.5

H24A—C24—H24C	109.5
H18A—C18—H18C	109.5
H24B—C24—H24C	109.5
H18B—C18—H18C	109.5
O3—C14—C13	124.9 (2)
C11—C16—C15	121.1 (2)
O3—C14—C15	115.0 (2)
C11—C16—H16	119.4
C13—C14—C15	120.1 (2)
C15—C16—H16	119.4
C14—C13—C12	119.5 (2)
C1—C7—C8	103.73 (18)
C14—C13—H13	120.2
C1—C7—C10	118.3 (2)
C12—C13—H13	120.2
C8—C7—C10	125.8 (2)
C11—C12—C13	120.9 (2)
C1—C7—C9	113.39 (17)
C11—C12—H12	119.5
C8—C7—C9	59.31 (15)
C13—C12—H12	119.5
C10—C7—C9	122.2 (2)
C16—C11—C12	118.5 (2)
C7—C10—H10A	109.5
C16—C11—C9	121.9 (2)
C7—C10—H10B	109.5
C12—C11—C9	119.5 (2)
H10A—C10—H10B	109.5
C17—C9—C11	116.43 (19)
C7—C10—H10C	109.5
C17—C9—C8	113.5 (2)

H10A—C10—H10C	109.5
C11—C9—C8	120.41 (18)
H10B—C10—H10C	109.5
C17—C9—C7	113.55 (19)
C6—C1—C2	120.5 (2)
C11—C9—C7	121.86 (18)
C6—C1—C7	128.9 (2)
C8—C9—C7	58.41 (15)
C2—C1—C7	110.55 (19)
N1—C8—C7	107.15 (18)
C3—C2—C1	120.9 (2)
N1—C8—C9	116.18 (19)
C3—C2—N1	130.4 (2)
C7—C8—C9	62.28 (15)
C1—C2—N1	108.73 (18)
N1—C8—H8	119.2
C4—C3—C2	117.3 (3)
C7—C8—H8	119.2
C4—C3—H3	121.3
C9—C8—H8	119.2
C2—C3—H3	121.3
O4—C19—O5	127.7 (2)
C5—C4—C3	122.3 (3)
O4—C19—N1	121.9 (2)
C5—C4—H4	118.8
O5—C19—N1	110.33 (19)
C3—C4—H4	118.8
O5—C20—C21	109.7 (2)
C4—C5—C6	120.3 (3)
O5—C20—C23	109.7 (2)
C4—C5—H5	119.8

C21—C20—C23	113.5 (3)
C6—C5—H5	119.8
O5—C20—C22	101.5 (2)
C5—C6—C1	118.7 (3)
C21—C20—C22	110.7 (2)
C5—C6—H6	120.6
C23—C20—C22	111.1 (2)
C1—C6—H6	120.6
C20—C23—H23A	109.5
C20—C21—H21A	109.5
C20—C23—H23B	109.5
C20—C21—H21B	109.5
H23A—C23—H23B	109.5
H21A—C21—H21B	109.5
C20—C23—H23C	109.5
C20—C21—H21C	109.5
H23A—C23—H23C	109.5
H21A—C21—H21C	109.5
H23B—C23—H23C	109.5
H21B—C21—H21C	109.5

Symmetry transformations used to generate equivalent atoms:

6.4.3. Single crystal X-ray structure of compound 8i′.

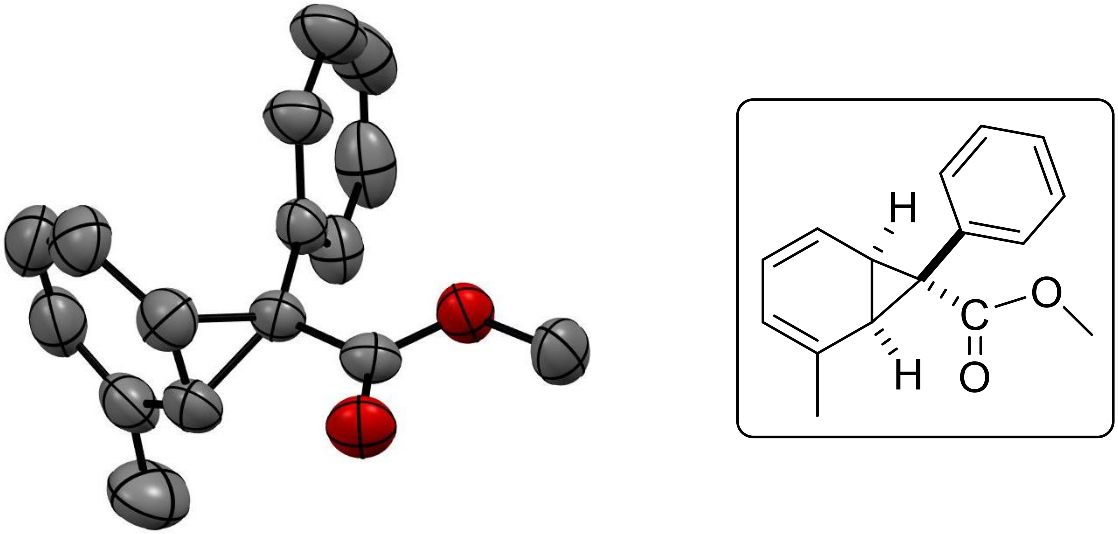

Figure S40. Single crystal X-ray structure of compound **8i′** (ORTEP plot, all the atoms are drawn at 50% probability level). H atoms are omitted for clarity.

Table S33. X-ray crystallographic parameters for compound **8i′**.

Chemical formula	$C_{16}H_{16}O_2$
Formula weight	240.29
CCDC Number	2092320
Crystal size (mm)	0.20 × 0.18 × 0.15
Crystal system	Monoclinic
Space group	$P2_1/c$
a (Å)	11.421 (3)
b (Å)	15.783 (4)
c (Å)	7.4458 (16)

α (deg)	90
β (deg)	93.411 (6)
γ (deg)	90
V (Å^3)	1339.8 (5)
Z	4
T (K)	298
λ (Å)	0.71073
D_{calc} (g cm^{-3})	1.191
μ (mm^{-1})	0.08
R_{int}	0.054
R_1 [$I > 2\sigma(I)$]^a	0.081
wR_2 (all data)^b	0.210
Total reflections	18974
Independent reflections	2773
Reflections ; $I > 2\sigma(I)$	2031
$\Delta\rho_{max}$	+ 0.29 e Å^{-3}
$\Delta\rho_{min}$	-0.26 e Å^{-3}
GooF	1.19

$^{a}R_1 = \Sigma||F_o| - |F_c||/\Sigma|F_o|$; $^{b}wR_2 = \{\Sigma[w(F_o^2 - F_c^2)^2]/\Sigma[w(F_o^2)^2]\}^{1/2}$

Table S34. Bond lengths [Å] and angles [°] for compound **8i′**.

O2—C15	1.324 (3)
C8—H8	0.9800
O2—C16	1.453 (3)
C8—C13	1.471 (4)
O1—C15	1.213 (3)
C11—H11	0.9300
C6—C7	1.500 (3)
C11—C12	1.424 (5)
C6—C5	1.382 (4)
C4—H4	0.9300
C6—C1	1.386 (4)
C4—C3	1.372 (6)
C7—C15	1.493 (4)
C2—H2	0.9300
C7—C9	1.539 (4)
C2—C3	1.361 (6)
C7—C8	1.539 (4)
C16—H16A	0.9600
C5—H5	0.9300
C16—H16B	0.9600
C5—C4	1.399 (4)
C16—H16C	0.9600
C9—H9	0.9800
C13—H13	0.9300
C9—C10	1.474 (4)

C13—C12	1.334 (5)
C9—C8	1.514 (4)
C14—H14A	0.9600
C10—C11	1.338 (5)
C14—H14B	0.9600
C10—C14	1.489 (5)
C14—H14C	0.9600
C1—H1	0.9300
C3—H3	0.9300
C1—C2	1.379 (4)
C12—H12	0.9300

C15—O2—C16	115.6 (2)
C13—C8—C9	116.3 (3)
C5—C6—C7	121.0 (2)
C13—C8—H8	116.1
C5—C6—C1	118.7 (3)
C10—C11—H11	118.9
C1—C6—C7	120.1 (2)
C10—C11—C12	122.1 (3)
C6—C7—C9	121.7 (2)
C12—C11—H11	118.9
C6—C7—C8	120.7 (2)
C5—C4—H4	119.8
C15—C7—C6	117.6 (2)
C3—C4—C5	120.4 (3)

C15—C7—C9	112.0 (2)
C3—C4—H4	119.8
C15—C7—C8	112.8 (2)
C1—C2—H2	119.8
C8—C7—C9	58.94 (19)
C3—C2—C1	120.4 (4)
O2—C15—C7	112.3 (2)
C3—C2—H2	119.8
O1—C15—O2	123.5 (3)
O2—C16—H16A	109.5
O1—C15—C7	124.2 (2)
O2—C16—H16B	109.5
C6—C5—H5	120.1
O2—C16—H16C	109.5
C6—C5—C4	119.7 (3)
H16A—C16—H16B	109.5
C4—C5—H5	120.1
H16A—C16—H16C	109.5
C7—C9—H9	115.7
H16B—C16—H16C	109.5
C10—C9—C7	120.2 (2)
C8—C13—H13	119.5
C10—C9—H9	115.7
C12—C13—C8	121.0 (3)
C10—C9—C8	117.7 (3)
C12—C13—H13	119.5

C8—C9—C7	60.51 (18)
C10—C14—H14A	109.5
C8—C9—H9	115.7
C10—C14—H14B	109.5
C9—C10—C14	116.5 (3)
C10—C14—H14C	109.5
C11—C10—C9	120.2 (3)
H14A—C14—H14B	109.5
C11—C10—C14	123.3 (3)
H14A—C14—H14C	109.5
C6—C1—H1	119.6
H14B—C14—H14C	109.5
C2—C1—C6	120.9 (3)
C4—C3—H3	120.0
C2—C1—H1	119.6
C2—C3—C4	119.9 (3)
C7—C8—H8	116.1
C2—C3—H3	120.0
C9—C8—C7	60.55 (18)
C11—C12—H12	118.8
C9—C8—H8	116.1
C13—C12—C11	122.4 (3)
C13—C8—C7	120.2 (2)
C13—C12—H12	118.8

Symmetry transformations used to generate equivalent atoms:

7. ^{1}H and ^{13}C NMR spectra of cyclopropanated carboxylate derivatives (8)

^{1}H NMR spectrum of 2-(*Tert*-butyl)-6-ethyl-2-azabicyclo[3.1.0]hex-3-ene-2,6-dicarboxylate (8a) (400 MHz, $CDCl_3$, 298 K) (signal broadening occurs due to the presence of rotamers).

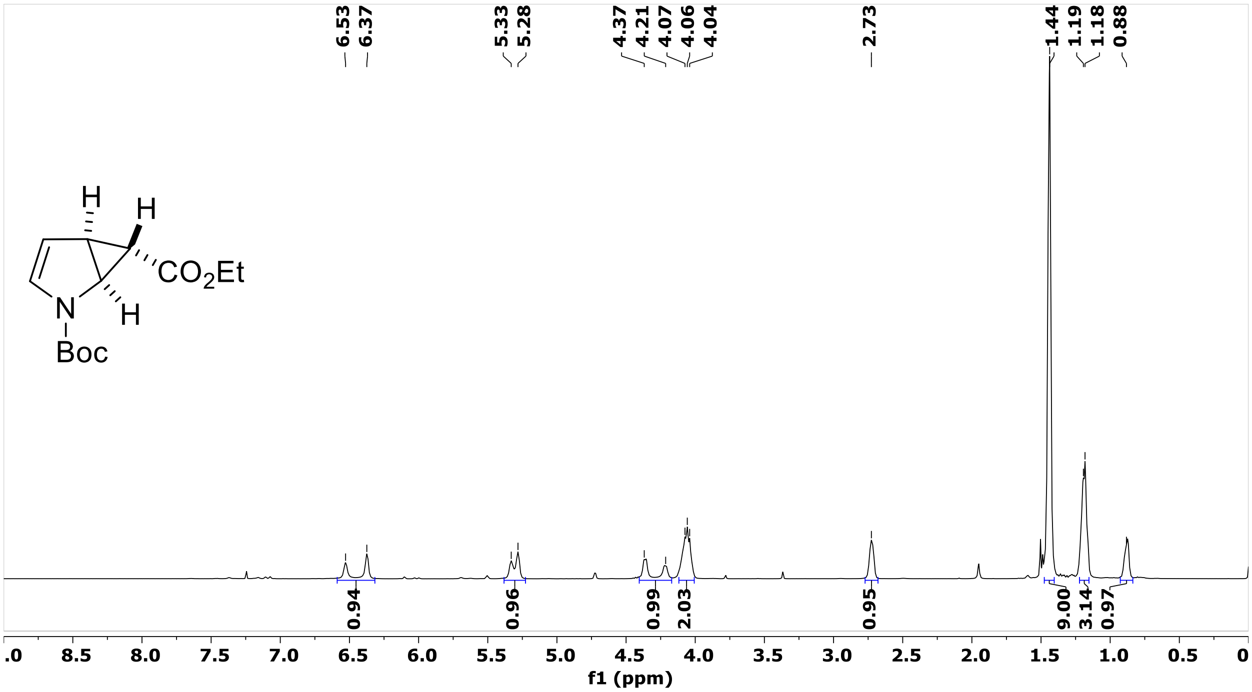

^{13}C NMR spectrum of 2-(*Tert*-butyl)-6-ethyl-2-azabicyclo[3.1.0]hex-3-ene-2,6-dicarboxylate (8a) (101 MHz, $CDCl_3$, 298 K).

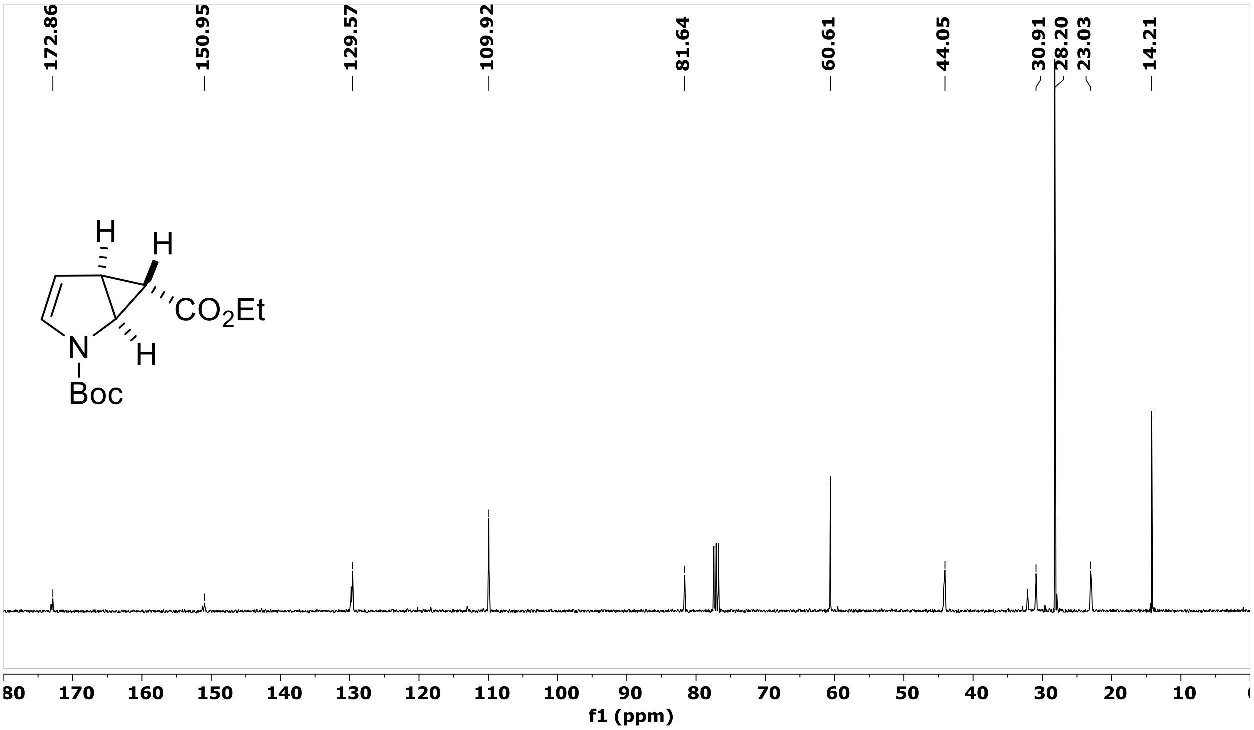

^{1}H NMR spectrum of Di-*tert*-butyl-2-azabicyclo[3.1.0]hex-3-ene-2,6-dicarboxylate (8b) (400 MHz, $CDCl_3$, 298 K) (signal broadening occurs due to the presence of rotamers).

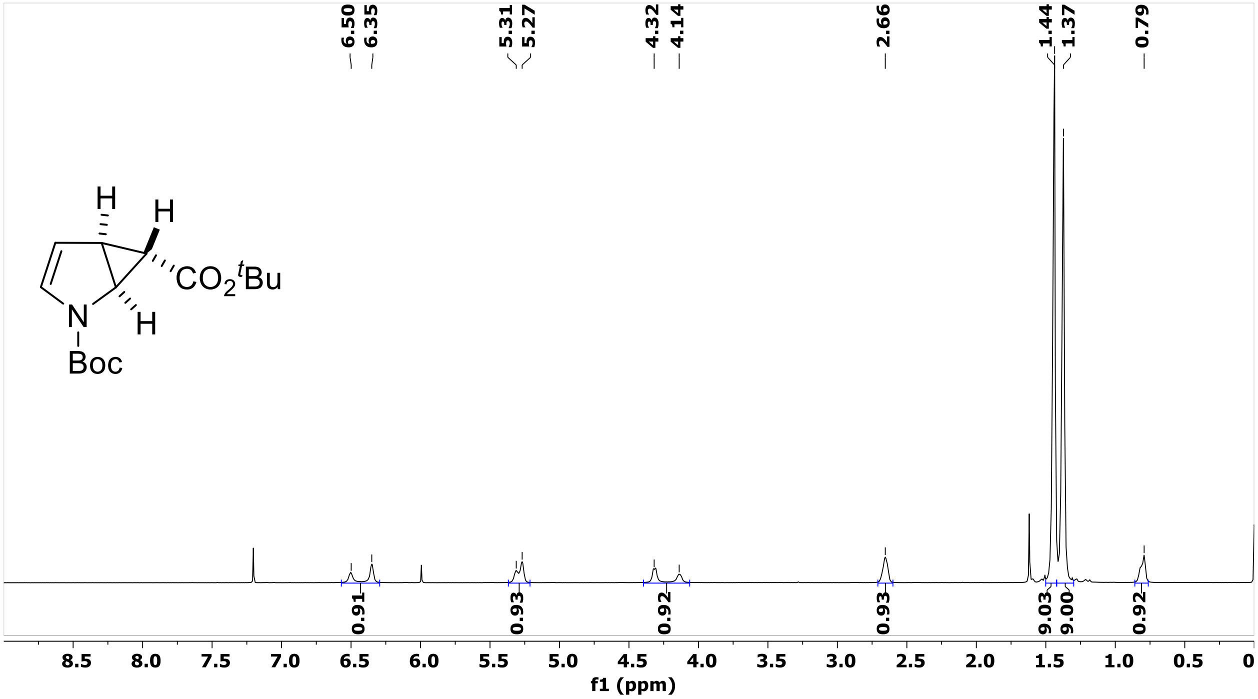

^{13}C NMR spectrum of Di-*tert*-butyl-2-azabicyclo[3.1.0]hex-3-ene-2,6-dicarboxylate (8b) (101 MHz, $CDCl_3$, 298 K)

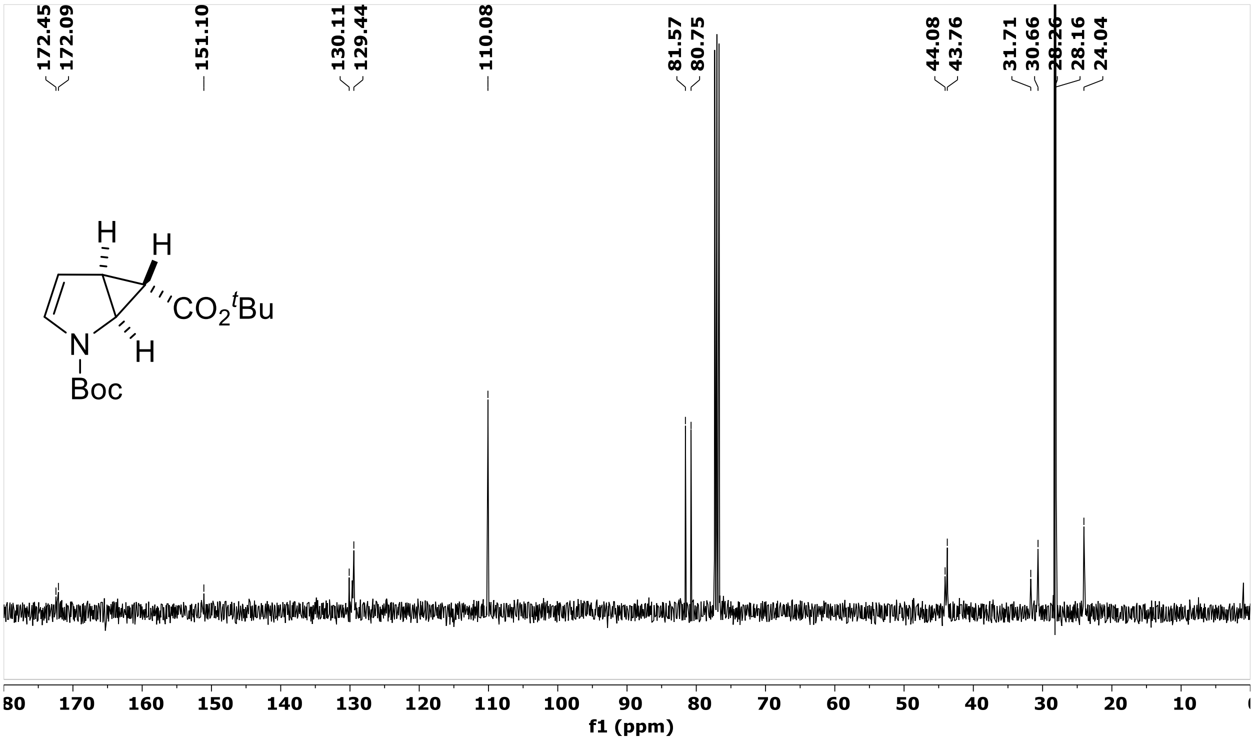

^{1}H NMR spectrum of Di-*tert*-butyl fumarate (8b′) (400 MHz, $CDCl_3$, 298 K).

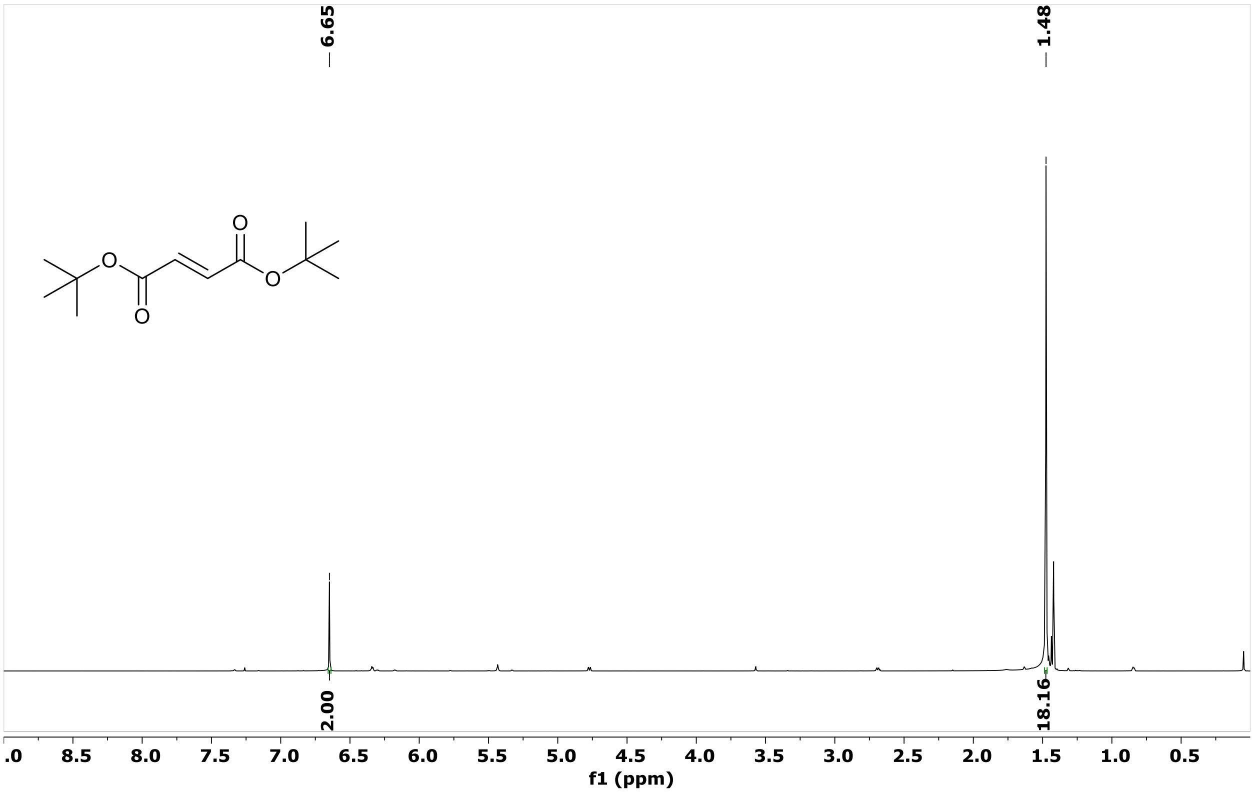

^{13}C NMR spectrum of Di-*tert*-butyl fumarate (8b′) (400 MHz, $CDCl_3$, 298 K).

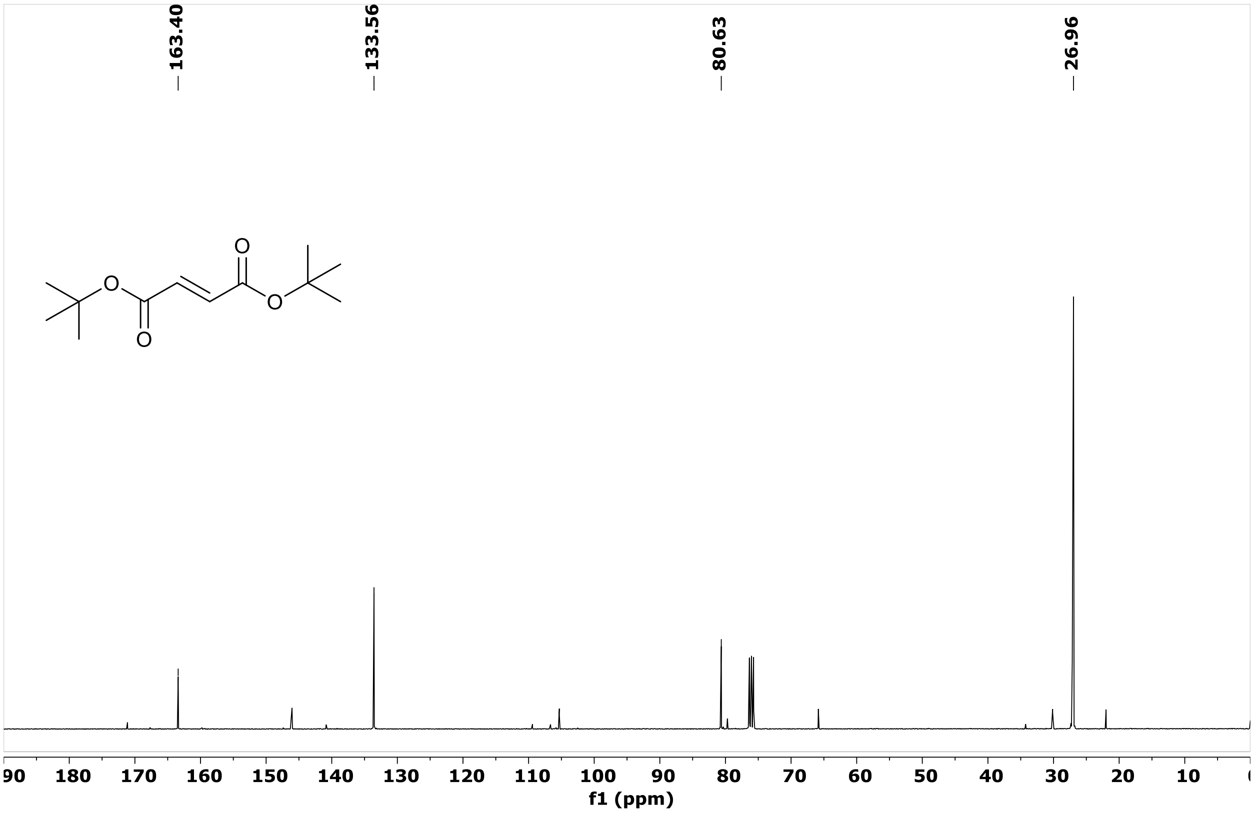

^{1}H NMR spectrum of 2-(*tert*-butyl) 6-methyl (1S,5S,6R)-6-phenyl-2-azabicyclo[3.1.0]hex-3-ene-2,6-dicarboxylate (8c) (400 MHz, CDCl$_3$, 298 K).

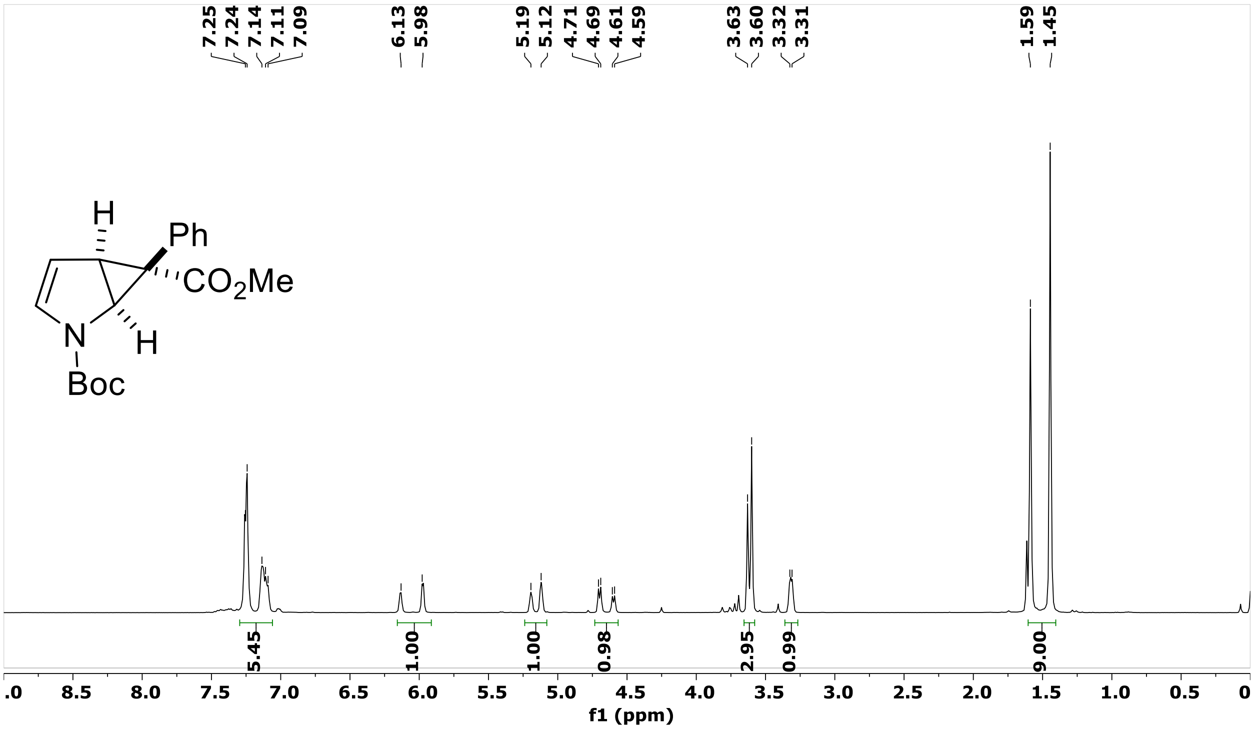

^{13}C NMR spectrum of 2-(*tert*-butyl) 6-methyl (1S,5S,6R)-6-phenyl-2-azabicyclo[3.1.0]hex-3-ene-2,6-dicarboxylate (8c) (101 MHz, CDCl$_3$, 298 K).

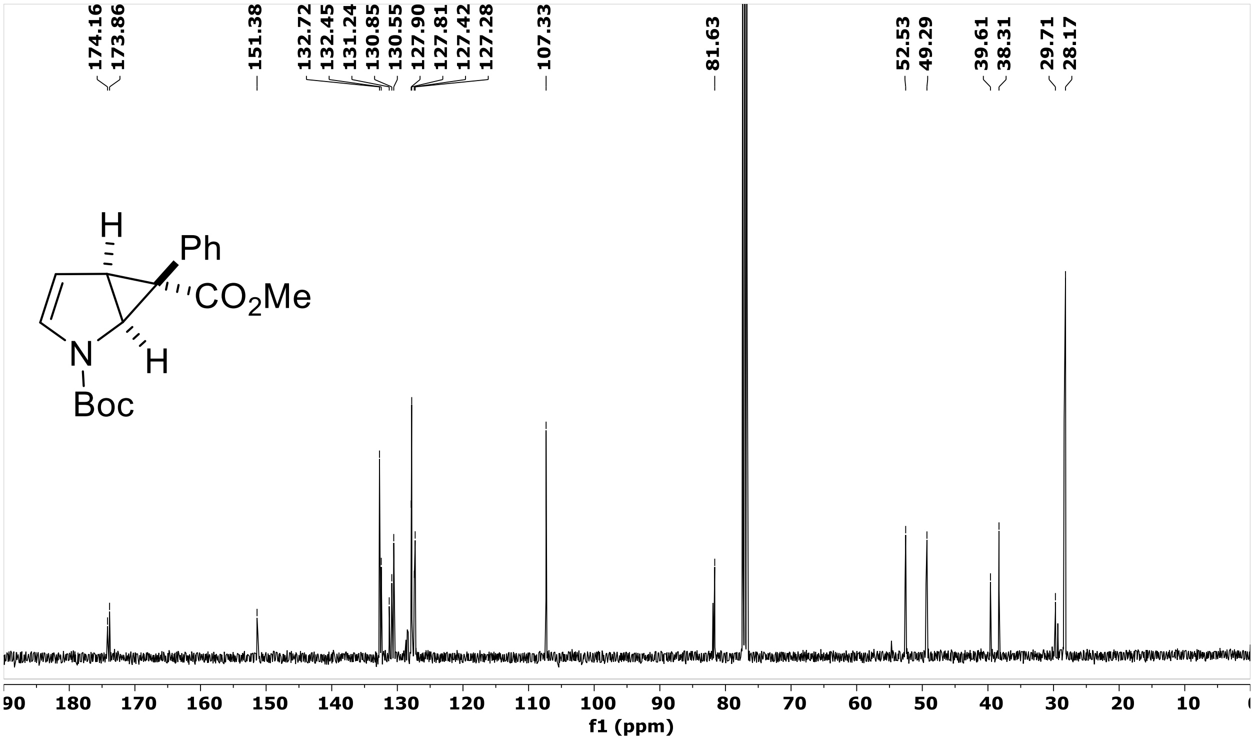

^{1}**H NMR spectrum of 2-(*tert*-butyl) 6-methyl (1S,5S,6R)-6-phenyl-2-azabicyclo[3.1.0]hex-3-ene-2,6-dicarboxylate (8d) (400 MHz, CDCl$_3$, 298 K).**

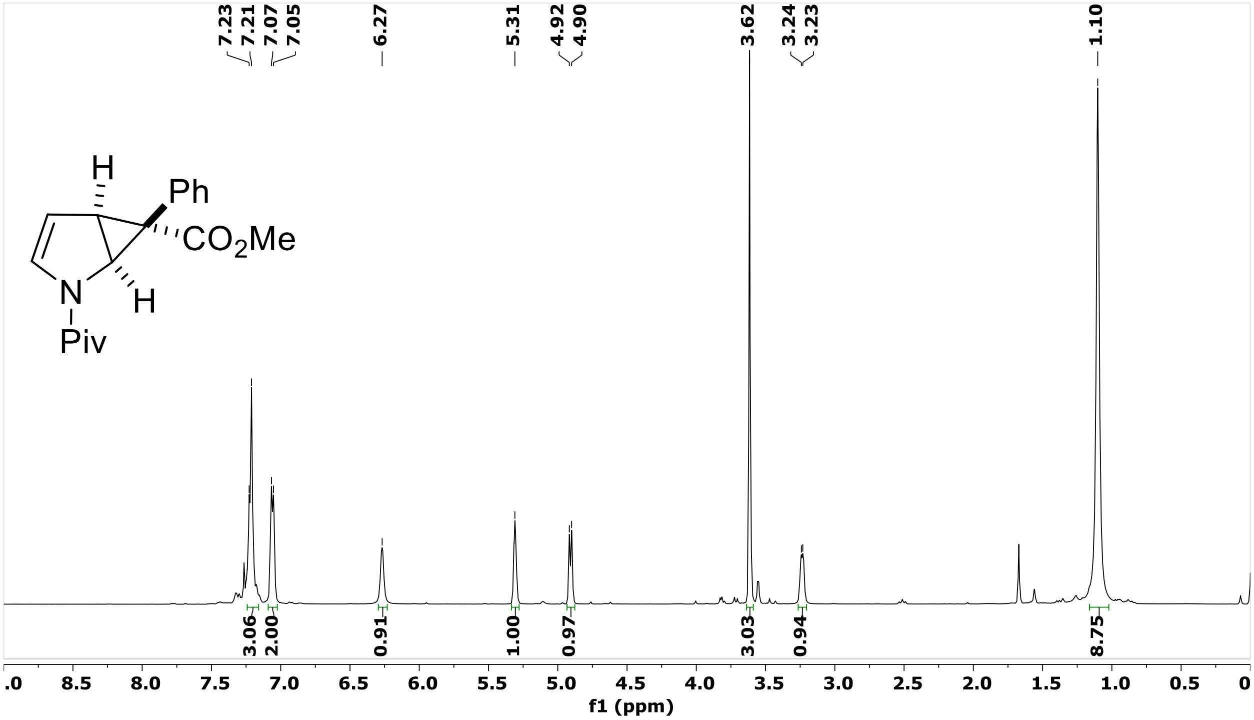

^{13}**C NMR spectrum of methyl (1S,5S,6R)-6-phenyl-2-pivaloyl-2-azabicyclo[3.1.0]hex-3-ene-6-carboxylate (8d) (101 MHz, CDCl$_3$, 298 K).**

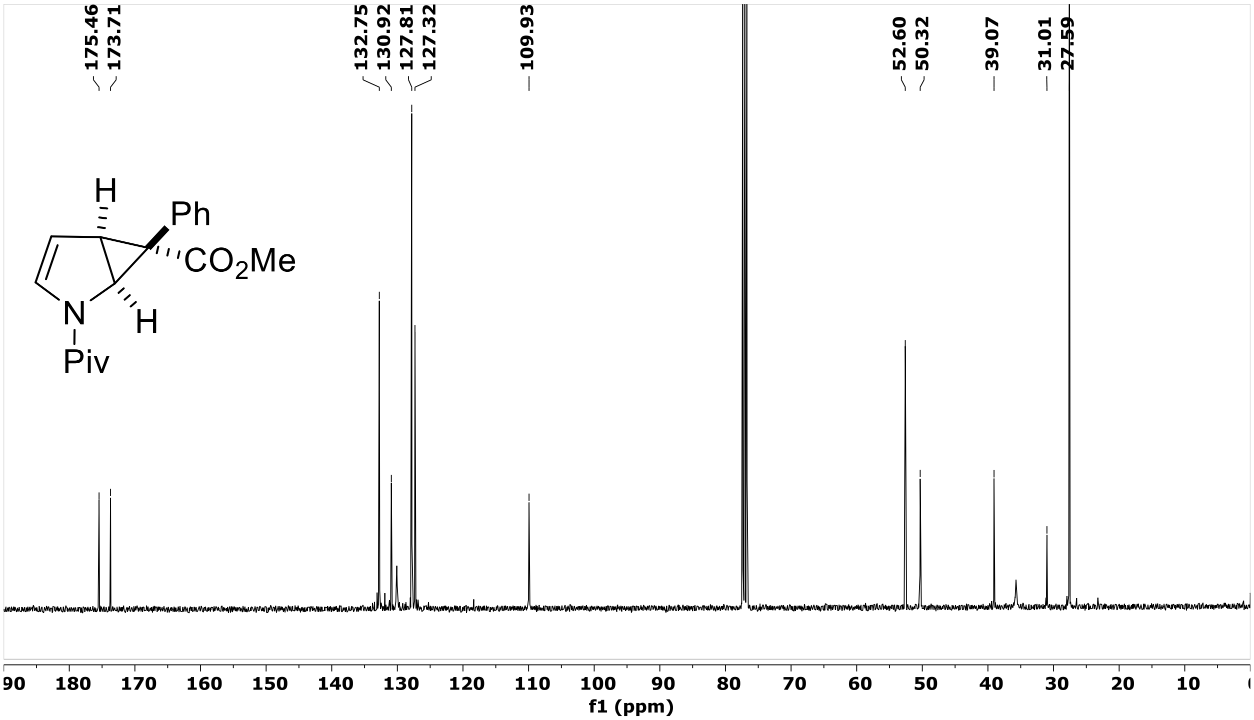

^{1}H NMR spectrum of 2-(*tert*-butyl) 6-methyl (1S,5S,6R)-6-(4-methoxyphenyl)-2-azabicyclo[3.1.0]hex-3-ene-2,6-dicarboxylate (8e) (400 MHz, CDCl$_3$, 298 K).

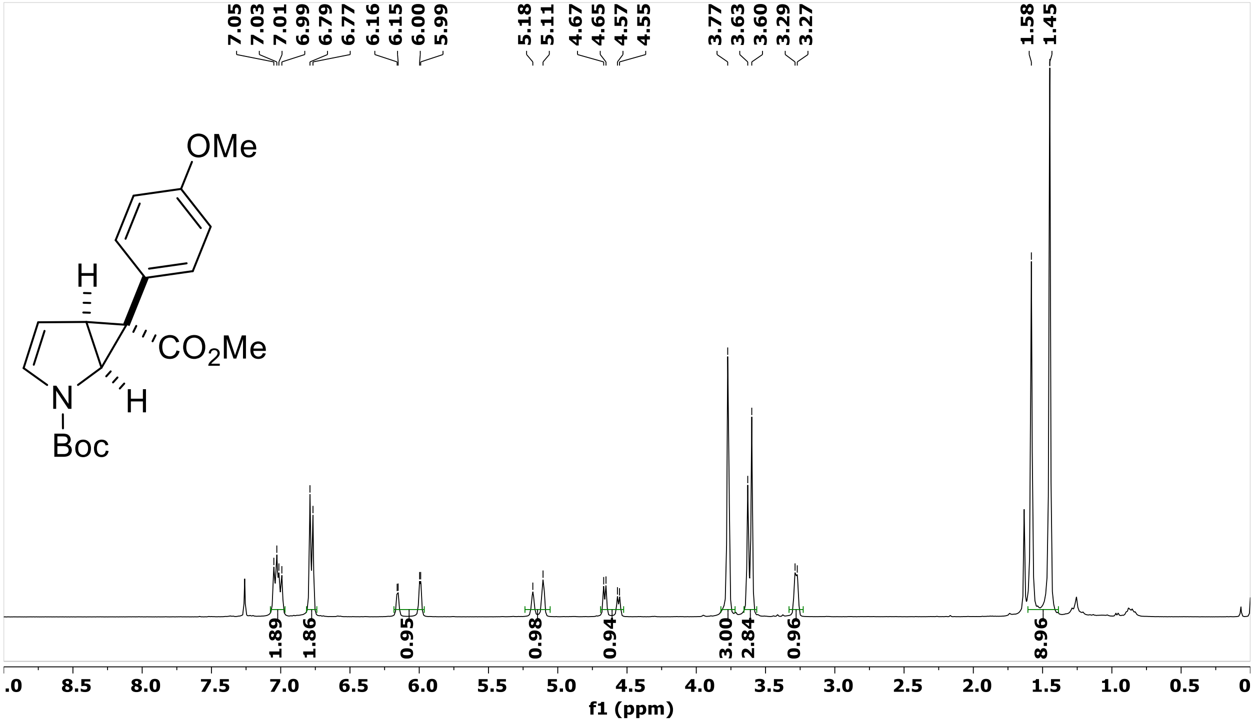

^{13}C NMR spectrum of 2-(*tert*-butyl) 6-methyl (1S,5S,6R)-6-(4-methoxyphenyl)-2-azabicyclo[3.1.0]hex-3-ene-2,6-dicarboxylate (8e) (101 MHz, CDCl$_3$, 298 K).

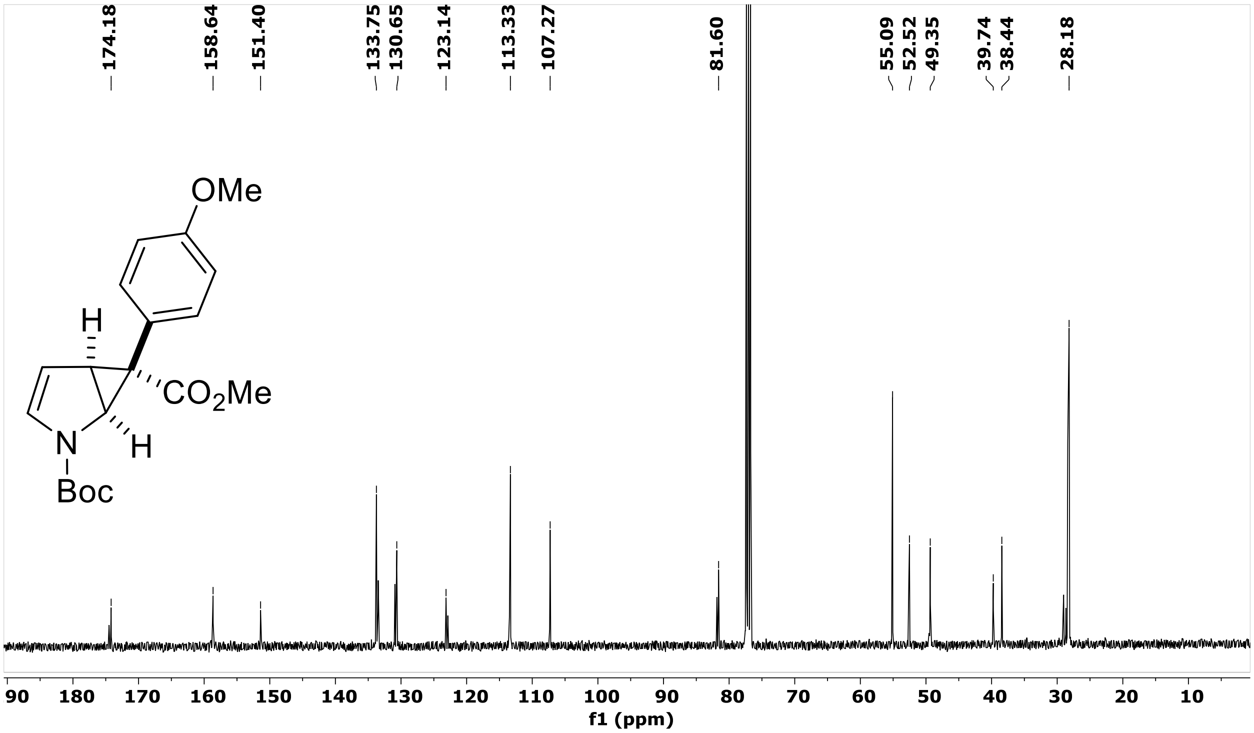

^{1}H NMR spectrum of methyl (1S,5S,6R)-6-(4-methoxyphenyl)-2-pivaloyl-2-azabicyclo[3.1.0]hex-3-ene-6-carboxylate (8f) (400 MHz, $CDCl_3$, 298 K).

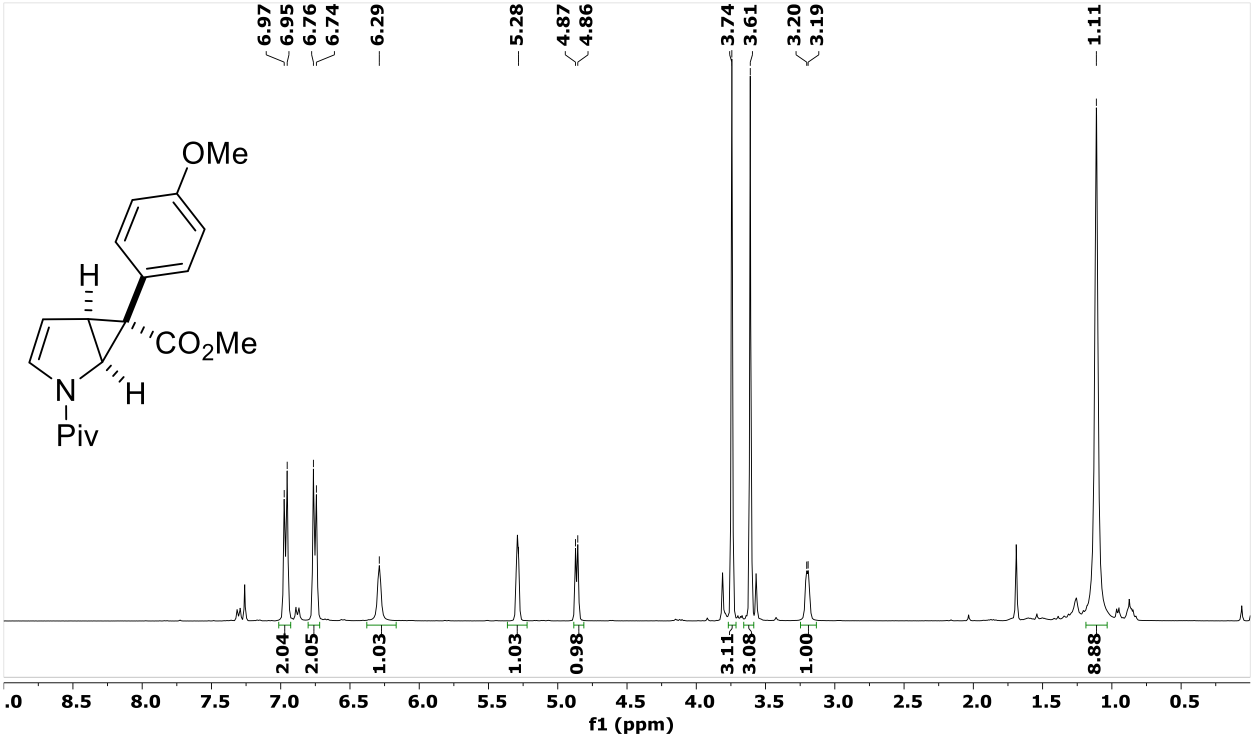

^{13}C NMR spectrum of methyl (1S,5S,6R)-6-(4-methoxyphenyl)-2-pivaloyl-2-azabicyclo[3.1.0]hex-3-ene-6-carboxylate (8f) (101 MHz, $CDCl_3$, 298 K).

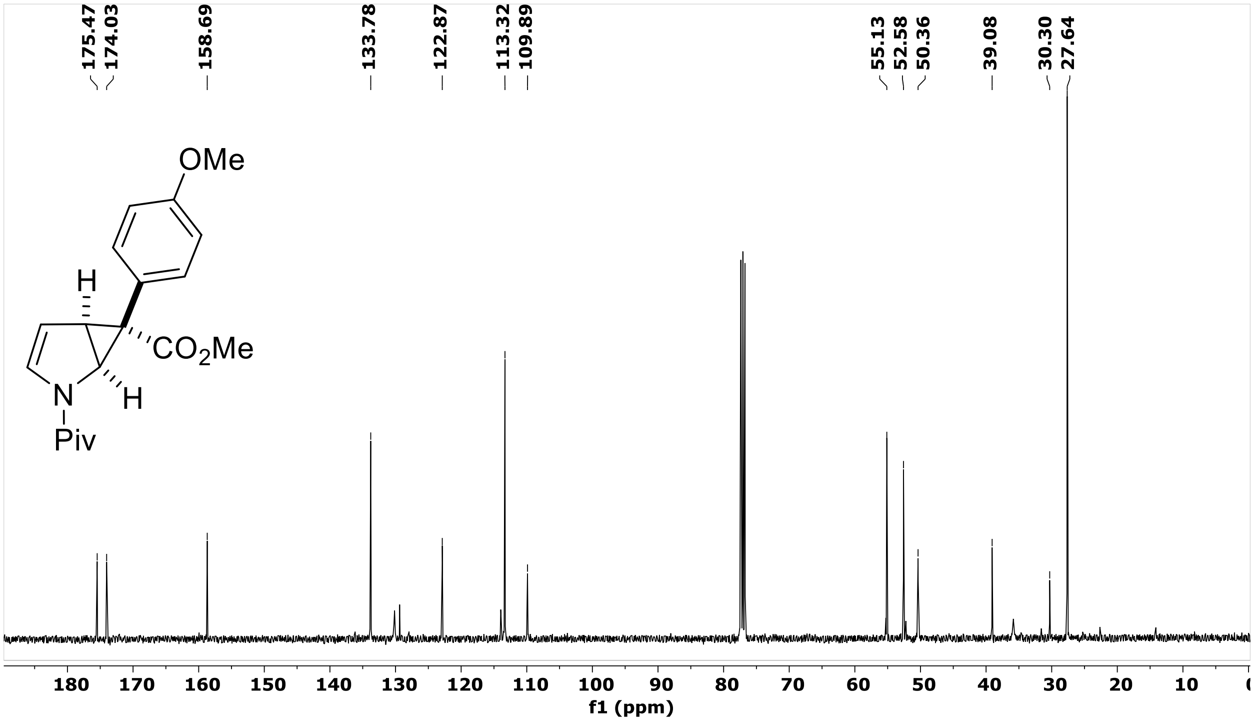

^{1}H NMR spectrum of 2-(*Tert*-butyl)1-ethyl-1a,6b-dihydrocyclopropa[b]indole-1,2(1H)-dicarboxylate (8g) (400 MHz, $CDCl_3$, 298 K).

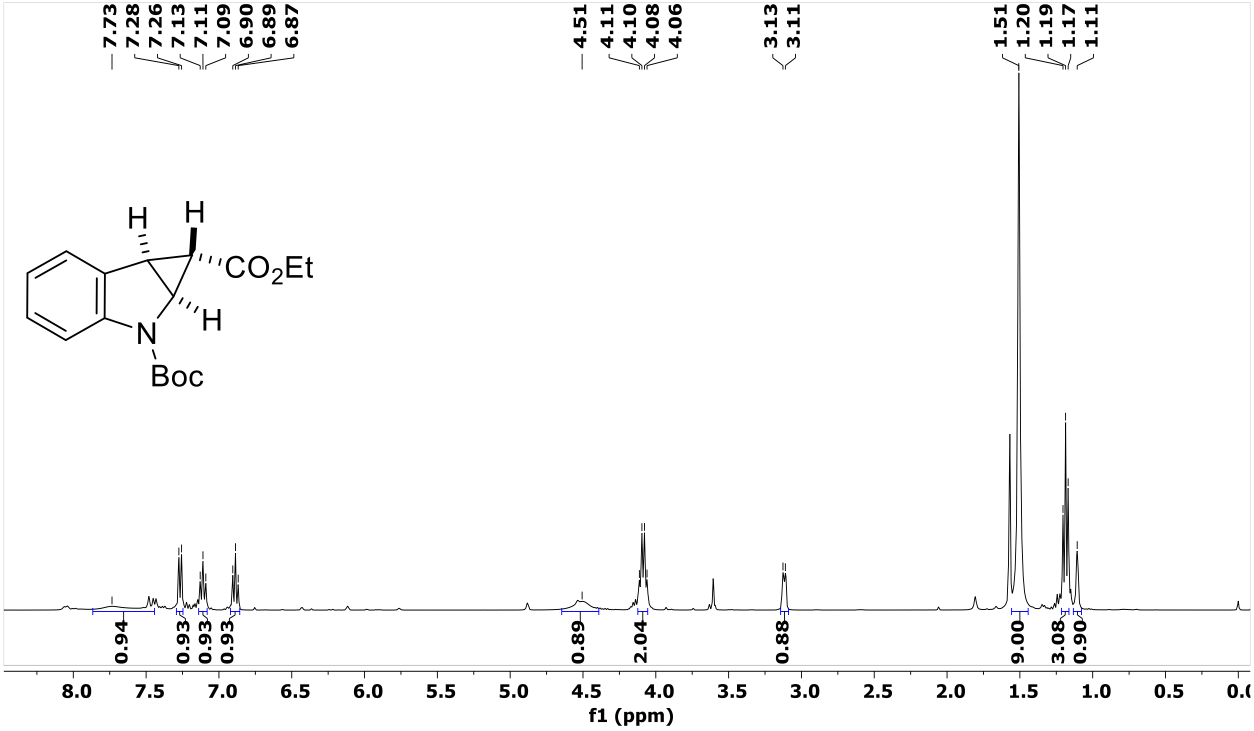

^{13}C NMR spectrum of 2-(*Tert*-butyl)1-ethyl-1a,6b-dihydrocyclopropa[b]indole-1,2(1H)-dicarboxylate (8g) (101 MHz, $CDCl_3$, 298 K).

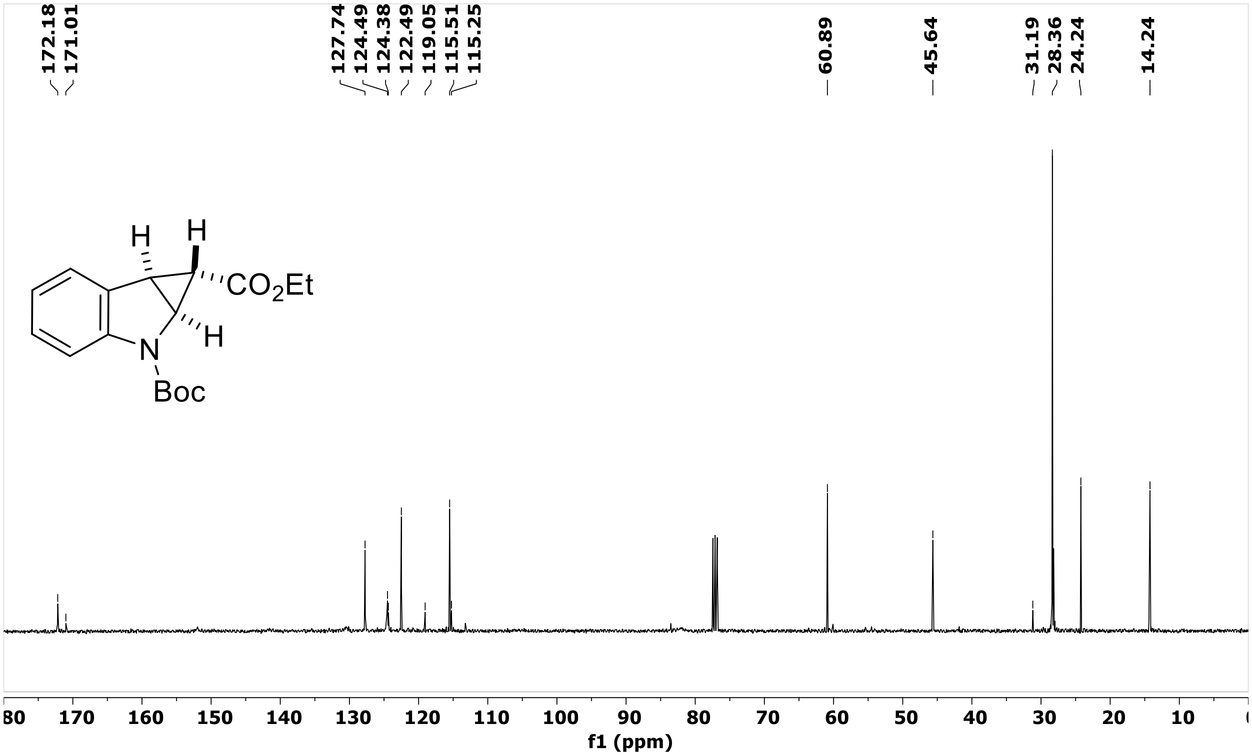

^{1}H NMR spectrum of Di-*tert*-butyl-1a,6b-dihydrocyclopropa[b]indole-1,2(1H)-dicarboxylate (8h) (400 MHz, CDCl$_3$, 298 K)

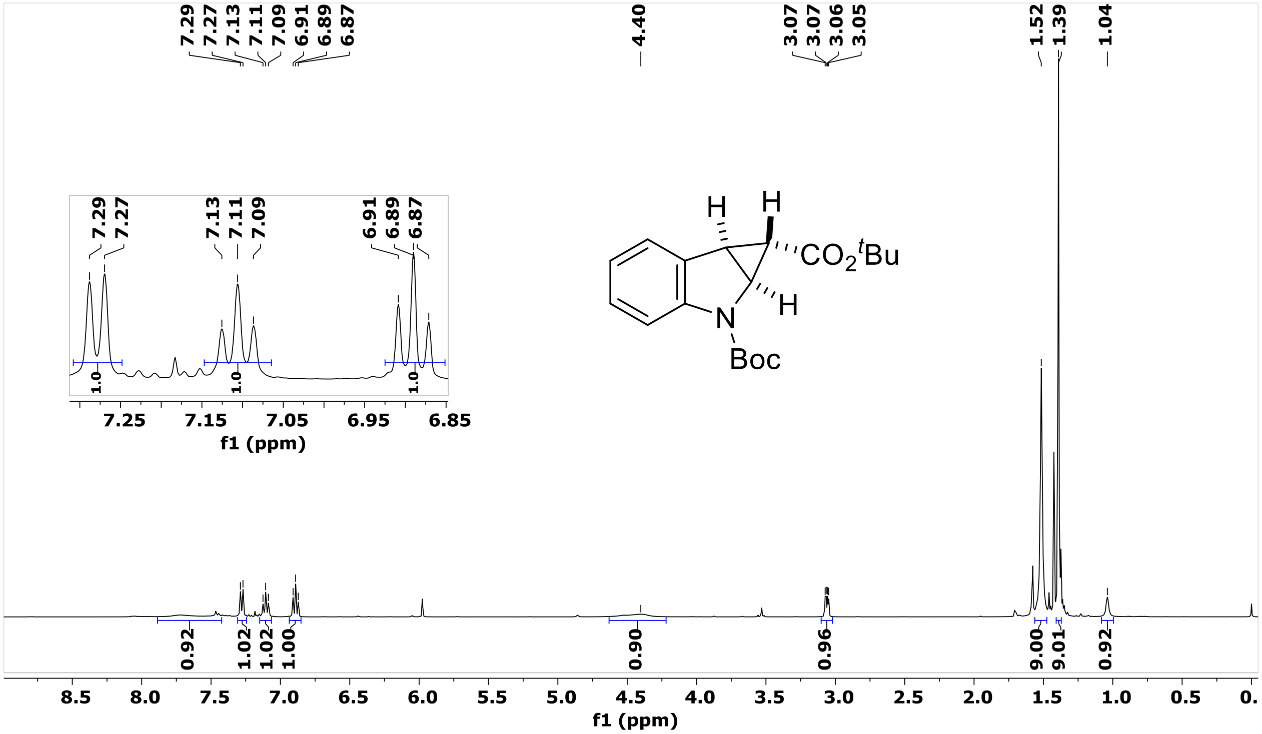

^{13}C NMR spectrum of Di-*tert*-butyl-1a,6b-dihydrocyclopropa[b]indole-1,2(1H)-dicarboxylate (8h) (101 MHz, CDCl$_3$, 298 K)

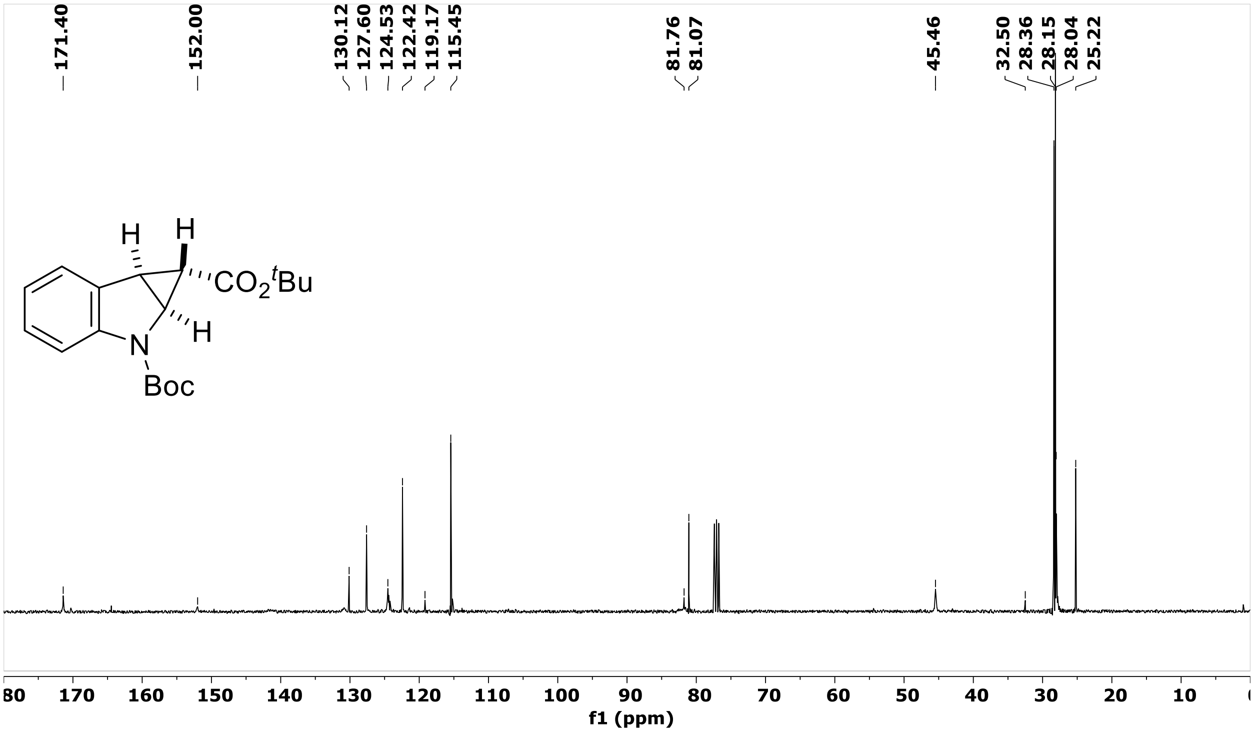

^{1}H NMR spectrum of 2-(*Tert*-butyl)1-methyl-6b-methyl-1-phenyl-1a,6b-dihydrocyclopropa[b]indole-1,2(1H)- dicarboxylate (8i, major product) (400 MHz, CDCl$_3$, 298 K).

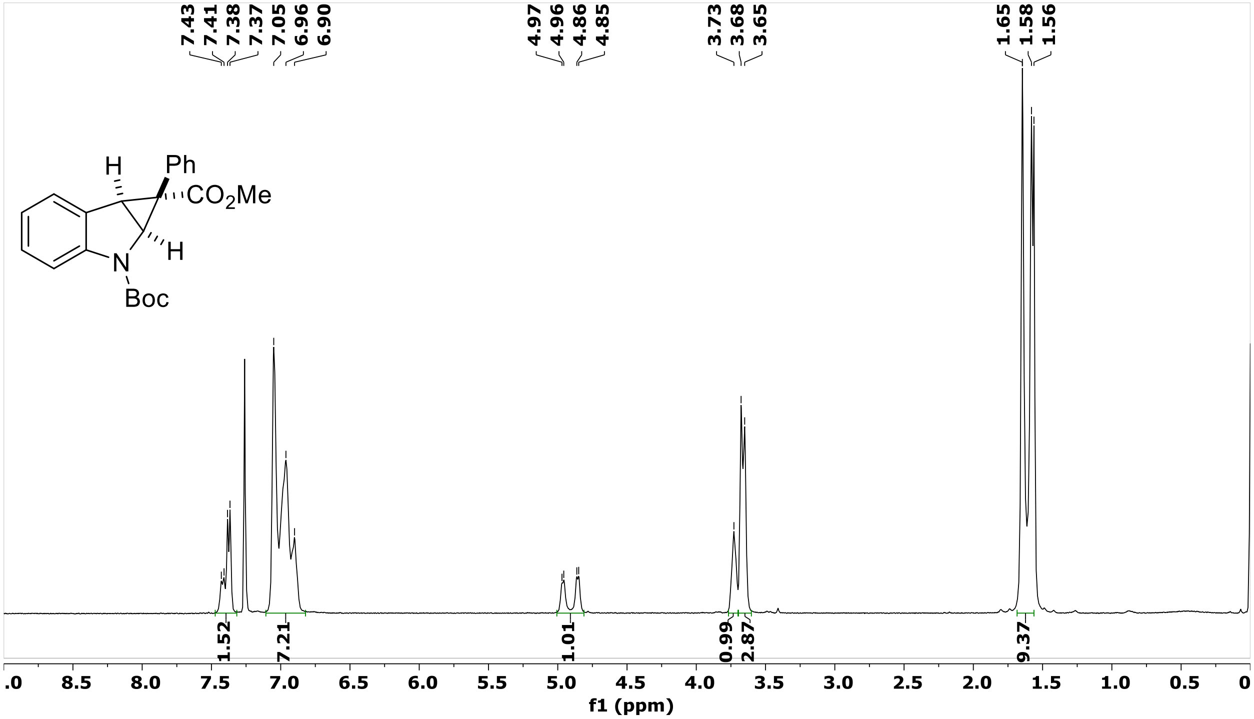

^{13}C NMR spectrum of 2-(*Tert*-butyl)1-methyl-6b-methyl-1-phenyl-1a,6b-dihydrocyclopropa[b]indole-1,2(1H)- dicarboxylate (8i, major product) (101 MHz, CDCl$_3$, 298 K).

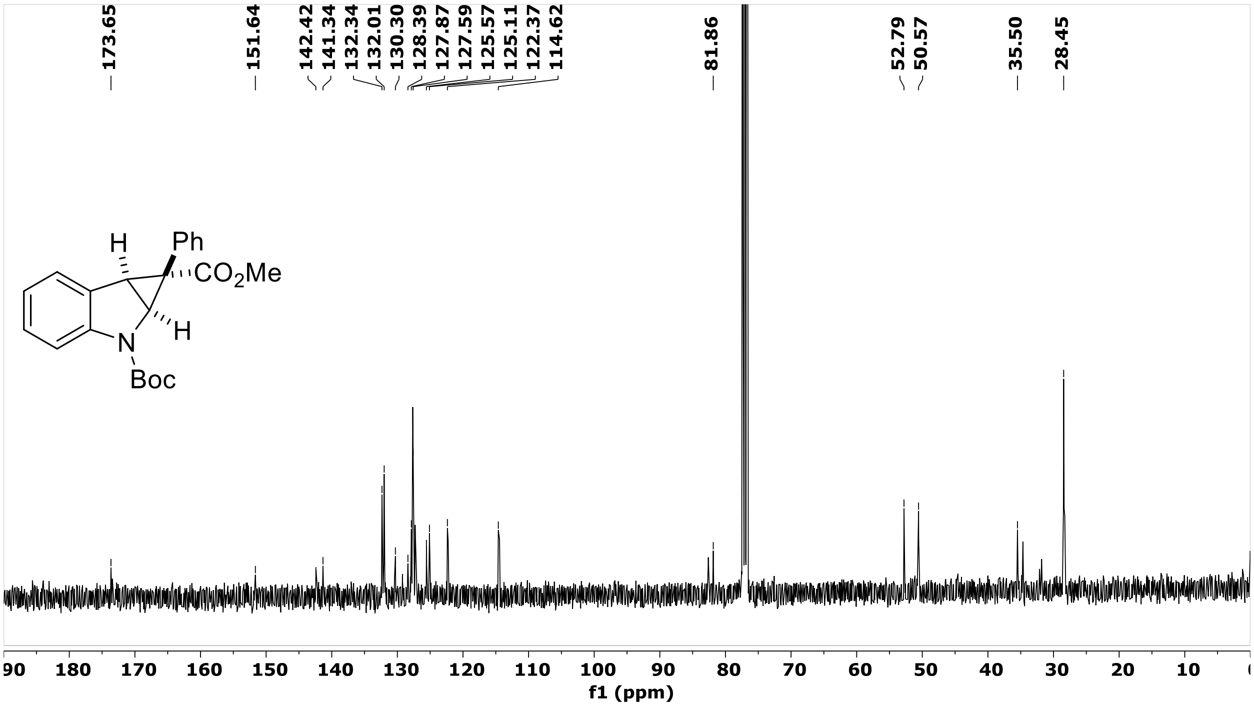

^{1}H NMR spectrum of methyl 2-methyl-7-phenylbicyclo[4.1.0]hept-3-ene-7-carboxylate (8i′, minor product) (400 MHz, $CDCl_3$, 298 K).

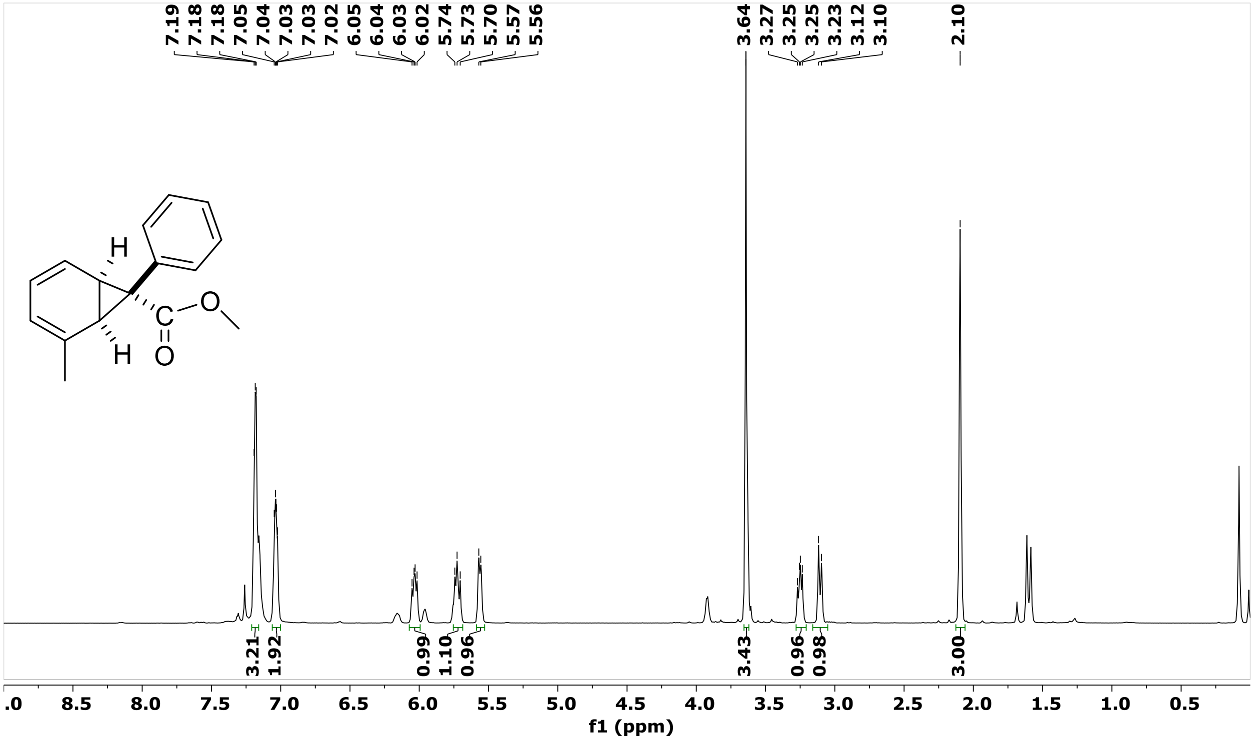

^{13}C NMR spectrum of methyl 2-methyl-7-phenylbicyclo[4.1.0]hept-3-ene-7-carboxylate (8i′, minor product) (101 MHz, $CDCl_3$, 298 K).

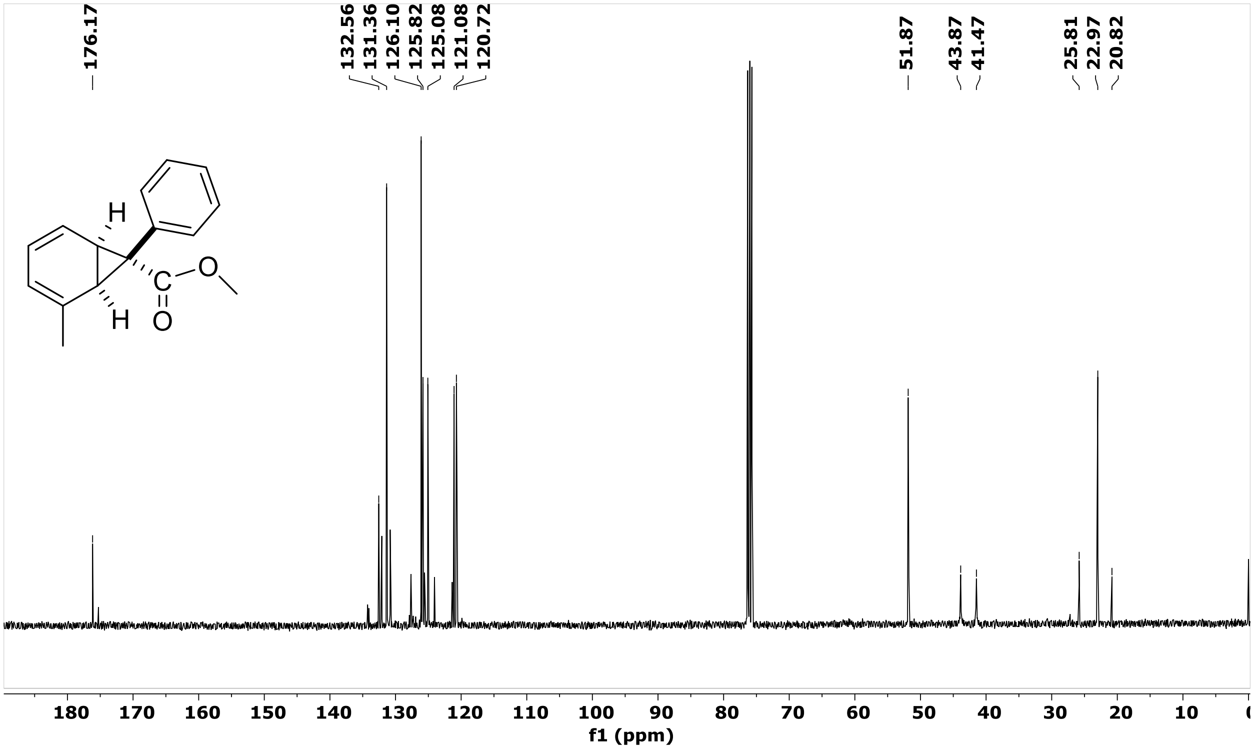

^{1}H NMR spectrum of methyl (1R,1aS,6bS)-1-phenyl-2-pivaloyl-1,1a,2,6b-tetrahydrocyclopropa[b]indole-1-carboxylate (8j) (400 MHz, $CDCl_3$, 298 K).

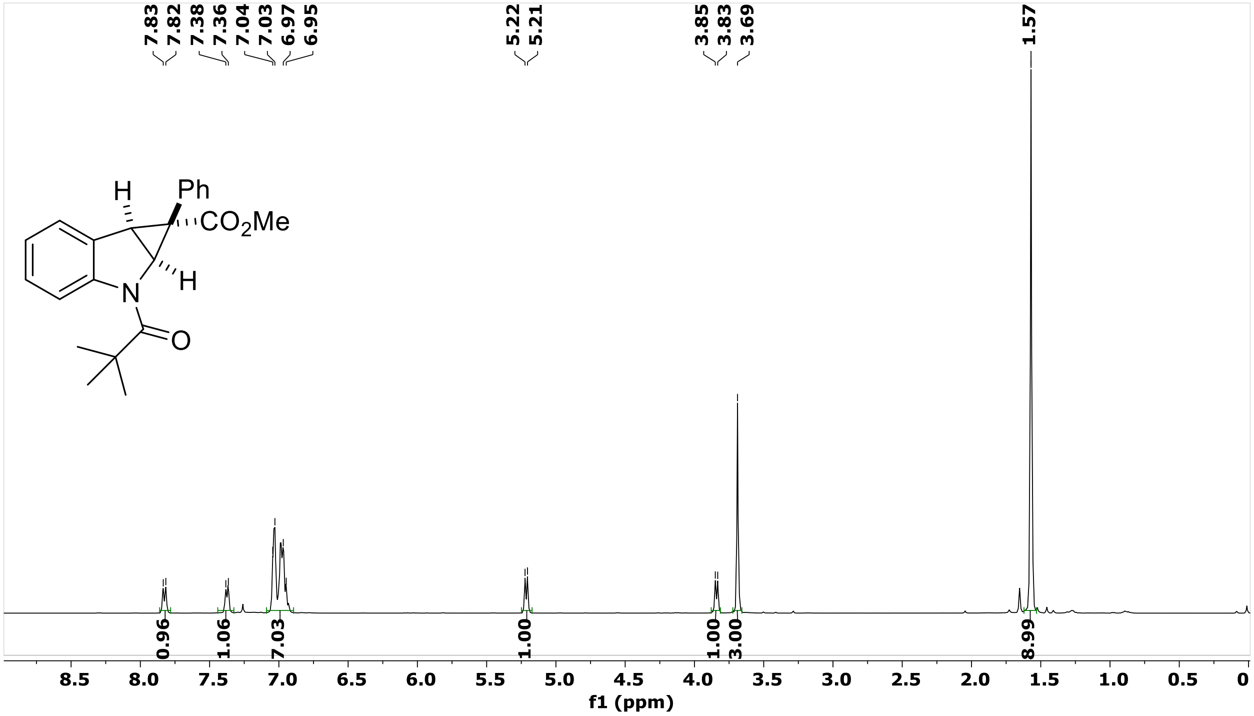

^{13}C NMR spectrum of methyl (1R,1aS,6bS)-1-phenyl-2-pivaloyl-1,1a,2,6b-tetrahydrocyclopropa[b]indole-1-carboxylate (8j) (101 MHz, $CDCl_3$, 298 K).

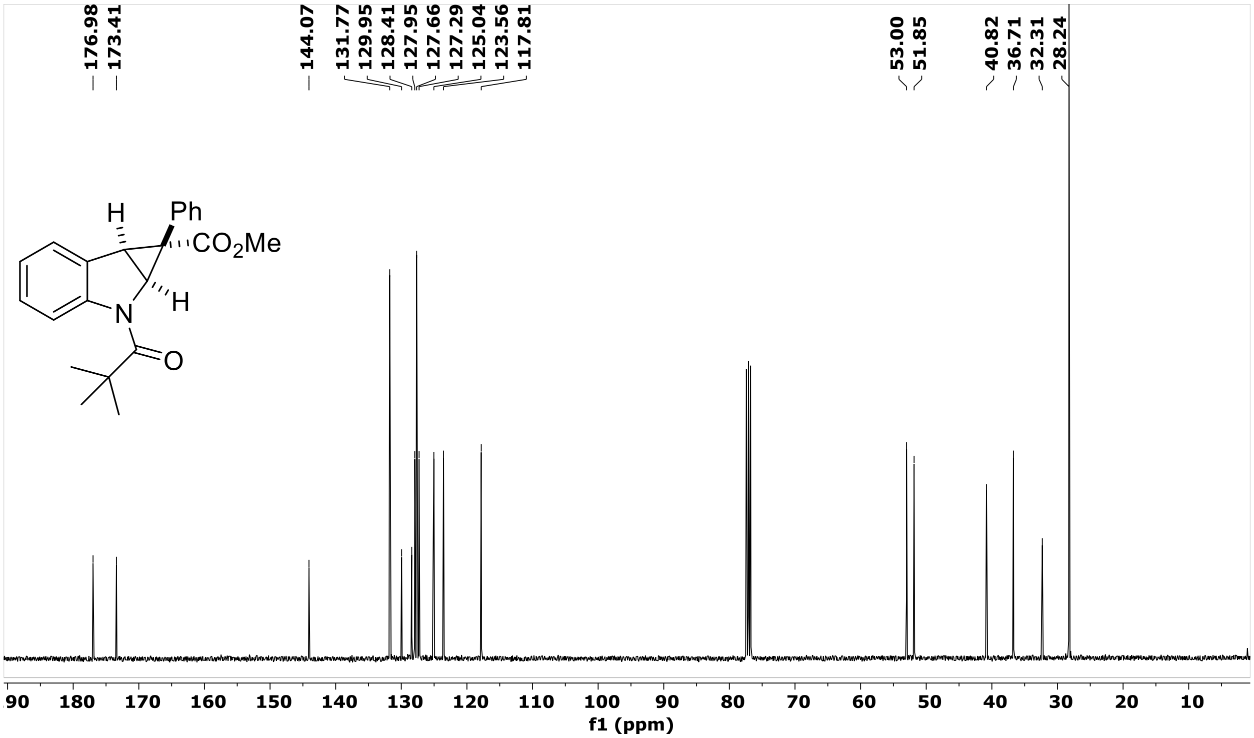

^{1}H NMR spectrum of methyl (1R,1aS,6bS)-2-acetyl-1-phenyl-1,1a,2,6b-tetrahydrocyclopropa[b]indole-1-carboxylate (8k) (400 MHz, $CDCl_3$, 298 K).

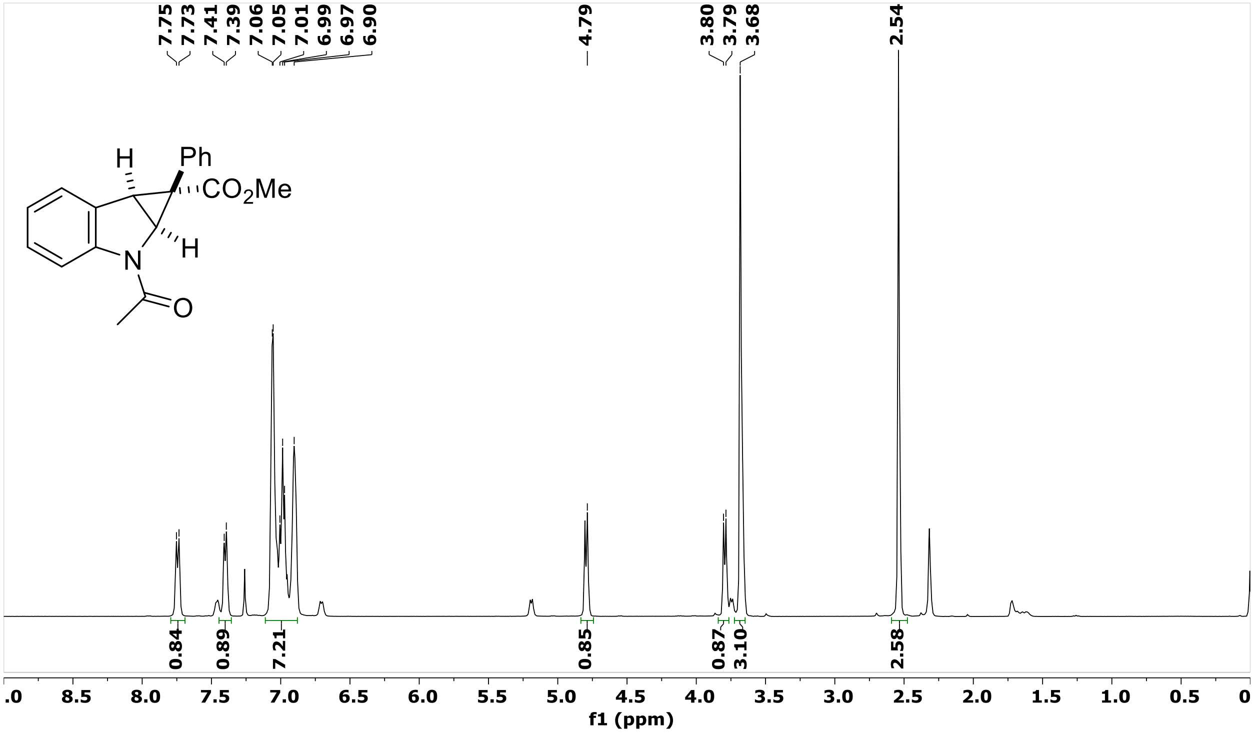

^{13}C NMR spectrum of methyl (1R,1aS,6bS)-2-acetyl-1-phenyl-1,1a,2,6b-tetrahydrocyclopropa[b]indole-1-carboxylate (8k) (101 MHz, $CDCl_3$, 298 K).

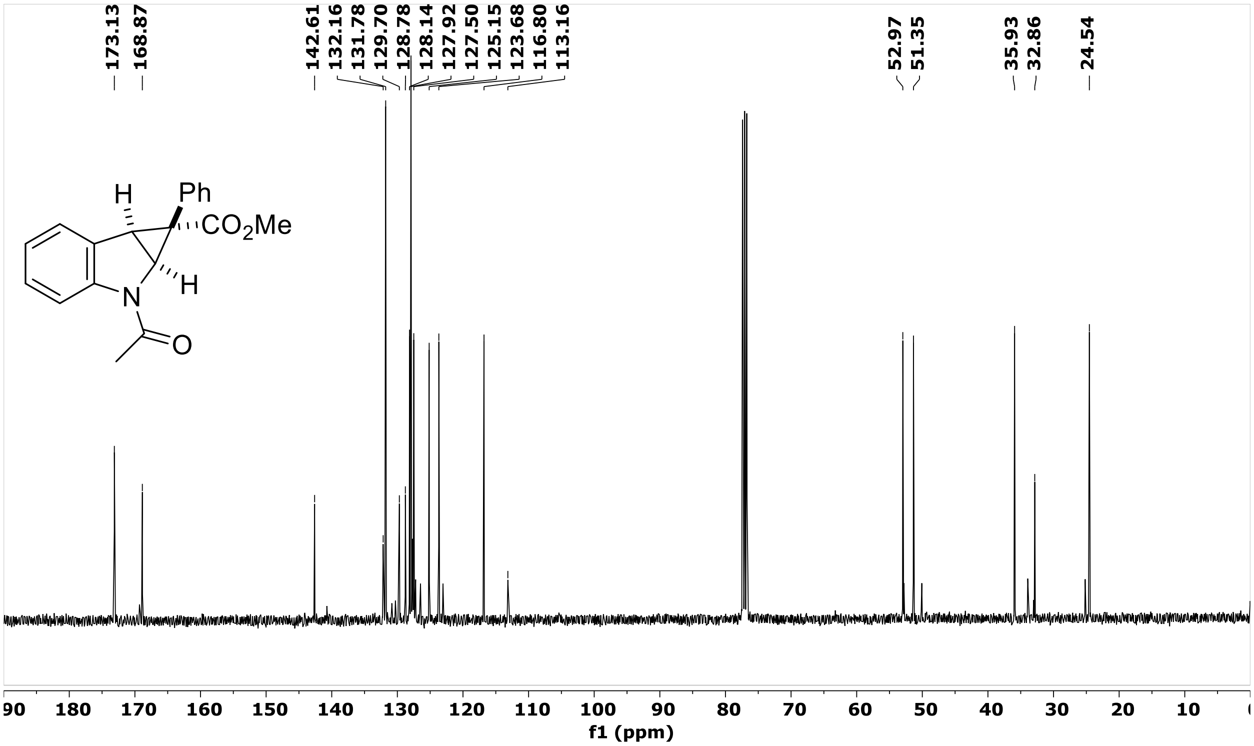

^{1}H NMR spectrum of methyl (1S,5S,6R)-6-(4-methoxyphenyl)-2-pivaloyl-2-azabicyclo[3.1.0]hex-3-ene-6-carboxylate (8l, major product) (400 MHz, CDCl3, 298 K).

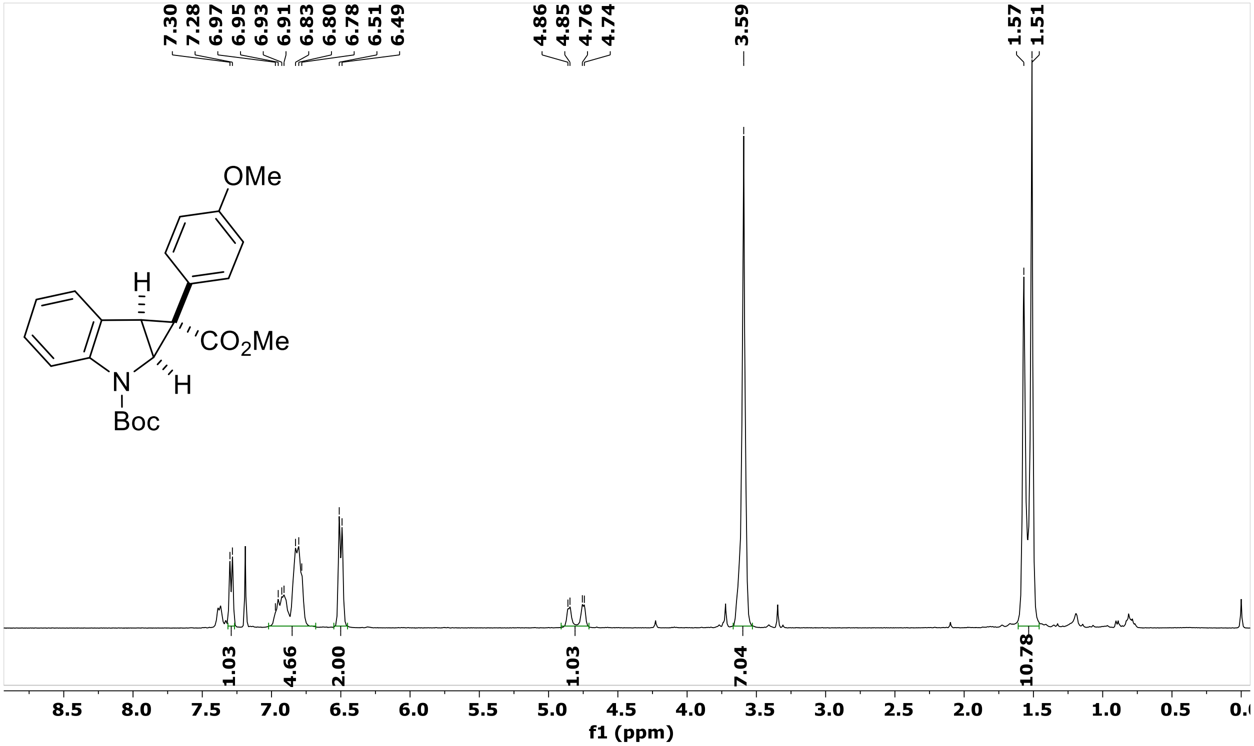

^{13}C NMR spectrum of methyl (1S,5S,6R)-6-(4-methoxyphenyl)-2-pivaloyl-2-azabicyclo[3.1.0]hex-3-ene-6-carboxylate (8l, major product) (101 MHz, CDCl$_3$, 298 K):

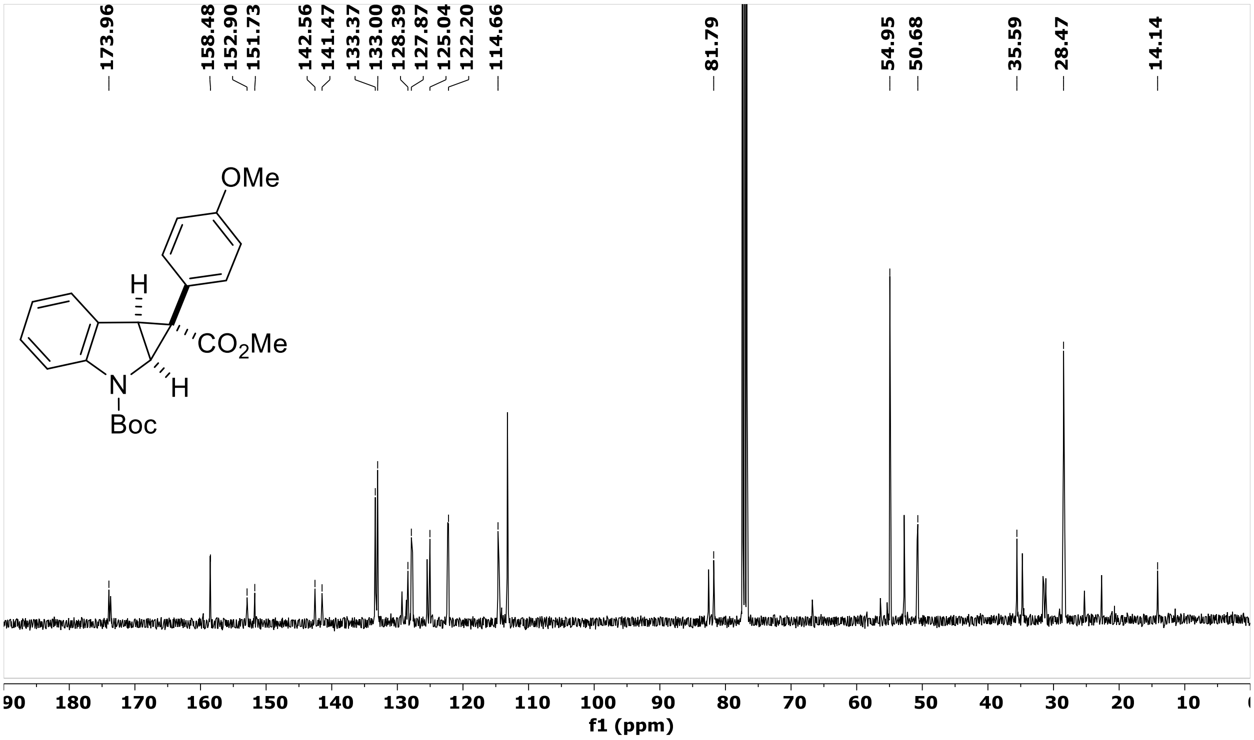

^{1}H NMR spectrum of methyl 7-(4-methoxyphenyl)-2-methylbicyclo[4.1.0]hept-3-ene-7-carboxylate (8l′, minor product) (400 MHz, CDCl3, 298 K).

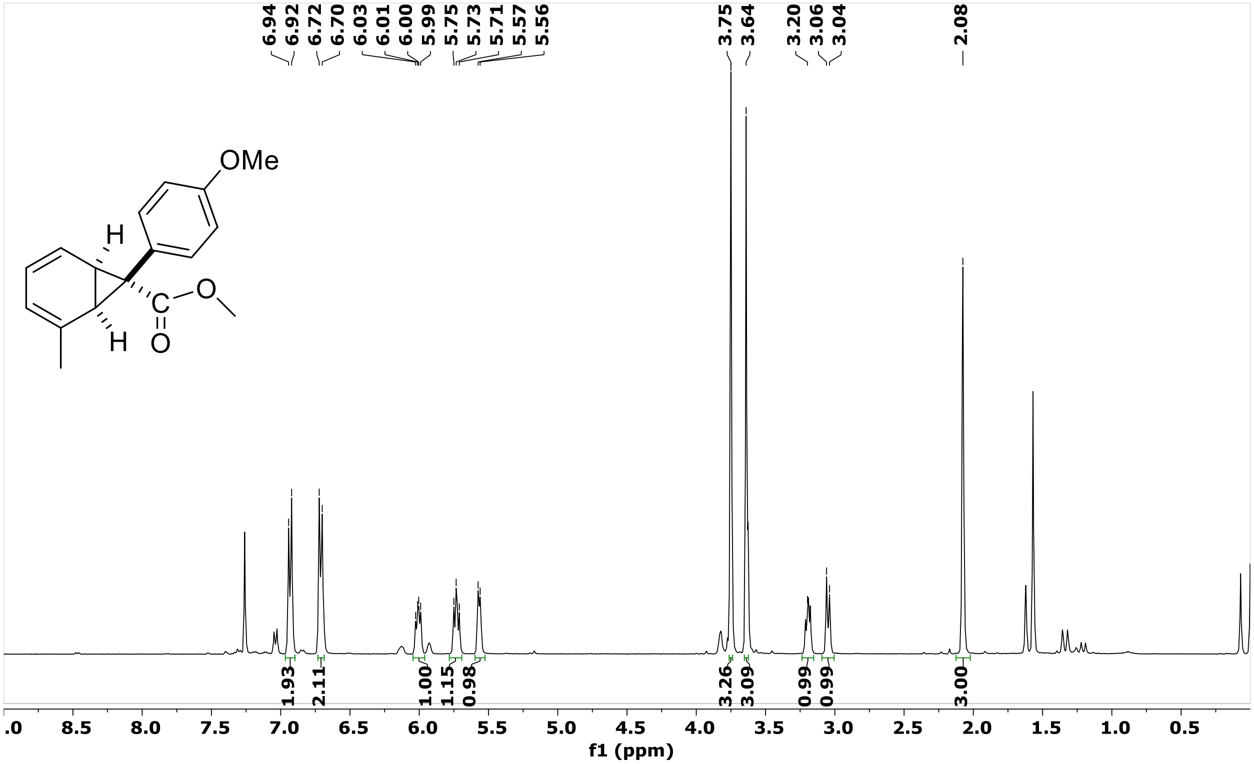

^{13}C NMR spectrum of methyl 7-(4-methoxyphenyl)-2-methylbicyclo[4.1.0]hept-3-ene-7-carboxylate (8l′, minor product) (101 MHz, $CDCl_3$, 298 K)

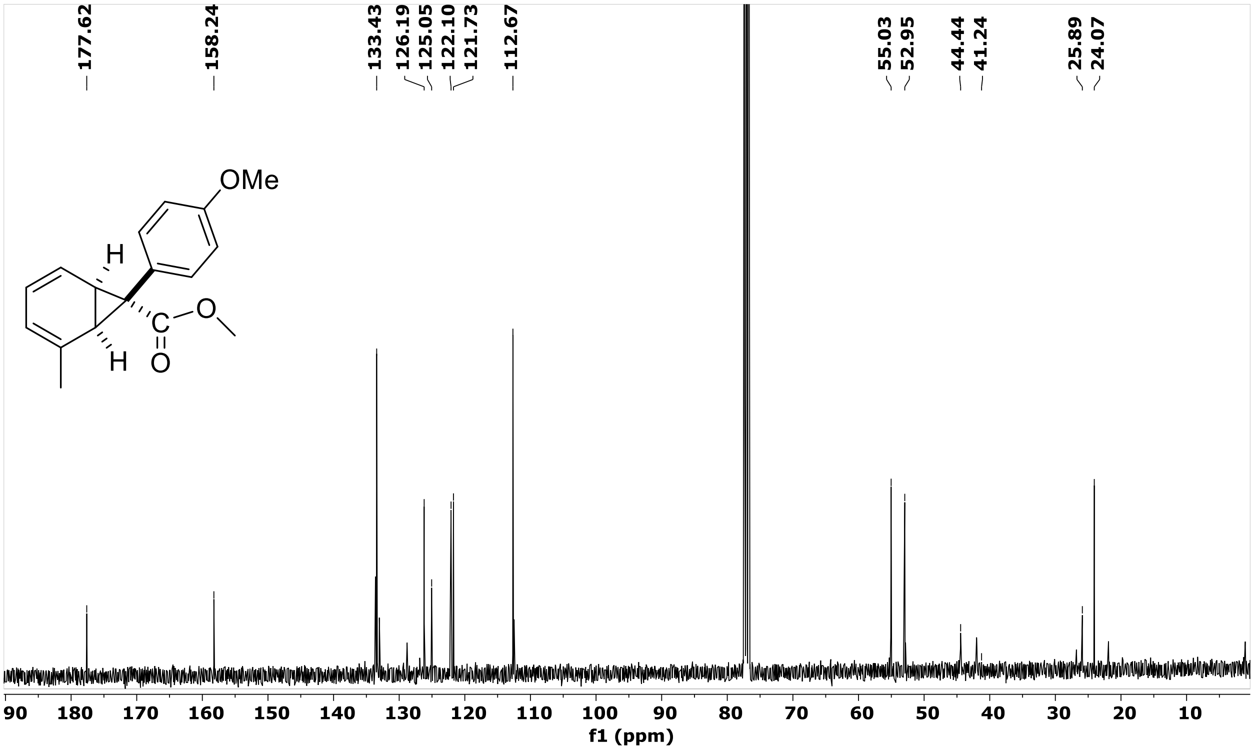

^{1}H NMR spectrum of 2-(*tert*-butyl) 1-methyl (1R,1aS,6bS)-1-(4-chlorophenyl)-1a,6b-dihydrocyclopropa[b]indole-1,2(1H)-dicarboxylate (8m) (400 MHz, CDCl3, 298 K).

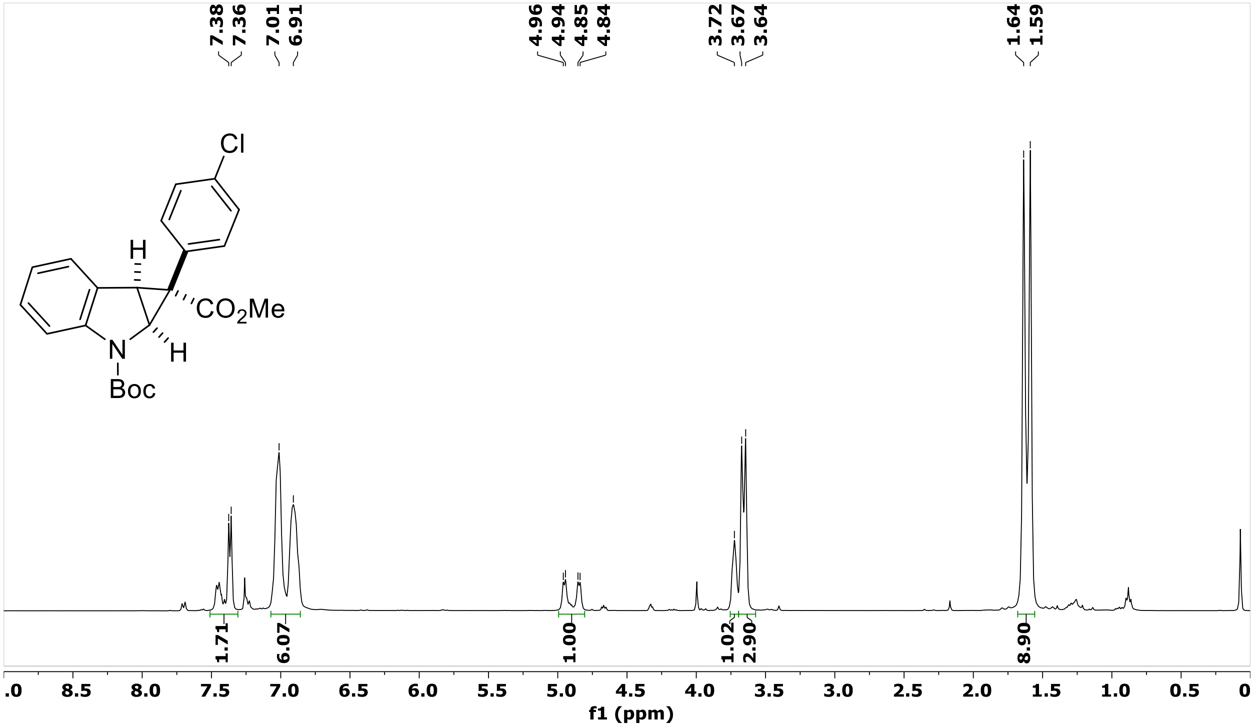

^{13}C NMR spectrum 2-(*tert*-butyl) 1-methyl (1R,1aS,6bS)-1-(4-chlorophenyl)-1a,6b-dihydrocyclopropa[b]indole-1,2(1H)-dicarboxylate (8m) (101 MHz, CDCl$_3$, 298 K).

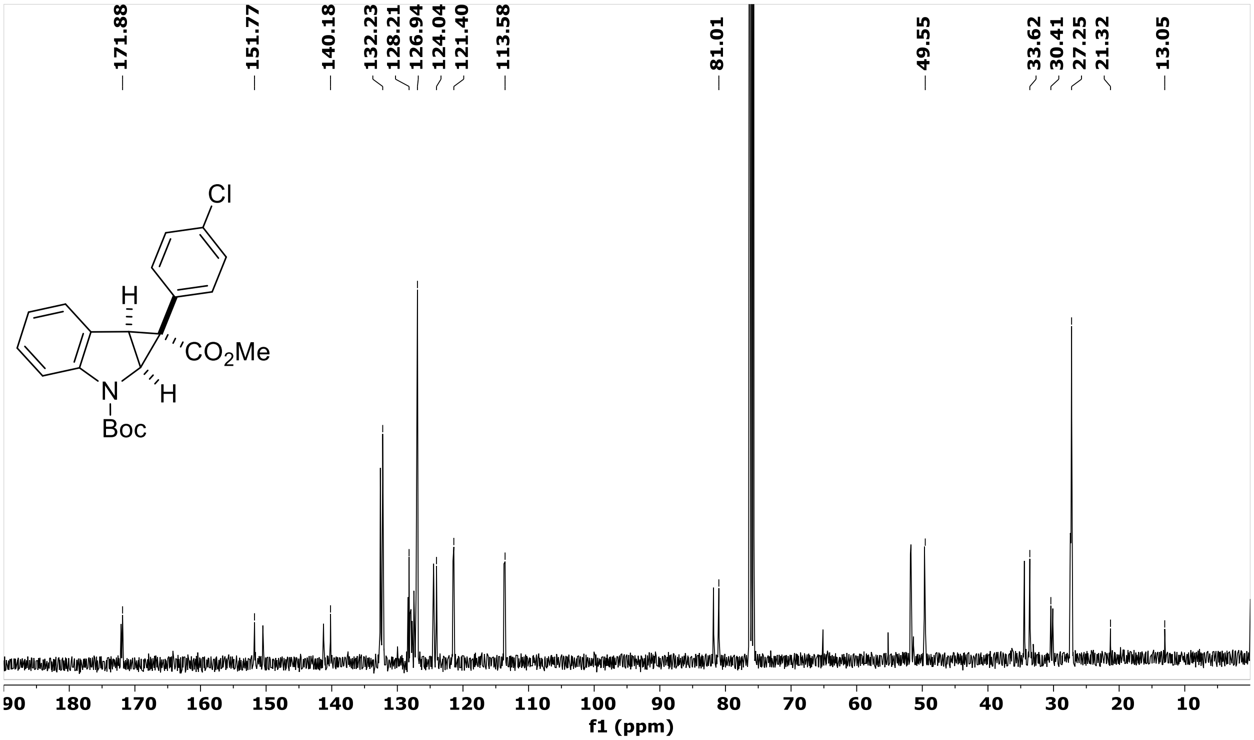

^{1}H NMR spectrum 2-(*tert*-butyl) 6-methyl (1S,5S,6R)-6-(4-methoxyphenyl)-2-azabicyclo[3.1.0]hex-3-ene-2,6-dicarboxylate (8n) (400 MHz, $CDCl_3$, 298 K).

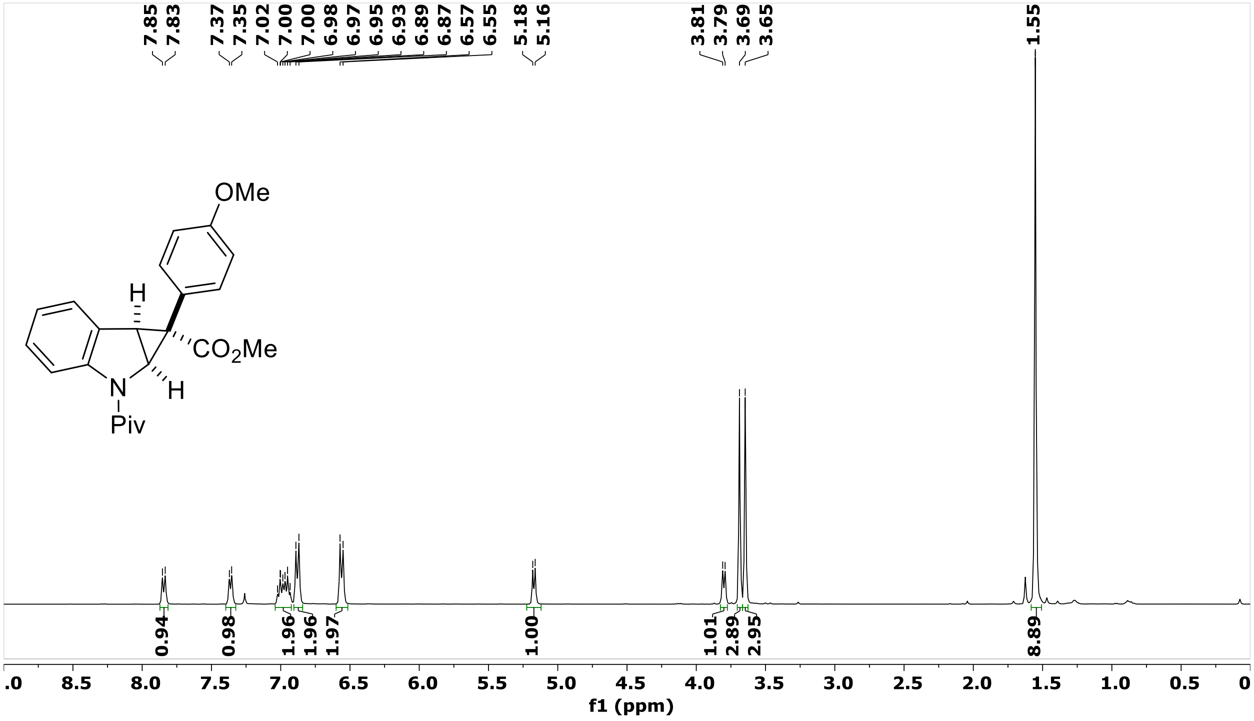

^{13}C NMR spectrum 2-(*tert*-butyl) 6-methyl (1S,5S,6R)-6-(4-methoxyphenyl)-2-azabicyclo[3.1.0]hex-3-ene-2,6-dicarboxylate (8n) (101 MHz, $CDCl_3$, 298 K).

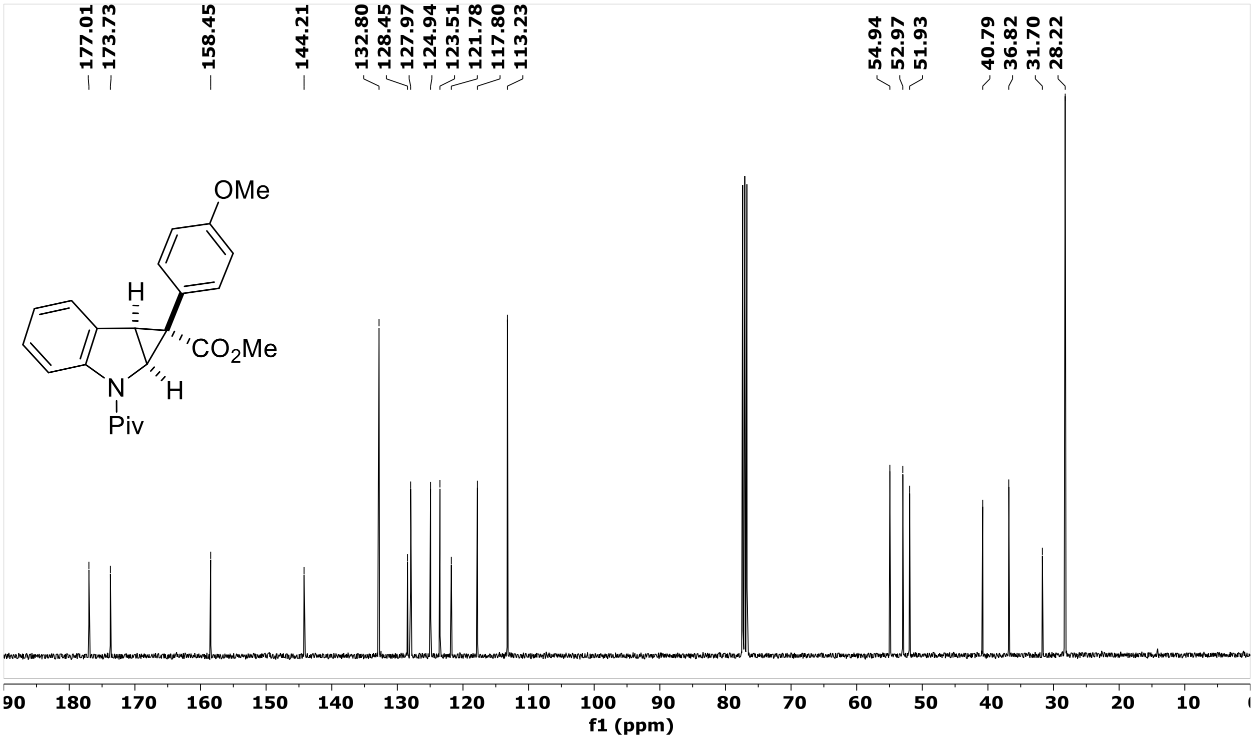

^{1}H NMR spectrum methyl (1R,1aS,6bS)-2-acetyl-1-(4-methoxyphenyl)-1,1a,2,6b-tetrahydrocyclopropa[b]indole-1-carboxylate (8o) (400 MHz, $CDCl_3$, 298 K).

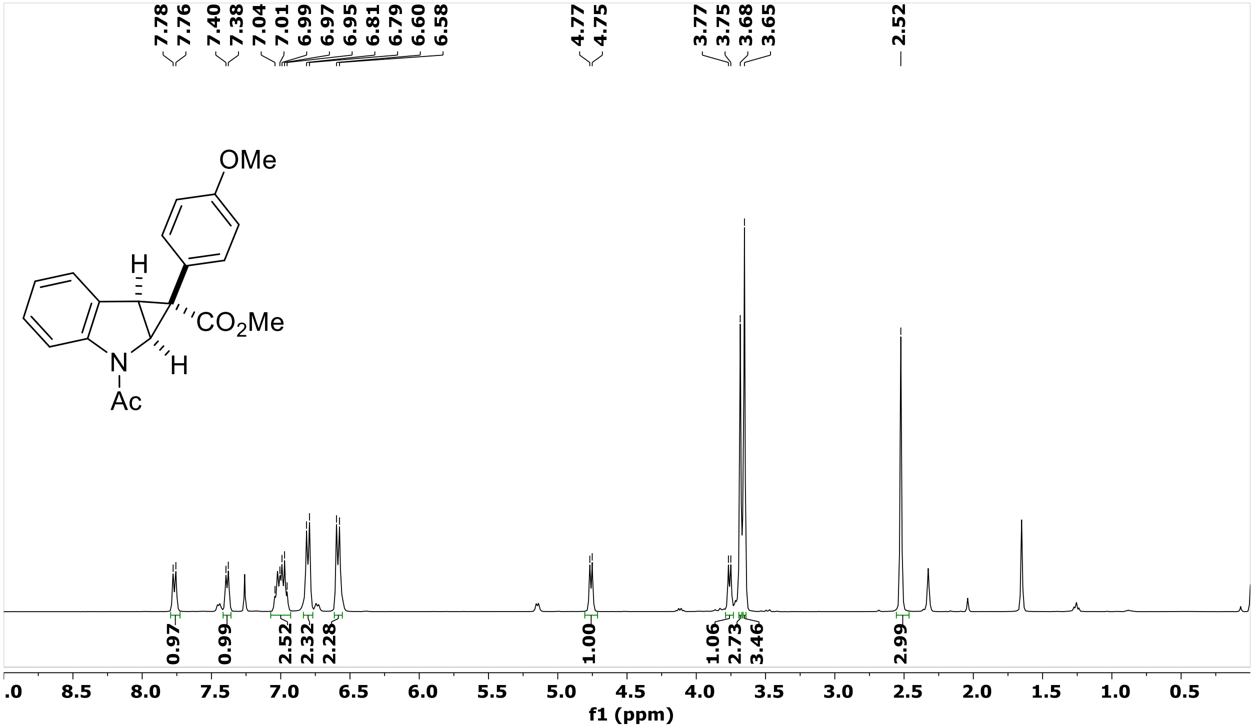

^{13}C NMR spectrum methyl (1R,1aS,6bS)-2-acetyl-1-(4-methoxyphenyl)-1,1a,2,6b-tetrahydrocyclopropa[b]indole-1-carboxylate (8o) (101 MHz, $CDCl_3$, 298 K).

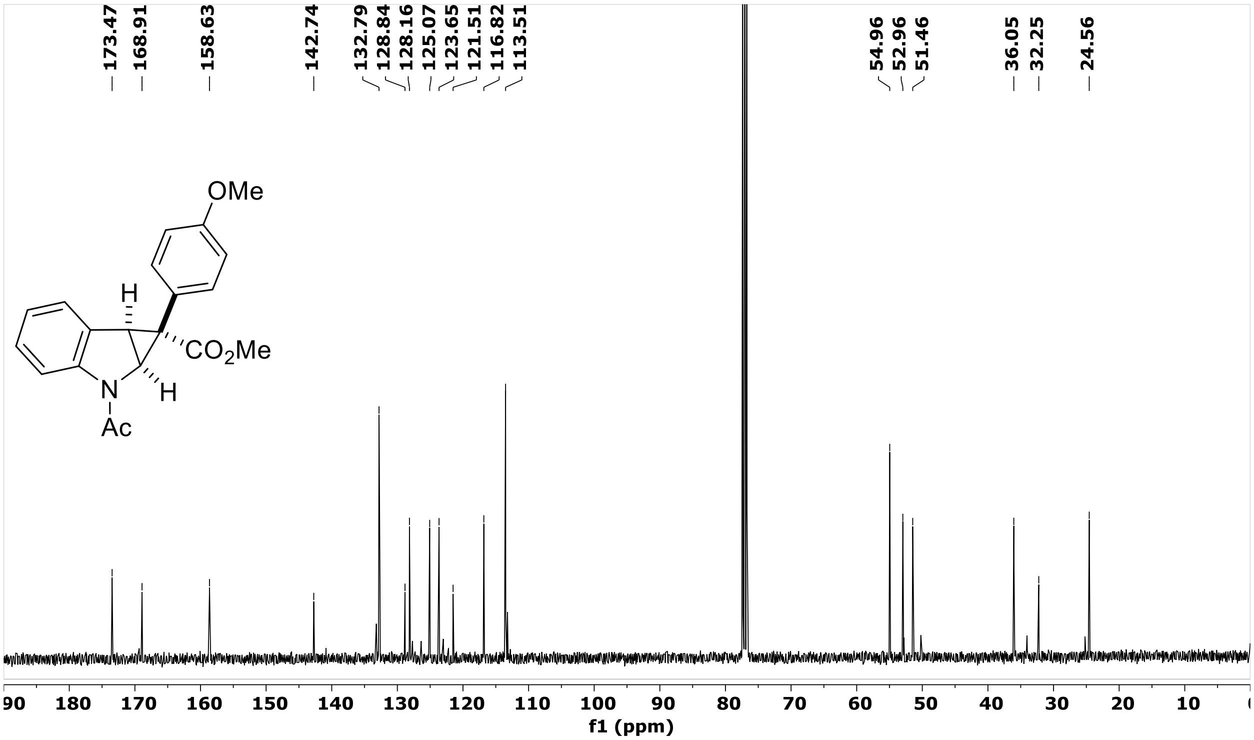

^1H NMR spectrum of 2-(*Tert*-butyl) 1-ethyl (1R,1aS,6bS)-1-(3,4-dimethoxyphenyl)-1a,6b-dihydrocyclopropa[b]indole-1,2(1H)-dicarboxylate (8p).

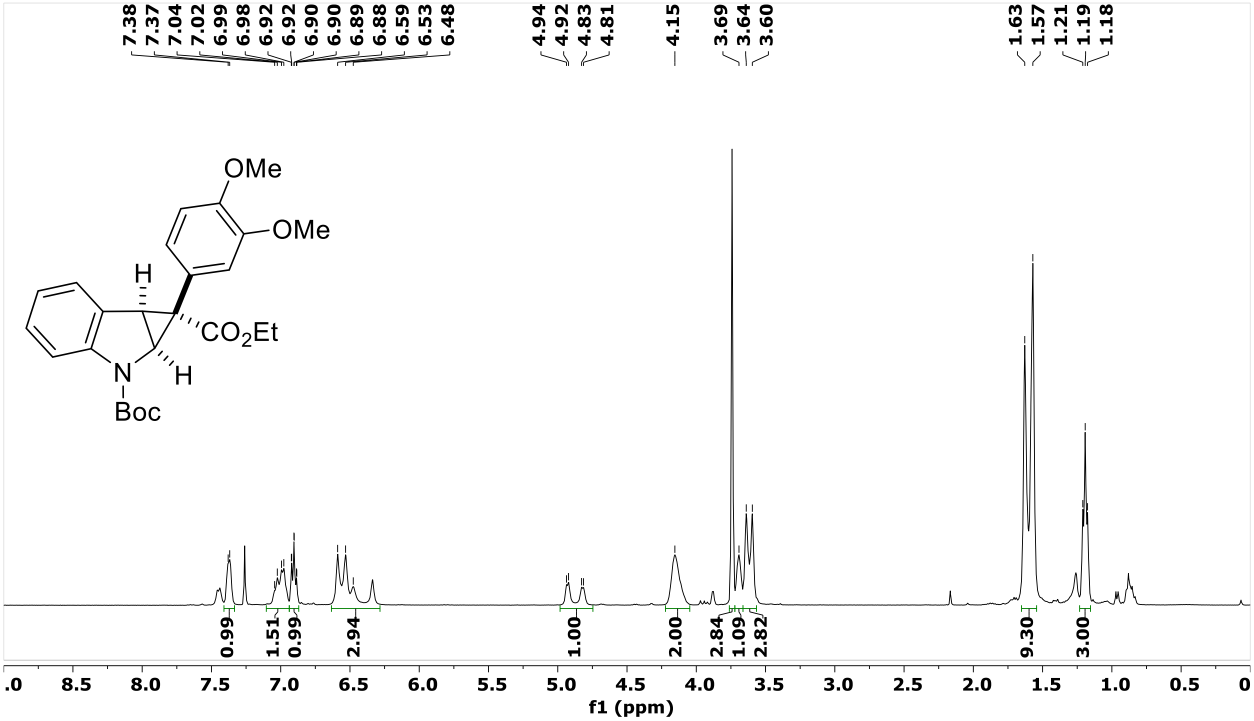

^{13}C NMR spectrum of 2-(*Tert*-butyl) 1-ethyl (1R,1aS,6bS)-1-(3,4-dimethoxyphenyl)-1a,6b-dihydrocyclopropa[b]indole-1,2(1H)-dicarboxylate (8p).

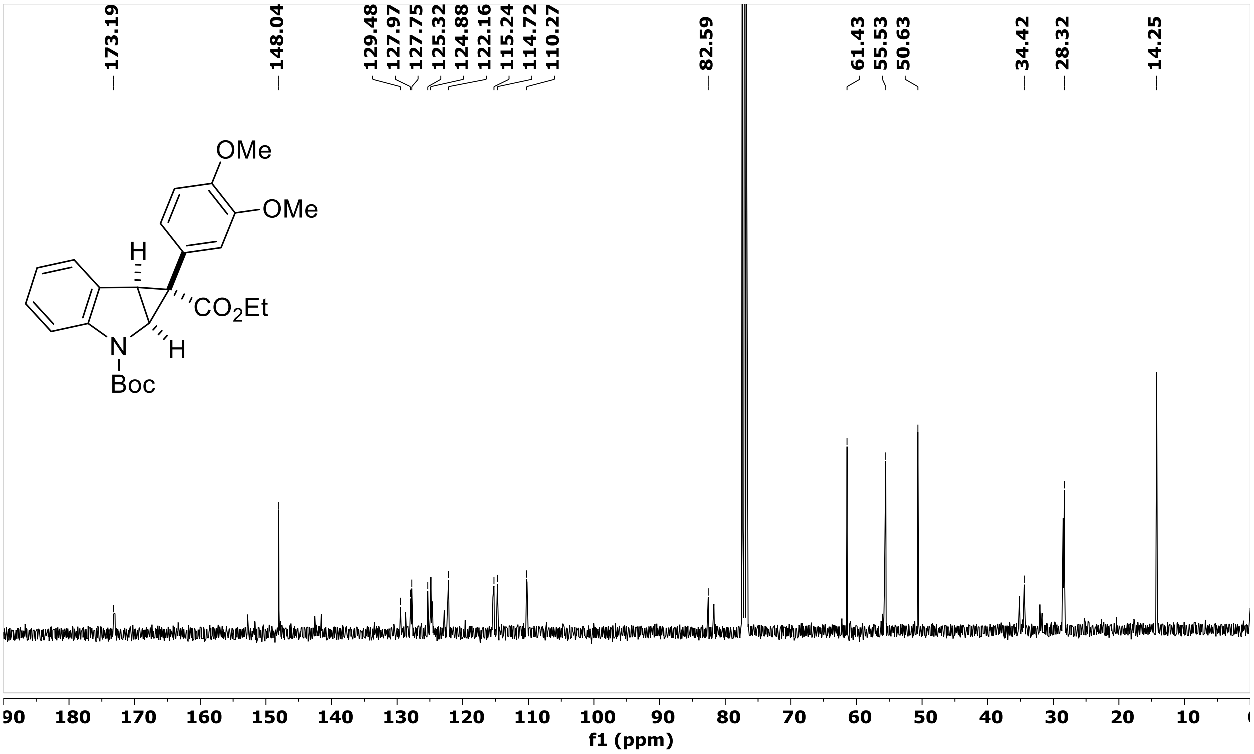

^{1}H NMR spectrum of ethyl (1R,1aS,6bS)-1-(3,4-dimethoxyphenyl)-2-pivaloyl-1,1a,2,6b-tetrahydrocyclopropa[b]indole-1-carboxylate (8q) (400 MHz, $CDCl_3$, 298 K).

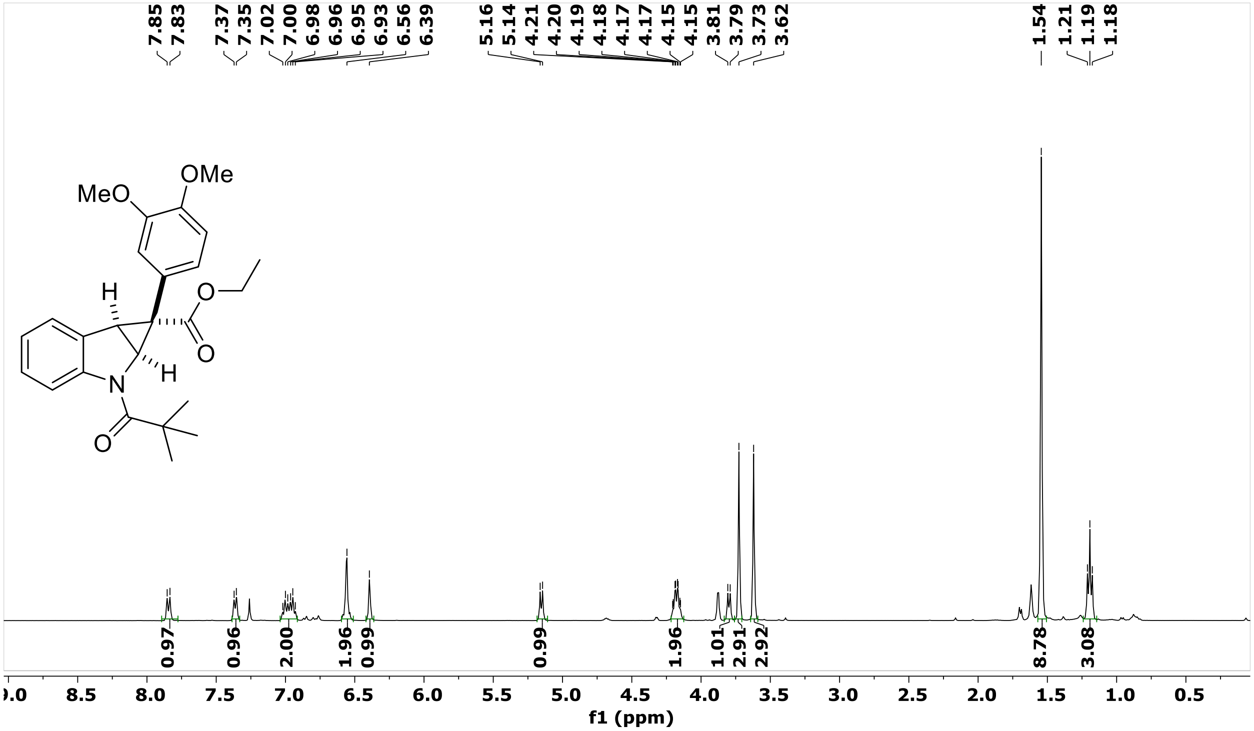

^{13}C NMR spectrum ethyl (1R,1aS,6bS)-1-(3,4-dimethoxyphenyl)-2-pivaloyl-1,1a,2,6b-tetrahydrocyclopropa[b]indole-1-carboxylate (8q) (101 MHz, $CDCl_3$, 298 K) .

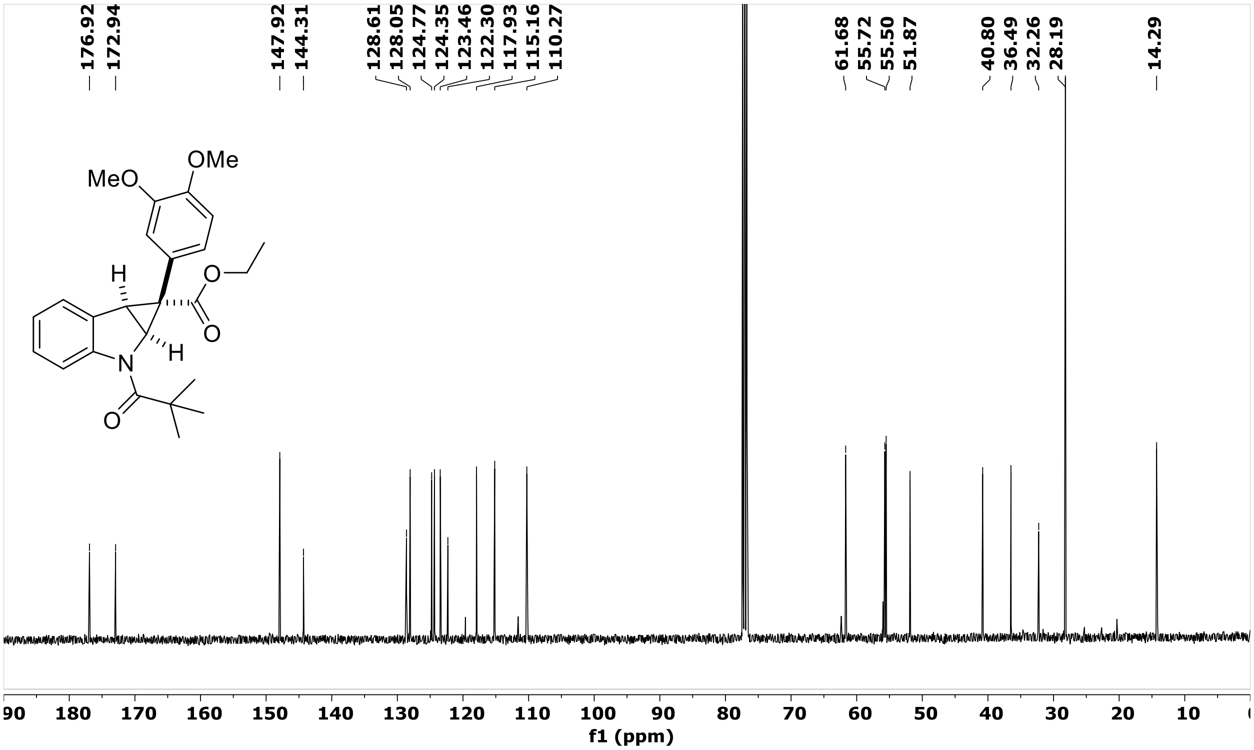

^{1}H NMR spectrum of 2-(*Tert*-butyl) 1-ethyl 6b-methyl-1a,6b-dihydrocyclopropa[b]indole-1,2(1H)-dicarboxylate (8r) (400 MHz, $CDCl_3$, 298 K).

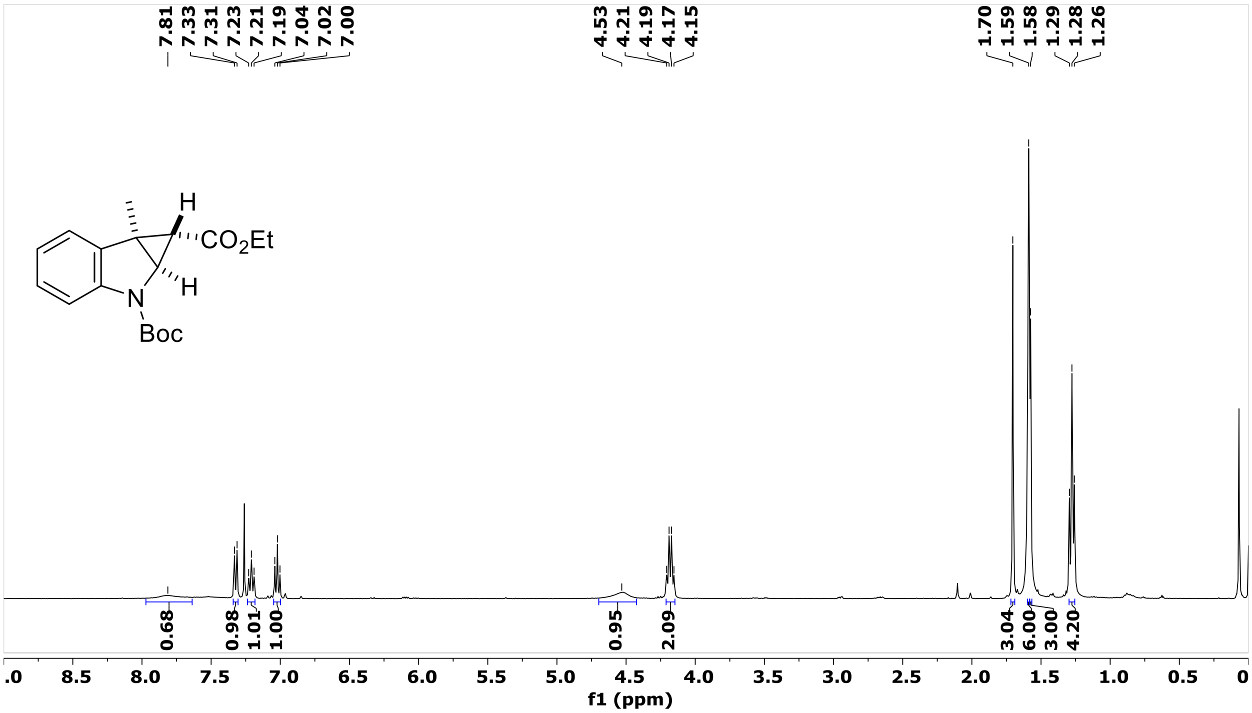

^{13}C NMR spectrum of 2-(*Tert*-butyl) 1-ethyl 6b-methyl-1a,6b-dihydrocyclopropa[b]indole-1,2(1H)-dicarboxylate (8r) (101 MHz, $CDCl_3$, 298 K).

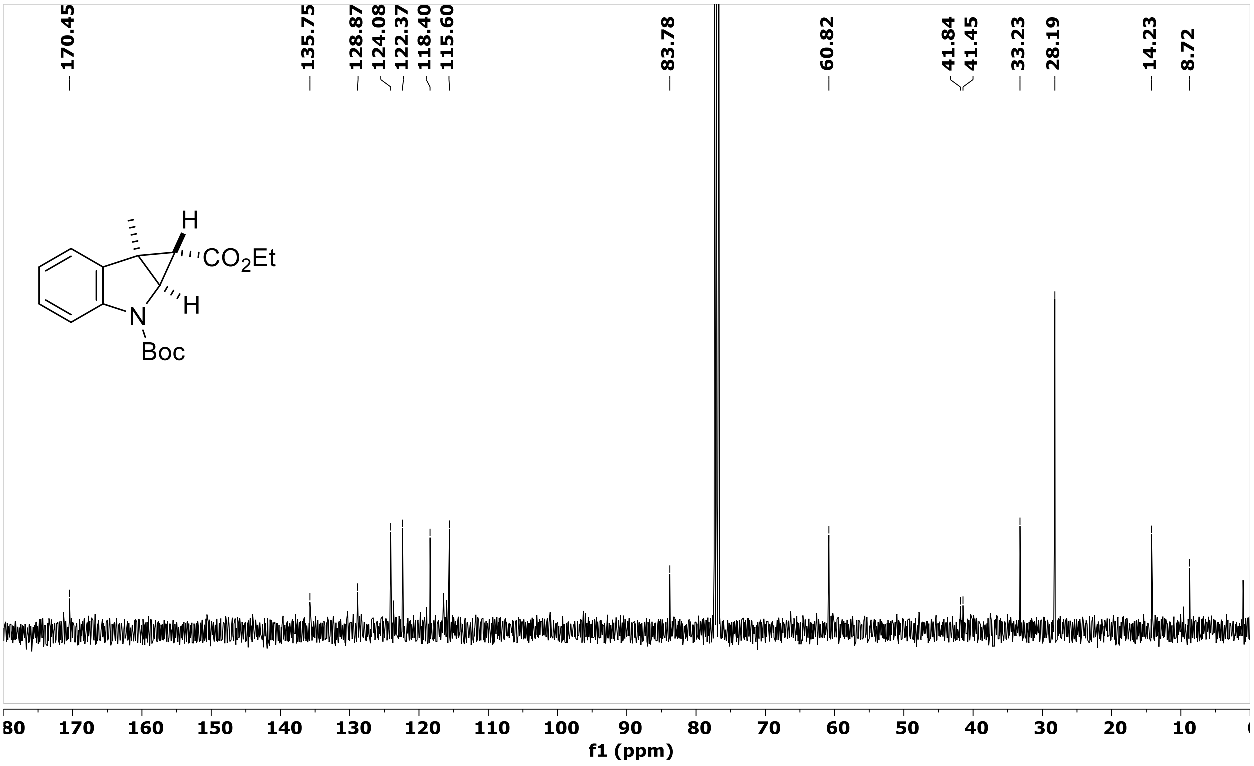

^{1}H NMR spectrum of Di-*tert*-butyl-6b-methyl-1a,6b-dihydrocyclopropa[b]indole-1,2(1H)-dicarboxylate (8r′) (400 MHz, $CDCl_3$, 298 K) (signal broadening occurs due to the presence of rotamers).

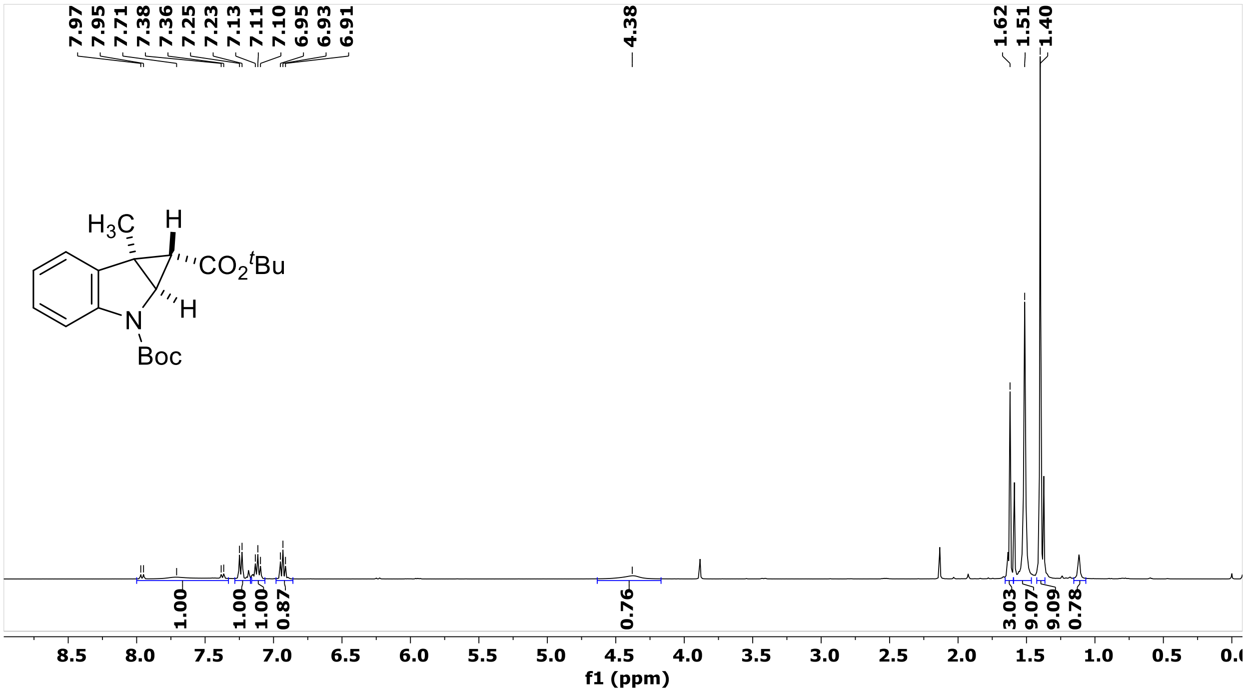

^{13}C NMR spectrum of Di-*tert*-butyl-6b-methyl-1a,6b-dihydrocyclopropa-[b]indole-1,2(1H)-dicarboxylate (8r′) (101 MHz, $CDCl_3$, 298 K) (signal doubling occurs due to the presence of rotamers).

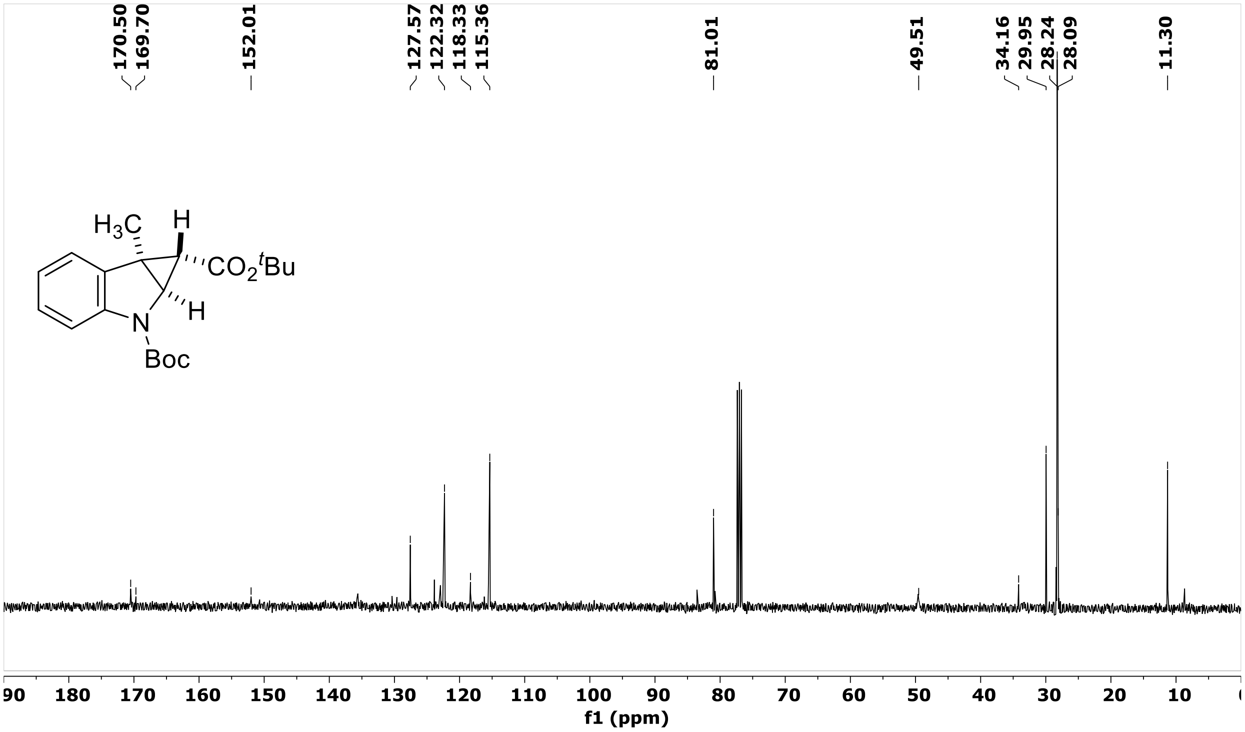

^{1}H NMR spectrum of 2-(*Tert*-butyl) 1-methyl-6b-methyl-1-phenyl-1a,6b-dihydrocyclopropa[b]indole-1,2(1H)- dicarboxylate (8s) (400 MHz, $CDCl_3$, 298 K).

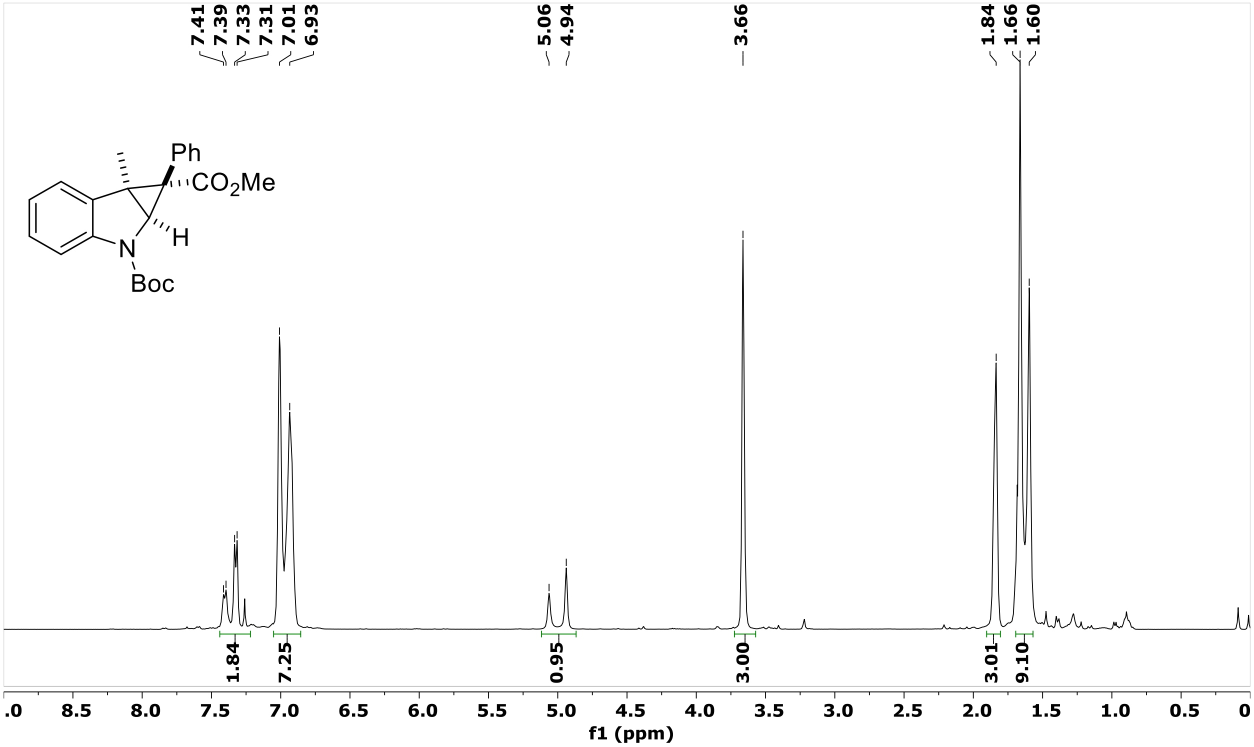

^{13}C NMR spectrum of 2-(*Tert*-butyl) 1-methyl-6b-methyl-1-phenyl-1a,6b-dihydrocyclopropa[b]indole-1,2(1H)- dicarboxylate (8s) (101 MHz, $CDCl_3$, 298 K).

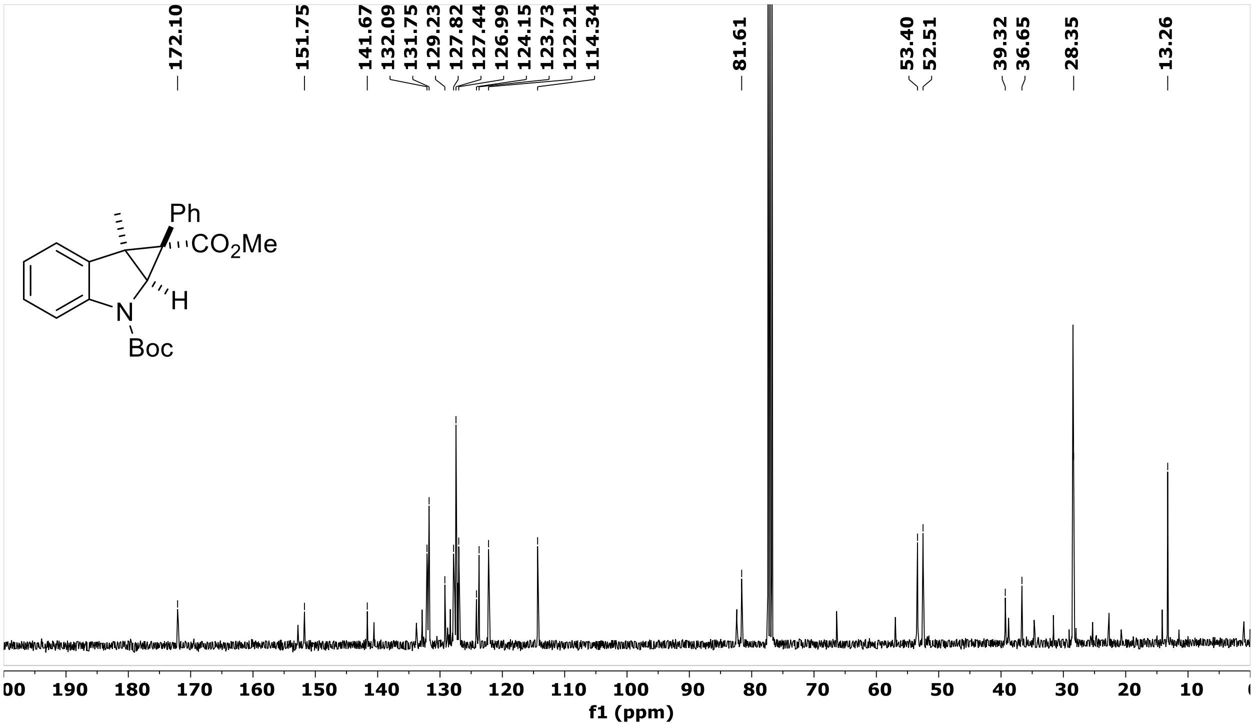

^{1}H NMR spectrum of methyl (1S,1aS,6bS)-6b-methyl-1-phenyl-2-pivaloyl-1,1a,2,6b-tetrahydrocyclopropa[b]indole-1-carboxylate (8t) (400 MHz, $CDCl_3$, 298 K).

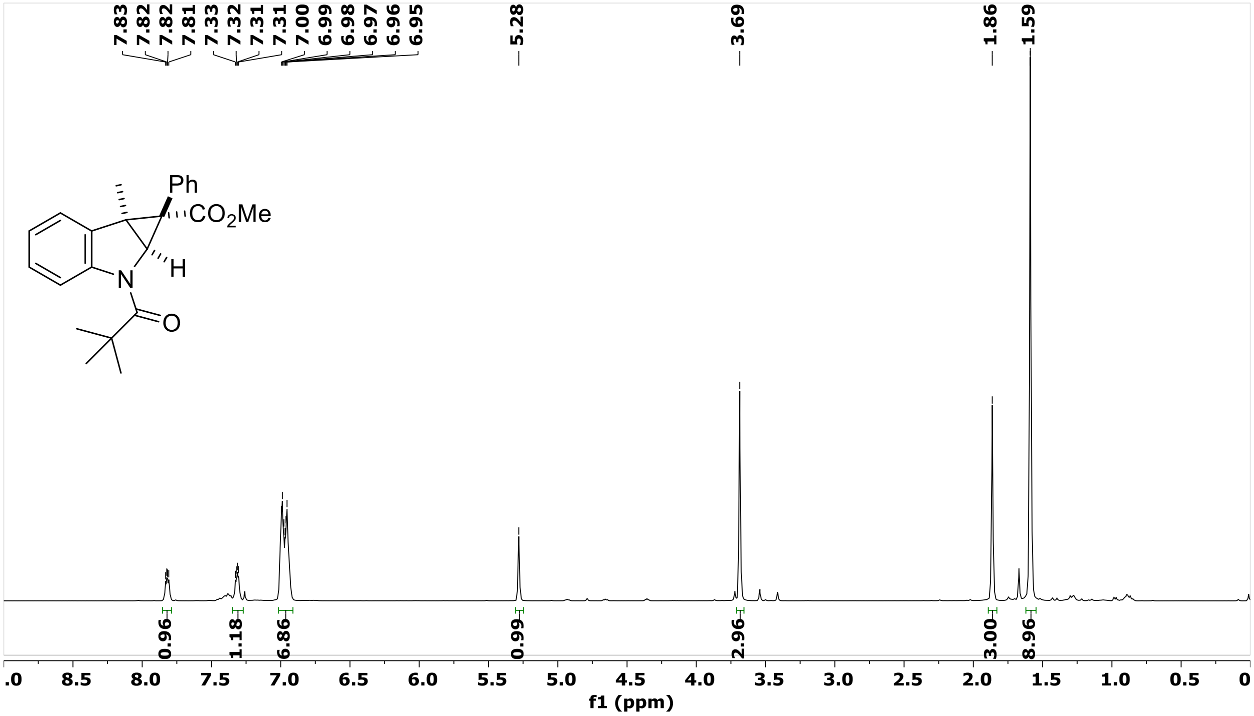

^{13}C NMR spectrum methyl (1S,1aS,6bS)-6b-methyl-1-phenyl-2-pivaloyl-1,1a,2,6b-tetrahydrocyclopropa[b]indole-1-carboxylate (8t) (101 MHz, $CDCl_3$, 298 K).

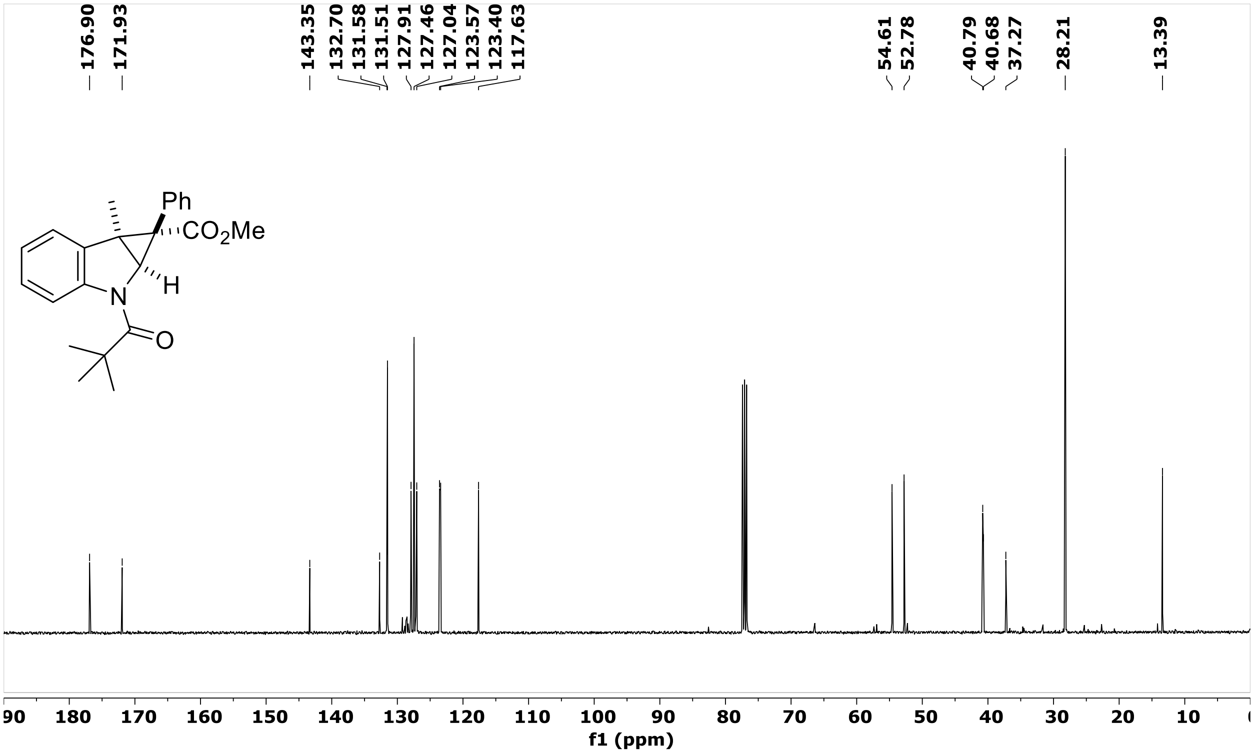

^{1}H NMR spectrum of Di-*tert*-butyl-6b-methyl-1a,6b-dihydrocyclopropa[b]indole-1,2(1H)-dicarboxylate (6f) (400 MHz, $CDCl_3$, 298 K) (signal broadening occurs due to the presence of rotamers).

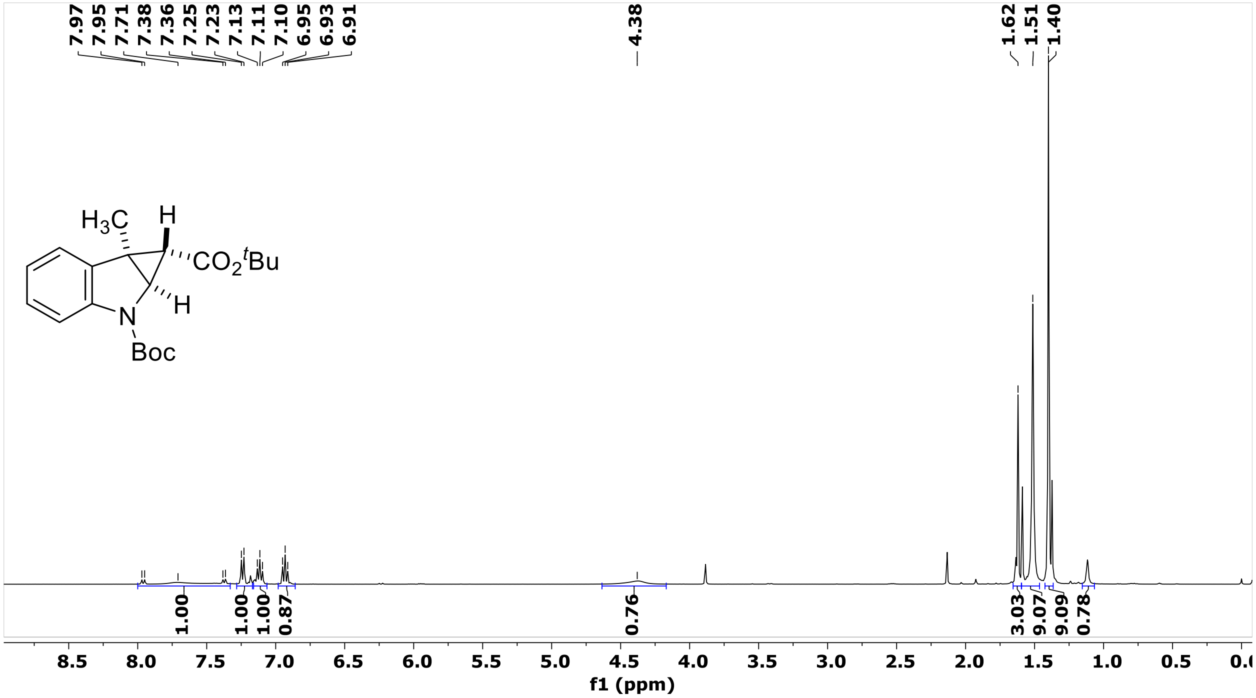

^{13}C NMR spectrum of Di-*tert*-butyl-6b-methyl-1a,6b-dihydrocyclopropa-[b]indole-1,2(1H)-dicarboxylate (6f) (101 MHz, $CDCl_3$, 298 K) (signal doubling occurs due to the presence of rotamers).

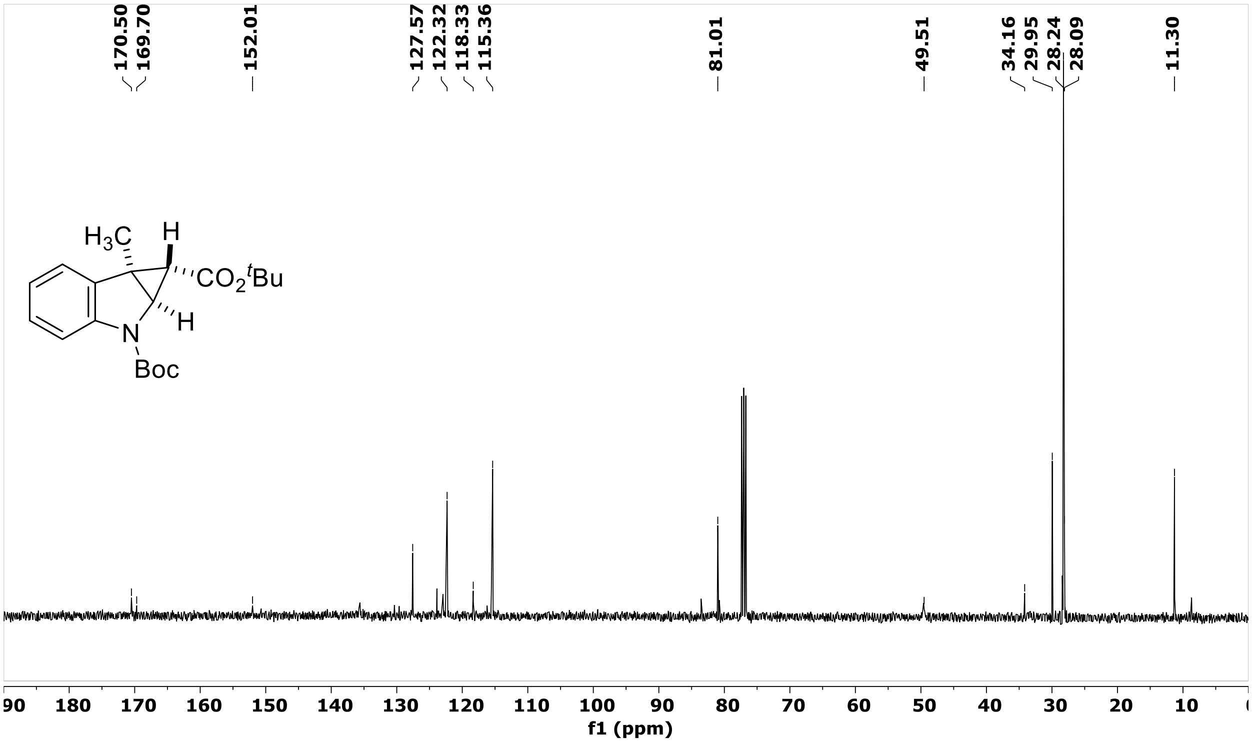

^{1}H NMR spectrum 2-(tert-butyl) 1-methyl (1S,1aS,6bS)-1-(4-methoxyphenyl)-6b-methyl-1a,6b-dihydrocyclopropa[b]indole-1,2(1H)-dicarboxylate (8u) (400 MHz, CDCl3, 298 K).

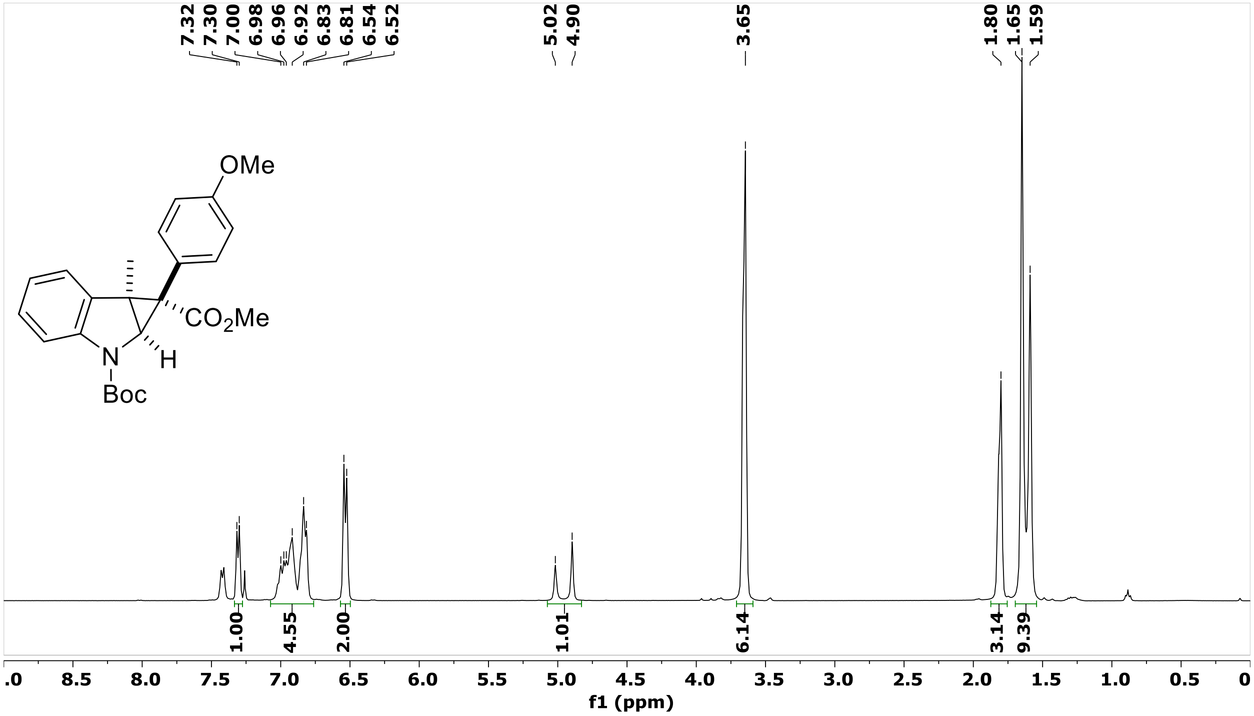

^{13}C NMR spectrum 2-(tert-butyl) 1-methyl (1S,1aS,6bS)-1-(4-methoxyphenyl)-6b-methyl-1a,6b-dihydrocyclopropa[b]indole-1,2(1H)-dicarboxylate (8u) (101 MHz, CDCl$_3$, 298 K).

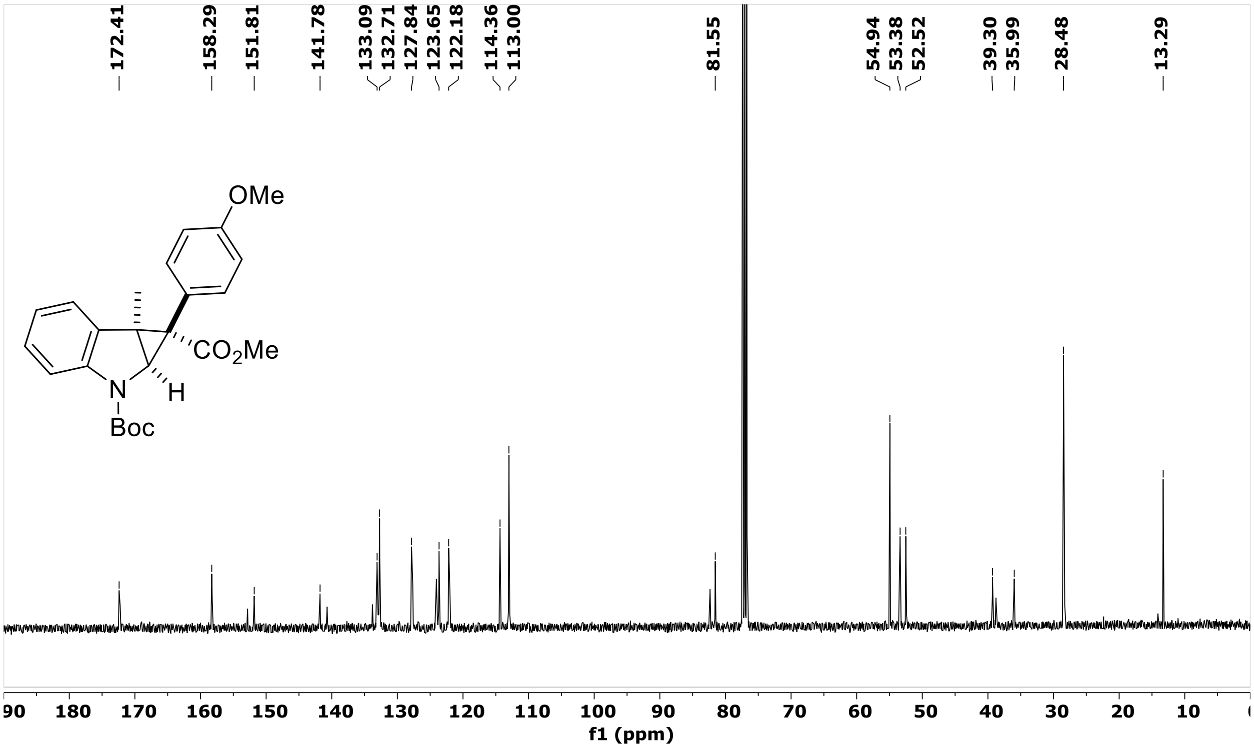

^{1}H NMR spectrum of *Tert*-butyl 3-((2S)-2-(methoxycarbonyl)-2-phenylcyclopropyl)-1H-indole-1-carboxylate (8v).

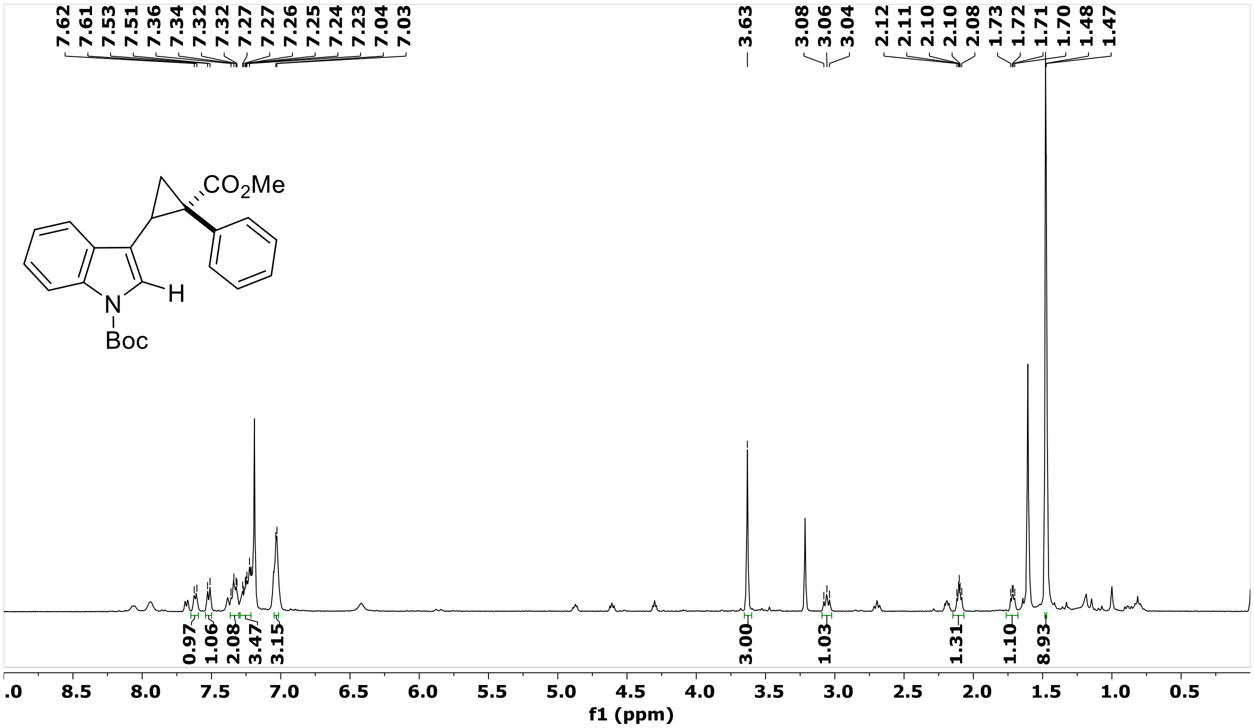

^{13}C NMR spectrum of *Tert*-butyl 3-((2S)-2-(methoxycarbonyl)-2-phenylcyclopropyl)-1H-indole-1-carboxylate (8v).

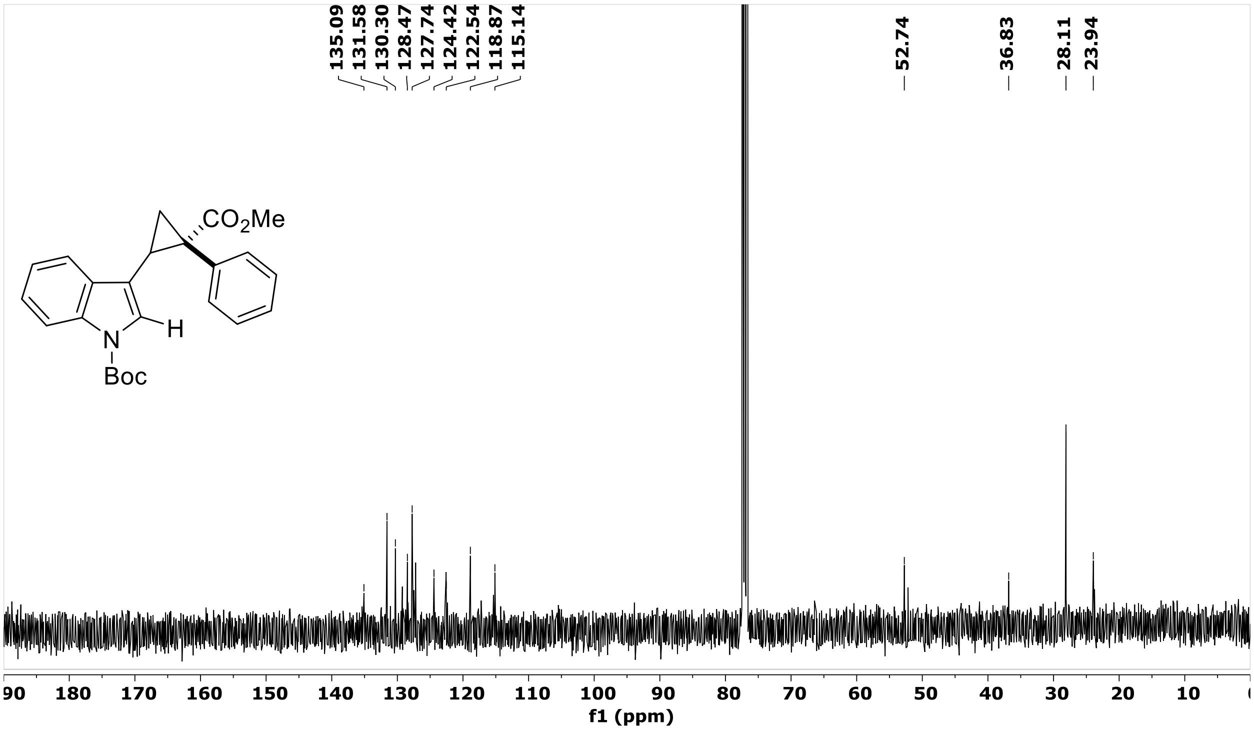

^{1}H NMR spectrum of *tert*-butyl 3-((1S,2S)-2-(methoxycarbonyl)-2-(4-methoxyphenyl)cyclopropyl)-1H-indole-1-carboxylate (8w) (400 MHz, $CDCl_3$, 298 K).

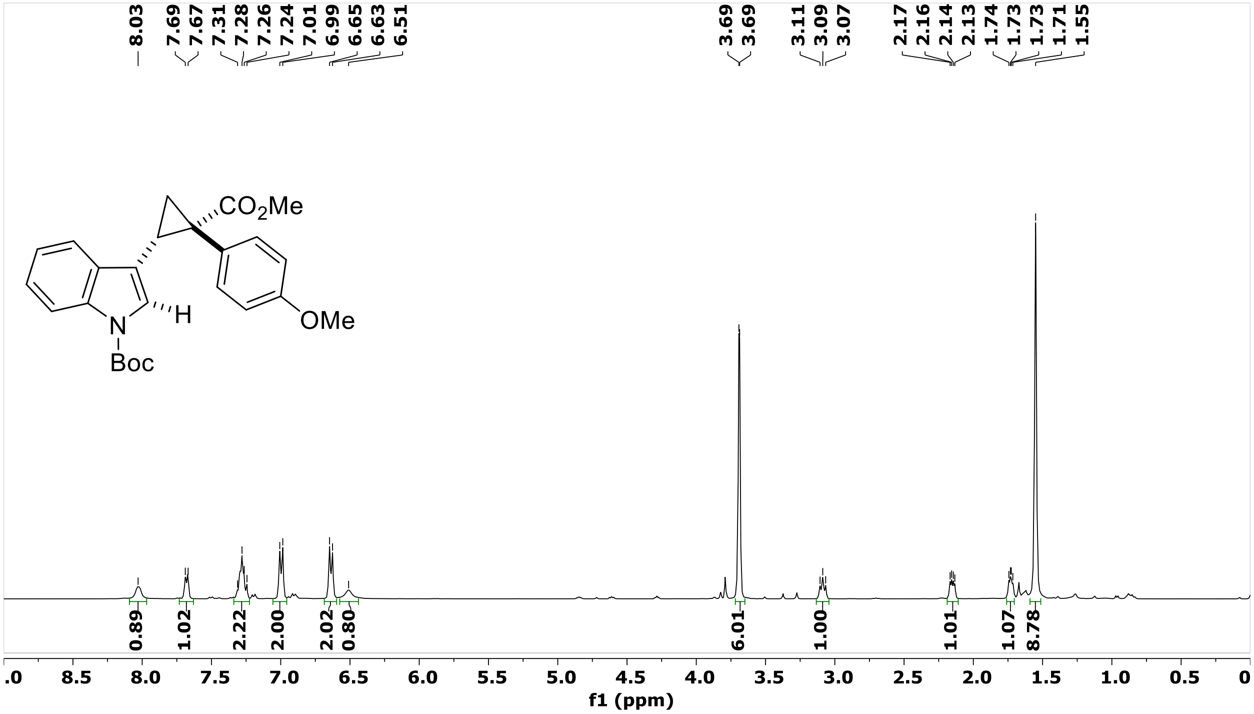

^{13}C NMR spectrum of *tert*-butyl 3-((1S,2S)-2-(methoxycarbonyl)-2-(4-methoxyphenyl)cyclopropyl)-1H-indole-1-carboxylate (8w) (101 MHz, $CDCl_3$, 298 K).

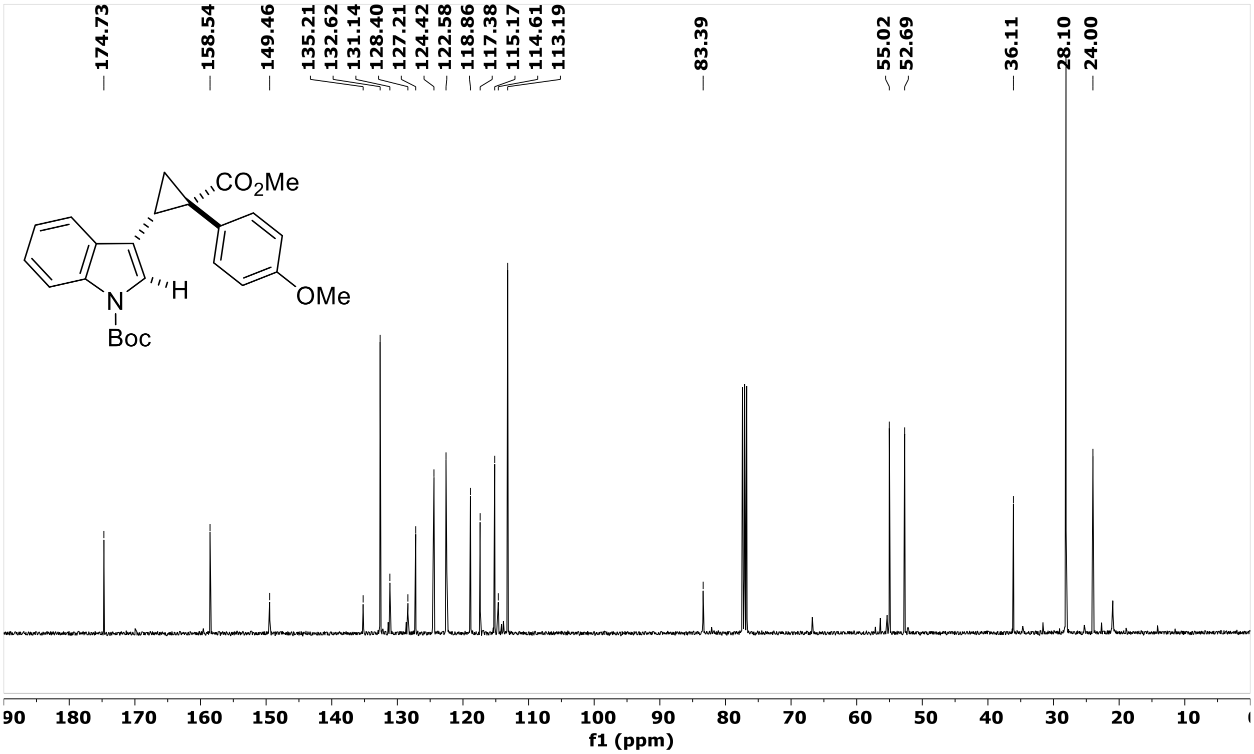

^{1}H NMR spectrum of *Tert*-butyl 3-((2S)-2-(3,4-dimethoxyphenyl)-2-(ethoxycarbonyl)cyclopropyl)-1H-indole-1-carboxylate (8x):

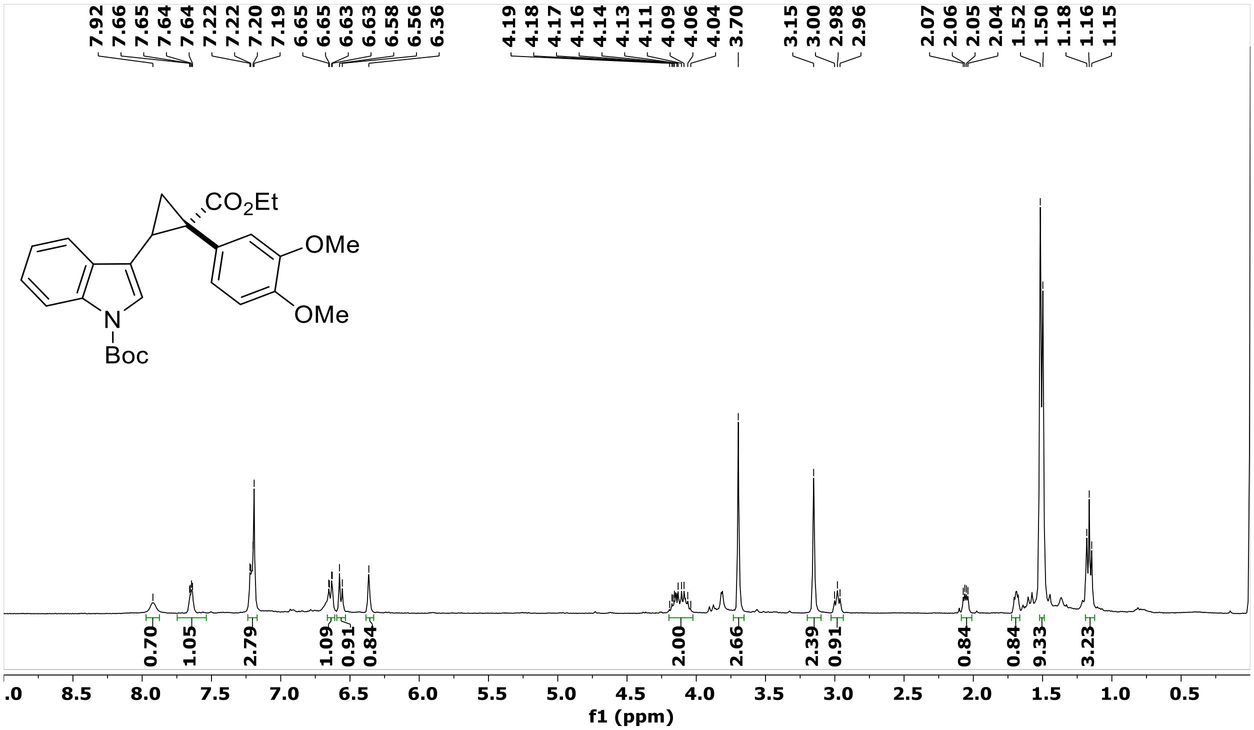

^{13}C NMR spectrum of *Tert*-butyl 3-((2S)-2-(3,4-dimethoxyphenyl)-2-(ethoxycarbonyl)cyclopropyl)-1H-indole-1-carboxylate (8x):

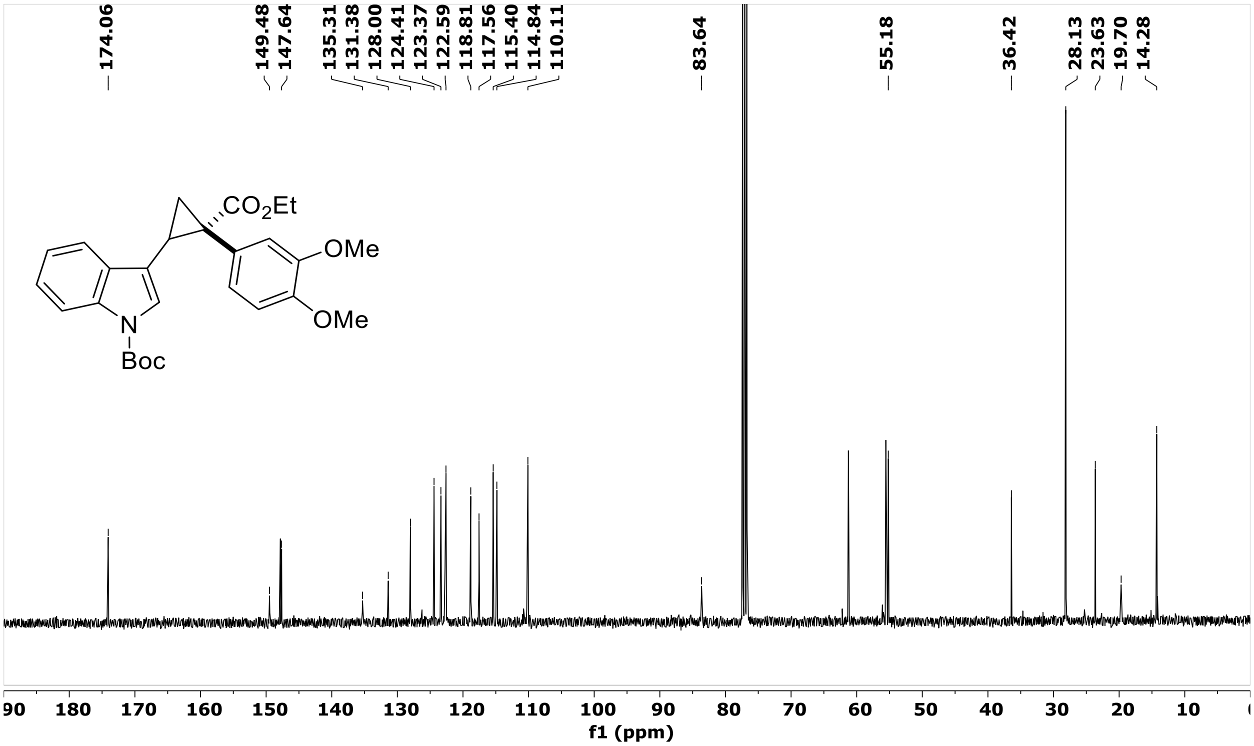

8. Mechanistic investigations and mass spectrometric analysis

8.1. HRESI-MS measurement:

HRESI-MS measurements were conducted at a capillary temperature of 225 °C. Aliquots of the solution were injected into the device at 2.00 μL/min. The mass spectrometer used for the measurements was an Agilent Technologies 6545 Q-TOF LC/MS and the data were collected in positive ion modes. The spectrometer was previously calibrated with the standard tune mix to give a precision of ca. 2.0 ppm. within the region of 100−3000 m/z. The capillary voltage was 2.5 kV, the tube lens voltage was 1.0 kV, and the skimmer voltage was 65 V.

The GC vials were evacuated using a needle which was connected to the vacuum line. The vials were purged with argon. This process was repeated three times to make it air free. MeOH (1.4 mL) was injected inside the GC vial and reaction solution (0.2 mL) was also injected after wards. Separately the needle/syringe was made oxygen free (before use) by purging argon into it. The methanol was boiled under argon atmosphere for 2 h in Schlenk flask to make it O_2 free.

Freshly distilled toluene (boiled with Na/K alloy in the presence of benzophenone under argon flow) and DCM (boiled with $CaCl_2$ under argon) were utilized for reaction with studying the binding of diazoester (**7b**) in DCM and toluene. Catalyst **3** (0.1 mmol) which was isolated as orange precipitate from MeOH was reacted with **7b** (0.2 mmol) in toluene and/or DCM (10 mL) at room temperature. The orange brown solution was sampled over different time intervals to study binding with the nickel centers of the catalyst.

8.2. Study of reaction mechanism of $[Ni_4((O^-)_2L\text{-}Me)_4(s)_4]$ (3) [s = solvent = MeOH/H_2O]:

For mass spectrometric analysis a 1:1 molar mixture of $NiCl_2{\cdot}6H_2O$ (0.5 mmol; 134 mg) and (H_2L-Me) (0.5 mmol; 128 mg) was dissolved in 20 mL of MeOH and stirred for 20 min to obtain a clear solution. Et_3N (1 mmol; 100 mg) (two equivalents) was added dropwise to obtain a clear orange-brown solution. The 0.1 mL of the reaction solution was sampled every time and diluted with MeOH to study the reaction mechanism for the step wise formation of complex **3**. The ESI-MS samples were prepared in every five minutes after the addition of base. **3′** = **3** - 4s.

For simplicity of $(OH)_2L$-Me = H_2L-Me = $C_{15}H_{15}NO_3$, $(O^-)_2L$-Me = $(L\text{-}Me)^{2-}$ = $C_{15}H_{13}NO_3$, $(O^-)(OH)L$-Me = HL-Me^- = $C_{15}H_{14}NO_3$. For simplicity, similarly $(OH)_2L$-H = H_2L-H = $C_{14}H_{13}NO_3$, $(O^-)_2L$-H = $(L\text{-}H)^{2-}$ = $C_{14}H_{11}NO_3$, $(O^-)(OH)L$-H = HL-H^- = $C_{14}H_{12}NO_3$.

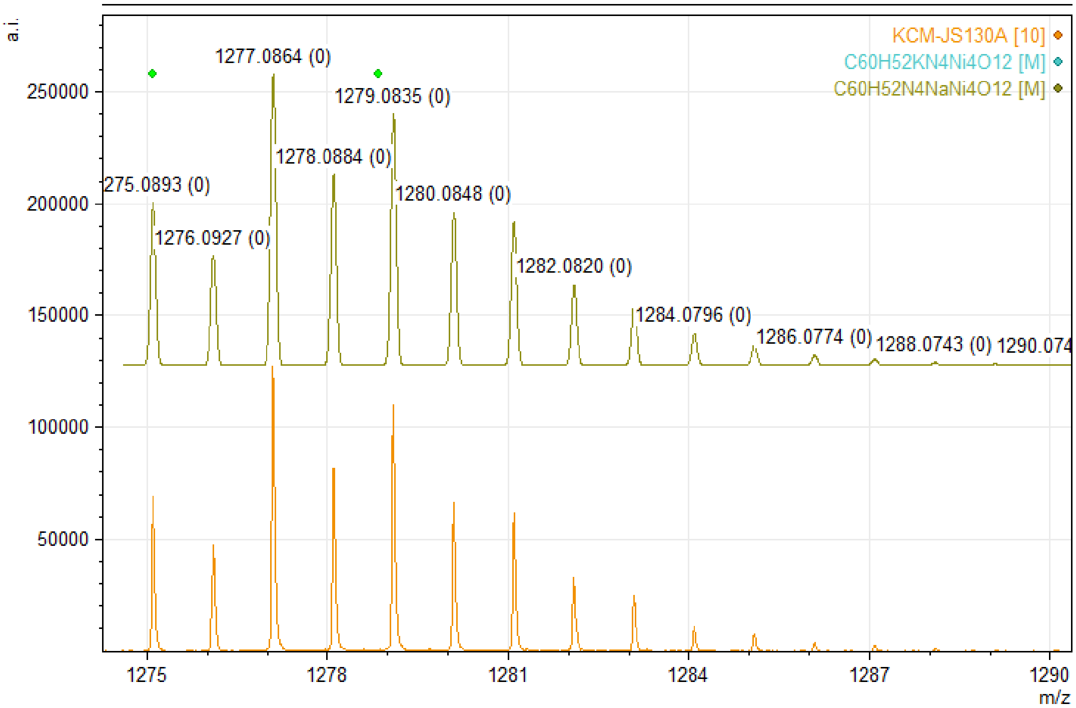

Figure S41. Experimental (bottom) and calculated (top) ESI mass spectrum of $[Ni_4(L\text{-}Me)_4 + Na]^+$ (**3′ + Na**)$^+$. Reaction of **3** with $N_2CHCO_2{}^tBu$ after 1 h. For simplicity, $(O^-)_2L\text{-}Me = (L\text{-}Me)^{2-} = C_{15}H_{13}NO_3$ and **3′** = **3** - 4s [s = solvent = H_2O or MeOH].

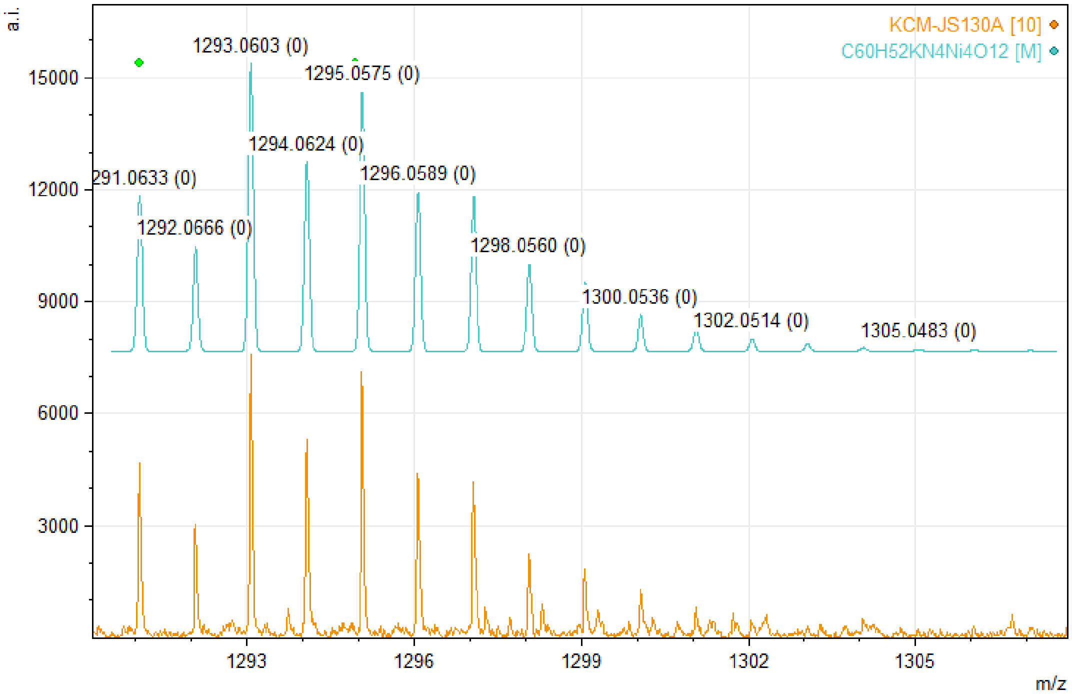

Figure S42. Experimental (bottom) and calculated (top) ESI mass spectrum of $[Ni_4(L\text{-}Me)_4 + K]^+$ (**3′ + K**)$^+$. Reaction of **3** with $N_2CHCO_2{}^tBu$ after 1 h. For simplicity, $(O^-)_2L\text{-}Me = (L\text{-}Me)^{2-} = C_{15}H_{13}NO_3$ and **3′** = **3** - 4s [s = solvent = H_2O or MeOH].

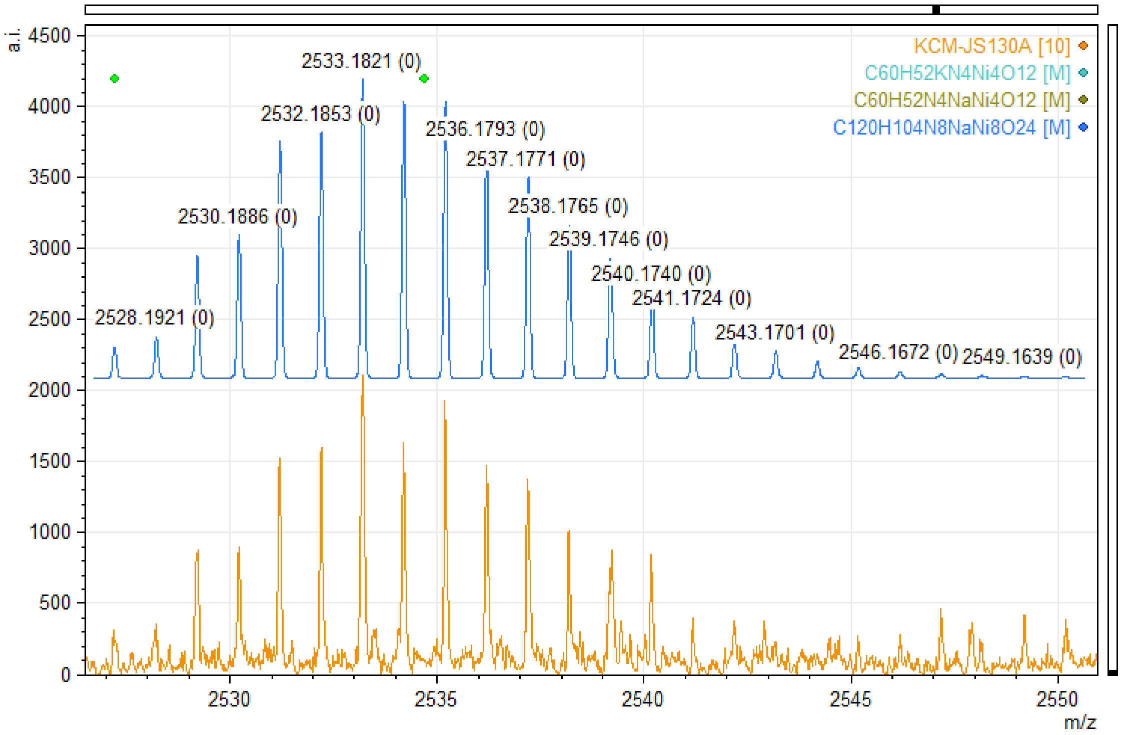

Figure S43. Experimental (bottom) and calculated (top) ESI mass spectrum of $[Ni_8(L\text{-}Me)_8 + Na]^+$ $[\mathbf{9}+\mathbf{Na}]^+$ *m/z* = 2527.19. Reaction of **3** with $N_2CHCO_2{}^tBu$ after 1 h.

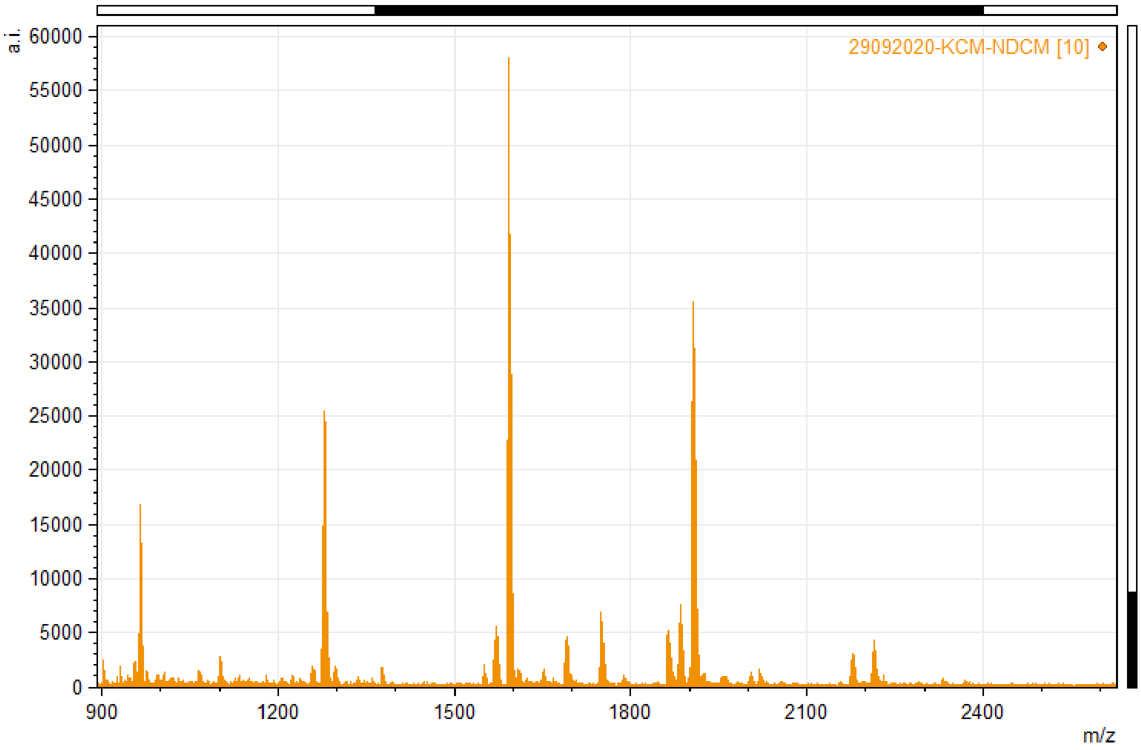

Figure S44. Experimental ESI mass spectrum of **3** recorded in DCM solvent.

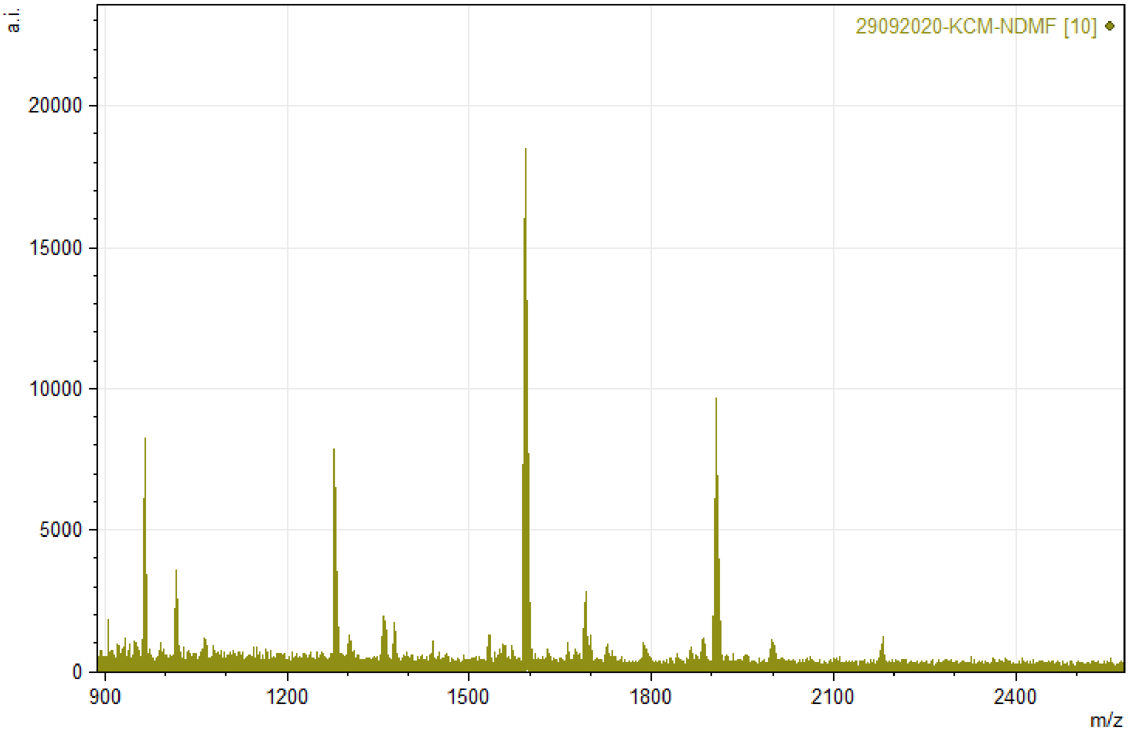

Figure S45. Experimental ESI mass spectrum of **3** in DMF solvent.

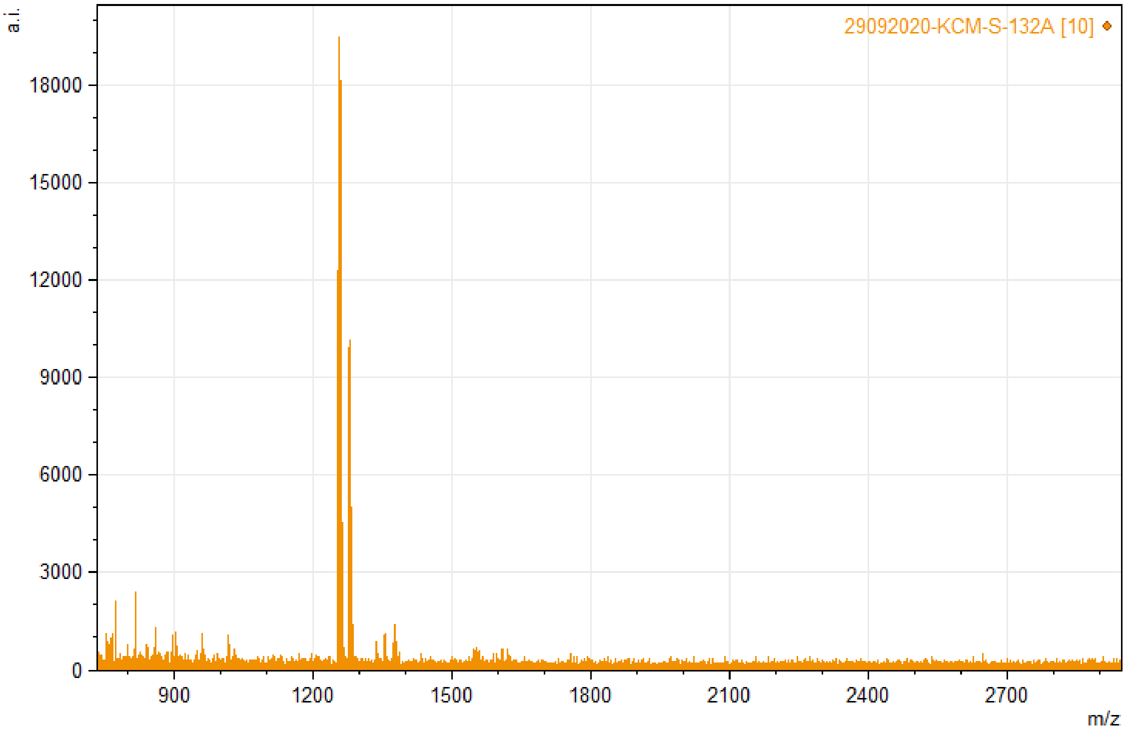

Figure S46. Experimental ESI mass spectrum of the reaction solution [$NiCl_2 \cdot 6H_2O$:H_2L-Me:Et_3N = 1:1:1] in MeOH solvent. The reaction solution was diluted with MeCN and ESI-MS spectrum was recorded. At *m/z* = 1253, [Ni_4(L-Me)$_4$ + H]$^+$; 1275, [Ni_4(L-Me)$_4$ + Na]$^+$. [**3′** = Ni_4(L-Me)$_4$].

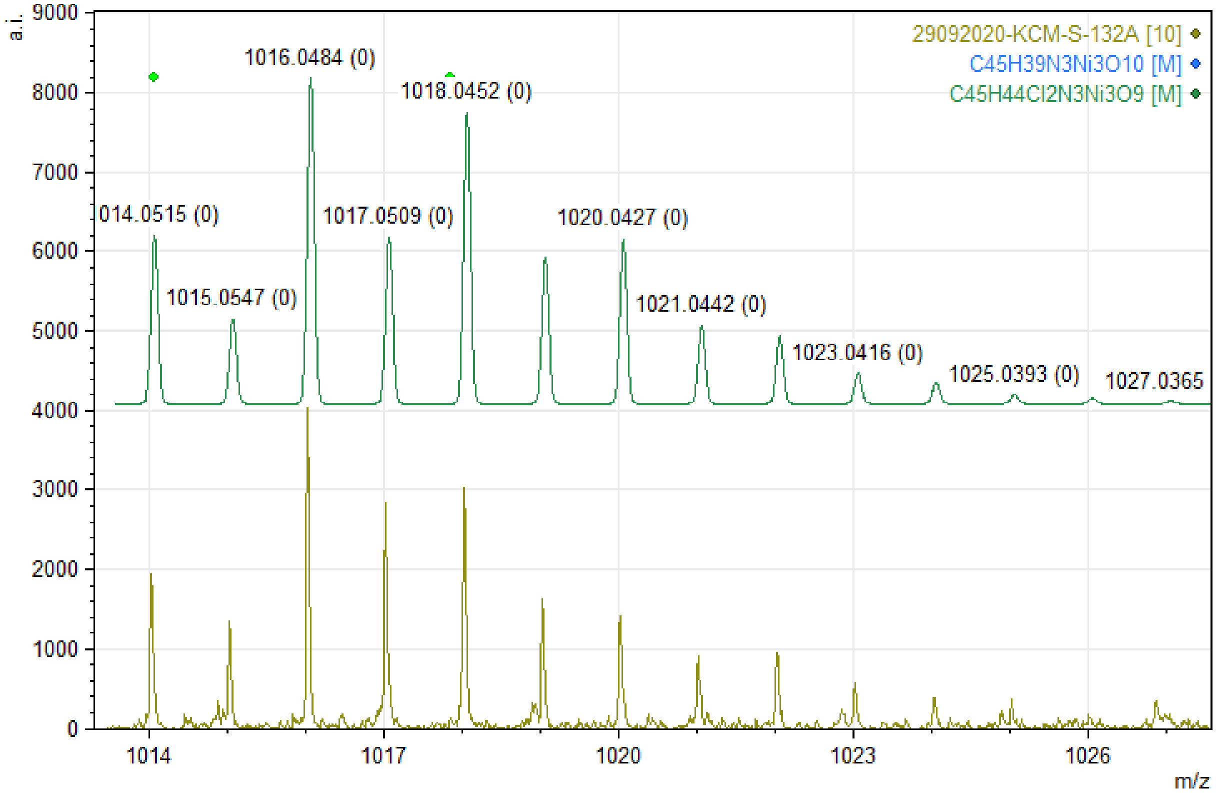

Figure S47. Experimental ESI mass spectrum of the reaction solution [$NiCl_2{\cdot}6H_2O$:H_2L-Me:Et_3N = 1:1:1] in MeOH after 5 min. The reaction solution was diluted with MeCN and ESI-MS spectrum was recorded. $[Ni_3(L\text{-}Me)_3(KCl)+H]^+$, *m/z* = 1014.02.

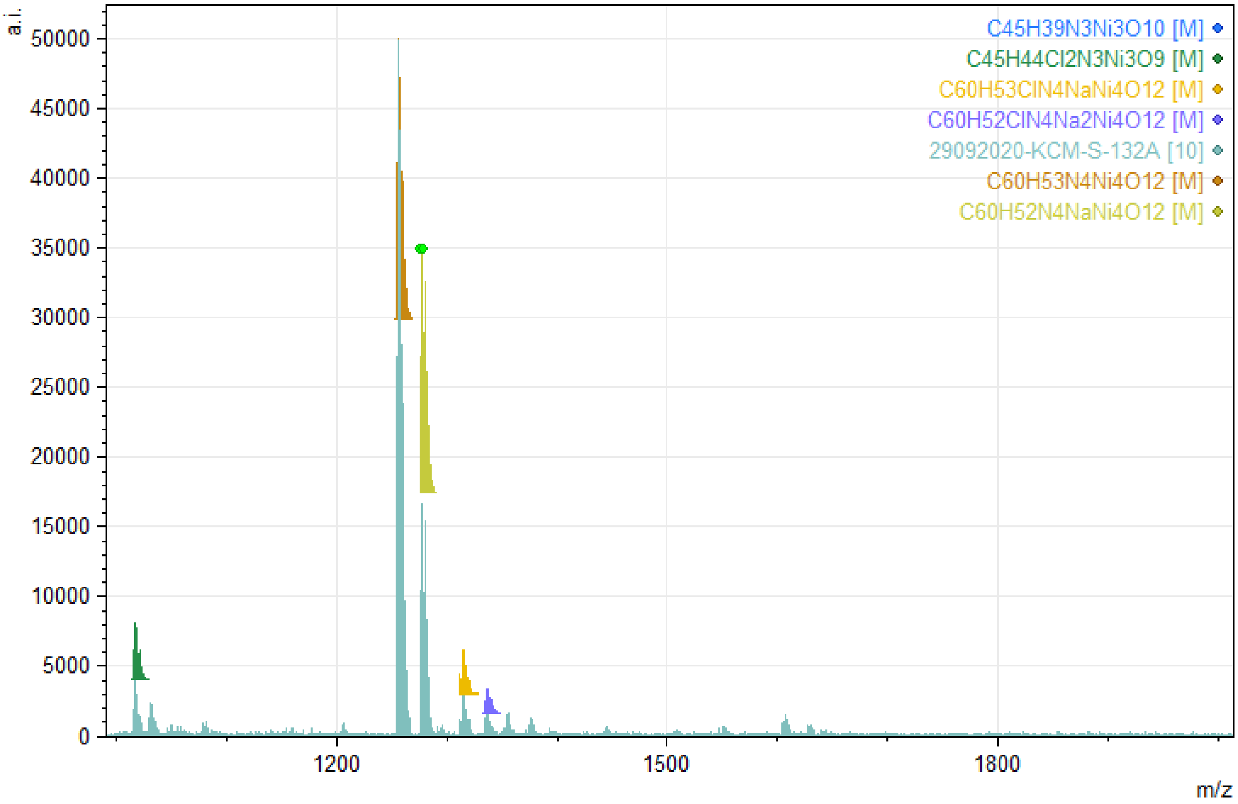

Figure S48. Experimental ESI mass spectrum (green) of the reaction solution [$NiCl_2 \cdot 6H_2O$:H_2L-Me:Et_3N = 1:1:1] in MeOH after 10 min. The reaction solution was diluted with MeCN and ESI-MS spectrum was recorded. (left to right, calculated) [Ni_3(HL-Me)$_3$+2HCl]$^+$, [**3′**+H]$^+$, [**3′**+Na]$^+$, [Ni_4(L-Me)$_3$(HL-Me)Cl+Na]$^+$, [Ni_4(L-Me)$_3$(HL-Me)Cl-H+2Na]$^+$. [**3′** = Ni_4(L-Me)$_4$].

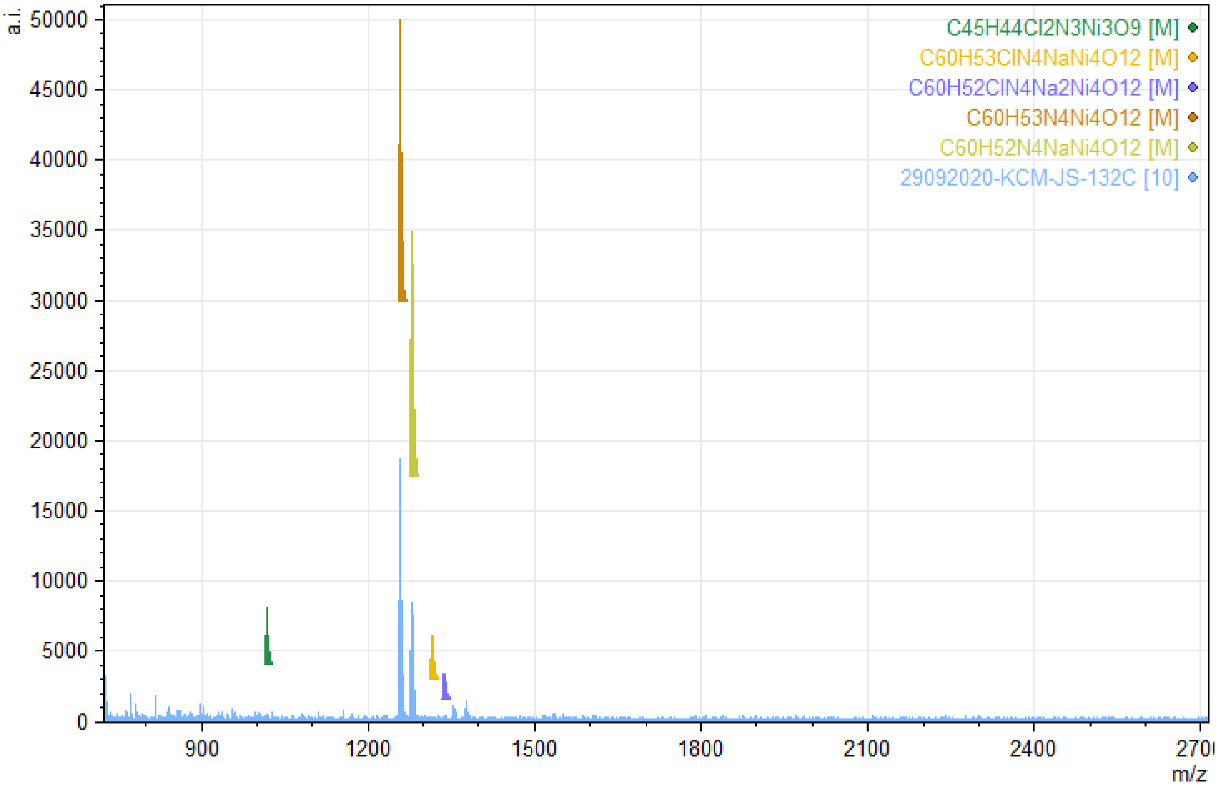

Figure S49. Experimental ESI mass spectrum (green) of the reaction solution [$NiCl_2 \cdot 6H_2O$:H_2L-Me:Et_3N = 1:1:1] in MeOH after 30 min. The reaction solution was diluted with MeCN and ESI-MS spectrum was recorded. (in the middle) [**3′**+H]$^+$, [**3′**+Na]$^+$.

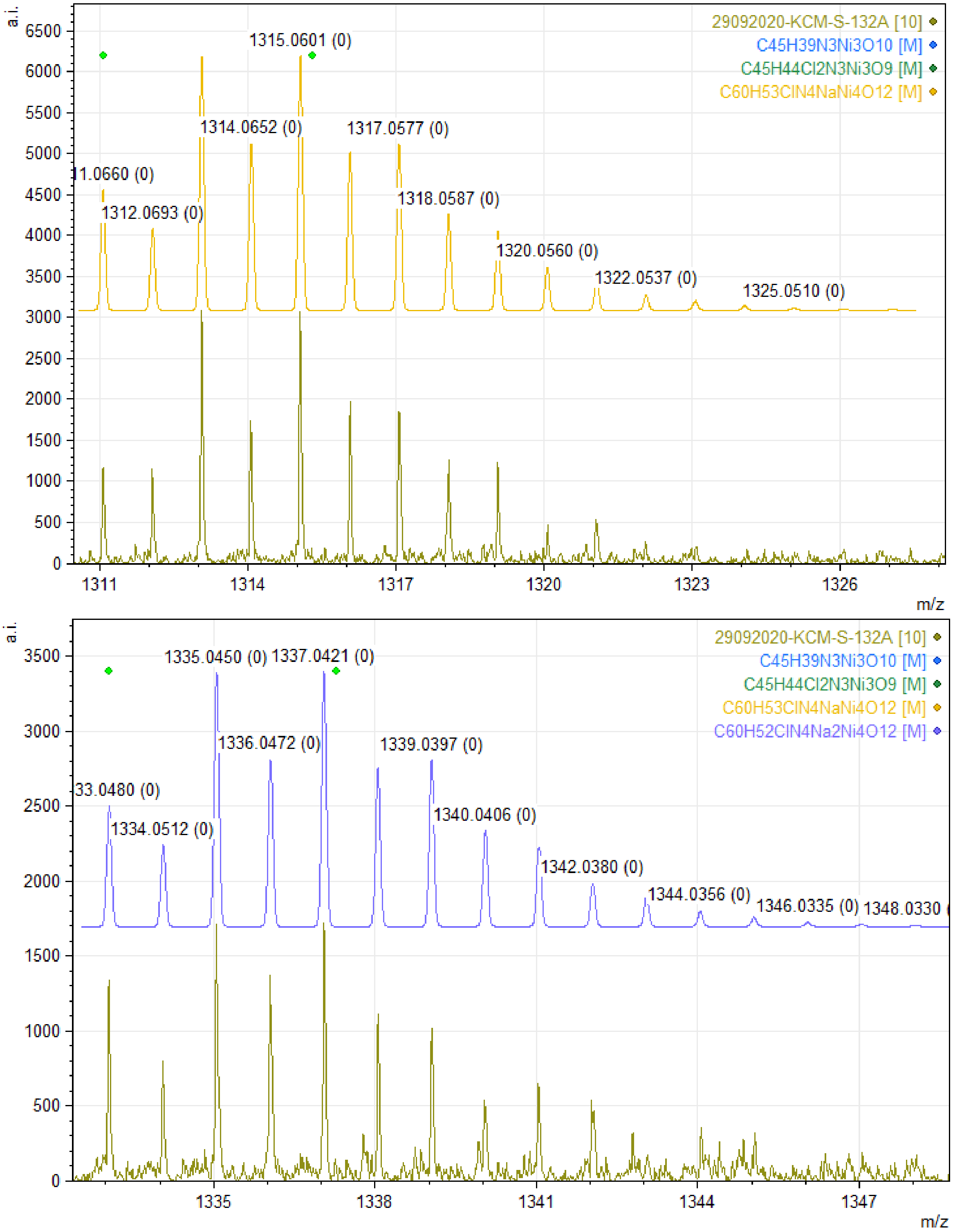

Figure S50. Experimental ESI mass spectrum of the reaction solution [$NiCl_2{\cdot}6H_2O$:H_2L-Me:Et_3N = 1:1:1] in MeOH after 10 min. The reaction solution was diluted with MeCN and ESI-MS spectrum was recorded. [Ni_4(L-Me)$_3$(HL-Me)Cl+Na]$^+$ [**2**+Na]$^+$ (top) [Ni_4(L-Me)$_3$(HL-Me)Cl-H+2Na]$^+$ [**2**-H+2Na]$^+$ (bottom).

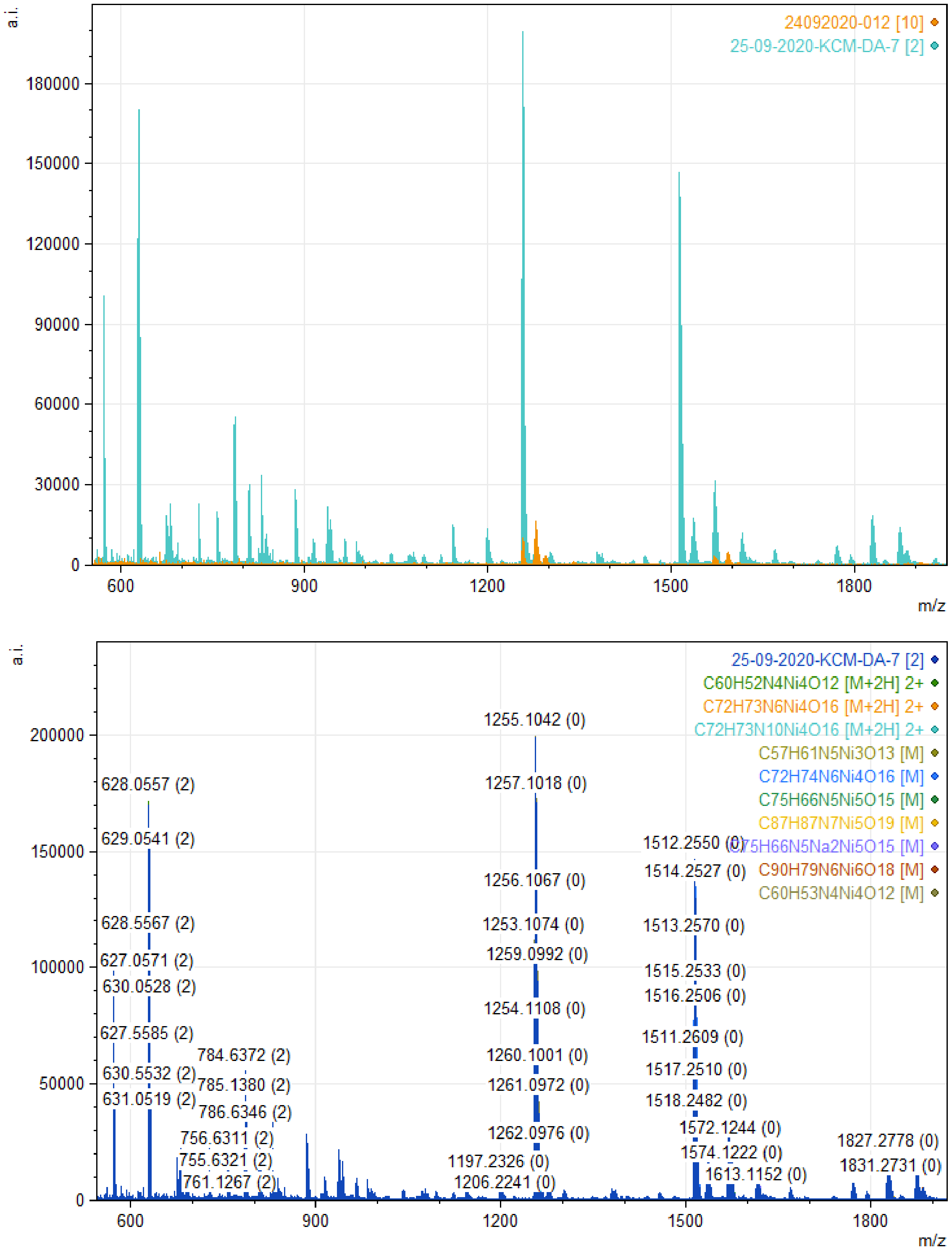

Figure S51. Experimental mass spectrum of **3** (top, orange), reaction solution with $N_2CHCO_2{}^tBu$ (top, green) after 1 h and masses due to calculated species in solution (bottom).

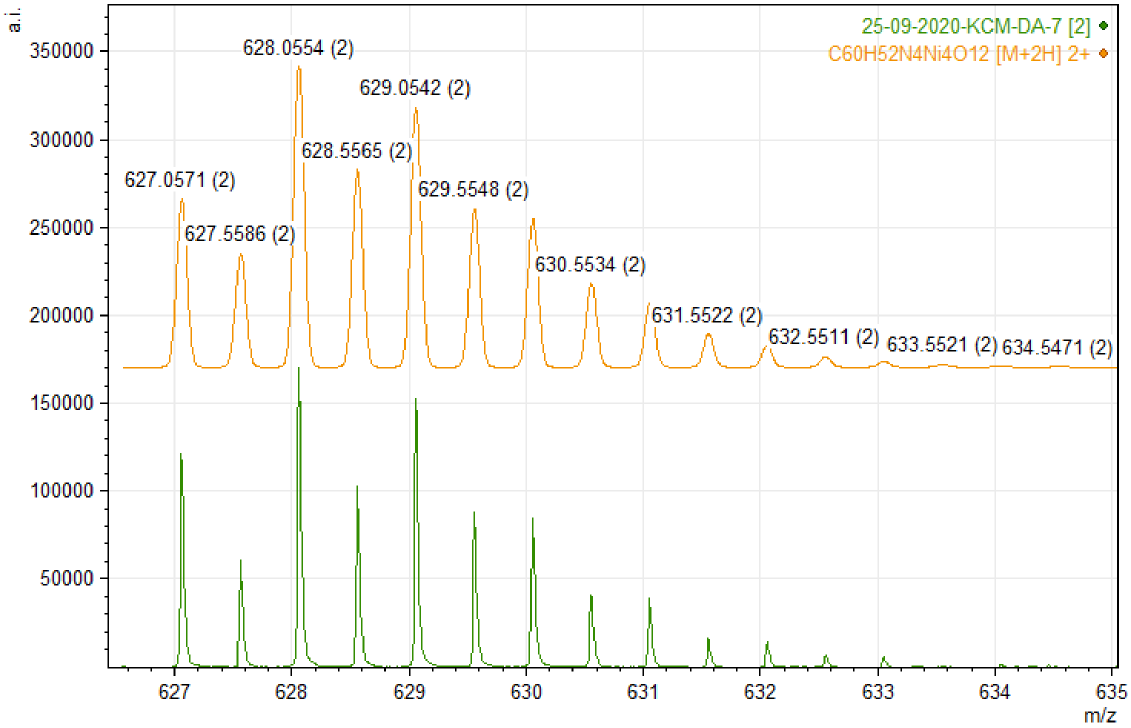

Figure S52. Experimental mass spectrum of **3′** (top, orange), m/z = 627, [Ni$_4$(L-Me)$_4$+2H]$^{2+}$ di-cation. [**3′**+2H]$^{2+}$.

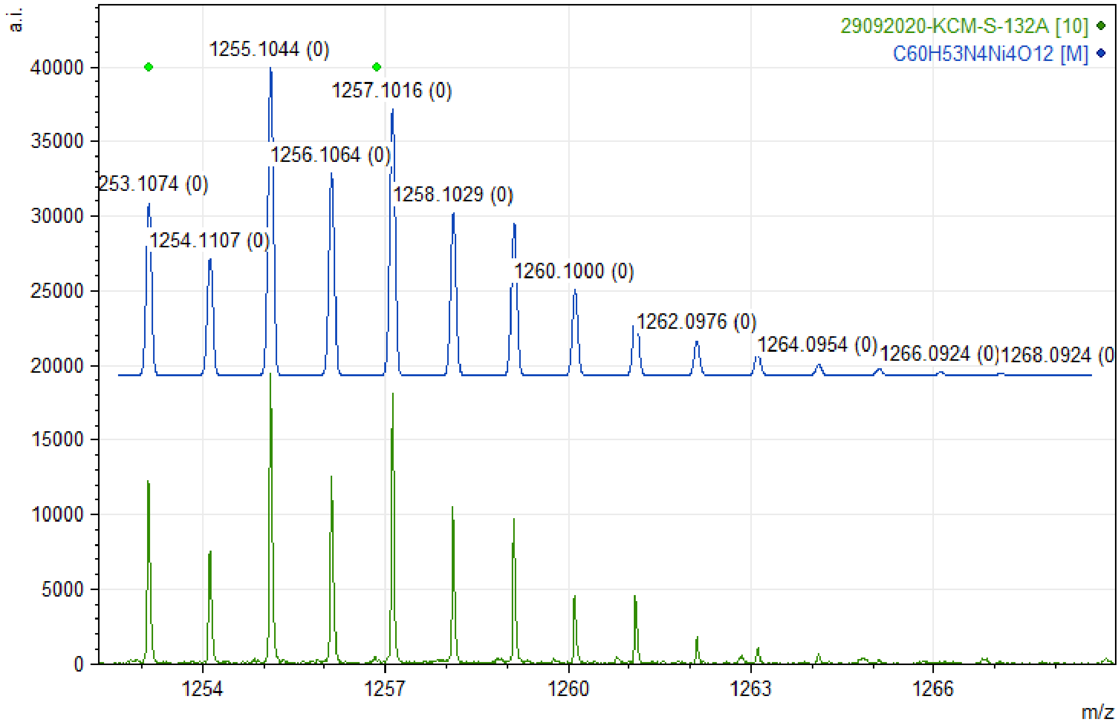

Figure S53. Experimental mass spectrum of **3′** (top, orange), m/z = 1253, [Ni$_4$(L-Me)$_4$+H]$^{+}$ mono-cation. [**3′**+H]$^{+}$.

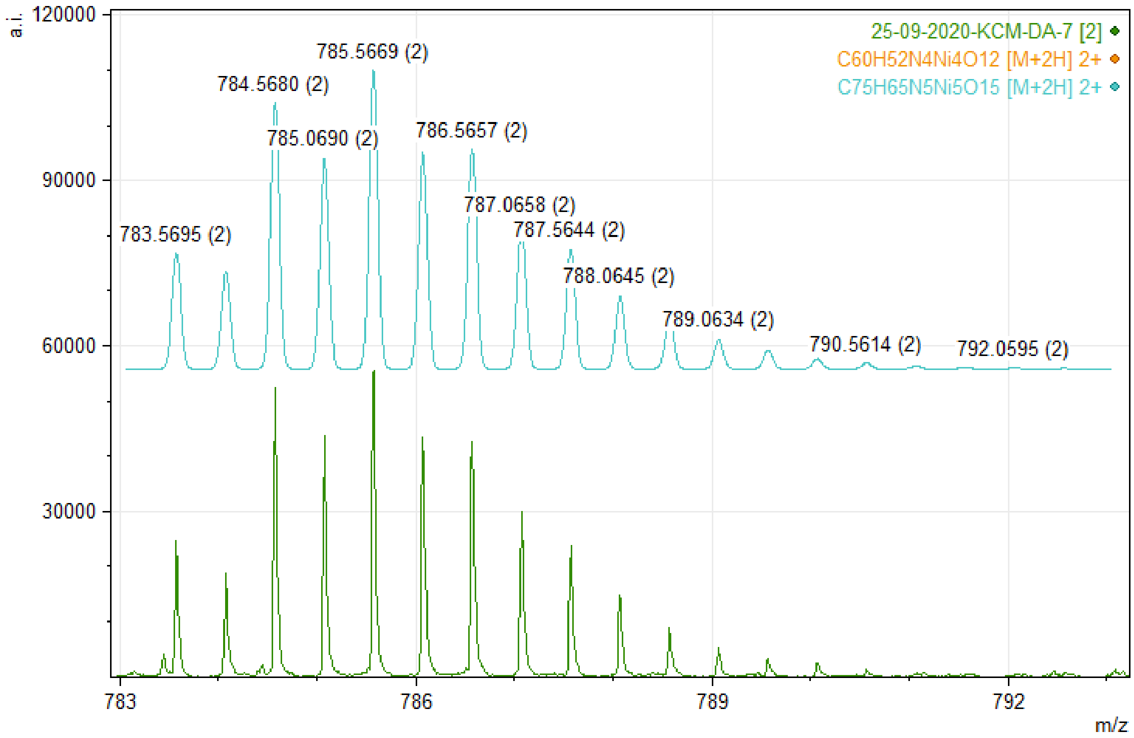

Figure S54. Experimental mass spectrum of pentameric oligomer **5** (top, orange), m/z = 783, [Ni$_5$(L-Me)$_5$+2H]$^{2+}$ di-cation. [**5**+2H]$^{2+}$.

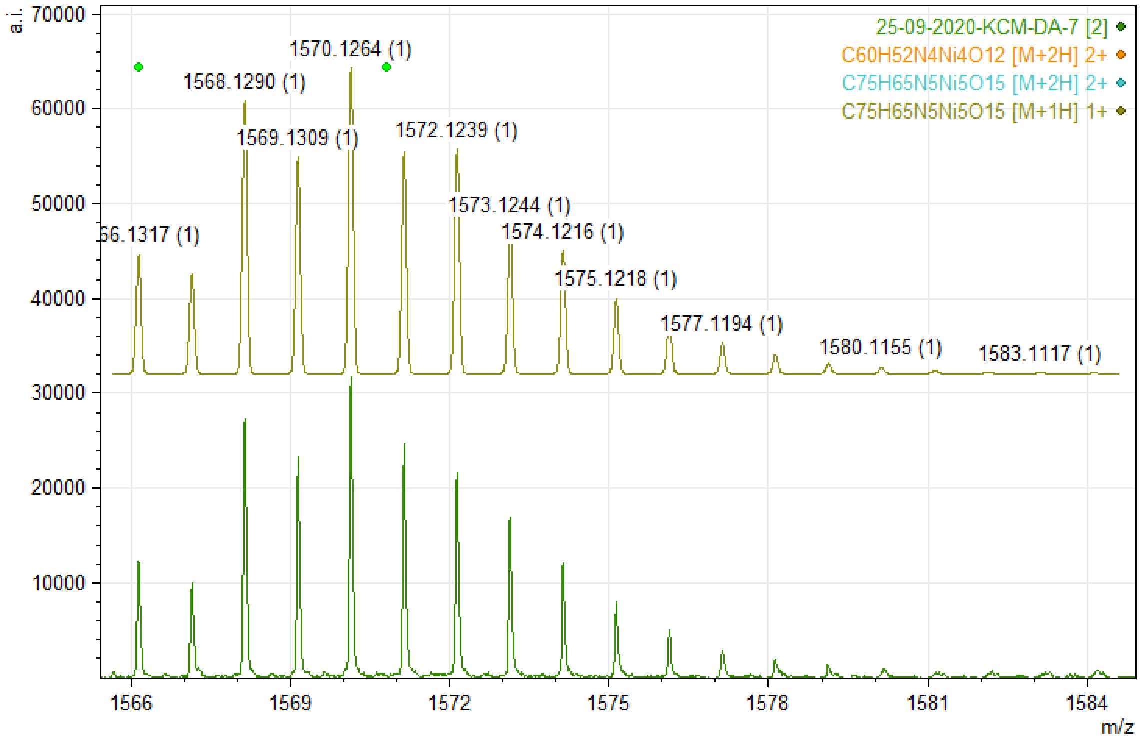

Figure S55. Experimental mass spectrum of pentameric oligomer **5** (top, orange), m/z = 1566, [Ni$_5$(L-Me)$_5$+H]$^{+}$ di-cation. [**5**+H]$^{+}$.

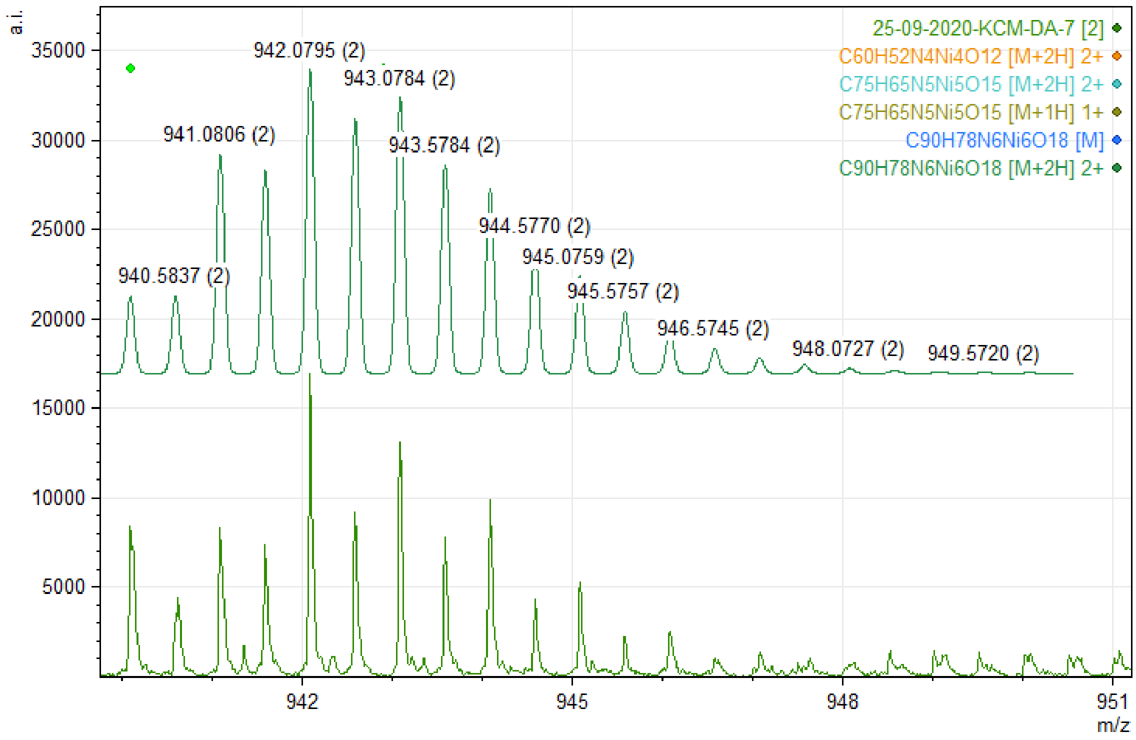

Figure S56. Experimental mass spectrum of hexameric oligomer **5′′′** (top, orange), m/z = 940.08, [Ni$_6$(L-Me)$_6$+2H]$^{2+}$ di-cation. [**5′′′**+2H]$^{2+}$.

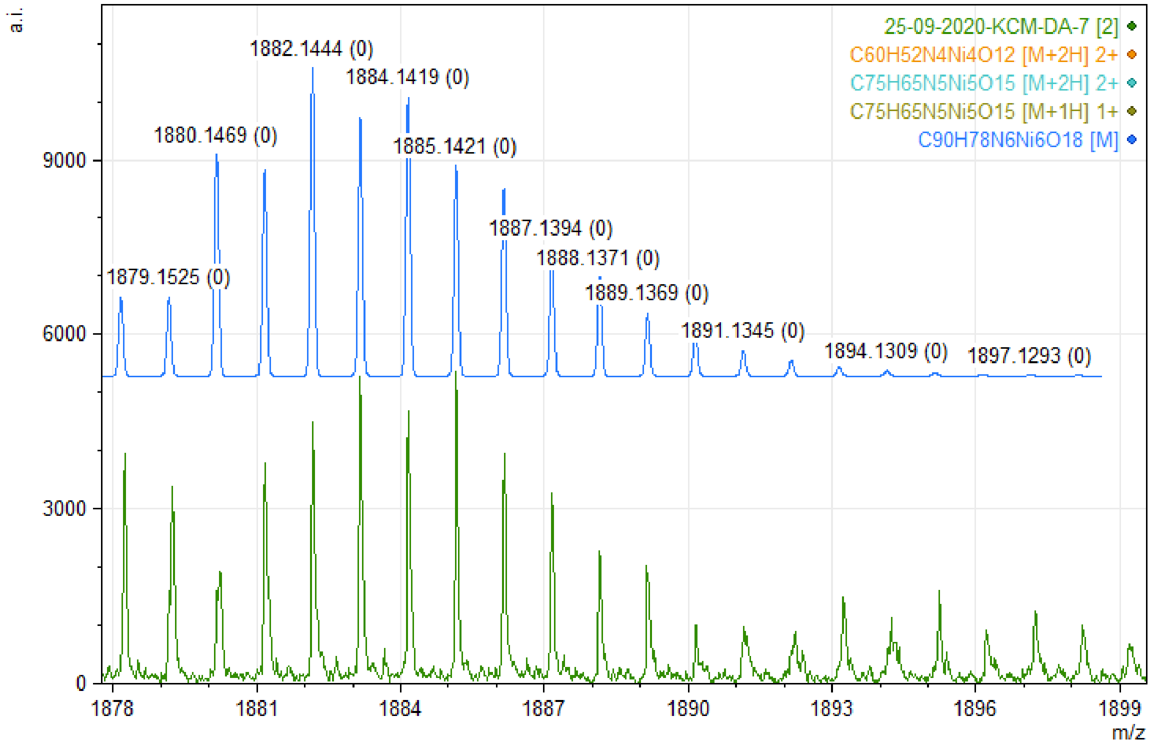

Figure S57. Experimental mass spectrum of hexameric oligomer **5′′′** (top, orange), m/z = 1879.15, [Ni$_6$(L-Me)$_6$+H]$^+$ mono-cation. [**5′′′** +H]$^+$.

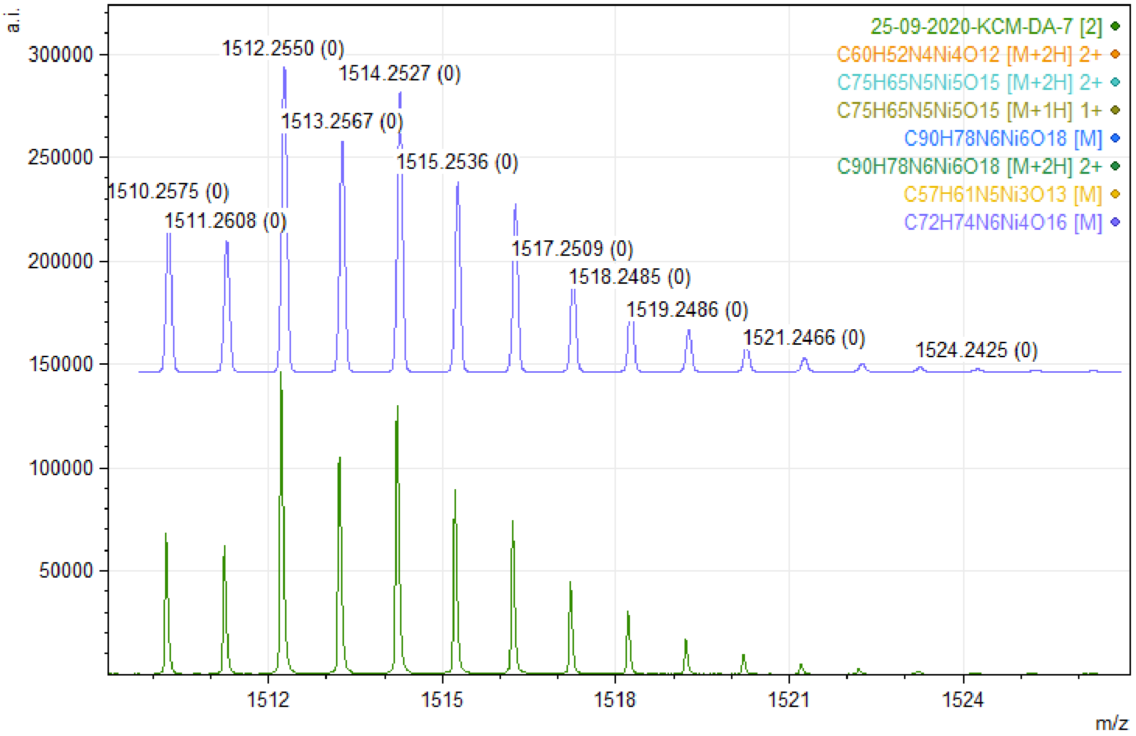

Figure S58. Experimental mass spectrum of trimeric oligomer **4** (top, orange), *m/z* = 1510, [Ni_4(L-Me)$_4$+(**7b**)+(**7b-N$_2$**)+2H]$^+$ = [**4** +2H]$^+$. **7b** = $N_2CHCO_2{}^t$Bu, **7b-N$_2$** = :$CHCO_2{}^t$Bu.

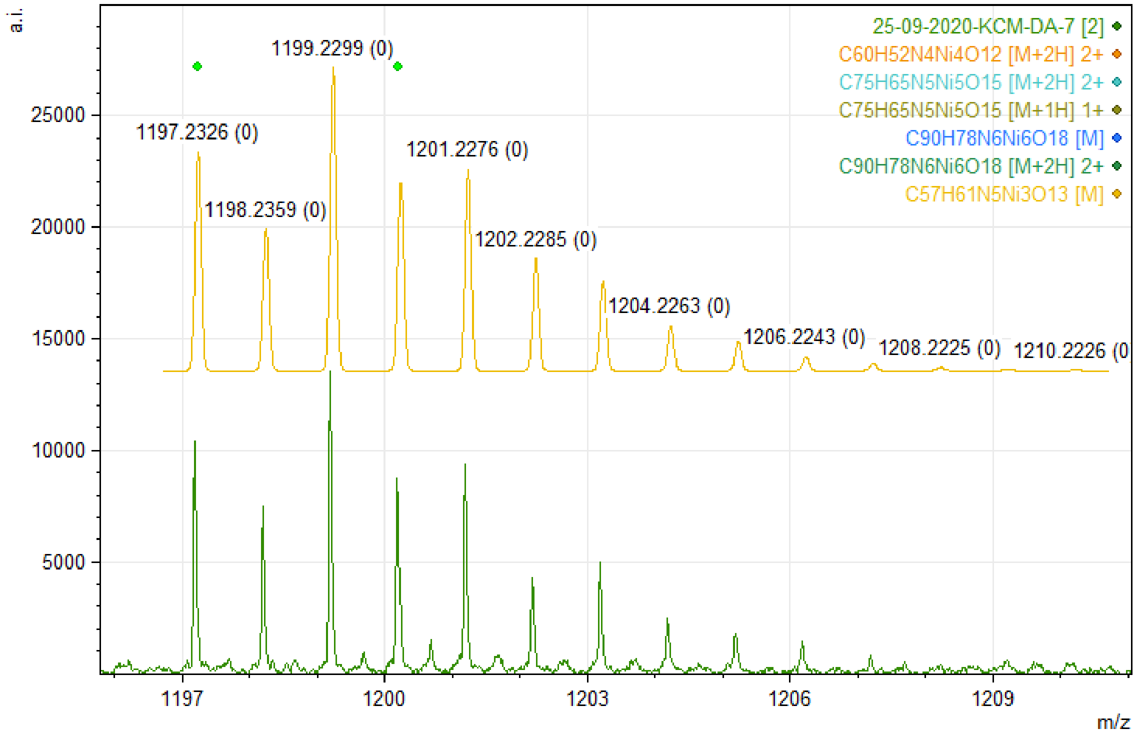

Figure S59. Experimental mass spectrum of trimeric oligomer **5″** (top, orange), *m/z* = 1197, [Ni_3(L-Me)$_3$+(**7b**)+(**7b-N$_2$**)+2H]$^+$ = [**5″** +2H]$^+$. **7b** = $N_2CHCO_2{}^t$Bu, **7b-N$_2$** = :$CHCO_2{}^t$Bu.

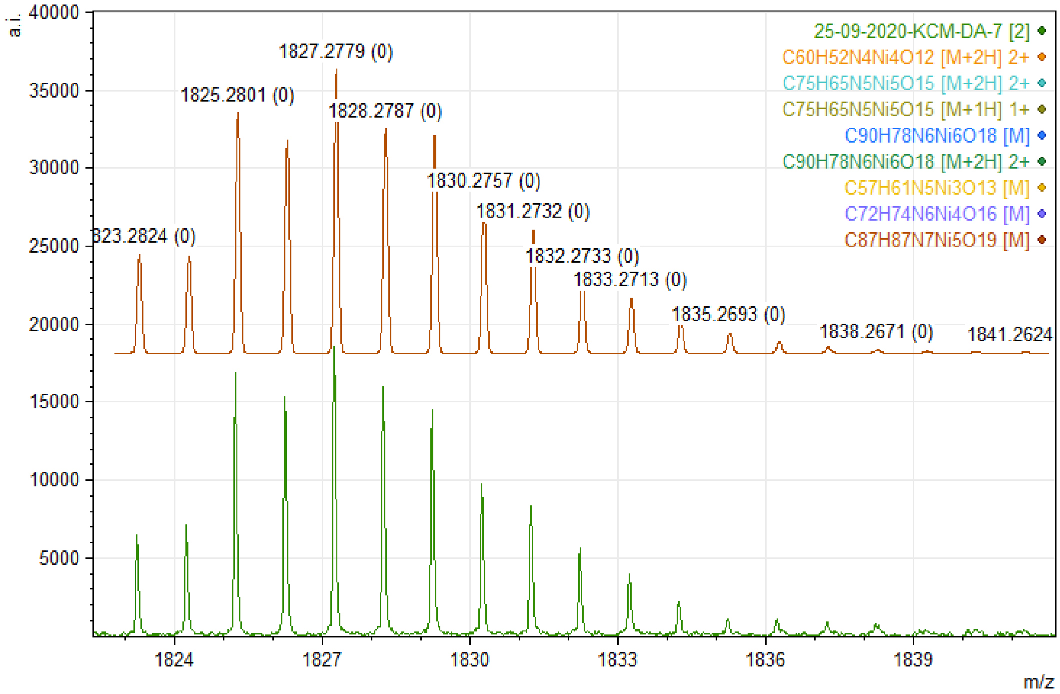

Figure S60. Experimental mass spectrum of trimeric oligomer **5′** (top, orange), *m/z* = 1823, [Ni$_5$(L-Me)$_5$+(**7b**)+(**7b-N$_2$**)+2H]$^+$ = [**5′** +2H]$^+$. **7** = N$_2$CHCO$_2$^{t}Bu, **7b-N$_2$** = :CHCO$_2$^{t}Bu.

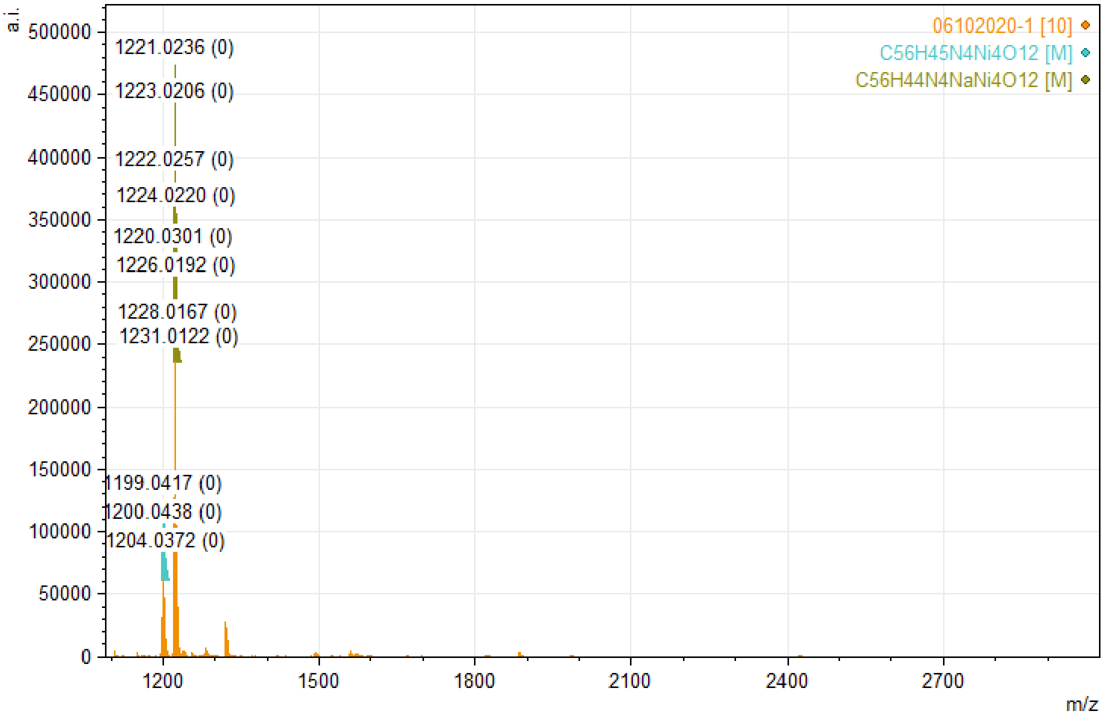

Figure S61. Experimental ESI mass spectrum (green) of cubane Ni$_4$(L-H)$_4$(MeOH)$_2$ prepared in DCM solution. The reaction solution was diluted with DCM and ESI-MS spectrum was recorded. (left to right, calculated) [Ni$_4$(L-H)$_4$+H]$^+$, [Ni$_4$(L-H)$_4$+Na]$^+$. Ligand = (OH)$_2$L-H = H$_2$L-H = C$_{14}$H$_{13}$NO$_3$, L-H = C$_{14}$H$_{11}$NO$_3$ here. Ni$_4$(L-H)$_4$(MeOH)$_2$ does not seems to display oligomerization in DCM.

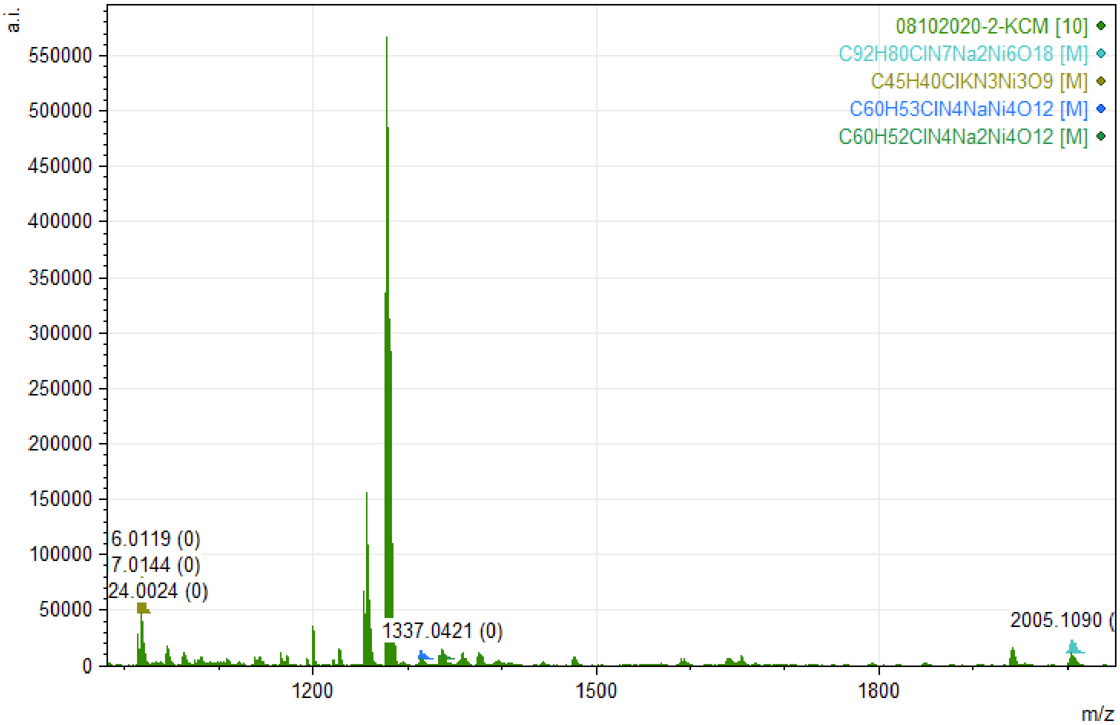

Figure S62. The reaction of $NiCl_2 \cdot 6H_2O$, H_2L-Me, NaOMe in 1:1:1 molar ratio in MeOH at 0 ºC. *m/z* = 1014, $[Ni_3(L\text{-}Me)_3+KCl+H]^+$; 1999, $[Ni_6(L\text{-}Me)_6Na(CH_3CN)NaCl\text{-}H]^+$; 1311, $[Ni_4(L\text{-}Me)_4(HCl)+Na]^+$ and 1333, $[Ni_4(L\text{-}Me)_4(NaCl)Na]^+$. The high intensity m/z are at 1253 and 1275 due to formation of $[\mathbf{3'}+H]^+$ and $[\mathbf{3'}+Na]^+$ respectively.

$[Ni_4((O^-)_2L\text{-}Me)_4]$ (**3'**)

Characterized by ESI Mass

as [**3'** + H]$^+$ and [**3'** + 2H]$^{2+}$

m/z 1253; 627

$[Ni_4((O^-)_2L\text{-}Me)_4(:CHCO_2Et)(N_2CHCO_2{}^tBu)]$ (**4**)

Characterized by ESI Mass

as [**4** + 2H]$^+$ and [**4** + 3H]$^{2+}$

m/z 1510; 755

$[Ni_5((O^-)_2L\text{-}Me)_5]$ (**5**)

Characterized by ESI Mass

as [**5** + H]$^+$ and [**5** + 2H]$^{2+}$

m/z 1566; 783

$[Ni_5((O^-)_2L\text{-}Me)_5(:CHCO_2Et)(N_2CHCO_2{}^tBu)]$(**5'**)

Characterized by ESI Mass

as [**5'** + 2H]$^+$ and [**5'** + 3H]$^{2+}$

m/z 1823; 912

$[Ni_6((O^-)_2L\text{-}Me)_6]$ (**5'''**)

Characterized by ESI Mass

as [**5'''** + H]$^+$ and [**5'''** + 2H]$^{2+}$

m/z 1879; 940

$[Ni_3((O^-)_2L\text{-}Me)_3(:CHCO_2Et)(N_2CHCO_2{}^tBu)]$(**5''**)

Characterized by ESI Mass

as [**5''** + 2H]$^+$

m/z 1197

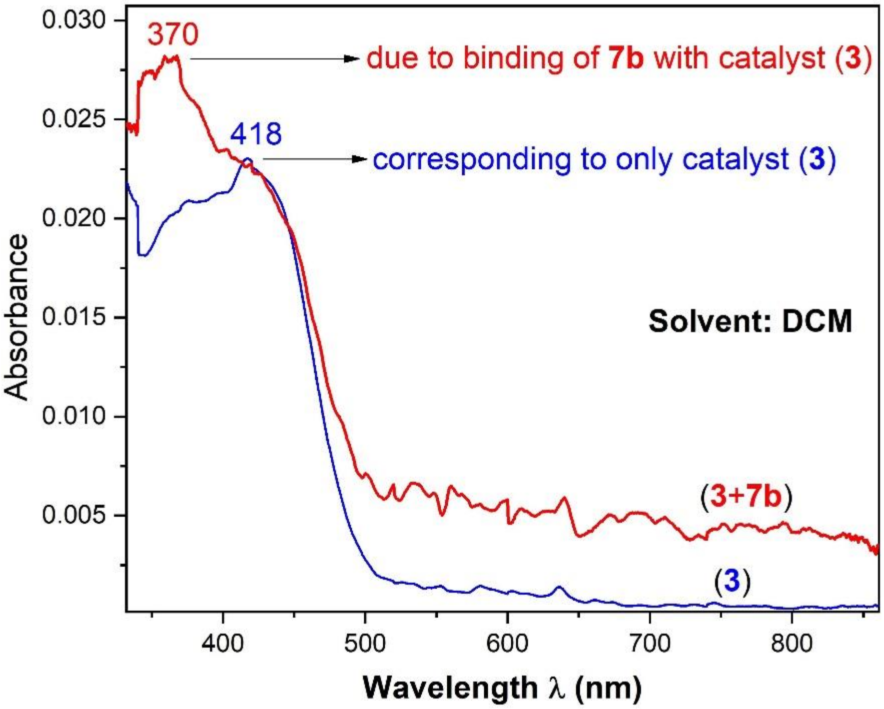

Figure S63. UV-vis spectra of catalyst **3** (blue) and **3**+**7b** (red) recorded in DCM. An absorption band at 418 nm corresponds to catalyst **3**. The additional absorption band at 370 nm is possibly due to binding of catalyst **3** with tertiary butyl-diazoester (**7b**).

Coordinates:

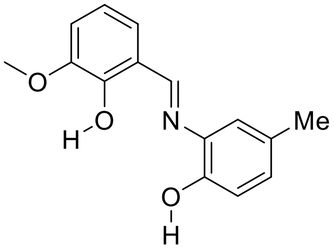

6	3.080439000	-1.944718000	-0.839786000
6	1.748235000	-1.613582000	-0.670244000
6	1.383415000	-0.359466000	-0.139695000
6	2.386066000	0.548676000	0.212749000
6	3.746862000	0.205307000	0.037988000
6	4.091145000	-1.033755000	-0.485004000
1	3.359446000	-2.917727000	-1.250453000
1	0.952752000	-2.311510000	-0.939130000
1	5.139840000	-1.303000000	-0.621650000
6	-0.024942000	0.010200000	0.057163000
1	-0.214772000	1.010035000	0.483097000
7	-0.978217000	-0.786004000	-0.231475000
8	2.068583000	1.758703000	0.721282000
1	2.891607000	2.251882000	0.906285000
8	4.612108000	1.174796000	0.422384000
6	5.996864000	0.926586000	0.287899000
1	6.509961000	1.826206000	0.654048000
1	6.301133000	0.055815000	0.894347000
1	6.264534000	0.753935000	-0.769065000
6	-2.306670000	-0.361826000	-0.078104000

6	-3.249056000	-1.309790000	0.378720000
6	-2.748764000	0.923709000	-0.408601000
6	-4.584963000	-0.940060000	0.514786000
6	-4.091717000	1.303853000	-0.285376000
1	-2.021752000	1.638966000	-0.805849000
6	-5.000263000	0.352569000	0.185364000
1	-5.302480000	-1.680037000	0.882043000
1	-6.056220000	0.617433000	0.291449000
6	-4.528463000	2.693861000	-0.671831000
1	-3.953994000	3.460039000	-0.123541000
1	-4.369387000	2.876097000	-1.749073000
1	-5.597538000	2.847222000	-0.455398000
8	-2.794436000	-2.548703000	0.689840000
1	-3.534771000	-3.111059000	0.978992000

……

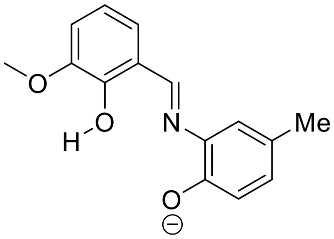

6	3.054585000	-2.017063000	-0.649930000
6	1.724836000	-1.660756000	-0.502677000
6	1.368359000	-0.361692000	-0.087878000
6	2.383423000	0.563947000	0.172480000
6	3.739254000	0.198267000	0.018618000
6	4.074991000	-1.086398000	-0.390836000

1	3.322172000	-3.026853000	-0.970112000
1	0.921469000	-2.373747000	-0.699313000
1	5.120969000	-1.373443000	-0.510256000
6	-0.039723000	0.033783000	0.080055000
1	-0.217041000	1.073008000	0.405189000
7	-0.994920000	-0.787651000	-0.123630000
8	2.076969000	1.820035000	0.576386000
1	2.905049000	2.317621000	0.719026000
8	4.615558000	1.194276000	0.304252000
6	5.996900000	0.919698000	0.196501000
1	6.519969000	1.844646000	0.475564000
1	6.292476000	0.107929000	0.883887000
1	6.264735000	0.643941000	-0.838416000
6	-2.338254000	-0.399405000	-0.023465000
6	-3.280725000	-1.443286000	0.322149000
6	-2.771215000	0.910734000	-0.290859000
6	-4.647080000	-1.004002000	0.395178000
6	-4.110573000	1.294757000	-0.224682000
1	-2.027221000	1.652087000	-0.603685000
6	-5.039792000	0.299282000	0.136053000
1	-5.389782000	-1.762701000	0.665108000
1	-6.102976000	0.560811000	0.199040000
6	-4.557597000	2.695261000	-0.564768000
1	-5.216598000	3.112799000	0.217098000
1	-3.693782000	3.372103000	-0.671712000

1	-5.124592000	2.730276000	-1.513522000
8	-2.936871000	-2.642269000	0.568348000

……

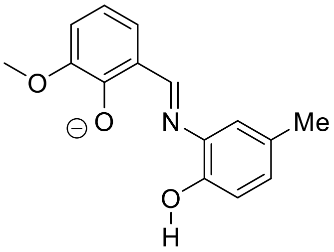

6	3.118552000	-1.894450000	-0.893441000
6	1.791487000	-1.583273000	-0.708436000
6	1.400117000	-0.349092000	-0.131490000
6	2.368125000	0.628541000	0.285738000
6	3.760245000	0.248054000	0.062376000
6	4.113874000	-0.958933000	-0.499222000
1	3.420086000	-2.846180000	-1.337459000
1	1.003159000	-2.282790000	-1.001604000
1	5.166341000	-1.210332000	-0.648893000
6	0.000706000	-0.029555000	0.060403000
1	-0.195996000	0.964821000	0.500101000
7	-0.968768000	-0.822521000	-0.231603000
8	2.085269000	1.743876000	0.809554000
8	4.645792000	1.202123000	0.468446000
6	6.016627000	0.939271000	0.300872000
1	6.555831000	1.818299000	0.683100000
1	6.329508000	0.045557000	0.871873000
1	6.272594000	0.792164000	-0.764758000

6	-2.284939000	-0.376828000	-0.080125000
6	-3.250892000	-1.301123000	0.384364000
6	-2.713018000	0.913059000	-0.417819000
6	-4.579501000	-0.909869000	0.516480000
6	-4.050158000	1.318411000	-0.294608000
1	-1.975579000	1.614678000	-0.820468000
6	-4.976561000	0.388559000	0.180188000
1	-5.308866000	-1.636347000	0.888253000
1	-6.028036000	0.671386000	0.284629000
6	-4.459713000	2.715518000	-0.686688000
1	-3.890091000	3.472886000	-0.120928000
1	-4.270403000	2.900616000	-1.758570000
1	-5.532009000	2.882393000	-0.496933000
8	-2.821124000	-2.549809000	0.705344000
1	-3.574372000	-3.088766000	1.004586000

……

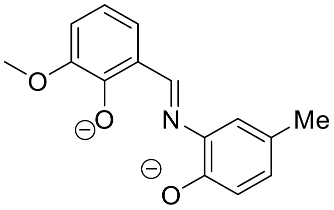

6	3.104936000	-1.901754000	-0.882372000
6	1.775389000	-1.589595000	-0.692235000
6	1.383012000	-0.356437000	-0.122129000
6	2.350011000	0.624299000	0.283999000
6	3.738867000	0.247186000	0.057256000
6	4.097386000	-0.963676000	-0.499089000

1	3.404625000	-2.856037000	-1.322486000
1	0.986158000	-2.291730000	-0.977210000
1	5.150507000	-1.211177000	-0.650971000
6	-0.026254000	-0.042610000	0.077050000
1	-0.225545000	0.957603000	0.504136000
7	-0.988173000	-0.844483000	-0.197602000
8	2.064954000	1.745392000	0.804722000
8	4.626495000	1.207015000	0.454118000
6	5.996324000	0.944702000	0.284639000
1	6.536124000	1.826568000	0.659950000
1	6.313019000	0.055055000	0.860196000
1	6.251116000	0.791279000	-0.780560000
6	-2.320331000	-0.422798000	-0.050262000
6	-3.266642000	-1.414709000	0.427909000
6	-2.740625000	0.864346000	-0.397227000
6	-4.612810000	-0.946806000	0.527083000
6	-4.077140000	1.285890000	-0.295067000
1	-1.994879000	1.560317000	-0.800187000
6	-5.000159000	0.347662000	0.179917000
1	-5.355968000	-1.664799000	0.891825000
1	-6.054899000	0.633241000	0.271463000
6	-4.486584000	2.677158000	-0.713124000
1	-3.907651000	3.454175000	-0.181983000
1	-4.331153000	2.847321000	-1.794583000
1	-5.554271000	2.854387000	-0.501093000

8	-2.915481000	-2.597655000	0.751990000

……

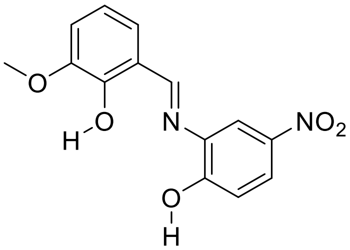

6	-3.719005000	1.773492000	-0.984367000
6	-2.363730000	1.608294000	-0.765532000
6	-1.878511000	0.445626000	-0.132232000
6	-2.783109000	-0.540815000	0.272803000
6	-4.168462000	-0.366058000	0.047317000
6	-4.631600000	0.783476000	-0.577733000
1	-4.093428000	2.674740000	-1.474899000
1	-1.643233000	2.368559000	-1.074051000
1	-5.699640000	0.921930000	-0.753994000
6	-0.446193000	0.246312000	0.113217000
1	-0.161014000	-0.691775000	0.619079000
7	0.426054000	1.113700000	-0.226389000
8	-2.345299000	-1.663502000	0.879310000
1	-3.108717000	-2.239594000	1.079635000
8	-4.932308000	-1.393000000	0.490930000
6	-6.331326000	-1.313338000	0.305500000
1	-6.752805000	-2.235423000	0.728166000
1	-6.749146000	-0.439930000	0.835730000

1	-6.582598000	-1.250869000	-0.767621000
6	1.782753000	0.837663000	-0.028639000
6	2.624483000	1.912088000	0.359801000
6	2.353470000	-0.412697000	-0.255948000
6	3.997896000	1.707049000	0.533882000
6	3.725955000	-0.585124000	-0.080479000
1	1.737024000	-1.245490000	-0.596436000
6	4.560180000	0.456709000	0.314121000
1	4.623135000	2.548953000	0.842042000
1	5.630505000	0.292160000	0.439041000
8	2.041633000	3.100633000	0.563281000
1	2.701482000	3.775758000	0.809138000
7	4.305135000	-1.898299000	-0.335333000
8	5.495365000	-2.044826000	-0.158823000
8	3.571022000	-2.787166000	-0.710201000

……

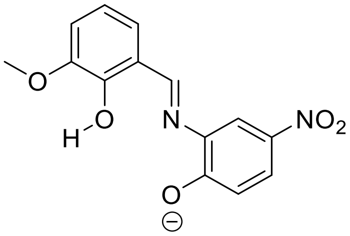

6	-3.708661000	1.820842000	-0.905117000
6	-2.352919000	1.641846000	-0.694155000
6	-1.868398000	0.454960000	-0.108275000
6	-2.777531000	-0.542315000	0.256465000
6	-4.161794000	-0.355935000	0.038256000

6	-4.624551000	0.819092000	-0.539298000
1	-4.079513000	2.743225000	-1.357949000
1	-1.629625000	2.411554000	-0.971203000
1	-5.692249000	0.967183000	-0.709317000
6	-0.432503000	0.247677000	0.132171000
1	-0.148283000	-0.703444000	0.614868000
7	0.437627000	1.123726000	-0.185125000
8	-2.343427000	-1.692506000	0.818307000
1	-3.111284000	-2.268316000	0.999562000
8	-4.928894000	-1.399578000	0.439323000
6	-6.327665000	-1.306690000	0.262067000
1	-6.751720000	-2.244716000	0.645489000
1	-6.741093000	-0.455841000	0.831159000
1	-6.582766000	-1.196753000	-0.806370000
6	1.802838000	0.864962000	-0.002711000
6	2.630726000	2.018673000	0.364970000
6	2.366700000	-0.376326000	-0.219010000
6	4.045057000	1.745329000	0.513113000
6	3.754035000	-0.569569000	-0.069678000
1	1.745075000	-1.214090000	-0.540531000
6	4.589629000	0.503835000	0.303308000
1	4.679667000	2.589944000	0.795438000
1	5.662364000	0.335512000	0.412061000
8	2.144724000	3.152948000	0.553975000
7	4.313631000	-1.846045000	-0.322807000

8	5.521626000	-2.009114000	-0.187219000
8	3.578578000	-2.765037000	-0.668176000

……………………………………………………………………………………

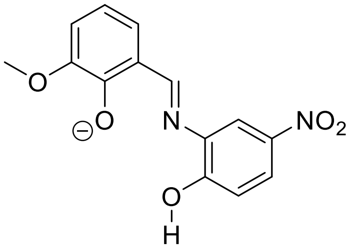

6	-3.749099000	1.742333000	-0.991203000
6	-2.401532000	1.592630000	-0.769301000
6	-1.889099000	0.440194000	-0.118191000
6	-2.753920000	-0.615449000	0.339047000
6	-4.175881000	-0.405621000	0.070817000
6	-4.644998000	0.722677000	-0.562239000
1	-4.145035000	2.629222000	-1.491635000
1	-1.689602000	2.358952000	-1.089237000
1	-5.714775000	0.848047000	-0.744136000
6	-0.473155000	0.282492000	0.108725000
1	-0.182096000	-0.660634000	0.604850000
7	0.416936000	1.157146000	-0.214658000
8	-2.361863000	-1.660254000	0.927939000
8	-4.959751000	-1.428927000	0.513269000
6	-6.347780000	-1.324971000	0.312890000
1	-6.796699000	-2.235510000	0.735659000
1	-6.765100000	-0.441041000	0.829677000

1	-6.596899000	-1.263285000	-0.762608000
6	1.762439000	0.855807000	-0.030066000
6	2.635739000	1.913614000	0.346308000
6	2.318202000	-0.405243000	-0.251086000
6	4.005160000	1.686775000	0.513496000
6	3.689293000	-0.602484000	-0.078731000
1	1.688075000	-1.230809000	-0.583247000
6	4.546771000	0.424071000	0.302881000
1	4.645678000	2.520762000	0.812399000
1	5.614235000	0.240957000	0.424650000
8	2.078381000	3.118442000	0.544815000
1	2.754547000	3.777200000	0.788216000
7	4.242580000	-1.927499000	-0.326864000
8	5.431170000	-2.097164000	-0.153863000
8	3.491839000	-2.806139000	-0.693912000

……

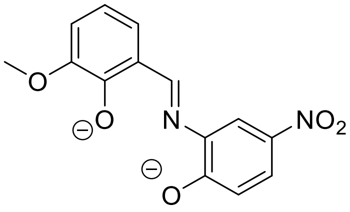

6	-3.731158000	1.692913000	-1.097449000
6	-2.384327000	1.556498000	-0.845594000
6	-1.880149000	0.446674000	-0.125106000
6	-2.748979000	-0.582195000	0.376792000
6	-4.164090000	-0.392420000	0.075235000

6	-4.629601000	0.698300000	-0.627331000
1	-4.118702000	2.550173000	-1.653240000
1	-1.668406000	2.305267000	-1.197207000
1	-5.697146000	0.808379000	-0.831240000
6	-0.457470000	0.306818000	0.128581000
1	-0.166146000	-0.619127000	0.657792000
7	0.428669000	1.171554000	-0.212438000
8	-2.363151000	-1.593565000	1.032739000
8	-4.954716000	-1.393744000	0.561008000
6	-6.338863000	-1.304839000	0.333845000
1	-6.792853000	-2.192787000	0.797700000
1	-6.767278000	-0.396072000	0.795886000
1	-6.572555000	-1.301822000	-0.747020000
6	1.783370000	0.885696000	-0.011681000
6	2.631227000	2.007986000	0.412834000
6	2.333499000	-0.356222000	-0.254465000
6	4.036174000	1.704710000	0.577981000
6	3.717696000	-0.584008000	-0.081065000
1	1.702193000	-1.171279000	-0.612977000
6	4.564750000	0.459707000	0.340689000
1	4.678763000	2.528105000	0.902540000
1	5.631667000	0.268334000	0.466915000
8	2.163965000	3.145979000	0.633627000
7	4.257761000	-1.859319000	-0.359043000
8	5.461072000	-2.053468000	-0.202484000

8	3.514452000	-2.755517000	-0.749687000

……………………………………………………………………………………

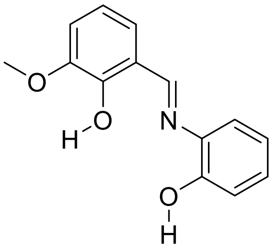

6	2.654833000	2.071618000	0.604974000
6	1.351676000	1.618968000	0.504494000
6	1.082708000	0.287873000	0.125936000
6	2.150843000	-0.571949000	-0.146044000
6	3.481544000	-0.105193000	-0.039531000
6	3.731290000	1.208612000	0.332906000
1	2.859600000	3.104204000	0.896627000
1	0.505594000	2.277280000	0.712076000
1	4.756483000	1.573581000	0.414913000
6	-0.293103000	-0.213509000	0.007306000
1	-0.406132000	-1.266441000	-0.302078000
7	-1.304120000	0.529667000	0.234827000
8	1.926162000	-1.852495000	-0.511188000
1	2.784099000	-2.295218000	-0.662948000
8	4.416990000	-1.041804000	-0.329112000
6	5.778867000	-0.671403000	-0.256246000
1	6.357691000	-1.564199000	-0.529303000
1	6.003068000	0.144576000	-0.965078000

1	6.046977000	-0.357758000	0.767673000
6	-2.594145000	-0.016628000	0.166999000
6	-3.626178000	0.798323000	-0.348956000
6	-2.918548000	-1.295501000	0.638310000
6	-4.933744000	0.314144000	-0.409394000
6	-4.228285000	-1.773429000	0.586022000
1	-2.128478000	-1.907037000	1.082277000
6	-5.234999000	-0.966449000	0.056596000
1	-5.714817000	0.958498000	-0.823997000
1	-6.265892000	-1.326533000	0.010755000
8	-3.286515000	2.032132000	-0.791271000
1	-4.078578000	2.505363000	-1.102536000
1	-4.460420000	-2.769509000	0.970164000

……

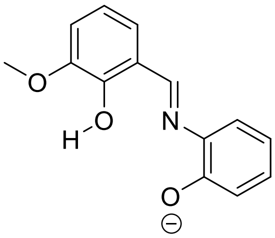

6	2.616478000	2.103875000	0.483261000
6	1.317764000	1.632964000	0.393293000
6	1.061067000	0.281094000	0.088170000
6	2.142651000	-0.579697000	-0.120761000
6	3.466966000	-0.096552000	-0.025751000
6	3.704229000	1.238960000	0.274355000

1	2.807099000	3.153729000	0.718154000
1	0.462259000	2.292801000	0.551942000
1	4.725443000	1.616350000	0.347787000
6	-0.313322000	-0.235151000	-0.020701000
1	-0.412650000	-1.303709000	-0.277529000
7	-1.328545000	0.517142000	0.154723000
8	1.934148000	-1.884535000	-0.416447000
1	2.798824000	-2.325009000	-0.528074000
8	4.415361000	-1.040512000	-0.251624000
6	5.772262000	-0.652687000	-0.188331000
1	6.362754000	-1.553839000	-0.403254000
1	5.996254000	0.122451000	-0.941834000
1	6.028407000	-0.276288000	0.817498000
6	-2.634458000	0.005744000	0.107915000
6	-3.668743000	0.930251000	-0.320272000
6	-2.951053000	-1.301359000	0.504693000
6	-4.996109000	0.380607000	-0.332396000
6	-4.260228000	-1.782340000	0.486986000
1	-2.147336000	-1.945562000	0.876458000
6	-5.280273000	-0.920760000	0.055208000
1	-5.798292000	1.051796000	-0.657718000
1	-6.317330000	-1.272847000	0.035429000
8	-3.422541000	2.123494000	-0.676953000
1	-4.484738000	-2.797145000	0.824256000

……

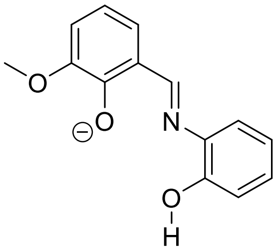

6	2.706256000	2.038822000	0.620616000
6	1.405047000	1.603582000	0.522771000
6	1.103199000	0.275094000	0.131661000
6	2.138745000	-0.675101000	-0.173626000
6	3.500044000	-0.158823000	-0.057487000
6	3.765442000	1.138193000	0.323122000
1	2.939302000	3.063238000	0.920858000
1	0.568936000	2.274106000	0.742092000
1	4.796754000	1.489741000	0.400510000
6	-0.268646000	-0.174655000	0.020285000
1	-0.389784000	-1.226789000	-0.293241000
7	-1.295654000	0.567181000	0.242805000
8	1.933894000	-1.874182000	-0.517498000
8	4.453342000	-1.086141000	-0.361951000
6	5.799979000	-0.688340000	-0.289298000
1	6.403400000	-1.563138000	-0.572342000
1	6.014362000	0.141469000	-0.987951000
1	6.074448000	-0.375340000	0.735086000
6	-2.572018000	0.001591000	0.172158000
6	-3.623113000	0.794333000	-0.347352000

6	-2.884381000	-1.283924000	0.638211000
6	-4.921191000	0.289157000	-0.414388000
6	-4.185667000	-1.787169000	0.575398000
1	-2.087633000	-1.884883000	1.084747000
6	-5.205437000	-0.999535000	0.044673000
1	-5.710915000	0.921440000	-0.831919000
1	-6.229496000	-1.377725000	-0.008690000
8	-3.306341000	2.038654000	-0.787712000
1	-4.106995000	2.491518000	-1.105735000
1	-4.399520000	-2.789907000	0.953783000

……

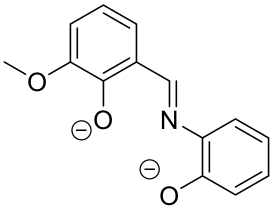

6	2.689688000	2.035572000	0.631584000
6	1.385827000	1.599414000	0.525725000
6	1.082589000	0.275967000	0.131191000
6	2.117185000	-0.674026000	-0.169410000
6	3.475619000	-0.160739000	-0.050378000
6	3.745950000	1.136582000	0.335334000
1	2.920851000	3.058828000	0.937690000
1	0.548717000	2.269692000	0.742858000
1	4.778320000	1.484294000	0.416363000
6	-0.300539000	-0.168036000	0.009614000

1	-0.425542000	-1.225860000	-0.285486000
7	-1.319541000	0.584706000	0.206002000
8	1.910009000	-1.876689000	-0.515657000
8	4.431626000	-1.088364000	-0.358033000
6	5.776856000	-0.687229000	-0.293725000
1	6.381220000	-1.558950000	-0.584829000
1	5.984783000	0.145984000	-0.990598000
1	6.059612000	-0.377291000	0.729498000
6	-2.616143000	0.045740000	0.141595000
6	-3.649835000	0.897603000	-0.421212000
6	-2.926379000	-1.222484000	0.643505000
6	-4.961884000	0.323405000	-0.430631000
6	-4.228346000	-1.738212000	0.614702000
1	-2.123401000	-1.809645000	1.102310000
6	-5.242583000	-0.946374000	0.067262000
1	-5.761250000	0.941529000	-0.854428000
1	-6.271703000	-1.320783000	0.036003000
8	-3.404036000	2.055325000	-0.892880000
1	-4.443629000	-2.726012000	1.030221000

……………………………………………………………………………………

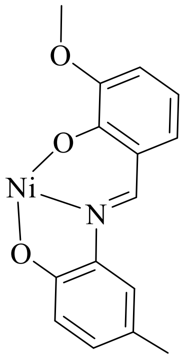

28	-0.061276000	-1.674262000	0.002213000
8	-1.883784000	-2.217406000	-0.020283000
8	1.746336000	-1.157264000	0.003599000
7	-0.772984000	0.199599000	0.002621000
8	4.319755000	-0.933276000	0.014581000
6	-0.039153000	1.256666000	-0.014141000
6	1.412564000	1.253659000	-0.012229000
6	-2.698262000	-1.171767000	-0.012205000
6	-2.181519000	0.154223000	0.001649000
6	3.410523000	2.647989000	-0.017263000
1	3.883794000	3.630435000	-0.023623000
6	-4.098546000	-1.319418000	-0.016435000
1	-4.509014000	-2.331226000	-0.027987000
6	4.211922000	1.488330000	-0.004842000
1	5.297198000	1.588199000	-0.001397000
6	-4.932841000	-0.208311000	-0.005224000
1	-6.016413000	-0.355445000	-0.008475000
6	3.628282000	0.233208000	0.002817000
6	-5.352081000	2.287532000	0.026507000
1	-6.011558000	2.266612000	0.907771000

1	-4.791376000	3.231880000	0.044566000
1	-6.001722000	2.295039000	-0.862323000
6	5.728777000	-0.866789000	0.022522000
1	6.090587000	-1.901412000	0.033243000
1	6.111860000	-0.358727000	-0.877376000
1	6.100776000	-0.343949000	0.918622000
6	2.040219000	2.526703000	-0.021071000
1	1.405602000	3.415701000	-0.030067000
6	-3.036952000	1.262516000	0.016201000
1	-2.618424000	2.271647000	0.033994000
6	-4.422188000	1.102057000	0.012199000
6	2.201716000	0.067694000	-0.001541000
1	-0.507911000	2.251194000	-0.032090000

……

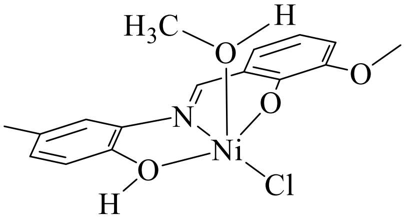

28	-0.002170000	-1.253054000	-0.247206000
8	1.806361000	-0.489047000	-0.515959000
8	-2.067334000	-1.656874000	-0.021874000
8	0.364005000	-1.511748000	1.775700000
8	4.368669000	-0.103492000	-0.545573000
7	-0.810863000	0.642936000	-0.080522000
6	2.192191000	0.693639000	-0.188097000

6	-2.221817000	0.690060000	-0.105920000
6	1.337612000	1.779478000	0.174105000
6	3.612547000	0.964602000	-0.188180000
6	1.889421000	3.045690000	0.521158000
1	1.202036000	3.851158000	0.789963000
6	-3.004185000	1.849872000	-0.186418000
1	-2.523006000	2.828073000	-0.235064000
6	3.244613000	3.258960000	0.516637000
1	3.659958000	4.231064000	0.784216000
6	-4.398751000	1.785889000	-0.240295000
6	-5.014734000	0.526327000	-0.226691000
1	-6.103569000	0.457657000	-0.278589000
6	-4.260246000	-0.641460000	-0.157712000
1	-4.734386000	-1.624770000	-0.151929000
6	5.767821000	0.065041000	-0.583902000
6	-2.874591000	-0.554314000	-0.100570000
6	-0.100205000	1.692870000	0.176020000
1	-0.609671000	2.634567000	0.424853000
6	4.115292000	2.202380000	0.154863000
1	5.191390000	2.377310000	0.150789000
6	-0.257428000	-2.611278000	2.438101000
1	0.140090000	-2.711545000	3.457207000
1	-1.331428000	-2.397413000	2.492877000
1	-0.098320000	-3.541059000	1.873117000
6	-5.228583000	3.040510000	-0.307445000

1	-4.611285000	3.913822000	-0.556292000
1	-6.023454000	2.948998000	-1.061393000
1	-5.717338000	3.237239000	0.659650000
17	0.321672000	-3.438896000	-0.957707000
1	-2.485407000	-2.473436000	-0.341426000
1	1.327804000	-1.603485000	1.843942000
1	6.167262000	0.333310000	0.407840000
1	6.191794000	-0.896775000	-0.894982000
1	6.058557000	0.841173000	-1.310619000

……

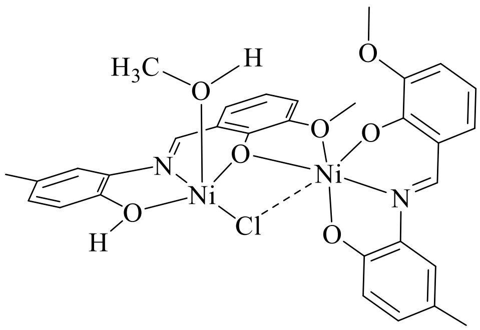

28	-1.339572000	-0.520005000	0.316416000
28	1.689054000	-0.814158000	-0.601315000
8	0.586432000	-0.601314000	1.049692000
8	-2.039939000	-2.251776000	1.070233000
8	3.199399000	-1.298604000	-1.961585000
8	-0.933009000	1.346368000	-0.351622000
8	1.469468000	1.124664000	-1.210333000
8	-1.440926000	0.393507000	2.308351000
7	-3.290825000	-0.316139000	-0.306783000

7	3.380995000	-0.472317000	0.530592000
8	0.073874000	3.671305000	-0.852081000
6	-3.836604000	0.762161000	-0.748690000
6	-3.164516000	2.030018000	-0.985091000
6	-3.249075000	-2.496440000	0.649777000
6	0.870005000	0.286529000	1.973722000
6	-3.987024000	-1.524326000	-0.095029000
6	4.577502000	-0.897418000	-0.085573000
6	2.181457000	0.711115000	2.296505000
6	-0.215382000	0.858458000	2.699886000
6	2.373826000	1.646894000	3.342797000
1	3.394290000	1.948129000	3.588487000
6	-3.452967000	4.335118000	-1.732253000
1	-4.089615000	5.141625000	-2.097721000
6	-3.906092000	-3.726225000	0.907080000
1	-3.362794000	-4.481300000	1.480003000
6	-2.075204000	4.566557000	-1.538922000
1	-1.658442000	5.550833000	-1.753957000
6	5.836395000	-0.945503000	0.526336000
1	5.940813000	-0.643618000	1.570137000
6	-5.191478000	-3.971834000	0.447769000
1	-5.660736000	-4.936024000	0.664544000
6	-1.259571000	3.551130000	-1.073405000
6	1.303816000	2.181639000	4.028458000
1	1.462452000	2.909893000	4.824083000

6	6.961406000	-1.401981000	-0.162761000
6	6.805410000	-1.827604000	-1.490246000
1	7.672903000	-2.194825000	-2.043093000
6	5.562213000	-1.803933000	-2.115211000
1	5.438815000	-2.143629000	-3.145495000
6	-2.607152000	1.040383000	2.793178000
6	-7.291751000	-3.320809000	-0.811727000
1	-7.971892000	-3.591812000	0.010676000
1	-7.721091000	-2.454291000	-1.333240000
1	-7.285031000	-4.168190000	-1.515372000
6	0.700554000	4.884004000	-1.202804000
1	1.768900000	4.755577000	-0.992245000
1	0.564080000	5.110376000	-2.272999000
1	0.312009000	5.723898000	-0.604247000
6	-3.978134000	3.091877000	-1.458981000
1	-5.043013000	2.898369000	-1.607953000
6	4.454966000	-1.344914000	-1.411513000
6	-5.280754000	-1.799898000	-0.560648000
1	-5.812047000	-1.052537000	-1.155271000
6	-5.906557000	-3.017646000	-0.300933000
6	3.368820000	0.240941000	1.604305000
1	4.319051000	0.567553000	2.049970000
6	-0.008909000	1.790101000	3.698956000
1	-0.855182000	2.220319000	4.235045000
6	-1.773755000	2.242400000	-0.780698000

6	1.386234000	1.364773000	-2.606818000
1	1.269289000	2.441437000	-2.801574000
1	2.317783000	1.020925000	-3.075943000
1	0.539579000	0.816633000	-3.049825000
6	8.314185000	-1.440363000	0.496697000
1	8.238348000	-1.240006000	1.573437000
1	8.792751000	-2.420612000	0.358107000
1	8.984119000	-0.685460000	0.056864000
1	-4.913689000	0.772728000	-0.972106000
17	-0.260693000	-1.627908000	-1.700974000
1	3.139254000	-1.743088000	-2.823110000
1	0.579876000	1.388007000	-0.811468000
1	-2.598564000	2.107713000	2.522363000
1	-3.456818000	0.536301000	2.318299000
1	-2.683870000	0.930859000	3.884431000

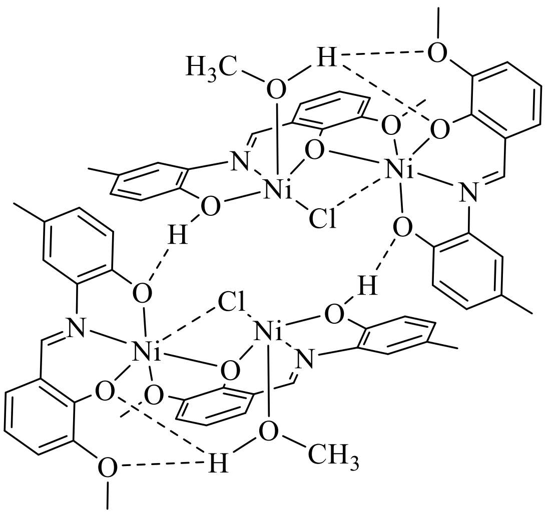

6	-3.118047000	2.007237000	-2.569317000
6	-3.364945000	3.278416000	-3.102281000
1	-4.233167000	3.853656000	-2.772996000
6	-2.506095000	3.832061000	-4.051747000
6	-1.392768000	3.072846000	-4.461631000
1	-0.714675000	3.490926000	-5.211082000
6	-1.128344000	1.815924000	-3.934951000
1	-0.254052000	1.239066000	-4.246675000
6	-1.984839000	1.253801000	-2.964824000
6	-5.023235000	1.773626000	-1.147502000
1	-5.410087000	2.736395000	-1.506749000
6	-5.851094000	1.092985000	-0.176899000
6	-5.469593000	-0.138003000	0.417919000
6	-6.405750000	-0.746545000	1.320860000
6	-7.604110000	-0.133729000	1.638557000
1	-8.293565000	-0.610895000	2.335434000
6	-7.948764000	1.105630000	1.057159000
1	-8.896854000	1.577607000	1.317120000
6	-7.087614000	1.700196000	0.163885000
1	-7.342412000	2.653628000	-0.304530000
6	-2.740852000	5.206706000	-4.622827000
1	-2.847521000	5.173923000	-5.718247000
1	-3.650649000	5.660783000	-4.207103000
1	-1.895510000	5.877519000	-4.401288000
6	-6.760996000	-2.539940000	2.832877000

1	-6.210158000	-3.432792000	3.151391000
1	-6.881624000	-1.860490000	3.692590000
1	-7.757068000	-2.838502000	2.467261000
6	-1.736861000	-2.936870000	-0.715141000
6	-2.619045000	-3.302241000	-1.790739000
6	-2.594734000	-4.564424000	-2.353115000
1	-3.273806000	-4.808957000	-3.169934000
6	-1.681493000	-5.526092000	-1.886738000
1	-1.662095000	-6.517633000	-2.340985000
6	-0.844685000	-5.220476000	-0.828838000
1	-0.161658000	-5.973771000	-0.429809000
6	-0.873361000	-3.949625000	-0.215608000
6	-0.085920000	-3.798563000	0.995148000
1	0.531531000	-4.666794000	1.259968000
6	0.506086000	-2.744963000	3.044222000
6	0.297619000	-1.513171000	3.711075000
6	0.897681000	-1.349474000	4.979461000
1	0.755877000	-0.400308000	5.500068000
6	1.658978000	-2.367681000	5.533585000
1	2.116676000	-2.217078000	6.515590000
6	1.863208000	-3.594315000	4.869544000
6	1.273695000	-3.765614000	3.618341000
1	1.417598000	-4.711805000	3.091918000
6	2.690947000	-4.680239000	5.507406000
1	2.766584000	-5.558732000	4.851983000

1	3.712145000	-4.330265000	5.724538000
1	2.253803000	-5.008803000	6.463300000
6	2.214809000	2.175087000	-3.003102000
6	2.252953000	3.145175000	-3.993118000
1	2.643340000	2.901090000	-4.981105000
6	1.773600000	4.438070000	-3.730598000
1	1.799476000	5.194475000	-4.515828000
6	1.260888000	4.733777000	-2.484407000
1	0.871609000	5.730512000	-2.267154000
6	1.237711000	3.765919000	-1.453242000
6	1.725516000	2.463858000	-1.696767000
6	0.695419000	4.194130000	-0.174309000
1	0.265220000	5.204071000	-0.167933000
6	-0.572384000	5.121599000	2.333898000
1	-0.829732000	5.761135000	1.486701000
6	-1.024165000	5.469577000	3.605930000
6	-0.694330000	4.618704000	4.678926000
1	-1.041706000	4.876394000	5.683506000
6	0.048048000	3.460146000	4.497341000
1	0.288180000	2.806621000	5.338558000
6	0.502645000	3.094987000	3.211612000
6	0.185256000	3.960987000	2.137190000
6	-1.851699000	6.707658000	3.836946000
1	-1.374167000	7.377445000	4.568756000
1	-1.992519000	7.270505000	2.904131000

1	-2.847710000	6.455295000	4.233110000
6	3.097747000	0.483550000	-4.447427000
1	3.342034000	-0.581338000	-4.353129000
1	2.330490000	0.616738000	-5.225687000
1	4.005235000	1.043037000	-4.722506000
6	2.294194000	-2.877988000	-1.849824000
6	1.039111000	-2.159103000	-2.297235000
6	0.130904000	-2.834051000	-3.199371000
1	-0.710790000	-2.262232000	-3.590150000
6	0.389300000	-4.119690000	-3.523883000
1	-0.248968000	-4.647661000	-4.234495000
6	1.521932000	-4.865984000	-2.958312000
6	2.439292000	-4.258224000	-2.138915000
1	3.296401000	-4.823552000	-1.774769000
6	4.331208000	-2.489331000	-0.745951000
1	4.509658000	-3.568142000	-0.711945000
6	5.338595000	-1.674489000	-0.282201000
6	6.535134000	-2.305425000	0.231644000
1	6.551239000	-3.394261000	0.295943000
6	7.599238000	-1.559339000	0.611460000
1	8.499858000	-2.036176000	0.999044000
6	7.577796000	-0.121742000	0.506562000
1	8.461213000	0.438827000	0.812851000
6	6.481214000	0.533420000	0.031681000
6	5.281630000	-0.205582000	-0.359697000

6	7.413380000	2.689838000	0.292390000
1	7.075603000	3.721803000	0.147779000
1	7.660100000	2.524869000	1.352881000
1	8.305219000	2.500089000	-0.325203000
6	1.664577000	-6.291307000	-3.359137000
1	2.508517000	-6.776529000	-2.856257000
1	0.734106000	-6.837166000	-3.138858000
1	1.808208000	-6.347001000	-4.451055000
6	-4.108003000	-2.419824000	-3.434656000
1	-4.580543000	-1.446048000	-3.610317000
1	-3.388242000	-2.634513000	-4.240268000
1	-4.881662000	-3.202192000	-3.411705000
6	-3.568987000	-0.683641000	3.322692000
1	-4.638003000	-0.732036000	3.595804000
1	-2.978853000	-0.742511000	4.248272000
1	-3.362003000	0.292469000	2.851979000
7	3.147084000	-2.056743000	-1.259045000
7	-0.142763000	-2.791390000	1.790724000
7	-3.909918000	1.325078000	-1.615691000
7	0.710257000	3.504564000	0.907445000
8	-5.996550000	-1.941031000	1.811761000
8	-4.344852000	-0.756796000	0.206197000
8	-1.779743000	0.075885000	-2.428850000
8	0.884885000	-1.001275000	-1.903207000
8	4.294394000	0.450401000	-0.748799000

8	2.614677000	0.891700000	-3.184309000
8	1.736822000	1.502614000	-0.779443000
8	1.203550000	2.010644000	2.981388000
8	-0.421864000	-0.585283000	3.139832000
8	-1.783364000	-1.714071000	-0.246535000
8	-3.447835000	-2.317212000	-2.189017000
8	6.340814000	1.859707000	-0.112350000
8	-3.193069000	-1.753804000	2.482707000
28	-2.994373000	-0.280478000	-1.024566000
28	-1.000558000	-1.077447000	1.413274000
28	1.465193000	1.721039000	1.130036000
28	2.508771000	-0.231833000	-1.083239000
17	-1.504293000	1.097371000	0.883061000
17	2.323635000	-0.396474000	1.502864000
8	3.804686000	2.790142000	0.972802000
1	4.250423000	2.359649000	0.226181000
1	-3.660849000	-1.612289000	1.633318000
6	4.449260000	2.363483000	2.154417000
1	4.567151000	1.267191000	2.183141000
1	5.437997000	2.836747000	2.280594000
1	3.819238000	2.653102000	3.007284000

Additional Information:

The diprotic Schiff base ligand which was synthesized by condensation of *o*-vanillin and functionalized 2-aminophenol [$(OH)_2L-NO_2$ / $(OH)_2L$-Me] has two phenolic HO-groups. The HO-group of nitro-aminophenol part of $(OH)_2L-NO_2$ is more acidic than that of *o*-vanillin part of $(OH)_2L-NO_2$. This trend of $(OH)_2L$-Me is opposite to that $(OH)_2L-NO_2$ (see the proton affinity values given in Scheme 1 in the Manuscript). The proton affinity value of aminophenolate part of $(OH)_2L$-Me are 10-12 kcal/mol.

Previous report showed that **$(OH)_2L'-NO_2$** reacted with $Ni(NO_3)_2{\cdot}6H_2O$ to produce a mixture of dinuclear $[Ni_2((O^-)_2L'-NO_2)_2(DMSO)_2(MeOH)_2]$ (**A**) and tetranuclear $[Ni_4((O^-)_2L'-NO_2)_4(DMF)_2(MeOH)_2]$ (**B**) complexes. The Ni-O core of **B** has a defect-dicubane topology. $Ni(NO_3)_2{\cdot}6H_2O$ or $NiCl_2{\cdot}6H_2O$ was reported to react with $(OH)_2L$-H in the presence of Et_3N leading to the isolation of tetranuclear $[Ni_4((O^-)_2L-H)_4(MeOH)_2]$ complex (**C**) with distorted cubane like Ni-O core topology. **$(OH)_2L-NO_2$** and **$(OH)_2L$-H** are doubly deprotonated to [**$(O^-)_2L'-NO_2$**] and **$(O^-)_2L$-H** in all three complexes **A-C** by Et_3N. All the Ni(II)-ceneters of **A-C** are hexa-coordinated. The mechanistic path ways for the formation of complexes **A-C** were not studied.

9. References:

S1. (a) Grehn, L.; Ragnarsson, U. *Angew. Chem. Int. Ed*. **1984**, *23*, 296-301. (b) Coulton, S.; Gilchrist, T. L.; Graham, K. *Tetrahedron* **1997**, *53*, 791-798.

S2. Harrar, K.; Reiser, O. *Chem. Comm.* **2012**, *48*, 3457-3459.

S3. Kushvaha, S. K.; Arumugam, S.; Shankar, B.; Sarkar, R. S.; Ramkumar, V.; Mondal, K. C. Isolation and Characterization of Different Homometallic and Heterobimetallic Complexes of Nickel and Zinc Ions by Controlling Molar Ratios and Solvents. *Eur. J. Inorg. Chem*. **2019**, 2871-2882.

S4. Gorantla, S. M. N. V.T.; Reddy, P. G.; Shakoor, S. M. A.; Mandal, R.; Roy, S.; Mondal, K. C. Tetranuclear 3 d/4 f Coordination Complexes as Homogeneous Catalysts for Bis(indolyl)methane Syntheses. *ChemistrySelect* **2019**, *4*, 7722-7727.

S5. (a) Saha, S.; Jana, S.; Gupta, S.; Ghosh, A.; Nayek, H. P. Syntheses, Structures and Biological Activities of Square Planar Ni(II), Cu(II) Complexes. *Polyhedron* **2016**, *107*, 183-189. (b) Nag, E.; Gorantla, S. M. N. V. T.; Arumugam, S.; Kulkarni, A.; Mondal, K. C.; Roy, S. Tridentate Nickel(II)-Catalyzed Chemodivergent C–H Functionalization and Cyclopropanation: Regioselective and Diastereoselective Access to Substituted Aromatic Heterocycles. *Org. Lett.* **2020**, *22*, 6313-6318.

S6. Bader, R. F.W. *Atoms in Molecules-A Quantum Theory*, Oxford University Press, New York, **1990**.

S7. Matta, C. F. R.; Boyd, J. *The Quantum Theory of Atoms in Molecules: From Solid State to DNA and Drug Design* (Eds.:), *Chapter 1. An Introduction to the Quantum Theory of Atoms in Molecules*, Wiley, Hoboken, **2007**, 1-34.

S8. (a) Bader, R. F. W. *Acc. Chem. Res.* **1985**, *18*, 9-15. (b) Bader, R. F. W. *Chem. Rev*. **1991**, *94*, 893-928.

S9. Bruker (2008). *APEX2* (Version 2008.1-0). Bruker AXS Inc., Madison, Wisconsin, USA.

S10. Bruker (2001b). SAINT-V6.28A. Data Reduction Software.

S11. Sheldrick, G. M. (1996). *SADABS. Program for Empirical Absorption Correction*. University of Gottingen, Germany.

S12. Farrugia, L. J. *J. Appl. Cryst*. **1999**, *32*, 837.

S13. Sheldrick, G.M. (1997) SHELXL-97. Program for the Refinement of Crystal.

S14. Sheldrick, G.M. *Acta Cryst.* **1990**, *A46*, 467.

S15. S. Coulton, T. L. Gilchrist and K. Graham, *Tetrahedron*, **1997**, *53*, 791.

S16. D. R. Stuart, E. Villemure and K. Fagnou, *J. Am. Chem. Soc.*, **2007**, *129*, 12072.

S17. H. Keipour, A. Jalba, L. Delage-Laurin and T. Ollevier, *J. Org. Chem.*, **2017**, *82*, 3000.